U.PORTO

DOUTORAMENTO

BIOTECNOLOGIA MOLECULAR E CELULAR APLICADA ÀS CIÊNCIAS DA SAÚDE

Production of compatible solutes using the cyanobacterium *Synechocystis* sp. PCC 6803 as photoautotrophic chassis

Eunice Miguel Azevedo Ferreira

D

2022

U.PORTO

Eunice Miguel Azevedo Ferreira. Production of compatible solutes using the cyanobacterium *Synechocystis* sp. PCC 6803 as photoautotrophic chassis

Production of compatible solutes using the cyanobacterium *Synechocystis* sp. PCC 6803 as photoautotrophic chassis

Eunice Miguel Azevedo Ferreira

D.ICBAS **2022**

SEDE ADMINISTRATIVA

INSTITUTO DE CIÊNCIAS BIOMÉDICAS ABEL SALAZAR

FACULDADE DE FARMÁCIA

EUNICE MIGUEL AZEVEDO FERREIRA

Production of compatible solutes using the cyanobacterium *Synechocystis* sp. PCC 6803 as photoautotrophic chassis

Tese de Candidatura ao grau de Doutor em
Biotecnologia Molecular e Celular Aplicada às
Ciências da Saúde;
Programa Doutoral da Universidade do Porto
(Instituto de Ciências Biomédicas Abel Salazar e
Faculdade de Farmácia)

Orientador – Paula Tamagnini
Categoria – Professora Associada
Afiliação – Faculdade de Ciências,
i3S – Instituto de Investigação e Inovação em Saúde,
IBMC – Instituto de Biologia Molecular e Celular,
Universidade do Porto, Portugal

Co-orientador – Javier Urchueguía
Categoria – Full Professor
Afiliação – Universitat Politècnica de València,
Spain

Co-orientador – Robert Kourist
Categoria – Full Professor
Afiliação – Institut für Molekulare Biotechnologie,
TU Graz, Austria

The one who plants trees, knowing that he will never sit in their shade,

has at least started to understand the meaning of life.

Rabindranath Tagore

Nobel Prize in Literature, 1913

This work was funded by Fundação para a Ciência e a Tecnologia through PhD fellowship SFRH/BD/117508/2016.

This work was also funded by European Commission through the 7th Framework Programme FP7-ENERGY-2012-1-STAGE-308518 project CyanoFactory [308518], and by Fundo Europeu de Desenvolvimento Regional (FEDER) funds, under the PORTUGAL 2020 Partnership Agreement, supported by Norte Portugal Regional Operational Programme (NORTE 2020), NORTE-01-0145-FEDER-000012 - Structured Programme on Bioengineering Therapies for Infectious Diseases and Tissue Regeneration, and under the COMPETE 2020 Operacional Programme for Competitiveness and Internationalisation (POCI), and by Portuguese funds through the Fundação para a Ciência e a Tecnologia (FCT) / Ministério da Ciência, Tecnologia e Ensino Superior within the scope of UIDB/04293/2020, UIDP/04293/2020 and POCI-01-0145-FEDER-029540 (PTDC/BIA-OUT/29540/2017). Part of the work from Chapters IV and V was awarded by funds of the European Molecular Biology Organisation (EMBO) by a European Molecular Biology Laboratory (EMBL) Advanced Training Centre Corporate Partnership Programme fellowship.

Table of Contents

Acknowledgements / Agradecimentos

I would like to express my gratitude to all the people that directly or indirectly helped me on this journey. This work was not possible, and most likely I would not survive to PhD, without a supportive network, namely supervisor, collaborators, lab colleagues, friends, and family. In particular, I would like to thank: / Gostaria de demonstrar a minha gratidão a todas as pessoas que direta ou indiretamente me ajudaram nesta caminhada. Este trabalho não seria possível, e muito provavelmente não sobreviveria ao PhD, sem o apoio nomeadamente da minha orientadora, colaboradores, colegas de laboratório, amigos e família. Em particular, gostaria de agradecer:

À minha orientadora Prof. Paula Tamagnini, pela oportunidade de realizar o trabalho de doutoramento no grupo "Bioengineering & Synthetic Microbiology" (BSM), pelos conhecimentos transmitidos, pelo apoio e paciência, pela liberdade e incentivo para traçar o meu próprio caminho.

To my co-supervisor Javier Urchueguía, for the huge opportunity to be completely outside of my comfort zone and learn computational language during my stay in Universitat Politecnica de Valencia. To David Fuente, for the great hospitality, kindness, and patience for teaching me from scratch the complex world of FBA computations and COBRA Toolbox written in MATLAB; and to Maria Siurana, for the good mood and all the scientific discussions. To Meritxell Notari (Méri) for the friendship and taking me to taste the best horchata and fartons like a real Valencian girl.

To Prof. Martin Hagemann (University of Rostock, Germany), Prof. Pauli Kallio (University of Turku, Finland), Prof. Peter Lindblad (Uppsala University, Sweden) and my co-supervisor Prof. Robert Kourist (Graz University of Technology, Austria), for all the valuable scientific discussions and helpful advices.

A toda a família BSM: D. Helena Pinho, Marta Mendes, Pedro Albuquerque, Sara Pereira, Rita Mota, Ângela Brito, Cátia Gonçalves, Delfim Cardoso (…) por tornarem o ambiente labor(atori)al incrível, pelo apoio e companheirismo. Em especial, à Catarina Pacheco, por todo o apoio e partilha de conhecimento, por ter sido o meu ombro amigo, a nível profissional e pessoal, pela dedicação e paciência. Ao Paulo Oliveira pelas sábias palavras na hora certa, apoio e incentivo. Ao Filipe Pinto e João Rodrigues pela boa disposição, apoio e entusiasmo pelo maravilhoso mundo da biologia sintética. Ao Carlos Flores (Carlitos), pela boa disposição e companheirismo e à Marina Santos, pela preocupação e incentivo. Obrigada por, juntamente com a Rute Oliveira, Steeve Lima e José Leite, terem feito do nosso cantinho o melhor *guetto* de sempre! À Rutezinha, pela amizade, pela força que tem e me transmite, por ter sido a minha luz especialmente quando tudo corria mal. Ao Steevezinho, por ser o meu resmungão preferido, por poder contar sempre com ele. Ao

Zé, por ser uma inspiração, pelo incansável apoio e incentivo, pela sua emocionalidade racional.

À Prof. Helena Santos (ITQB, Universidade Nova de Lisboa), por me ter dado a oportunidade de conhecer o seu laboratório e aprender a técnica de extração de solutos compatíveis com a ajuda e amabilidade da Sara Rebelo; e ao Pedro Lamosa por ter estabelecido connosco uma importante colaboração para a quantificação de solutos compatíveis no serviço CERMAX (ITQB).

À Prof. Paula Gomes (LAQV-REQUIMTE, FCUP), que me deu a possibilidade de realizar a técnica de extração de solutos compatíveis no seu laboratório, com o seu equipamento, com a ajuda das suas alunas. Obrigada especialmente à Luísa Aguiar, pela disponibilidade, apoio e paciência; à Mélanie Fonte por toda ajuda com o equipamento laboratorial e boa disposição e à Ana Gomes pela simpatia e partilha de momentos.

À Prof. Cecília Arraiano e à Patrícia Apura (ITQB), pelo entusiasmo pelo meu trabalho e boa companhia no Workshop da EMBO (Heidelberg, Alemanha) e no congresso Microbiotec (Universidade de Coimbra, Portugal).

Ao ex-Diretor do programa doutoral BiotechHealth (ICBAS), Prof. Mário Barbosa, por ter acompanhado o meu trabalho apresentado nos simpósios e pelas palavras motivadoras e compreensivas que sempre proferia com muito apreço. Ao Diretor Prof. Manuel Vilanova pela disponibilidade e compreensão.

Aos colegas do meu ano de doutoramento do BiotechHealth: Filipe Marques, Mafalda Gonçalves, João Brás, José Mateus, Joana Ferreira, Andreia Granja e Rita Pinto, pela camaradagem, entre-ajuda e todos os bons momentos que passámos.

Às “Meneinas” Leandra Neto, Paula Costa, Patrícia Simões e Joana Requeijo pela amizade.

Aos meus “Miguitos” Ana Matos, Mariana Silva, Pedro Loureiro, Ana Castro e Tiago Ferreira, pela constante e contagiante boa disposição, pela preocupação e bonita amizade de muitos anos.

Às minhas fofinhas Ana Laço e Raquel Brandão por serem o meu porto de abrigo em todas as ocasiões, para celebrar sucessos e desabafar tristezas.

Ao Tiago Oliveira e família, por todo o amor, cuidado e preocupação.

À minha família, mãe, pai, irmão, cunhada e avós, pelo apoio e amor incondicionais, por acreditarem em mim, a maior parte das vezes mais do que eu, por verem uma versão de mim melhor do que a que eu vejo.

Ao meu sobrinho e afilhado Bernardo Ferreira, por me iluminar com o sorriso mais bonito que há neste mundo.

List of Publications

This thesis is based on the following publications and some unpublished results:

Ferreira, E. A., Pacheco, C. C., Pinto, F., Pereira, J., Lamosa, P., Oliveira, P., Kirov, B., Jaramillo, A., & Tamagnini, P. (2018). Expanding the toolbox for *Synechocystis* sp. PCC 6803: validation of replicative vectors and characterization of a novel set of promoters. *Synthetic Biology, 3*(1), ysy014. https://doi.org/10.1093/synbio/ysy014.

Ferreira, E. A., Pacheco, C. C., Rodrigues, J. S., Pinto, F., Lamosa, P., Fuente, D., Urchueguía, J., & Tamagnini, P. (2022). Heterologous production of glycine betaine using *Synechocystis* sp. PCC 6803-based chassis lacking native compatible solutes. *Frontiers in Bioengineering and Biotechnology*, *9*:821075. https://doi.org/10.3389/fbioe.2021.821075.

Pacheco, C. C., Ferreira, E. A., Oliveira, P., & Tamagnini, P., "Synthetic biology of cyanobacteria"; in: Kourist, R., & Schmidt, S. (ed.) of book The Autotrophic Biorefinery: Raw Materials from Biotechnology, Berlin, Boston: De Gruyter, 2021, pp. 131-172, fig. 6.1-6.5. https://doi.org/10.1515/9783110550603-006.

Other publications:

Lindblad, P., Fuente, D., Borbe, F., Cicchi, B., Conejero, J. A., Couto, N., Čelešnik, H., Diano, M. M., Dolinar, M., Esposito, S., Evans, C., Ferreira, E. A., Keller, J., Khanna, N., Kind, G., Landels, A., Lemus, L., Noirel, J., Ocklenburg, S., Oliveira, P., Pacheco, C. C., Parker, J. L., Pereira, J., Pham, T. K., Pinto, F., Rexroth, S., Rögner, M., Schmitz, H.-J., Benavides, A. M. S., Siurana, M., Tamagnini, P., Touloupakis, E., Torzillo, G., Urchueguía, J. F., Wegelius, A., Wiegand, K., Wright, P. C., Wutschel, M., & Wünschiers, R. (2019). CyanoFactory, a European consortium to develop technologies needed to advance cyanobacteria as chassis for production of chemicals and fuels. *Algal Research, 41* (101510). https://doi.org/10.1016/j.algal.2019.101510.

Jurkaš, V., Winkler, C. K., Poschenrieder, S., Oliveira, P., Pacheco, C. C., Ferreira, E. A., Weissenteiner, F., De Santis, P., Kara, S., Kourist, R., Tamagnini, P., & Kroutil, W. (2022). Expression and activity of heterologous hydroxyisocaproate dehydrogenases in *Synechocystis* sp. PCC 6803 Δ*hoxYH*. *Engineering Microbiology*, *2*(1), 100008. https://doi.org/10.1016/j.engmic.2021.100008.

List of Abbreviations

αKG	α-ketoglutarate
Abs	Absorbance
AcCoA	Acetyl-coenzyme A
ADP	Adenosine diphosphate
AHL	Acyl-homoserine lactone
Amp	Ampicillin
ANOVA	Analysis of variance
AsD	L-aspartate-β-semialdehyde dehydrogenase
AsK	Aspartate kinase
ASW	Artificial seawater
aTc	Anhydrotetracycline hydrochloride
ATP	Adenosine triphosphate
A-tract	Adenosine-rich tract
A.U.	Arbitrary units
BB/BBa	BioBrick
BCD	Bicistronic design
bp	Base pairs
Byr	Billion years
CAI	Codon adaptation index
Cas	CRISPR-associated protein
CBB cycle	Calvin–Benson–Bassham cycle
cDNA	Complementary DNA
CDS	Coding sequence
CFKB	CyanoFactory KnowledgeBase
Chl *a*	Chlorophyll *a*
Cm	Chloramphenicol
CoA	Coenzyme A
COBRA Toolbox	Constraint-based reconstruction and analysis Toolbox
CPS	Capsular polysaccharides
CRISPR	Clustered regularly interspaced short palindromic repeats
CRISPRi	CRISPR interference
crRNA	*Cis*-repressed RNA
Cs	*Chromohalobacter salexigens*
CS	Compatible solute
Cys	Cysteine
dCas9	Dead Cas9
DCW	Dry cell weight
DldhE	D-lactate dehydrogenase from *E. coli*

DMT	Dimethylglycine-N-methyltransferase
DNA	Deoxyribonucleic acid
DNAse	Deoxyribonuclease
dNTP	Deoxyribonucleotide triphosphate
DW	Dry weight
EctA	L-diaminobutyric acid acetyltransferase
EctB	L-diaminobutyric acid transaminase
EctC	Ectoine synthase
EctD	Ectoine hydroxylase
EDTA	Ethylenediaminetetraacetic acid
EFE	Ethylene-forming enzyme
EPS	Extracellular polymeric substances
EYFP/eYFP	Enhanced yellow fluorescent protein
FBA	Flux balance analysis
FbFP	Flavin mononucleotide based fluorescent protein
FI	Forward inner
FMN	Flavin mononucleotide
FO	Forward outer
FSC	Forward scatter
F_v/F_m	Variable fluorescence / Maximum fluorescence
FW	Fresh weight
G-3P	Glycerol-3-phosphate
GB	Glycine betaine
gDNA	Genomic DNA
GDP-mannose	Guanosine diphosphate mannose
GFP	Green fluorescent protein
GG	Glucosylglycerol
GghA	Glucosylglycerol hydrolase A
GgpP	Glucosylglycerol-phosphate phosphatase
GgpS	Glucosylglycerol-phosphate synthase
Glc	Glucose
Glc-1P	Glucose-1-phosphate
GOE	Great Oxidation Event
GOI	Gene of interest
GSMT	Glycine-sarcosine-N-methyltransferase
HR	Homologous recombination
HRP	Horseradish peroxidase
HSP	Heat shock response protein
HT-GSM	High-throughput genome scale metabolic
IgG	Immunoglobulin G

IOMA	Integrative omics-metabolic analysis
IPTG	Isopropyl β-D-1-thiogalactopyranoside
IsaR1	Iron-stress activated RNA 1
kb	Kilo base pairs
kDa	Kilo Daltons
KEGG	Kyoto encyclopedia of genes and genomes
Km	Kanamycin
LB	Luria Broth
LED	Light-emitting diodes
M	Molecular marker
Ma	*Methylomicrobium alcaliphilum*
Mb	Mega base pairs
met	Methionine
metX	S-adenosyl-methionine synthase
MgsD	Mannosyl-3-phosphoglycerate synthase / phosphatase
MIQE	Minimum information for publication of quantitative real-time PCR experiments
MoClo	Modular cloning system
MOMA	Minimization of metabolic adjustment
MpgP	Mannosyl-3-phosphoglycerate phosphatase
MpgS	Mannosyl-3-phosphoglycerate synthase
mRNA	Messenger RNA
MW	Molecular weight
N.A.	Not available / not applicable
n.s.	Not significant
NAD	Nicotinamide adenine dinucleotide
NADP	Nicotinamide adenine dinucleotide phosphate
ND	Not detected
NIS	Nuclease/nuclease inhibitor system
NMR	Nuclear magnetic resonance
NOE	Neoproterozoic Oxidation Event
NTC	No template control
OCD	Oxygen consuming device
OD	Optical density
OmpC	Outer membrane porin C
OmpF	Outer membrane porin F
ORF	Open reading frame
PAR	Photosynthetically active radiation
PBR	PhotoBioReactor
PCC	Pasteur culture collection
PCI	Peripheral component interconnect

PCR	Polymerase chain reaction
PHA	Polyhydroxyalkanoate
PHB	Polyhydroxybutyrate
P_i	Inorganic phosphate
PP	Polymer polypropylene
PSI	Photosystem I
PSII	Photosystem II
PVC	Polyvinyl chloride
PVDF	Polyvinylidene fluoride
RBS	Ribosome binding site
RI	Reverse inner
RNA	Ribonucleic acid
RNase	Ribonuclease
RO	Reverse outer
rpm	Revolutions per minute
RPS	Released polysaccharides
rRNA	Ribosomal RNA
RT	Room temperature
RT-PCR	Reverse transcription PCR
RT-qPCR	Reverse transcription quantitative PCR
RuBisCO	Ribulose-1,5-bisphosphate carboxylase-oxygenase
SAH	S-adenosyl-homocysteine
SAM	S-adenosylmethionine
SB	Synthetic biology
SBGN	Systems biology graphical notation
SBML	System biology markup language
SCX	Strong cation exchange
SD sequence	Shine-Dalgarno sequence
SDS-PAGE	Sodium dodecyl sulfate-polyacrylamide gel electrophoresis
SEM	Standard error of the mean
SEVA	Standard european vector architecture
sgRNA	Single-guide RNA
SigF	Sigma factor F
Sm	Streptomycin
SNPs	Single-nucleotide polymorphisms
Sp	Spectinomycin
Sp.	Species
Spp	Sucrose-phosphate phosphatase
Sps	Sucrose-phosphate synthase
SSC	Side scatter
ssrA	Small stable RNA A

Succ	Succinate
SyInv	*Synechocystis* invertase
T_a	Annealing temperature
tacrRNA	Trans-activating crRNA
TAE	Tris-acetate-EDTA
TALENs	Transcription activator-like effector nucleases
taRNA	*Trans*-activating RNA
TCA cycle	Tricarboxylic acid cycle
Ter	Trans-enoyl-CoA reductase
Tm	Melting temperature
T_{mix}	Mixing time
UDP	Uridine diphosphate
UTR	Untranslated region
U-tract	Uracil-rich tract
UV	Ultraviolet
Vol/vol	Volume/volume
WholeCell KB	WholeCell Knowledge Base
WT	Wild-type
Wt/vol	Weight/volume
YFP	Yellow fluorescent protein
ZFNs	Zinc fingers

Abstract

Cyanobacteria are photoautotrophic organisms with minimal nutritional requirements and high metabolic plasticity that use sunlight and CO_2 as energy and carbon sources, respectively. The unicellular *Synechocystis* sp. PCC 6803 was the first photosynthetic organism to have its genome sequenced and rapidly became the best studied cyanobacterium. However, to be used as an efficient and robust photoautotrophic chassis it requires a customized and well-characterized synthetic biology toolbox. The availability of regulatory elements and vectors is crucial for the sustainable production of added-value compounds by *Synechocystis*. In this context, compatible solutes, that are organic molecules involved in the halo and thermotolerance mechanisms in several organisms, emerge as a promising choice due to their stabilizing, protecting and moisturizing properties, that make them valuable to the cosmetics, pharmaceutical and biomedical industries.

In this study, a comprehensive approach was followed envisaging the production of heterologous compatible solutes using *Synechocystis* / *Synechocystis*-based chassis. For this purpose, the molecular toolbox for this unicellular cyanobacterium was expanded, customized chassis were generated, and synthetic devices were assembled and introduced into the chassis. Initially, fourteen heterologous or redesigned promoters were characterized exhibiting a wide range of activities varying from 0.13- to 41-fold compared with the cyanobacterial reference promoter P_{rnpB}. From this set of promoters, three of them could be efficiently repressed / derepressed using suitable inducers. In addition, three self-replicative vectors from the SEVA repository (Standard European Vector Architecture) were validated to be used in *Synechocystis*. The presence of the plasmids did not lead an evident phenotype or hindered *Synechocystis* growth, with most of the cells being able to maintain the plasmid even in the absence of selective pressure, for at least two weeks. The functionality of the developed toolbox was firstly demonstrated by using some of the tools to restore the production of the native compatible solute glucosylglycerol in a *Synechocystis* deficient mutant, Δ*ggpS*. Subsequently, an updated version of the *Synechocystis* genome-scale metabolic model *i*Syn811 was used to simulate production rates of compatible solutes. Regarding heterologous compatible solutes, the analysis showed that the maximum production rate was obtained for glycine betaine, followed by (hydroxy)ectoine and mannosylglycerate. Therefore, a synthetic device aiming at producing glycine betaine was designed, assembled and implemented into *Synechocystis* wild-type and mutants deficient in the synthesis of native compatible solutes (glucosylglycerol Δ*ggpS* or both sucrose and glucosylglycerol Δ*sps*Δ*ggpS*). These mutants were generated to avoid redundancy and to redirect metabolic fluxes towards the heterologous compounds. Their

characterization showed that they accumulate glycogen as the main carbon storage compound but can redirect carbon flux towards the production of other carbon-based compounds, namely extracellular polymeric substances and compatible solutes, as a mechanism to survive under saline conditions. Glycine betaine was detected in all the mutants harboring the synthetic device (WT, Δ*ggpS* and Δ*sps*Δ*ggpS*), reaching 64.29 µmol/gDW in the Δ*ggpS* mutant grown in 3% NaCl, after four days. In addition, the production of glycine betaine in this mutant led to a significant growth improvement and supported its survival under 5% NaCl. Furthermore, with the aim of producing other heterologous compatible solutes, two constructs were designed to produce (hydroxy)ectoine, and one synthetic device envisaging the production of mannosylglycerate was assembled and implemented into *Synechocystis* wild-type and Δ*ggpS* chassis. Preliminary studies showed that although the *mgsD* gene was transcribed, no mannosylglycerate could be detected, maybe due to the small culture volumes utilized.
Overall, this work contributed to expand the synthetic toolbox for the model cyanobacterium *Synechocystis*, allowed an insight into the key players responsible for the survival of *Synechocystis* under saline conditions, and provided an important stepping-stone to produce glycine betaine or other relevant compatible solutes using *Synechocystis* / *Synechocystis*-based chassis.

Keywords: compatible solutes, cyanobacteria, glucosylglycerol, glycine betaine, promoters, *Synechocystis*, sucrose, synthetic biology, synthetic biology toolbox.

Resumo

As cianobactérias são organismos fotoautotróficos com requisitos nutricionais mínimos e alta plasticidade metabólica que utilizam respetivamente a luz solar e o CO_2 como fontes de energia e carbono. O genoma da cianobactéria unicelular *Synechocystis* sp. PCC 6803 foi o primeiro a ser sequenciado de entre os organismos fotossintéticos e isto fez com que rapidamente se tornasse a cianobactéria mais bem estudada. Contudo para ser usada como um *chassi* fotoautotrófico eficiente e robusto é necessário um conjunto de ferramentas de biologia sintética adequadas e bem caracterizadas. Neste contexto, a disponibilidade de elementos regulatórios e vetores é crucial para a produção sustentável de compostos de valor acrescentado por *Synechocystis* ou *chassis* derivados de *Synechocystis*. Os solutos compatíveis (moléculas orgânicas envolvidas nos mecanismos de halo e termotolerância em diversos organismos, incluindo cianobactérias) surgem como uma escolha promissora devido às suas propriedades estabilizadoras, protetoras e hidratantes, de grande interesse para as indústrias cosmética, farmacêutica e biomédica.

Neste trabalho, foi adotada uma abordagem abrangente com vista à produção de solutos compatíveis heterólogos usando *Synechocystis* e *chassis* derivados de *Synechocystis*. Com este propósito expandimos a caixa de ferramentas moleculares disponível para esta cianobactéria, gerámos *chassis* adaptados ao fim em vista e construímos dispositivos sintéticos que foram posteriormente implementados nesses mesmos *chassis*. Inicialmente, caracterizámos catorze promotores heterólogos ou redesenhados que apresentaram uma gama de força variável entre 0,13 e 41 vezes em relação ao promotor de referência das cianobactérias - P_{rnpB}. Deste conjunto de promotores, três podem ser eficazmente reprimidos / desreprimidos usando os indutores adequados. Avaliámos, também, a utilização de três vetores replicativos do repositório SEVA (*Standard European Vector Architecture*). A presença destes plasmídeos não originou nenhum fenótipo evidente nem alterou a taxa de crescimento de *Synechocystis*, sendo que a maioria das células manteve o plasmídeo mesmo na ausência de pressão seletiva, durante pelo menos duas semanas. A funcionalidade da caixa de ferramentas desenvolvida neste trabalho foi demonstrada restituindo a produção do soluto compatível glucosilglicerol num mutante que não sintetiza este composto devido à ausência de uma das enzimas da via - Δ*ggpS*. Posteriormente, utilizámos uma versão atualizada do modelo metabólico de *Synechocystis* - *i*Syn811 - para simular taxas de produção de solutos compatíveis. No que diz respeito aos solutos heterólogos, a taxa mais elevada foi obtida para a glicina betaína, seguida da (hidroxi)ectoína e do manosilglicerato. Tendo em conta este facto, desenhámos e construímos um módulo sintético para a produção de glicina betaína, que foi posteriormente introduzido na estirpe selvagem de *Synechocystis* e nos *chassis* previamente gerados: mutantes deficientes na síntese dos solutos compatíveis nativos,

nomeadamente glucosilglicerol (Δ*ggpS*) ou sacarose e glucosilglicerol (Δ*sps*Δ*ggpS*). Estes mutantes foram concebidos de forma a evitar redundância e redirecionar os fluxos metabólicos para a produção dos solutos heterólogos. A sua caracterização mostrou que acumulam glicogénio, como o principal composto de reserva de carbono. Podem, contudo, como um mecanismo de sobrevivência em condições salinas, redirecionar o fluxo de carbono para a produção de outros compostos, nomeadamente substâncias poliméricas extracelulares e solutos compatíveis. A glicina betaína foi detetada em todos as estirpes onde foi introduzido o módulo sintético (WT, Δ*ggpS* e Δ*sps*Δ*ggpS*), tendo atingido 64.3 µmol/g peso seco no mutante Δ*ggpS* crescido em 3% de NaCl, após quatro dias de cultura. Para além disso, a produção de glicina betaína aumentou significativamente o crescimento deste mutante e permitiu a sua sobrevivência em 5% de NaCl. Com o objetivo de produzir outros solutos compatíveis heterólogos, desenhámos ainda duas construções para a produção de (hidroxi)ectoína e construímos um módulo sintético com vista à produção de manosilglicerato. Este último foi introduzido na estirpe selvagem de *Synechocystis* e no mutante Δ*ggpS.* Estudos preliminares demonstraram que o gene *mgsD* é transcrito, contudo não foi possível detetar a produção de manosilglicerato provavelmente devido ao reduzido volume de cultura utilizado.

Em suma, este trabalho contribuiu para expandir o conjunto de ferramentas sintéticas para a cianobactéria modelo *Synechocystis*, elucidar os mecanismos responsáveis pela sobrevivência de *Synechocystis* em condições salinas e avançar com a produção de glicina betaína ou outros solutos compatíveis de interesse em *Synechocystis* / *chassis* derivados de *Synechocystis.*

Palavras-chave: biologia sintética, caixa de ferramentas de biologia sintética, cianobactérias, glicina betaína, glucosilglicerol, promotores, sacarose, solutos compatíveis, *Synechocystis*.

Chapter I. General introduction

1.1 Cyanobacteria

Phylum Cyanobacteria: A phylogenetic lineage of organisms in the domain bacteria able to carry out oxygenic photosynthesis with water as an electron donor and to reduce carbon dioxide as a source of carbon, or those secondarily evolved from such organisms.

Synonyms: blue–green algae, cyanophyta, oxyphotobacteria, oxychlorobacteria, myxophyceae.

From Garcia-Pichel *et al.* (2020).

1.1.1 Evolutionary and ecological importance

Cyanobacteria, previously known as blue-green algae, occupy a pioneered position since they are among the earliest inhabitants of the planet, being the subject of many evolutionary, biological and ecological studies. Although there is still considerable controversy about the exact time cyanobacteria appeared on Earth, there is no doubt that they are extremely ancient organisms. There is evidence that oxygenic photosynthesis occurred even in the Archean era, > 3.5 billion years (Byr) ago (Knoll, 1980; Olson, 2006; Rosing & Frei, 2004), almost since the origin of the Earth (~ 4 Byr). In the Proterozoic era (2.5 and 0.54 Byr), termed as “the age of blue-green algae”, the atmosphere turned from anoxic to oxygenated due to the emergence of organisms capable of oxygenic photosynthesis (Schopf, 2000). For this reason, the majority of cyanobacterial diversity evolved after the Great Oxidation Event (GOE) (Sánchez-Baracaldo, 2015) (Figure 1). The second major oxygenation event known as Neoproterozoic Oxidation Event (NOE) (0.8 Byr) significantly increased atmospheric O_2 concentrations similar to those found in the atmosphere today (Sánchez-Baracaldo & Cardona, 2020; Scott *et al.*, 2008). The NOE has been linked to the origin of animals and, more recently, to the emergence of marine planktonic groups (Brocks *et al.*, 2017) (Figure 1). Apart from the oxygenation, cyanobacteria also influenced the advancements of life on Earth by shaping themselves as the ancestors of plastids (Sergeev *et al.*, 2002). A fateful endosymbiosis between a cyanobacteria and a heterotrophic unicellular eukaryote (Parfrey *et al.*, 2011) turned out to be one of the most transformative events in life’s history – the emergence of the first photosynthetic eukaryotes (Archibald, 2015). These plastids further evolved into semiautonomous organelles (chloroplasts), giving rise to the remarkable evolution and diversity of algae and land plants (Maréchal, 2018). Cyanobacteria continue to affect life on Earth today as the major oxygen producers on this planet. As primary producers and efficient fixers of atmospheric nitrogen, cyanobacteria play a significant role in Earth’s carbon and nitrogen cycles respectively (Karl *et al.*, 2002). Cyanobacteria perform more than 35% of global CO_2 fixation, despite the fact that they comprise less than 0.2% of

photosynthetic biomass (Falkow *et al.*, 2006). Plants fix CO_2 into building blocks for growth by performing photosynthesis in chloroplasts, while cyanobacteria fix carbon in a special compartment called carboxysome. Even though carbon fixation in chloroplasts and carboxysomes depend upon the same class of enzymes called RuBisCO (ribulose-1,5-bisphosphate carboxylase-oxygenase), the process is two times more efficient in carboxysome than in chloroplast (Gough, 2020; NREL, 2020). Their unprecedented ability of CO_2 fixation allows cyanobacteria to make a significant contribution to global carbon fixation (Fang *et al.*, 2018), alleviating climate change.

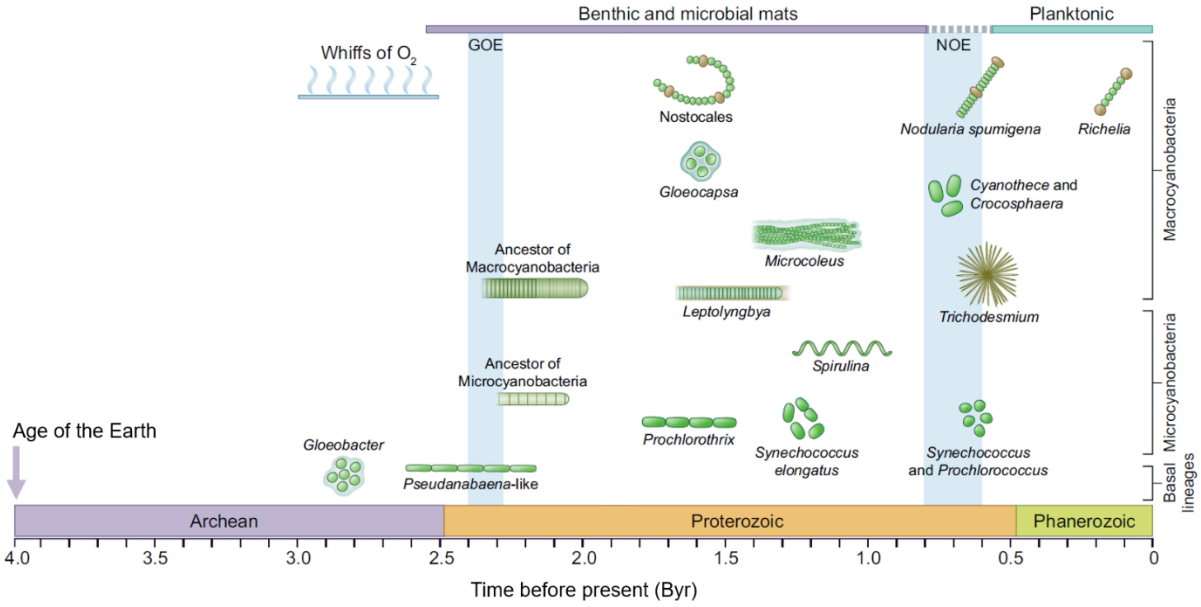

Figure 1. Evolutionary course of cyanobacterial lineages. Taxa with smaller cell diameter (basal lineages and Microcyanobacteria) are shown at the bottom and larger cell diameter (Macrocyanobacteria) at the top. Not to scale. GOE, Great Oxidation Event; NOE, Neoproterozoic Oxidation Event; Byr, Billion years. Adapted from Sánchez-Baracaldo and Cardona (2020).

1.1.2 Biodiversity and environmental adaptation

The long evolutionary process of cyanobacteria gave rise to the biodiversity we find today. Within prokaryotic groups, cyanobacteria are one of the most morphologically diverse groups, ranging from unicellular to colonial or filamentous (Castenholz, 2015; Shih *et al.*, 2013). The earlier cyanobacteria forms were unicellular with small cell diameters (*Gloeobacter*, *Synechococcus*) (Larsson *et al.*, 2011). Filamentous forms appeared shortly afterwards (*Pseudanabaena* lineages) (Schirrmeister *et al.*, 2011). The origin of multicellular forms of cyanobacteria increased the biologic complexity, size and diversity after the GOE, including the recently described groups Microcyanobacteria (cell diameters ranging from 1 to 2 µm) and Macrocyanobacteria (cell diameters larger than 3 µm and up to 50 µm) (Sánchez-Baracaldo, 2015; Schirrmeister *et al.*, 2013) (Figure 1). Most of the strains can

divide by binary fission while others can undergo multiple divisions. This is the case of cyanobacteria that form a large number of small daughter cells named baeocytes that subsequently grow out to normal-sized cells (Castenholz, 2015). Some filamentous strains are capable of cell differentiation to fix nitrogen (heterocysts), to survive under adverse environmental conditions (akinetes) or to move and infect plants (hormogonia) (Adams & Duggan, 2012; Castenholz, 2015). Moreover, there are cyanobacteria that exhibit branching trichomes, constituting what may be the most advanced type of morphological structure attained in the prokaryotic world (Castenholz, 2015). The notable biodiversity of cyanobacteria is also reflected in their genomes, the sizes of which vary from 1.4 to 9 Mb (Larsson *et al.*, 2011).

The biodiversity and the high plasticity allow cyanobacteria to colonize a large variety of habitats. The vast majority of cyanobacteria is found in terrestrial, freshwater and marine environments. However, they can inhabit the harshest environments such as drylands, glaciers, hot springs and hypersaline environments (Whitton, 2012). This ubiquitous feature is a consequence of the great capacity of cyanobacteria to adapt to any place. Among a variety of adaptive strategies, cyanobacteria have the remarkable ability to move to areas where conditions are most favourable, in response to a light or chemical signals/stimuli (phototaxis or chemotaxis, respectively) (Schuergers *et al.*, 2017). Some cyanobacteria are also capable of changing the ratio of pigments in response to the light spectrum (chromatic adaptation) (Castenholz, 2015). Moreover, cyanobacteria can produce compounds such as secondary metabolites, extracellular polymeric substances (EPS) or compatible solutes to cope with extreme environmental conditions (De Philippis *et al.*, 1998; Klähn & Hagemann, 2011; Kultschar & Llewellyn, 2018). Besides the ecological role of these compounds, they also have high biotechnological potential for industrial production.

1.1.3 Cyanobacteria as a source of compounds with biotechnological interest

The overwhelming available knowledge on the diversity, physiology and ecology of cyanobacteria allows for the exploitation of their applications in biotechnology. In the last few years, cyanobacteria have gained significant attention as a prolific source of *e.g.* bioactive compounds, biofuels, biopolymers, pigments, vitamins, and whole-food supplements (Figure 2). Cyanobacteria have been identified as a rich source of bioactive compounds. Isolated compounds belong to groups of lipopeptides, polyketides, amides, alkaloids, fatty acids and indoles (Abed *et al.*, 2009; Rao *et al.*, 2015). The range of biological properties of these secondary metabolites includes antibacterial, antifungal, antialgal, antiprotozoal, antiviral, molluscicidal, anti-inflammatory, cytotoxic, antitumor and antibiotic activities (Abed *et al.*, 2009; Niedermeyer, 2015; Nunnery *et al.*, 2010; Sharma *et*

al., 2013). The increased concern regarding limited petroleum-based fuel supplies and their contribution to atmospheric CO_2 levels, led to the utmost emergence of bioenergy production. In this context, cyanobacteria has been investigated for the sustainable production of different biofuels including biohydrogen, biodiesel, bioethanol and biomethane (Parmar *et al.*, 2011). Some cyanobacteria have also been found to accumulate polyhydroxyalkanoate (PHA), which is a biodegradable polymer that can replace petroleum-based plastics. Among PHA, the most important material is polyhydroxybutyrate (PHB). This biopolymer can replace the commodity polymer polypropylene (PP), being a promising bioplastic candidate in the present world to address rising environmental concerns (Markl *et al.*, 2018; Yashavanth *et al.*, 2021). Currently, PHB has been used in medical implants, bioremediation, tissue engineering, drug delivery, printing and photographic materials (Abed *et al.*, 2009; Sharma *et al.*, 2013; Yashavanth *et al.*, 2021). Cyanophycin is another biopolymer produced by cyanobacteria, that is constituted by two amino acids (aspartate and arginine) and serves as a nitrogen and carbon storage compound. It has attracted increasing attention due to its vast applicability in the fields of food, medicine, cosmetics, nutrition, and agriculture (Du *et al.*, 2019). Moreover, many cyanobacteria produce extracellular polymeric substances (EPS), mainly composed of polysaccharides, that can remain attached to cell surface as sheaths, capsules or slime (capsular polysaccharides - CPS) or be released into the surrounding environment (released polysaccharides - RPS) (Pereira *et al.*, 2009). The main areas for the possible application of cyanobacterial EPS are bioremediation, food, cosmetics, biomedicine, tissue engineering and pharmaceutics (Singh *et al.*, 2019). Recently, the release of extracellular vesicles by cyanobacteria has been explored and may constitute a target for packaging products of interest, highlighting potential application in the field of biomedicine (Lima *et al.*, 2020). Cyanobacteria pigments such as chlorophyll *a* (green), carotenoids (orange) and phycobiliproteins - phycocyanin (blue), allophycocyanin (blue) and phycoerythrin (red) - are historically used as food and cosmetic colorants, fluorescent probes, and have health potential as nutraceutical and pharmaceutical compounds due to the strong antioxidant, anti-inflammatory, neuroprotective and hepatoprotective effects (Castenholz, 2015; Mazard *et al.*, 2016; Raja *et al.*, 2016; Sharma *et al.*, 2013). Among pigments, cyanobacteria also synthesize “sunscreen” compounds such as mycosporines and scytonemin to protect themselves from UV exposure. Pharmacologically, they are known for their anti-inflammatory and antiproliferative activities and have huge potential to be used in sunscreen products in the cosmetic industry (Raja *et al.*, 2016). Some cyanobacteria also constitute potential sources for large-scale production of vitamins, such as vitamin B and E. For example, *Spirulina* sp. (*Arthrospira*) is considered to be the richest whole-food source of vitamin B12 (Watanabe *et al.*, 2002), having nowadays a considerable popularity in the health sector, food industry

and aquaculture (Soni *et al.*, 2017). Furthermore, production of compatible solutes by cyanobacteria has gained commercial interest due to the extent biotechnological applications (see more in detail in section 1.3 – Compatible solutes).

Figure 2. Schematic representation of some of the biotechnological relevant compounds produced by cyanobacteria.

The potential of cyanobacteria to produce compounds of interest is unlimited. Therefore, cyanobacteria have emerged as promising organisms to become “low-cost” cell factories, mainly due to their simple nutritional requirements, metabolic plasticity and obviously to the fact that they can utilize renewable feedstock (CO_2), water (electron source) and sunlight (energy source) to produce value-added compounds (Branco Dos Santos *et al.*, 2014; Knoot *et al.*, 2018). In recent years, a great effort has been made to maximize and customize the production of a variety of compounds. This has been addressed by optimizing industrial processes to develop more feasible cyanobacterial manufacturing in large-scale but also by genetic/metabolic engineering of cyanobacterial cells (Abed *et al.*, 2009; Luan & Lu, 2018). In this context, a significant effort is being made to expand and refine molecular and synthetic biology tools for the genetic manipulation of cyanobacteria, namely *Nostoc* sp. PCC 7120, *Synechococcus elongatus* PCC 7942, and particularly *Synechocystis* sp.

PCC 6803 (Carroll *et al.*, 2018; Hagemann & Hess, 2018; Luan & Lu, 2018; Pattharaprachayakul *et al.*, 2020; Santos-Merino *et al.*, 2019; Xia *et al.*, 2019).

1.2 Synthetic biology

Synthetic biology is the engineering of biology: the synthesis of complex, biologically based (or inspired) systems, which display functions that do not exist in nature. This engineering perspective may be applied at all levels of the hierarchy of biological structures - from individual molecules to whole cells, tissues and organisms. In essence, synthetic biology will enable the design of 'biological systems' in a rational and systematic way.

From Serrano *et al.* (2005).

1.2.1 Synthetic biology of cyanobacteria

This subject is presented as Chapter II, since it is a book chapter in which E. A. Ferreira is co-author ("Synthetic biology of cyanobacteria"; in: Kourist, R., & Schmidt, S. (ed.) of book The Autotrophic Biorefinery: Raw Materials from Biotechnology, GmbH, Berlin/Boston: De Gruyter, 2021, pp. 131-172).

1.3 Compatible solutes

A compatible solute is a substance compatible with the cellular metabolism that accumulates in the cytoplasm to balance external osmotic pressure. This accumulation can be due either to transport from the medium or to de novo *synthesis and helps maintaining turgor pressure, cell volume, and concentration of electrolytes, all needed for cell viability and proliferation.*

Synonyms: osmolytes, organic osmotic solutes, chemical chaperones.

From Antón (2011).

1.3.1 Main features and physiological roles

Living organisms have the ability to adapt to changes in the external environment to survive under harsh conditions. Under high salt concentrations, water usually moves out of the microbial cells along the osmotic gradient causing dehydration of the cytoplasm (turgor pressure) (Ladas & Papageorgiou, 2000). Therefore, to survive in these conditions, microorganisms have two distinct osmoadaptation mechanisms. Halophilic Archaea primarily use a "salt-in" strategy where osmotic balance is achieved by accumulating ions, mainly K^+ and Cl^-, and by adapting the entire intracellular enzymatic machinery (Galinski & Trüper, 1994). In contrast, most halophilic Bacteria and Eukarya, largely use a "salt-out"

strategy, which involves the active export of Na^+ and Cl^- as well as the intracellular accumulation of compatible solutes (Galinski, 1995). The accumulation of these compounds can be achieved by the uptake of solutes from the environment or by *de novo* synthesis. The first approach is energetically more favourable than the *de novo* synthesis and yields a much faster response (Galinski, 1995). However, when compatible solutes are not freely available externally or if those fail to meet an organism's biochemical requirements, microorganisms synthesize their own (da Costa *et al.*, 1998). Microorganisms that accumulate organic solutes can more easily adjust the osmotic pressure to salinity fluctuations than organisms that use the "salt-in" strategy. In some organisms, a combination of adaptive mechanisms may operate (DasSarma & DasSarma, 2015; Hagemann, 2011). The cellular concentration of compatible solutes is regulated according to the external salt conditions (Hagemann, 2013). Upon salt downshock, excess of compatible solutes can be excreted via mechanosensitive channels or converted, inside the cells, to osmotically inactive forms. Inorganic ions can be transiently accumulated following sudden increases of salinity, to be later replaced by newly synthesized organic solutes (Wood *et al.*, 2001). The term compatible solute was first used in 1972 (Brown & Simpson, 1972) and was later defined as a solute that, at high concentration, allows all essential cell processes to function effectively (Brown, 1990). They are low molecular mass organic molecules, generally uncharged or zwitterionic compounds with a high solubility (Poolman & Glaasker, 1998). Structurally they can be assigned to different classes, including sugars (sucrose, trehalose, mannosylglycerate), polyols (glycerol, sorbitol), heterosides [glucosylglycerol, glucosylglycerate, floridoside (galactosylglycerol)], amino acids (proline, glutamate) and amino acid derivatives (ectoine, hydroxyectoine, glycine betaine, glutamate betaine, homoserine betaine) (Hagemann, 2011; Hagemann & Pade, 2015; Kirsch *et al.*, 2019; Klähn *et al.*, 2010; Mackay *et al.*, 1984; Pade *et al.*, 2012; Pade *et al.*, 2016) (Figure 3A). In many extremophiles, compatible solutes are accumulated not only in response to increased salt concentrations, but also as a response to other environmental stresses such as temperature or desiccation (Eleutherio *et al.*, 1993; Potts, 1994). In addition to the osmotic equilibrium, compatible solutes can also exhibit direct protective effects towards nucleic acids, enzymes, proteins, membranes, cells and tissues (Jadhav *et al.*, 2018). The protective effect often explains why the accumulation of low amounts of compatible solutes (at concentrations not making big contributions to the intracellular osmotic potential) results in significant increase of salt or drought tolerance (Hagemann, 2013). The action of compatible solutes is currently best explained by the solute exclusion hypothesis (Galinski, 1995; Jadhav *et al.*, 2018). According to this model, compatible solutes do not directly interact with macromolecules, such as proteins and/or membranes, during their protective action. Instead, they are preferentially excluded from the surface of the macromolecule,

directing the remaining free water to the vicinity of the macromolecule surface, thereby retaining its hydration shell, favouring the folding and preventing denaturation. Furthermore, the accumulation of compatible solutes aids in stabilizing proteins by decreasing the accessible volume, which favours the more compact folded state (Minton, 2000).

1.3.2 Compatible solutes in cyanobacteria

Within cyanobacteria, there is a close correlation between the compatible solutes used to compensate osmotic potential and the natural habitat of the organism. Freshwater strains, resisting up to 3.5% NaCl (0.6 M, equivalent to seawater conditions), accumulate the sugars trehalose or sucrose. The moderately halotolerant strains can survive in environments with NaCl up to 10% (1.7 M) by accumulating glucosylglycerate or glucosylglycerol, while glutamate betaine and glycine betaine were identified as compatible solutes in halophilic cyanobacteria that can tolerate salt concentrations up to saturation (Hagemann, 2011; Mackay *et al.*, 1984; Reed *et al.*, 1986) (Figure 3B).

A Classes of compatible solutes

Sugars	Polyols	Heterosides	Amino acids and derivatives	
Sucrose	Glycerol	Glucosylglycerol	Proline	Ectoine
Trehalose	Sorbitol	Floridoside	Glutamate	Glycine betaine

B Compatible solutes in cyanobacteria

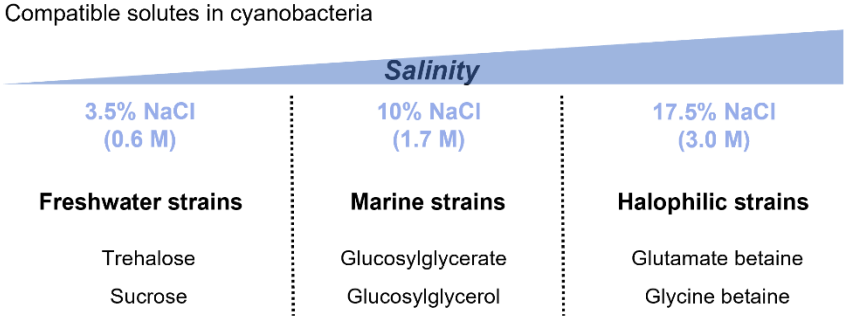

Figure 3. Classes of compatible solutes found in microorganisms (A) and the major compatible solutes produced by cyanobacteria in habitats with different salinity conditions. Adapted from Kirsch *et al.* (2019) and Hagemann (2011).

In contrast to heterotrophic bacteria, that often uptake compatible solutes, photoautotrophic organisms such as cyanobacteria prefer the *de novo* synthesis (Klähn & Hagemann, 2011). Among cyanobacteria, *Synechocystis* sp. PCC 6803 has become a popular model organism to study molecular mechanisms of osmotic adaptation based on extrusion of ions (Na^+, Cl^-) and uptake and/or synthesis of compatible solutes, as well as the bioenergetics basis of salt adaptation (Hagemann, 2013). Although *Synechocystis* sp. PCC 6803 is a freshwater strain, it is a moderately halotolerant organism that accumulates glucosylglycerol and sucrose as its main compatible solutes (Reed & Stewart, 1985). Sucrose is synthesized in a two-step reaction by the enzymes sucrose-phosphate synthase (Sps) and sucrose-phosphate phosphatase (Spp). The Sps catalyses the reaction of UDP-glucose and fructose 6-phosphate to sucrose 6-phosphate. This intermediate is dephosphorylated by Spp, forming sucrose (Hagemann & Marin, 1999; Lunn, 2002) (Figure 4). The biosynthetic pathway of glucosylglycerol involves the enzymes glucosylglycerol-phosphate synthase (GgpS) and glucosylglycerol-phosphate phosphatase (GgpP). GgpS is a glucosyltransferase that catalyses the synthesis of glucosylglycerol 3-phosphate from glycerol 3-phosphate and ADP-glucose. GgpP causes dephosphorylation of the intermediate and glucosylglycerol is released (Hagemann & Erdmann, 1994; Hagemann *et al.*, 1997; Marin *et al.*, 1998) (Figure 4). The synthesis and accumulation of both compatible solutes in *Synechocystis* is salt induced at both transcriptional and biochemical levels. In the case of sucrose, the increase in *sps* transcription occurs within minutes after a salt shock (Marin *et al.*, 2004). Recently, a possible negative regulation of *sps* by the response regulator 39 (Rre39) was identified (Song *et al.*, 2017). Furthermore, the quick accumulation of this sugar in salt-stressed cells is accompanied by a rapid activation of enzymes (Du *et al.*, 2013). However, the factors involved in the transcriptional and biochemical regulation are still largely unknown. In the case of glucosylglycerol, the increase in salinity induces *ggpS* transcription (Marin *et al.*, 2004). The transcription regulation involves several components: alternative sigma factors (*e.g.* SigF), a transcription factor (LexA) and a DNA-binding repressor protein (GgpR) (Huckauf *et al.*, 2000; Kizawa *et al.*, 2016; Klähn *et al.*, 2010; Marin *et al.*, 2002). Moreover, *ggpS* was also shown to be post-transcriptionally regulated by a small regulatory RNA, the iron-stress activated RNA 1 (IsaR1) (Rübsam *et al.*, 2018). In terms of biochemical regulation, GgpS is enzymatically inactivated by an electrostatic binding to nucleic acids (Novak *et al.*, 2011). After salt shock, inorganic ions flow into the cells and disrupt this bond, resulting in GgpS activation (Hagemann & Erdmann, 1994). Unlike the accumulation of compatible solutes upon increasing salinity, little is known about the cellular response of *Synechocystis* to a decreasing salt concentration. To prevent the cell from bursting, the compatible solutes intracellularly accumulated are released from the cell or enzymatically degraded by an invertase (SyInv),

in the case of sucrose, or by the glucosylglycerol hydrolase A (GghA), in the case of glucosylglycerol (Kirsch *et al.*, 2018; Kirsch *et al.*, 2017).

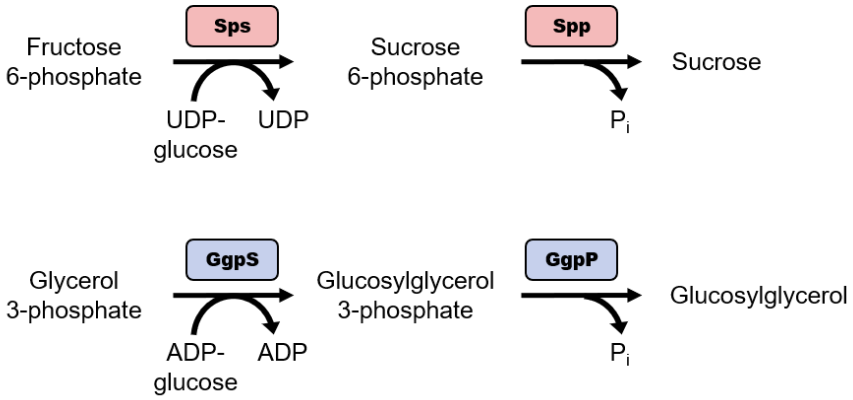

Figure 4. Biosynthetic pathways of sucrose and glucosylglycerol in *Synechocystis* sp. PCC 6803. Sps - sucrose-phosphate synthase; Spp - sucrose-phosphate phosphatase; GgpS - glucosylglycerol-phosphate synthase; GgpP - glucosylglycerol-phosphate phosphatase.

1.3.3 Biotechnological applications

The interesting properties of compatible solutes make them suitable for a variety of biotechnological applications. Besides their contribution to the osmotic balance, compatible solutes have an important role as stabilizers of biomolecules (enzymes, DNA, membranes), and whole cells (Margesin & Schinner, 2001) and can act as chemical chaperones for protein folding (Roberts, 2005). In this context, glycerol, sorbitol, hydroxyectoine and glycine betaine can increase the production of functional, stable and correctly folded recombinant proteins in *E. coli* (Barth *et al.*, 2000). Other studies have shown that ectoine, glycine betaine and trehalose inhibit insulin amyloid formation and; ectoine and hydroxyectoine inhibit aggregation and neurotoxicity of β-amyloid, constituting potential therapeutic compounds for the treatment of diabetes and Alzheimer's disease, respectively (Arora *et al.*, 2004; Kanapathipillai *et al.*, 2005). Mannosylglycerate showed to be a good stabilizer of proteins *in vivo* using a yeast model of Parkinson's disease (Faria *et al.*, 2013). The experimental effects of compatible solutes on macromolecules have shown that they also confer thermoprotection to proteins. Accumulation of glycine betaine in *E. coli* cells adapted to high salinity conditions showed a huge reduction in protein aggregation during heat shock (Diamant *et al.*, 2001). Mannosylglycerate showed the best performance as a thermoprotectant of enzyme activity *in vitro*, suggesting that it also fulfils a protein thermoprotective function *in vivo* (Borges *et al.*, 2002). In addition to thermoprotection, compatible solutes are also known as cell membranes stabilizers in plants and microorganisms during drought conditions (Hincha & Hagemann, 2004). In fact, the

insertion of genes encoding proteins responsible for the synthesis of compatible solutes allows the generation of stress-resistant transgenic organisms, constituting an advantage for the cultivation of commercially important crops. In particular, the genes related with the synthesis of ectoine, glycine betaine, glucosylglycerol or mannosylglycerate were transferred into *Arabidopsis thaliana* and tobacco plants, grasses and potato (*Solanum tuberosum*), improving their tolerance to salinity, temperature or/and drought (Alia *et al.*, 1998; Holmström *et al.*, 2000; Klähn *et al.*, 2009; Nakayama *et al.*, 2000; Scheller *et al.*, 2012; Sievers *et al.*, 2013). Within the molecular biology field, several compatible solutes, notably glycine betaine and ectoine, can also be used as enhancers for polymerase chain reactions (PCR) and PCR amplifications of GC-rich DNA templates by reducing the DNA melting temperature (Henke *et al.*, 1997; Schnoor *et al.*, 2004), and ectoine and hydroxyectoine can be used to decrease the accessibility of DNA regions to endonucleases (Malin *et al.*, 1999). Glucosylglycerol serves as stabilizer for the storage of enzymes and antibodies (Borges *et al.*, 2002; Luley-Goedl *et al.*, 2010). Glycine betaine and trehalose have been used as cryo-protectants for the freeze-drying of biomolecules and also for long-term preservation of microorganisms (Cleland *et al.*, 2004; Galinski & Tindall, 1992), while ectoine and hydroxyectoine have been identified as effective agents in cryopreservation of mononuclear cells derived from human umbilical cord blood, human endothelial cells or mesenchymal stem cells and erythrocytes (Bissoyi & Pramanik, 2013; El Assal *et al.*, 2014; Sun *et al.*, 2012). Moreover, the anti-inflammatory effect of ectoine suggests a medical oriented application in the future for treating lung inflammation, colitis and for tissue protection in ischemia (Abdel-Aziz *et al.*, 2013; Harishchandra *et al.*, 2011; Pech *et al.*, 2013; Sydlik *et al.*, 2009). Sucrose has also moved into biotechnological focus since it is an attractive nutritive sugar and feedstock (Hagemann & Hess, 2018).

In terms of commercially available products, a wide range of ectoine-based medical devices such as nasal/ear sprays and eye drops, for the treatment of allergic rhinitis, rhinoconjunctivitis, rhinosinusitis, acute pharyngitis and laryngitis, skin inflammatory conditions like atopic dermatitis, dry eye, and dry nose (Dwivedi *et al.*, 2014; Eichel *et al.*, 2013; Heinrich *et al.*, 2007; Marini *et al.*, 2014; Muller *et al.*, 2016) are currently commercialized by the German biotechnology company Bitop AG. From this company, “Ectoin® natural” (ectoine) and “Glycoin® natural” (glucosylglycerol) are multifunctional cosmetic active ingredients with cell protection and anti-aging properties for skin care (Buenger & Driller, 2004; Motitschke *et al.*, 2000). Bitop AG also commercializes what they call “BioStab products”: Ectoin®, Hydroxyectoin and Glucosylglycerol as chemically pure substances to “prevent loss of activity of diagnostic enzymes and antibodies during storage and to optimize PCR”. Furthermore, glycine betaine has been commercialized as “Betafin®” by IFF Nutrition & Biosciences company for animal food supplements to maintain

performance and reduce production costs. “BetaPower® Natural Betaine” from the same company is being commercialized as human dietary supplement to improve physical performance and hydration. Glycine betaine has been used as food supplement due to its proven physiological role as methyl donor that has beneficial stress-mitigating effects (Day & Kempson, 2016; Kumar *et al.*, 2012).

1.4 Main aims

The major aim of this study was to use the photoautotrophic cyanobacterium *Synechocystis* sp. PCC 6803 as a valuable platform/chassis for the production of compatible solutes. For this purpose, we aimed at:

i) Expanding the synthetic toolbox for *Synechocystis* sp. PCC 6803, by characterizing a novel set of promoters and validating replicative vectors (Chapter III);

ii) Generating and characterizing *Synechocystis* sp. PCC 6803 mutants deficient in the synthesis of native compatible solutes (Chapter IV);

iii) Designing and assembling synthetic devices meant for the production of heterologous compatible solutes (Chapters IV and V);

iv) Implementing the synthetic devices into the wild-type and the customized chassis (Chapters IV and V);

v) Evaluating the production of compatible solutes (Chapters IV and V).

1.5 References

Abdel-Aziz, H., Wadie, W., Abdallah, D. M., Lentzen, G., & Khayyal, M. T. (2013). Novel effects of ectoine, a bacteria-derived natural tetrahydropyrimidine, in experimental colitis. *Phytomedicine, 20*(7), 585-591.

Abed, R. M., Dobretsov, S., & Sudesh, K. (2009). Applications of cyanobacteria in biotechnology. *J Appl Microbiol, 106*(1), 1-12.

Adams, D. G., & Duggan, P. S. (2012). Signalling in cyanobacteria–plant symbioses. In B. F. Perotto S. (Ed.), *Signaling and communication in plant symbiosis* Vol. 11, 93-121: Springer.

Alia, Hayashi, H., Sakamoto, A., & Murata, N. (1998). Enhancement of the tolerance of *Arabidopsis* to high temperatures by genetic engineering of the synthesis of glycinebetaine. *Plant J, 16*(2), 155-161.

Antón, J. (2011). Compatible Solute. In M. Gargaud, R. Amils, J. C. Quintanilla, H. J. Cleaves, W. M. Irvine, D. L. Pinti, & M. Viso (Eds.), *Encyclopedia of Astrobiology* 351-352: Springer.

Archibald, J. M. (2015). Genomic perspectives on the birth and spread of plastids. *PNAS, 112*(33), 10147-10153.

Arora, A., Ha, C., & Park, C. B. (2004). Inhibition of insulin amyloid formation by small stress molecules. *FEBS Lett, 564*(1-2), 121-125.

Barth, S., Huhn, M., Matthey, B., Klimka, A., Galinski, E. A., & Engert, A. (2000). Compatible-solute-supported periplasmic expression of functional recombinant proteins under stress conditions. *Appl Environ Microbiol, 66*(4), 1572-1579.

Bissoyi, A., & Pramanik, K. (2013). Effects of non-toxic cryoprotective agents on the viability of cord blood derived MNCs. *Cryo Letters, 34*(5), 453-465.

Borges, N., Ramos, A., Raven, N. D., Sharp, R. J., & Santos, H. (2002). Comparative study of the thermostabilizing properties of mannosylglycerate and other compatible solutes on model enzymes. *Extremophiles, 6*(3), 209-216.

Branco Dos Santos, F., Du, W., & Hellingwerf, K. J. (2014). *Synechocystis*: not just a plug-bug for CO_2, but a green *E. coli*. *Front Bioeng Biotechnol, 2*(36).

Brocks, J. J., Jarrett, A. J., Sirantoine, E., Hallmann, C., Hoshino, Y., & Liyanage, T. (2017). The rise of algae in Cryogenian oceans and the emergence of animals. *Nature, 548*(7669), 578-581.

Brown, A. (1990). *Microbial water stress physiology. Principles and perspectives*: John Wiley & Sons.

Brown, A., & Simpson, J. R. (1972). Water relations of sugar-tolerant yeasts: the role of intracellular polyols. *Microbiol, 72*(3), 589-591.

Buenger, J., & Driller, H. (2004). Ectoin: An effective natural substance to prevent UVA-induced premature photoaging. *Skin Pharmacol Physiol, 17*(5), 232-237.

Carroll, A. L., Case, A. E., Zhang, A., & Atsumi, S. (2018). Metabolic engineering tools in model cyanobacteria. *Metab Eng, 50*, 47-56.

Castenholz, R. W. (2015). General characteristics of the cyanobacteria. In S. D. M.E. Trujillo, P. DeVos, B. Hedlund, P. Kämpfer, F.A. Rainey and W.B. Whitman (Ed.), *Bergey's Manual of Systematics of Archaea and Bacteria* 1-23: John Wiley & Sons, Inc.

Cleland, D., Krader, P., McCree, C., Tang, J., & Emerson, D. (2004). Glycine betaine as a cryoprotectant for prokaryotes. *J Microbiol Methods, 58*, 31-38.

da Costa, M. S., Santos, H., & Galinski, E. A. (1998). An overview of the role and diversity of compatible solutes in *Bacteria* and *Archaea*. In G. Antranikian (Ed.), *Biotechnol Extremophiles* 117-153: Springer, Berlin, Heidelberg.

DasSarma, S., & DasSarma, P. (2015). Halophiles and their enzymes: negativity put to good use. *Curr Opin Microbiol, 25*, 120-126.

Day, C. R., & Kempson, S. A. (2016). Betaine chemistry, roles, and potential use in liver disease. *Biochim Biophys Acta, 1860*, 1098-1106.

De Philippis, R., Margheri, M. C., Materassi, R., & Vincenzini, M. (1998). Potential of unicellular cyanobacteria from saline environments as exopolysaccharide producers. *Appl Environ Microbiol, 64*(3), 1130-1132.

Diamant, S., Eliahu, N., Rosenthal, D., & Goloubinoff, P. (2001). Chemical chaperones regulate molecular chaperones *in vitro* and in cells under combined salt and heat stresses. *J Biol Chem, 276*(43), 39586-39591.

Du, J., Li, L., & Zhou, S. (2019). Microbial production of cyanophycin: From enzymes to biopolymers. *Biotechnol Adv, 37*(7), 107400.

Du, W., Liang, F., Duan, Y., Tan, X., & Lu, X. (2013). Exploring the photosynthetic production capacity of sucrose by cyanobacteria. *Metab Eng, 19*, 17-25.

Dwivedi, M., Brinkkotter, M., Harishchandra, R. K., & Galla, H. J. (2014). Biophysical investigations of the structure and function of the tear fluid lipid layers and the effect of ectoine. Part B: artificial lipid films. *Biochim Biophys Acta, 1838*(10), 2716-2727.

Eichel, A., Wittig, J., Shah-Hosseini, K., & Mösges, R. (2013). A prospective, controlled study of SNS01 (ectoine nasal spray) compared to BNO-101 (phytotherapeutic dragées) in patients with acute rhinosinusitis. *Curr Med Res Opin, 29*(7), 739-746.

El Assal, R., Guven, S., Gurkan, U. A., Gozen, I., Shafiee, H., Dalbeyler, S., Abdalla, N., Thomas, G., Fuld, W., & Illigens, B. M. (2014). Bio-inspired cryo-ink preserves red blood cell phenotype and function during nanoliter vitrification. *Adv Mater, 26*(33), 5815-5822.

Eleutherio, E. C., Araujo, P. S., & Panek, A. D. (1993). Protective role of trehalose during heat stress in *Saccharomyces cerevisiae*. *Cryobiology, 30*(6), 591-596.

Falkow, S., Rosenberg, E., Schleifer, K.-H., Stackebrandt, E., & Dworkin, M. (2006). *The Prokaryotes: Symbiotic Associations, Biotechnology, Applied Microbiology* (Vol. 1): Springer, New York.

Fang, Y., Huang, F., Faulkner, M., Jiang, Q., Dykes, G. F., Yang, M., & Liu, L.-N. (2018). Engineering and modulating functional cyanobacterial CO_2-fixing organelles. *Front Plant Sci, 9*, 739.

Faria, C., Jorge, C. D., Borges, N., Tenreiro, S., Outeiro, T. F., & Santos, H. (2013). Inhibition of formation of α-synuclein inclusions by mannosylglycerate in a yeast model of Parkinson's disease. *Biochim Biophys Acta, 1830*(8), 4065-4072.

Galinski, E., & Tindall, B. (1992). Biotechnological prospects for halophiles and halotolerant micro-organisms. In R. Herbert & R. Sharp (Eds.), *Molecular biology and biotechnology of extremophiles* 76-114: Blackie & Sons Ltd.

Galinski, E. A. (1995). Osmoadaptation in bacteria. *Adv Microb Physiol, 37*, 273-328.

Galinski, E. A., & Trüper, H. G. (1994). Microbial behaviour in salt-stressed ecosystems. *FEMS Microbiol Rev, 15*(2-3), 95-108.

Garcia-Pichel, F., Zehr, J. P., Bhattacharya, D., & Pakrasi, H. B. (2020). What's in a name? The case of cyanobacteria. *J Phycol, 56*(1), 1-5.

Gough, N. R. (2020). Can Carbon Fixing Bacteria and Synthetic Biology Save the Planet? Retrieved from https://medium.com/swlh/can-carbon-fixing-bacteria-and-synthetic-biology-save-the-planet-b876960568fa

Hagemann, M. (2011). Molecular biology of cyanobacterial salt acclimation. *FEMS Microbiol Rev, 35*(1), 87-123.

Hagemann, M. (2013). Genomics of salt acclimation: synthesis of compatible solutes among cyanobacteria. In C. C.-C. Franck Chauvat (Ed.), *Adv Bot Res* Vol. 65, 27-55: Academic Press.

Hagemann, M., & Erdmann, N. (1994). Activation and pathway of glucosylglycerol synthesis in the cyanobacterium *Synechocystis* sp. PCC 6803. *Microbiol, 140*(6), 1427-1431.

Hagemann, M., & Hess, W. R. (2018). Systems and synthetic biology for the biotechnological application of cyanobacteria. *Curr Opin Biotechnol, 49*, 94-99.

Hagemann, M., & Marin, K. (1999). Salt-induced sucrose accumulation is mediated by sucrose-phosphate-synthase in cyanobacteria. *Plant Physiol, 155*(3), 424-430.

Hagemann, M., & Pade, N. (2015). Heterosides - compatible solutes occurring in prokaryotic and eukaryotic phototrophs. *Plant Biol, 17*(5), 927-934.

Hagemann, M., Schoor, A., Jeanjean, R., Zuther, E., & Joset, F. (1997). The *stpA* gene from *Synechocystis* sp. strain PCC 6803 encodes the glucosylglycerol-phosphate phosphatase involved in cyanobacterial osmotic response to salt shock. *J Bacteriol, 179*(5), 1727-1733.

Harishchandra, R. K., Sachan, A. K., Kerth, A., Lentzen, G., Neuhaus, T., & Galla, H. J. (2011). Compatible solutes: ectoine and hydroxyectoine improve functional nanostructures in artificial lung surfactants. *Biochim Biophys Acta, 1808*(12), 2830-2840.

Heinrich, U., Garbe, B., & Tronnier, H. (2007). In vivo assessment of ectoin: a randomized, vehicle-controlled clinical trial. *Skin Pharmacol Physiol, 20*(4), 211-218.

Henke, W., Herdel, K., Jung, K., Schnorr, D., & Loening, S. A. (1997). Betaine improves the PCR amplification of GC-rich DNA sequences. *Nucleic Acids Res, 25*(19), 3957-3958.

Hincha, D. K., & Hagemann, M. (2004). Stabilization of model membranes during drying by compatible solutes involved in the stress tolerance of plants and microorganisms. *Biochem J, 383*(2), 277-283.

Holmström, K. O., Somersalo, S., Mandal, A., Palva, T. E., & Welin, B. (2000). Improved tolerance to salinity and low temperature in transgenic tobacco producing glycine betaine. *J Exp Bot, 51*, 177-185.

Huckauf, J., Nomura, C., Forchhammer, K., & Hagemann, M. (2000). Stress responses of *Synechocystis* sp. strain PCC 6803 mutants impaired in genes encoding putative alternative sigma factors. *Microbiol, 146*(11), 2877-2889.

Jadhav, K., Kushwah, B., & Jadhav, I. (2018). Insight into compatible solutes from halophiles: exploring significant applications in biotechnology. In S. D. Singh J., Kumar G., Sharma N. (Ed.), *Microbial bioprospecting for sustainable development* 291-307: Springer, Singapore.

Kanapathipillai, M., Lentzen, G., Sierks, M., & Park, C. B. (2005). Ectoine and hydroxyectoine inhibit aggregation and neurotoxicity of Alzheimer's beta-amyloid. *FEBS Lett, 579*(21), 4775-4780.

Karl, D., Michaels, A., Bergman, B., Capone, D., Carpenter, E., Letelier, R., Lipschultz, F., Paerl, H., Sigman, D., & Stal, L. (2002). Dinitrogen fixation in the world's oceans. In H. R. W. Boyer E.W. (Ed.), *The nitrogen cycle at regional to global scales* 47-98: Springer, Dordrecht.

Kirsch, F., Klähn, S., & Hagemann, M. (2019). Salt-regulated accumulation of the compatible solutes sucrose and glucosylglycerol in cyanobacteria and its biotechnological potential. *Front Microbiol, 10*, 2139.

Kirsch, F., Luo, Q., Lu, X. F., & Hagemann, M. (2018). Inactivation of invertase enhances sucrose production in the cyanobacterium *Synechocystis* sp. PCC 6803. *Microbiol, 164*(10), 1220-1228.

Kirsch, F., Pade, N., Klahn, S., Hess, W. R., & Hagemann, M. (2017). The glucosylglycerol-degrading enzyme GghA is involved in acclimation to fluctuating salinities by the cyanobacterium *Synechocystis* sp. strain PCC 6803. *Microbiol, 163*, 1319-1328.

Kizawa, A., Kawahara, A., Takimura, Y., Nishiyama, Y., & Hihara, Y. (2016). RNA-seq profiling reveals novel target genes of LexA in the cyanobacterium *Synechocystis* sp. PCC 6803. *Front Microbiol, 7*(193), 1-14.

Klähn, S., & Hagemann, M. (2011). Compatible solute biosynthesis in cyanobacteria. *Environ Microbiol, 13*, 551-562.

Klähn, S., Höhne, A., Simon, E., & Hagemann, M. (2010). The gene *ssl3076* encodes a protein mediating the salt-induced expression of *ggpS* for the biosynthesis of the compatible solute glucosylglycerol in *Synechocystis* sp. strain PCC 6803. *J Bacteriol, 192*(17), 4403-4412.

Klähn, S., Marquardt, D. M., Rollwitz, I., & Hagemann, M. (2009). Expression of the *ggpPS* gene for glucosylglycerol biosynthesis from *Azotobacter vinelandii* improves the salt tolerance of *Arabidopsis thaliana*. *J Exp Bot, 60*(6), 1679-1689.

Klähn, S., Steglich, C., Hess, W. R., & Hagemann, M. (2010). Glucosylglycerate: a secondary compatible solute common to marine cyanobacteria from nitrogen-poor environments. *Environ Microbiol, 12*(1), 83-94.

Knoll, A. H. (1980). Archean photoautotrophy: some alternatives and limits. In M. L. Ponnamperuma C. (Ed.), *Limits of Life* Vol. 4, 133-147: Springer, Dordrecht.

Knoot, C. J., Ungerer, J., Wangikar, P. P., & Pakrasi, H. B. (2018). Cyanobacteria: promising biocatalysts for sustainable chemical production. *J Biol Chem, 293*(14), 5044-5052.

Kultschar, B., & Llewellyn, C. (2018). Secondary metabolites in cyanobacteria. In R. Vijayakumar & S. S. S. Raja (Eds.), *Secondary Metabolites - Sources and Applications* 23-36: IntechOpen.

Kumar, N., Jadhao, S. B., Chandan, N. K., & Rana, R. S. (2012). Dietary choline, betaine and lecithin mitigates endosulfan-induced stress in *Labeo rohita* fingerlings. *Fish Physiol Biochem, 38*(4), 989-1000.

Ladas, N. P., & Papageorgiou, G. C. (2000). Cell turgor: a critical factor for the proliferation of cyanobacteria at unfavorable salinity. *Photosynth Res, 65*(2), 155-164.

Larsson, J., Nylander, J. A., & Bergman, B. (2011). Genome fluctuations in cyanobacteria reflect evolutionary, developmental and adaptive traits. *BMC Evol Biol, 11*(1), 1-21.

Lima, S., Matinha-Cardoso, J., Tamagnini, P., & Oliveira, P. (2020). Extracellular vesicles: an overlooked secretion system in cyanobacteria. *Life, 10*(8), 129.

Luan, G., & Lu, X. (2018). Tailoring cyanobacterial cell factory for improved industrial properties. *Biotechnol Adv, 36*(2), 430-442.

Luley-Goedl, C., Sawangwan, T., Mueller, M., Schwarz, A., & Nidetzky, B. (2010). Biocatalytic process for production of α-glucosylglycerol using sucrose phosphorylase. *Food Technol Biotechnol, 48*, 276-283.

Lunn, J. E. (2002). Evolution of sucrose synthesis. *Plant Physiol, 128*(4), 1490-1500.

Mackay, M. A., Norton, R. S., & Borowitzka, L. J. (1984). Organic osmoregulatory solutes in cyanobacteria. *Microbiol, 130*(9), 2177-2191.

Malin, G., Iakobashvili, R., & Lapidot, A. (1999). Effect of tetrahydropyrimidine derivatives on protein-nucleic acids interaction. Type II restriction endonucleases as a model system. *J Biol Chem, 274*(11), 6920-6929.

Maréchal, E. (2018). Primary endosymbiosis: emergence of the primary chloroplast and the chromatophore, two independent events. In M. E. (Ed.), *Plastids Methods in Molecular Biology* Vol. 1829, 3-16: Humana Press, New York.

Margesin, R., & Schinner, F. (2001). Potential of halotolerant and halophilic microorganisms for biotechnology. *Extremophiles, 5*(2), 73-83.

Marin, K., Huckauf, J., Fulda, S., & Hagemann, M. (2002). Salt-dependent expression of glucosylglycerol-phosphate synthase, involved in osmolyte synthesis in the cyanobacterium *Synechocystis* sp. strain PCC 6803. *J Bacteriol, 184*(11), 2870-2877.

Marin, K., Kanesaki, Y., Los, D. A., Murata, N., Suzuki, I., & Hagemann, M. (2004). Gene expression profiling reflects physiological processes in salt acclimation of *Synechocystis* sp. strain PCC 6803. *Plant Physiol, 136*(2), 3290-3300.

Marin, K., Zuther, E., Kerstan, T., Kunert, A., & Hagemann, M. (1998). The *ggpS* gene from *Synechocystis* sp. strain PCC 6803 encoding glucosyl-glycerol-phosphate synthase is involved in osmolyte synthesis. *J Bacteriol, 180*(18), 4843-4849.

Marini, A., Reinelt, K., Krutmann, J., & Bilstein, A. (2014). Ectoine-containing cream in the treatment of mild to moderate atopic dermatitis: a randomised, comparator-controlled, intra-individual double-blind, multi-center trial. *Skin Pharmacol Physiol, 27*(2), 57-65.

Markl, E., Grünbichler, H., & Lackner, M. (2018). Cyanobacteria for PHB bioplastics production: a review. In Y. K. Wong (Ed.), *Algae*: IntechOpen.

Mazard, S., Penesyan, A., Ostrowski, M., Paulsen, I. T., & Egan, S. (2016). Tiny microbes with a big impact: the role of cyanobacteria and their metabolites in shaping our future. *Mar Drugs, 14*(5), 97.

Minton, A. P. (2000). Effects of excluded surface area and adsorbate clustering on surface adsorption of proteins: I. Equilibrium models. *Biophys Chem, 86*(2-3), 239-247.

Motitschke, L., Driller, H., & Galinski, E. (2000). Ectoin and ectoin derivatives as moisturizers in cosmetics. Patent US060071.

Muller, D., Lindemann, T., Shah-Hosseini, K., Scherner, O., Knop, M., Bilstein, A., & Mosges, R. (2016). Efficacy and tolerability of an ectoine mouth and throat spray compared with those of saline lozenges in the treatment of acute pharyngitis and/or laryngitis: a

prospective, controlled, observational clinical trial. *Eur Arch Otorhinolaryngol, 273*(9), 2591-2597.

Nakayama, H., Yoshida, K., Ono, H., Murooka, Y., & Shinmyo, A. (2000). Ectoine, the compatible solute of *Halomonas elongata*, confers hyperosmotic tolerance in cultured tobacco cells. *Plant Physiol, 122*(4), 1239-1248.

Niedermeyer, T. H. J. (2015). Anti-infective natural products from Cyanobacteria. *Planta Med, 81*(15), 1309-1325.

Novak, J. F., Stirnberg, M., Roenneke, B., & Marin, K. (2011). A novel mechanism of osmosensing, a salt-dependent protein-nucleic acid interaction in the cyanobacterium *Synechocystis* species PCC 6803. *J Biol Chem, 286*(5), 3235-3241.

NREL. (2020). Scientists Pinpoint Pathways for Carbon Dioxide Uptake of Cyanobacteria. Retrieved from https://www.nrel.gov/news/program/2020/scientists-pinpoint-pathways-for-carbon-dioxide-uptake-of-cyanobacteria.html

Nunnery, J. K., Mevers, E., & Gerwick, W. H. (2010). Biologically active secondary metabolites from marine cyanobacteria. *Curr Opin Biotechnol, 21*(6), 787-793.

Olson, J. M. (2006). Photosynthesis in the Archean Era. *Photosynth Res, 88*(2), 109-117.

Pade, N., Compaoré, J., Klähn, S., Stal, L. J., & Hagemann, M. (2012). The marine cyanobacterium *Crocosphaera watsonii* WH8501 synthesizes the compatible solute trehalose by a laterally acquired OtsAB fusion protein. *Environ Microbiol, 14*(5), 1261-1271.

Pade, N., Michalik, D., Ruth, W., Belkin, N., Hess, W. R., Berman-Frank, I., & Hagemann, M. (2016). Trimethylated homoserine functions as the major compatible solute in the globally significant oceanic cyanobacterium *Trichodesmium*. *PNAS, 113*(46), 13191-13196.

Parfrey, L. W., Lahr, D. J., Knoll, A. H., & Katz, L. A. (2011). Estimating the timing of early eukaryotic diversification with multigene molecular clocks. *PNAS, 108*(33), 13624-13629.

Parmar, A., Singh, N. K., Pandey, A., Gnansounou, E., & Madamwar, D. (2011). Cyanobacteria and microalgae: a positive prospect for biofuels. *Bioresour Technol, 102*(22), 10163-10172.

Pattharaprachayakul, N., Choi, J.-i., Incharoensakdi, A., & Woo, H. M. (2020). Metabolic engineering and synthetic biology of cyanobacteria for carbon capture and utilization. *Biotechnol Bioprocess Eng, 25*, 1-19.

Pech, T., Ohsawa, I., Praktiknjo, M., Overhaus, M., Wehner, S., von Websky, M., Abu-Elmagd, K., van Echten-Deckert, G., Kalff, J. C., & Schaefer, N. (2013). A natural tetrahydropyrimidine, ectoine, ameliorates ischemia reperfusion injury after intestinal transplantation in rats. *Pathobiol, 80*(2), 102-110.

Pereira, S., Zille, A., Micheletti, E., Moradas-Ferreira, P., De Philippis, R., & Tamagnini, P. (2009). Complexity of cyanobacterial exopolysaccharides: composition, structures, inducing factors and putative genes involved in their biosynthesis and assembly. *FEMS Microbiol Rev, 33*(5), 917-941.

Poolman, B., & Glaasker, E. (1998). Regulation of compatible solute accumulation in bacteria. *Mol Microbiol, 29*(2), 397-407.

Potts, M. (1994). Desiccation tolerance of prokaryotes. *Microbiol Rev, 58*(4), 755-805.

Raja, R., Hemaiswarya, S., Ganesan, V., & Carvalho, I. S. (2016). Recent developments in therapeutic applications of Cyanobacteria. *Crit Rev Microbiol, 42*(3), 394-405.

Rao, B. D., Babu, M. R., & Ellaswamy, N. (2015). Cyanotoxins and Their Potential Applications - A Review. *Nat Environ Pollut Technol, 14*(1).

Reed, R., Borowitzka, L., Mackay, M., Chudek, J., Foster, R., Warr, S., Moore, D., & Stewart, W. (1986). Organic solute accumulation in osmotically stressed cyanobacteria. *FEMS Microbiol Rev, 2*(1-2), 51-56.

Reed, R., & Stewart, W. (1985). Osmotic adjustment and organic solute accumulation in unicellular cyanobacteria from freshwater and marine habitats. *Mar Biol, 88*(1), 1-9.

Roberts, M. F. (2005). Organic compatible solutes of halotolerant and halophilic microorganisms. *Saline Syst, 1*(1), 1-30.

Rosing, M. T., & Frei, R. (2004). U-rich Archaean sea-floor sediments from Greenland–indications of >3700 Ma oxygenic photosynthesis. *Earth Planet Sci Lett, 217*(3-4), 237-244.

Rübsam, H., Kirsch, F., Reimann, V., Erban, A., Kopka, J., Hagemann, M., Hess, W. R., & Klähn, S. (2018). The iron-stress activated RNA 1 (IsaR1) coordinates osmotic acclimation and iron starvation responses in the cyanobacterium *Synechocystis* sp. PCC 6803. *Environ Microbiol, 20*(8), 2757-2768.

Sánchez-Baracaldo, P. (2015). Origin of marine planktonic cyanobacteria. *Sci Rep, 5*(1), 1-10.

Sánchez-Baracaldo, P., & Cardona, T. (2020). On the origin of oxygenic photosynthesis and Cyanobacteria. *New Phytol, 225*(4), 1440-1446.

Santos-Merino, M., Singh, A. K., & Ducat, D. C. (2019). New applications of synthetic biology tools for cyanobacterial metabolic engineering. *Front Bioeng Biotechnol, 7*(33).

Scheller, H. V., Harholt, J., & Ulvskov, P. (2012). Stress-tolerant plants expressing mannosylglycerate-producing enzymes. U.S. Patent Application No. 13/318,661.

Schirrmeister, B. E., Antonelli, A., & Bagheri, H. C. (2011). The origin of multicellularity in cyanobacteria. *BMC Evol Biol, 11*(1), 1-21.

Schirrmeister, B. E., de Vos, J. M., Antonelli, A., & Bagheri, H. C. (2013). Evolution of multicellularity coincided with increased diversification of cyanobacteria and the Great Oxidation Event. *PNAS, 110*(5), 1791-1796.

Schnoor, M., Voss, P., Cullen, P., Böking, T., Galla, H. J., Galinski, E. A., & Lorkowski, S. (2004). Characterization of the synthetic compatible solute homoectoine as a potent PCR enhancer. *Biochem Biophys Res Commun, 322*(3), 867-872.

Schopf, J. W. (2000). The fossil record: tracing the roots of the cyanobacterial lineage. In P. M. Whitton B.A. (Ed.), *The ecology of cyanobacteria* 13-35: Springer, Dordrecht.

Schuergers, N., Mullineaux, C. W., & Wilde, A. (2017). Cyanobacteria in motion. *Curr Opin Plant Biol, 37*, 109-115.

Scott, C., Lyons, T., Bekker, A., Shen, Y.-a., Poulton, S., Chu, X.-l., & Anbar, A. (2008). Tracing the stepwise oxygenation of the Proterozoic ocean. *Nature, 452*(7186), 456-459.

Sergeev, V., Gerasimenko, L., & Zavarzin, G. (2002). The proterozoic history and present state of cyanobacteria. *Microbiol, 71*(6), 623-637.

Serrano, L., Vancompernolle, K., Ball, P., Benenson, Y., Holliger, P., Panke, S., Rettberg, R., Stelling, J., & Weiss, R. (2005). *Synthetic Biology applying engineering to biology*. Retrieved from Report of a NEST High-Level Expert Group, European Communities.

Sharma, N. K., Rai, A. K., & Stal, L. J. (2013). *Cyanobacteria: an economic perspective*: John Wiley & Sons, Ltd.

Shih, P. M., Wu, D., Latifi, A., Axen, S. D., Fewer, D. P., Talla, E., Calteau, A., Cai, F., De Marsac, N. T., & Rippka, R. (2013). Improving the coverage of the cyanobacterial phylum using diversity-driven genome sequencing. *PNAS, 110*(3), 1053-1058.

Sievers, N., Muders, K., Henneberg, M., Klähn, S., Effmert, M., Junghans, H., & Hagemann, M. (2013). Establishing glucosylglycerol synthesis in potato (*Solanum tuberosum* L. cv. Albatros) by expression of the *ggpPS* gene from *Azotobacter vinelandii*. *J Plant Sci Mol Breed, 2*(1), 10-7243.

Singh, S., Kant, C., Yadav, R. K., Reddy, Y. P., & Abraham, G. (2019). Cyanobacterial exopolysaccharides: Composition, biosynthesis, and biotechnological applications. In A. K. Mishra, D. N. Tiwari, & A. N. Rai (Eds.), *Cyanobacteria - From Basic Science to Applications* 347-358: Academic Press.

Song, K., Hagemann, M., Tan, X., & Lu, X. (2017). The response regulator Slr1588 regulates *spsA* but is not crucial for salt acclimation of *Synechocystis* sp. PCC 6803. *Front Microbiol, 8*(1176).

Soni, R. A., Sudhakar, K., & Rana, R. (2017). *Spirulina*-From growth to nutritional product: A review. *Trends Food Sci Technol, 69*(Part A), 157-171.

Sun, H., Glasmacher, B., & Hofmann, N. (2012). Compatible solutes improve cryopreservation of human endothelial cells. *Cryo Letters, 33*(6), 485-493.

Sydlik, U., Gallitz, I., Albrecht, C., Abel, J., Krutmann, J., & Unfried, K. (2009). The compatible solute ectoine protects against nanoparticle-induced neutrophilic lung inflammation. *Am J Respir Crit Care Med, 180*(1), 29-35.

Watanabe, F., Takenaka, S., Kittaka-Katsura, H., Ebara, S., & Miyamoto, E. (2002). Characterization and bioavailability of vitamin B12-compounds from edible algae. *J Nutr Sci Vitaminol, 48*(5), 325-331.

Whitton, B. A. (2012). *Ecology of cyanobacteria II: their diversity in space and time*: Springer Science & Business Media.

Wood, J. M., Bremer, E., Csonka, L. N., Kraemer, R., Poolman, B., van der Heide, T., & Smith, L. T. (2001). Osmosensing and osmoregulatory compatible solute accumulation by bacteria. *Comp Biochem Physiol, Part A Mol Integr Physiol, 130*(3), 437-460.

Xia, P. F., Ling, H., Foo, J. L., & Chang, M. W. (2019). Synthetic biology toolkits for metabolic engineering of cyanobacteria. *Biotechnol J, 14*(6), 1800496.

Yashavanth, P., Das, M., & Maiti, S. K. (2021). Recent progress and challenges in cyanobacterial autotrophic production of polyhydroxybutyrate (PHB), a bioplastic. *J Environ Chem Eng, 9*(4), 105379.

Chapter II. Synthetic biology of cyanobacteria

Book Chapter published in:
Pacheco, C. C., Ferreira, E. A., Oliveira, P., & Tamagnini, P., “Synthetic biology of cyanobacteria”; in: Kourist, R., & Schmidt, S. (ed.) of book The Autotrophic Biorefinery: Raw Materials from Biotechnology, Berlin, Boston: De Gruyter, 2021, pp. 131-172, fig. 6.1-6.5. https://doi.org/10.1515/9783110550603-006.

Catarina C. Pacheco, Eunice A. Ferreira, Paulo Oliveira,
Paula Tamagnini

Chapter 6
Synthetic biology of cyanobacteria

Abstract: Synthetic biology has revolutionized the engineering and manipulation of microorganisms with valuable contributions to fundamental and applied science. In this context, cyanobacteria emerge as potential contenders as chassis, enabling the harnessing of solar energy and CO_2 fixation for the production of a variety of compounds. This chapter reviews key aspects of cyanobacterial synthetic biology, focusing on the strains that meet the characteristics to be used as chassis, namely *Synechocystis* and the fast-growing *Synechococcus* strains, the development of genome-scale metabolic models as tools to predict chassis behavior and design metabolic engineering strategies and; the significant efforts that are being made to expand and refine the available tools for the rational design of synthetic devices and for the genetic manipulation of this group of organisms. Furthermore, a selection of works focusing on the production of compounds using a synthetic biology-based approach is summarized and, the current limitations and future perspectives for cyanobacterial synthetic biology are discussed.

Keywords: cyanobacterial chassis, synthetic biology, metabolic flux models, genetic engineering, molecular toolbox

6.1 Principles of synthetic biology

Synthetic biology (SB) has emerged due to developments in computational and molecular biology, protein engineering, systems biology [1] and, most importantly, the cost-effective DNA sequencing and synthesis. This interdisciplinary field applies "science, technology and engineering to facilitate and accelerate the design, manufacture and/or modification of genetic materials in living organisms" [2]. The SB approach applies the engineering concepts of abstraction, decoupling and standardization to

Acknowledgements: This work was supported by FEDER – Fundo Europeu de Desenvolvimento Regional funds through the COMPETE 2020 – Operacional Programme for Competitiveness and Internationalisation (POCI), Portugal 2020, and by Portuguese funds through FCT – Fundação para a Ciência e a Tecnologia, I.P./Ministério da Ciência, Tecnologia e Ensino Superior, under the projects UIDB/04293/2020 and UIDP/04293/2020; and in the framework of the project POCI-01-0145-FEDER-029540 (PTDC/BIA-OUT/29540/2017). The authors also greatly acknowledge FCT for the scholarship SFRH/BD/117508/2016 (EAF), the Assistant Researcher contract CEECIND/00259/2017 (CCP) and FCT investigator grant IF/00256/2015 (PO).

https://doi.org/10.1515/9783110550603-006

biology, simplifying complex living systems through the establishment of different hierarchic levels [3].

Box 6.1: Synthetic biology

Synthetic biology – aims at designing and engineering biologically based parts, novel devices and systems as well as redesigning existing, natural biological systems.

Standardized biological part/BioBrick – oligonucleotide sequence with a specific biological function that cannot be subdivided into smaller functional units, such as a promoter or a coding sequence.

Composite part – is a DNA unit consisting of two or more basic parts assembled together.

Device – is a type of composite part that produces an output or operation in the cell.

Circuit – is a complex composite part composed of two or more synthetic devices, designed to perform logical functions.

Chassis – biological entity in which the devices or circuits are implemented, it can be a living organism (host) or an *in vitro* system for transcription and translation.

Scar – region of DNA formed where two separated parts are joined together, which cannot be cut by the enzymes that originally cut the two joined sequences.

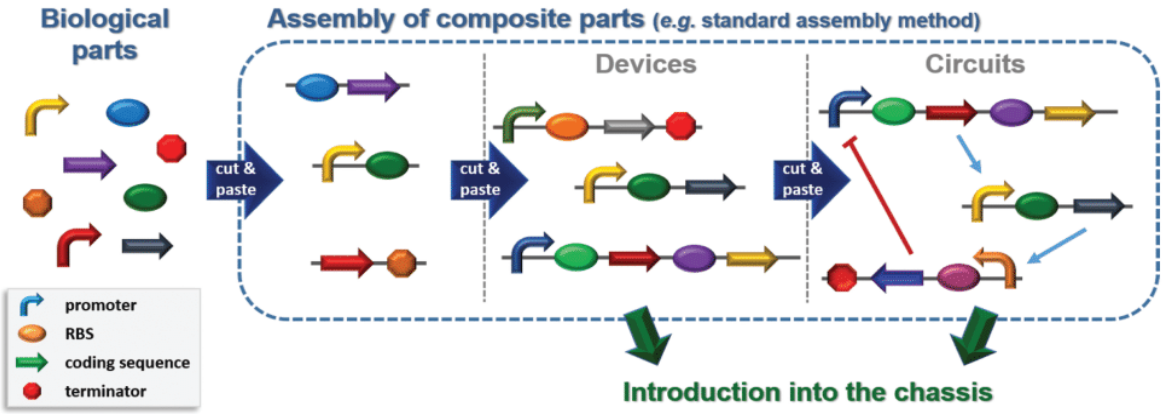

Figure 6.1: Schematic representation of the synthetic biology principles applied to DNA. Biological systems can be simplified by the establishment of biological parts with specific functions (e.g., promoters and RBS), built according to specifications that make them standardized. This enables the assembly of parts following methods, such as the "standard assembly", that resorts to simple molecular biology techniques (cut and paste = restriction and ligation) to generate composite parts. These devices and circuits are designed for specific purposes and must eventually be introduced into the host organism – the chassis.

At the bottom of the hierarchy are the biological parts or building blocks – DNA, RNA, proteins and metabolites – that are used for the next level, the assembly of devices that will function to regulate the flow of information and/or lead to biochemical reactions. In the third hierarchic level, devices are used to generate synthetic circuits that form functional complex pathways designed for specific purposes [3, 4]

(Box: 6.1, Figure 6.1). This rational approach is extended to the genetic building blocks – the biological parts or BioBricks that are oligonucleotide sequences with specific functions [e.g., promoters, ribosome binding sites (RBS), open reading frames (ORFs)], built according to specifications that make them standardized and interchangeable [5, 6]. Most biological parts available are compatible with the RFC[10] standard [7] that describes the structural features of BioBricks, in which the DNA sequence (part) must be flanked by a prefix (containing restriction sites for the enzymes *Eco*RI and *Xba*I) and by a suffix (containing restriction sites for the enzymes *Spe*I and *Pst*I). These specifications allow the use of the standard assembly method, resorting to simple molecular biology techniques for the generation of composite structures assembled from multiple parts that, in the end, maintain the prefix and suffix sequences thus increasing the speed and tractability of the cloning process (Figure 6.2). Between the assembled parts remains a six-nucleotide scar that is not recognized by any restriction enzyme, making it impossible to disassemble the composite. Several modifications and extensions of the RFC[10] standard have been proposed, mainly to alter or eliminate the stop codon present in the scar that is an undesirable feature when constructing devices with protein fusions or protein complexes with multiple domains [8, 9].

Moreover, the standard assembly method is iterative requiring steps of restriction enzyme digestion and ligation to assemble parts, which becomes inefficient for the generation of large devices/circuits and/or variant gene libraries. To overcome these hurdles, the Gibson Assembly, the Golden Gate, the MoClo or the Loop systems have been developed based on isothermal, single-reaction enzymatic assembly or in the use of type IIS restriction enzymes. These methods allow the assembly of multiple parts in one reaction, rapidly generating large DNA molecules [10–14]. Currently, type II assembly standards based on MoClo and Loop are accepted and the technical specifications of iGEM Type IIS standard – RFC[1000] – are already available [15]. Nevertheless, the RFC[10] standard is still widely used, much due to the iGEM – International Genetically Engineered Machine Competition – an annual, worldwide, SB event meant for undergraduate university students, as well as high school and graduate students. The iGEM teams build genetically engineered systems using BioBricks aiming at creating a positive contribution to their communities and the world [16]. Furthermore, iGEM is a program dedicated to the advancement of SB and is responsible for the Registry of Standard Biological Parts [17]. This registry is a database that gathers information on the design and characterization of the existing BioBricks as well as other tools and host organisms, which in the SB jargon are termed chassis. In addition, the iGEM Foundation also maintains a repository of all DNA parts that are in the registry providing a source of genetic parts to iGEM teams and academic laboratories all over the world. Therefore, the iGEM Foundation has played a key role in the dissemination of SB leveraging the development and characterization of numerous parts, devices and circuits with tremendous impact in fundamental and applied science.

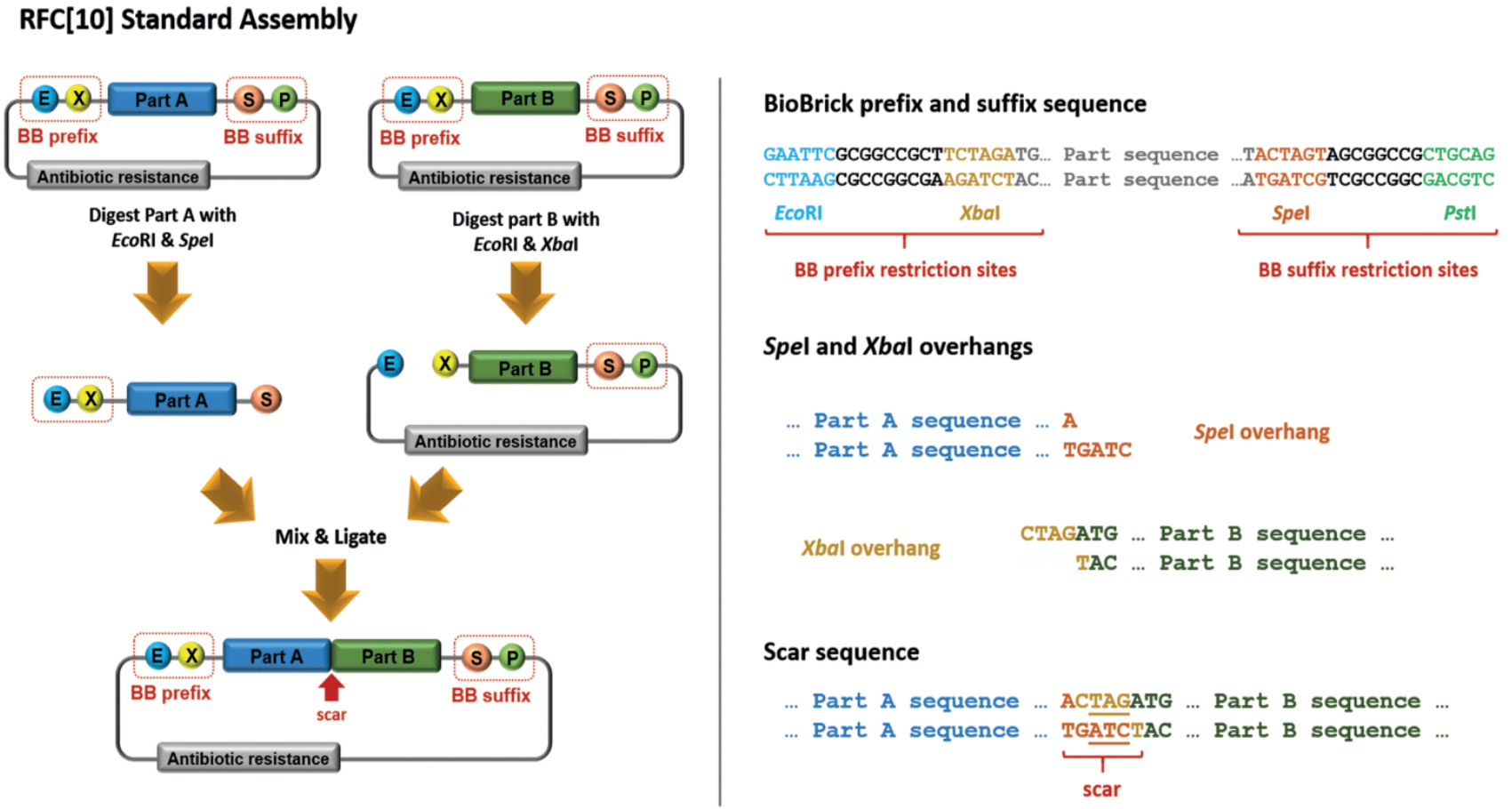

Figure 6.2: Schematic representation of the RFC[10] standard assembly (left panel) and sequence technical details (right panel). Biological parts compatible with the RFC[10] standard are flanked by a BB prefix harboring the *Eco*RI (E) and *Xba*I (X) restriction sites, and a BB suffix harboring the *Spe*I (S) and *Pst*I (P) restriction sites. For the assembly of two parts (A and B), part A is digested with *Eco*RI and *Spe*I restriction enzymes while part B must be digested with *Eco*RI and *Xba*I; the products of these restriction reactions are subsequently mixed and ligated. The *Xba*I and *Spe*I enzymes produce compatible overhangs that ligate, generating a scar sequence of 6 bp containing the TAG stop codon. In the end, a composite comprised of parts A and B is generated, maintaining the BB prefix and BB suffix.

6.2 Chassis

For an organism to be used as a chassis for SB applications, it must be well studied with a vast knowledge base, amenable to genetic manipulation, and have a relatively minimalist set of genes that allow retaining viability, avoiding possible cross talk between the synthetic devices/circuits and the genomic context [4, 18]. In the framework of the minimal genomes, the *Mycoplasma* genus has been the focus of attention. In 1995, the genome of *Mycoplasma genitalium* (0.58 Mb) was sequenced [19], at the time, it was the smallest known self-replicating organism harboring less than 500 genes, of which, 100 revealed to be non-essential [20]. Later on, the 1.08-Mb genome of *Mycoplasma mycoides* was chemically synthesized, assembled and subsequently, transferred to *M. capricolum* thus creating the first bacterium controlled by a synthetic genome – *M. mycoides* JCVI-syn1.0 [21]. The pursuit for a chassis with a minimal genome continued, and the JCVI-syn1.0 synthetic genome was streamlined down to 0.53 Mb – the JCVI-syn3.0 – harboring 473 genes, 149 with unknown function [22]. Apart from the minimal chassis, the model organisms established in molecular biology and genetic engineering, *Escherichia coli* and *Saccharomyces cerevisiae* emerged as primordial contenders to become universal chassis for SB [23]. These organisms, together with *Bacillus subtilis*, currently possess the largest SB toolboxes and efficient manipulation techniques that have allowed the successful implementation/optimization of complex pathways [24–30]. The increasing complexity and sophistication of synthetic devices and circuits has unveiled the need to have several chassis with robust performances in different scenarios/conditions. In this quest for new chassis, cyanobacteria are increasingly attractive biotechnology platforms due to their simple nutritional requirements, the ability to perform oxygenic photosynthesis and metabolic plasticity [31, 32]. In addition, the autotrophic metabolism enables the sustainable production of compounds through carbon sequestration. The metabolic network of these organisms is among the most complicated in nature, displaying redundant central carbon pathways that allow the mitigation of energy demands under multiple physiological conditions contributing to the ecological ubiquity of these organisms [31]. Compared to other photosynthetic organisms (namely plants), cyanobacteria are more amenable to genetic manipulation, have faster growth, culture scale-up is easier and still maintain some degree of subcellular compartmentalization [33, 34]. Within the *Cyanobacteria* phylum, the unicellular freshwater strains *Synechocystis* sp. PCC 6803 (*Synechocystis* 6803) and *Synechococcus elongatus* PCC 7942 (*S. elongatus* 7942), and the filamentous, heterocyst-forming strain *Nostoc* sp. PCC 7120 (*Nostoc* 7120) are among the most studied organisms. *Synechocystis* 6803 is a non-nitrogen-fixing bacterium capable of sustaining growth under autotrophic, mixotrophic (using glucose as carbon source) or heterotrophic (with a daily short light pulse) conditions [35], with doubling time around 6.6 h [36, 37] under fast growth conditions. This cyanobacterium has a medium-size genome of 3.6 Mb and harbors seven plasmids with sizes ranging from 2.3 to 120 kb, whose copy numbers

vary depending on growth phase and conditions [34, 38–40]. *Synechocystis* 6803 was the first photosynthetic cyanobacterium to have its genome sequenced and annotated [41], becoming the model organism in numerous proteomic, transcriptomic and metabolomics studies [42–47]. Furthermore, it can be genetically manipulated through different methods including natural transformation, conjugation or electroporation [48, 49]. More recently, genome-editing platforms based on clustered regularly interspaced short palindromic repeats (CRISPR) have been developed for this cyanobacterium (for more details on the CRISPR system, see Section 6.3.8 and Chapter 2) [50, 51].

The unicellular cyanobacterium *S. elongatus* 7942 has been extensively used as a model organism for the study of prokaryotic circadian clocks [52, 53]. *S. elongatus* 7942 is unable to fix nitrogen (similarly to *Synechocystis* 6803) and it is able to grow only under autotrophic conditions with doubling times down to 4.9 h [36]. This cyanobacterium harbors two plasmids (pANS with 7.8 kb and pANL with 46.2 kb) and a small genome of 2.7 Mb [34]. Genetic manipulation through natural DNA uptake was first reported for this cyanobacterium [54], and it is also amenable to transformation through conjugation and electroporation [48, 55]; and genome editing using CRISPR was also reported [51]. The generation of segregated mutants in *S. elongatus* 7942 is significantly less time consuming than in *Synechocystis* 6803, since it maintains 3–4 copies of the genome instead of the 12 reported and generally accepted for *Synechocystis* [39, 56]. One strategy envisaging the easier engineering of chassis is related to the simplification of biological complexity by genome streamlining and, in this context, Delaye et al. [57] generated a blueprint for a minimal *S. elongatus* 7942 genome by setting a guide to non-essential genes as targets for deletion. However, there have been no reports regarding the implementation of such plan.

In addition to the unicellular cyanobacteria mentioned above, the filamentous *Nostoc* 7120 is also considered a model organism, as it has been the subject of numerous studies focusing in nitrogen fixation and cellular differentiation [58, 59]. For many decades, this freshwater strain was considered an obligate photoautotroph, with doubling time of approximately 14 h [60], but recently its ability to sustain growth under mixotrophic and heterotrophic conditions was reported [61]. Conjugation and electroporation protocols for its genetic manipulation have long been established [62, 63], and since this is a filamentous strain, disruption of the filaments may be required to facilitate manipulation. This cyanobacterium has a large size genome of 6.4 Mb and six plasmids ranging from 5.6 to 408 kb [64].

Despite being the best-studied cyanobacteria within the phylum, the growth rates of these model organisms are modest and the robustness under high light and temperature fluctuations is limited [34]. In an effort to find a cyanobacterium more suitable for production purposes, the filamentous non-heterocystous *Leptolyngbya* sp. strain BL0902 (*Leptolyngbya* BL0902) was isolated based on its growth traits under outdoor cultivation conditions. The doubling times registered for this cyanobacterium are comparable to those of the *Arthrospira* genus, which are grown at industrial scale to be used as nutritional supplements [65]. Unlike the latter, this *Leptolyngbya* is amenable

to genetic transformation through conjugation [65]. Although this strain held promising capabilities and some tools were developed [66, 67], not much progress has been made using it. Nevertheless, several fast growing unicellular strains have emerged as candidates to become microbial cell factories: *Synechococcus* sp. PCC 7002, *S. elongatus* UTEX 2973 and *S. elongatus* PCC 11801 [36, 68, 69]. *Synechococcus* sp. PCC 7002 (*Synechococcus* 7002) is a unicellular marine strain, capable of growth under autotrophic and mixotrophic conditions, and is extremely tolerant to high light intensity and salinity conditions [68, 70, 71]. So far, this cyanobacterium was reported as one of the fastest growing within the group with a doubling time of 2.6 h under optimal conditions [68]. In addition, *Synechococcus* 7002 is amenable to genetic manipulation by natural transformation and conjugation [72–74], and advanced techniques for genetic manipulation have also been developed [75]. The sequence of the 3 Mb genome and of the six plasmids, with sizes ranging from 4.8 to 186 kb, have been publicly available since 2008 [76]. Other fast-growing strains were reported, including *S. elongatus* UTEX 2973 (*S. elongatus* 2973) and *S. elongatus* PCC 11801 (*S. elongatus* 11801), with doubling times of 1.9 and 2.3 h under optimal conditions, respectively [36, 69]. Genomic and proteomic analyzes were performed for both organisms to identify the determinants associated to the fast-growth phenotype [36, 69, 77–80]. *S. elongatus* 2973 has a genome of 2.7 Mb and its sequence is 99.8% similar to that of *S. elongatus* 7942, with a total of 55 differences (single-nucleotide polymorphisms (SNPs) and insertions–deletions) between the two genomes [36]. In addition, the photophysiology of these organisms was investigated revealing that *S. elongatus* 2973 has increased photosynthetic rates compared to 7942, due to differences in the photosynthetic apparatus such as increased content in plastocyanin, cytochrome b_6f and photosystem I (PSI) and decreased phycobilisomes [77]. A systematic mutational analysis using CRISPR was performed in *S. elongatus* 2973 associating the fast-growth phenotype to SNPs in the genes *atpA* (encoding the alpha subunit of the ATP synthase), *ppnK* (encoding a NAD^+ kinase) and *rpaA* (encoding the master regulator of the circadian clock) [78]. The SNPs in the *atpA* and *ppnK* resulted in enzymes with improved performance leading to an increase in the ATP and $NADP^+$ pools. However, the interactions between the energy balance and the circadian clock are complex and require further analysis to elucidate the fast-growth phenotype. In addition, the authors demonstrated that the insertion of these modifications in *S. elongatus* 7942 drastically reduces the doubling time from 6.8 to 2.3 h [78]. In terms of genetic manipulation, *S. elongatus* 2973 is not naturally competent, but can be transformed by conjugation through triparental mating and, as abovementioned, a CRISPR platform was also developed for this organism [36, 56]. *S. elongatus* 11801 shows the highest growth rate under atmospheric CO_2, high temperatures and light intensities, and tolerates sea salt concentrations [69]. Whole genome sequencing and annotation revealed that *S. elongatus* 11801 shares approximately 83% genome identity with *S. elongatus* 7942 and 2973. Compared to these two organisms, most of the proteins identified as unique in *S. elongatus* 11801 are involved in adaptation to abiotic stresses thus implying its robust phenotype [69]. This cyanobacterium

can be genetically manipulated since it was shown to be naturally competent, further demonstrating the potential of this strain to be used as a chassis [69]. The proteome of *S. elongatus* 11801 under different CO_2 concentrations was investigated envisaging future strategies for biofuel production [80]. Recently, *S. elongatus* PCC 11802 (*S. elongatus* 11802) was isolated, being closely related to *S. elongatus* 11801 with ~97% genome identity [81]. *S. elongatus* 11802 has a doubling time of 2.8 h at 1% CO_2, 1,000 μE m^{-2} s^{-1} and shows faster growth at high CO_2 and temperature conditions compared to 11801. Similar to the latter, *S. elongatus* 11802 can be manipulated by natural transformation. Analysis of the metabolic profile under high CO_2 shows that the accumulation of key intermediate metabolites of the Calvin–Benson–Bassham (CBB) cycle allied to the fast growth phenotype makes this cyanobacterium an ideal chassis for the synthesis of products primarily derived from the CBB cycle [81].

6.2.1 Development of genome-scale metabolic flux models for cyanobacteria

In addition to finding suitable chassis that can meet the requirements to fulfil the envisaged goals, it is equally important to develop accurate *in silico* models that are essential tools to predict chassis behavior, production rates, and aid in the design of more complex devices and circuits. In this context, genome-scale metabolic models based on flux balance analysis (FBA) have been developed (see Chapter 2). The FBA models represent the organism's metabolic network and consider all genes encoding proteins with associated reactions. Moreover, models are based on the premise that growth is in steady state as in the exponential growth phase, in which the rate of production of a given metabolite is equal to the rate of consumption [82]. The vast knowledge available for *Synechocystis* 6803 has enabled the construction of the first cyanobacterial genome-scale metabolic models [83–85] using FBA. The model by Fu et al. [83] considers 633 genes in a metabolic network of 831 reactions, enabling the simulation of cell growth and metabolite production. Two years later, a more comprehensive model was reported – the *i*Syn669 [84], considering 669 genes and 882 reactions including a more detailed representation of photosynthesis. Furthermore, the *i*Syn669 was used as a scaffold for the integration of transcriptomic data that allowed the identification of metabolic hotspots. This model was later upgraded to the *i*Syn811, consisting of 956 reactions accounting for 811 genes; flux-coupling analysis was also performed for this metabolic network leading to the identification of potential bottlenecks for compound production, namely hydrogen and ethanol [85]. Additional models for *Synechocystis* 6803 have been generated, updating pathway topologies and analyzing light/dark cycles of metabolism [86]; describing the photosynthetic process in mechanistic detail and analyzing it under different light, inorganic carbon conditions and genetic perturbations [87]. More recently, two updated models – the *i*SynCJ816 and the *i*mSyn716 – were generated based on metabolic networks or metabolic models available [88, 89]. The *i*SynCJ816

model was used to determine the possibility of engineering *Synechocystis* 6803 to increase carbon fixation [88]. The *i*mSyn716 includes 18 novel carbon pathways and 190 additional metabolites; using the updated network and performing instationary ^{13}C-metabolic flux analysis, it was possible to determine that 98% of the fixed carbon is directed to biomass generation with only small amounts channeled to organic acids and glycogen storage [89].

Building on the experience of the *Synechocystis* 6803 models, Triana et al. [90] reported the construction of the *S. elongatus* 7942 metabolic model – the *i*Syf715 that includes 851 reactions and 838 metabolites. Similarly, to the *i*Syn models, the *i*Syf allows simulations of *S. elongatus* 7942 behavior under photoautotrophic conditions, constituting an important tool for the use of this organism as a cell factory for industrially relevant products. Two years later, Broddrick et al. [91] generated the *i*JB785 model, a metabolic network of 850 reactions that highlighted areas of the cyanobacterial metabolism where knowledge is scarce, like the nucleotide salvage system and also unveiled the importance of metabolic features such as an abridged TCA cycle. *S. elongatus* 7942 harbors only the TCA enzymes required for the synthesis of oxaloacetate and 2-oxoglutarate that are necessary for many biomass components, and the latter is also the gateway for nitrogen assimilation [91]. Therefore, the *i*JB785 model constitutes not only an important tool for designing strategies in *S. elongatus* 7942 but it is also a source for biological discovery.

The vast knowledge base available for *Nostoc* 7120 also enabled the development of a genome-scale model, in this case with the particular aim of shedding light on the putative metabolic exchange reactions between vegetative cells and heterocysts [92]. This model led to the establishment of a more accurate metabolic network for this filamentous, heterocyst-forming cyanobacterium, and even though the need for model improvement is acknowledged, it constitutes an important tool for the use of *Nostoc* 7120 as chassis.

The first genome-scale metabolic model of *Synechococcus* 7002 – the *i*Syp611 – followed a rather different construction scheme. The *i*Syp611 was generated using the high-throughput genome-scale metabolic reconstruction pipeline (in the SEED framework), the organism's genome sequence, and the metabolic network of another cyanobacterium, *Cyanothece* sp. ATCC 54112 (*Cyanothece* 54112) [93–95]. This pipeline introduces automation in the generation of the network, bypassing time-consuming manual steps such as the annotation of the genome and the reaction network [93]. The *i*Syp611 was later updated to a version that accounts 708 reactions, the *i*Syp708; it was used together with other computational methods to predict the theoretical yields of several chemicals under dark and photoautotrophic conditions, examining also the effect light and CO_2 limitations in production [96]. In addition, this work also identifies gene knockouts with potential to increase production of specific compounds thus demonstrating the usefulness of the model as a tool for engineering *Synechococcus* 7002 [96]. A third version of the model was reported in 2016, in which the cyanobacterium's essential genes and metabolic robustness were reassessed, and strategies for improved

production of ethanol and glycerol were analyzed [97]. Qian et al. [98] reported the generation of the *i*Syp821 metabolic model that incorporates a light-dependent algorithm, enabling the consistent simulation of autotrophic growth under different light intensities. In addition, this model is able to predict the redistribution pattern of CO_2 uptake, amino acid, glycogen and lipid synthesis under nitrogen depletion.

A semi-automated method previously established [99] was used to generate a composite genome-scale metabolic model of *S. elongatus* 2973 and 7942; the *i*Syu683 was based on the genome sequences of both organisms and on the genome-scale metabolic models proposed for *Cyanothece* 51142, *Synechocystis* 6803 and *Synechococcus* 7002. Together with experimental data, the model was used to pinpoint the carbon uptake rate as the main factor contributing to the differences between the growth rates of *S. elongatus* 2973 and 7942 [79]. This compilation further highlights the relevance of constructing/refining reliable genome-scale metabolic models of cyanobacterial chassis for the identification of key steps in metabolic networks, as well as to unveil potential tweaking points for improved compound production.

6.3 Tools

The establishment of an organism as a cell factory for SB applications requires a customized toolbox comprising well-characterized parts such as regulatory elements (promoters, RBS, terminators), reporter genes, degradation tags and plasmids. The rational design of synthetic devices and circuits is based on standardized parts with a predictable behavior. In the advent of cyanobacterial SB, researchers have realized that the existing parts developed for the heterotrophic organisms *E. coli*, *B. subtilis* and *S. cerevisiae* work poorly or not at all in photoautotrophic bacteria [100]. In the last years, a tremendous effort has been made to develop tools for different cyanobacterial chassis. An overview of the existing SB tools for cyanobacteria is given here, focusing in the regulation of transcription by promoters, the fine tuning of translation by RBS and other RNA-based tools (riboswitches and riboregulators), and other tools such as reporter genes, degradation tags and terminators. In addition, some attention is dedicated to replicative plasmids, integrative plasmids and neutral sites as integration platforms. Finally, the generation of markerless mutants is addressed focusing on counter selection systems and the recent techniques for genome editing based on the CRISPR system.

Box 6.2: Genetics

Gene – DNA region that can be transcribed into a functional RNA molecule; most of the times into a messenger RNA (mRNA), that encodes the amino acid sequence of a polypeptide chain.

Promoter – DNA sequence located in the 5′ end of the gene, to which the RNA polymerase and necessary transcription factors (proteins) bind to initiate transcription. Promoters are the major elements used to control gene expression (at transcription level).

RBS – sequence located approximately six nucleotides upstream the initiation codon of the mRNA, to which ribosomes bind to initiate translation.

ORF – DNA region that contains the information for the sequence and structure of the gene product (usually a protein).

Terminator – DNA sequence present in the end of the gene that dictates the end of transcription. There are two types of terminators: the Rho-dependent, requiring the presence of the Rho protein for the termination of transcription to occur; and the Rho-independent, relying solely on the formation of a hairpin or stem-loop structure for the release of the RNA polymerase and the mRNA.

Transcription – process in which the information in a DNA sequence is converted into RNA by the enzyme RNA polymerase.

Translation – in this process, the information encoded in ribonucleotide sequences is converted into amino acid sequences. Protein synthesis is carried out by complexes composed of RNA and proteins – the ribosomes – that translate the information in the codons (groups of three nucleotides in mRNA) into specific amino acids to be incorporated into the nascent peptide.

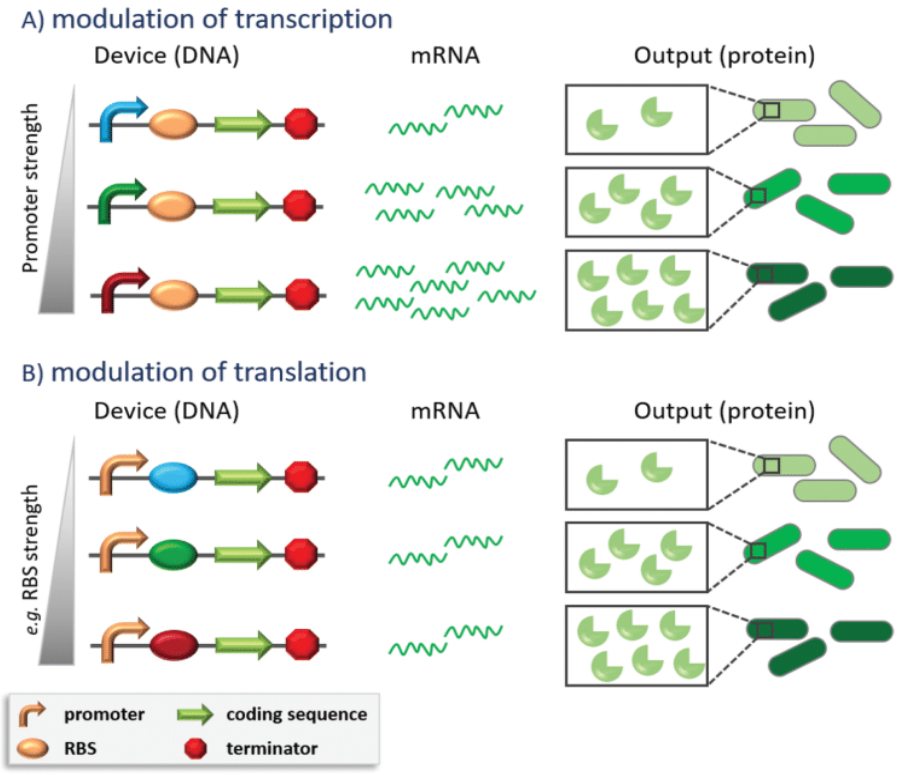

Figure 6.3: Schematic representation of the modulation of device regulation using standard biological parts. (A) Transcription can be regulated using promoters with different strengths (*e.g.* weak, medium or strong) leading to differential transcript (mRNA) levels that ultimately result in different protein levels. (B) At the translation level, the use of RBS with different strengths will not affect the mRNA levels, instead it will influence the recruitment of ribosomes that will carry out protein transcription. Translation can also be modulated using other types of biological parts like riboswitches or riboregulators. In the end, modulation of synthetic device regulation either at transcription or at translation will have an impact in the device output, *e.g.* chassis harboring GFP generators regulated by different elements can display different fluorescence levels.

6.3.1 Promoters

Promoters are crucial biological parts for the transcriptional regulation of genes in a synthetic circuit (Box: 6.2, Figure 6.3A). Cyanobacterial promoters can be categorized in three types (I, II and III), differing on the arrangement of the binding motifs. Type I promoters include both the –35 and –10 consensus elements spaced by 17 bp. Type II promoters have only the –10 box and can harbor enhancer-motif sequences or operators that bind activator proteins. Type III promoters are distinct from the first two, having –32 and –12 boxes spaced by 15 bp [101]. The transcription process is driven by the RNA polymerase holoenzyme, comprising a core enzyme and a sigma factor. The recognition and binding of the sigma factor to the operators is important for the efficiency of transcription initiation, and thus can define the strength of a promoter [102]. These regulatory elements can be organized in different categories depending on their origin and the host organism and are termed as native, heterologous, redesigned or synthetic promoters. When used in the native context, these regulatory parts have the advantage of responding to environmental stimuli in a dose-dependent manner, leading to the modulation of transcription [103]. On the other hand, these promoters are not insulated from the intrinsic regulation, which can lead to cross talk and compromise the predictability of the system. To overcome this limitation, promoters from other organisms or heterologous promoters have been commonly used. However, their characterization has shown that these elements can behave in a completely unexpected manner when in the genetic context of another organism [100, 104]. Consequently, the rational redesign of heterologous promoters and the generation of synthetic ones have been used as strategies to improve promoter insulation and efficiency [105, 106]. Another alternative to eliminate cross talk and ensure proper functionality/performance is the use of orthogonal parts. A successful example is the use of the bacteriophage T7 RNA polymerase to promote transcription that has been implemented in several prokaryotes, including cyanobacteria [107, 108].

Regarding the type of expression, constitutive promoters can be useful when an “always ON” gene expression is desired. However, for applications with a high metabolic burden, the use of this type of expression leads to toxicity/exhaustion of resources, hindering or impairing growth. In these situations, or when a more refined regulation is required, inducible promoters can be used having the obvious advantage that transcription is only “turned ON” when needed. Regulated promoters responding to many different stimuli have been reported, including light, metals, chemicals and metabolites, among others [105]. Despite the successful use of these regulatory elements in numerous applications, there are some disadvantages associated to their use. In the case of light-inducible promoters, there is the drawback of expression being dependent on specific light wavelength and intensity [109]. When metal- or chemical-inducible promoters are used, the inducer can be pumped out of the cells, degraded or cannot be removed from the culture resulting in lack of, or continuous expression [110, 111].

Overall, promoter characterization in cyanobacteria has been performed mainly for the model cyanobacterium *Synechocystis* 6803 (see Table 6.1, for a review see Till et al. [112]). Nevertheless, exciting progress is being made in characterizing and developing regulatory parts for *Synechococcus* 7002, *S. elongatus* 7942 (see Table 6.1) and also for the fast-growing strains *S. elongatus* 2973 and *S. elongatus* 11801 and 11802 [81, 113, 222]. The relentless search for promoters that are easy to use, have low leakiness and a dynamic range of induction and strength, is increasing the array of regulatory parts available in the cyanobacterial SB toolbox (Box: 6.2, Figure 6.3); which can be used in the construction of synthetic devices/circuits envisaging biotechnological applications using photoautotrophic organisms as chassis.

Table 6.1: Characteristics of promoters characterized in *Synechocystis* 6803, *Synechococcus* 7002 and *S. elongatus* 7942. The P*rnpB* is considered the reference promoter in cyanobacteria, with strength equal to 1. Therefore, the strength of constitutive promoters is presented relative to P*rnpB* whereas the strength of regulated promoters is represented as the ratio between induced versus non-induced expression.

Promoter	Source	Type of expression	Repressor (R)/ inducer (I) amount	Strength – output	Reference
Synechocystis 6803					
P*rnpB*	Native	Constitutive	NA	1-fold – GFPmut3B (Bba_E0040)	[100]
P*rbcL*	Native	Constitutive	NA	~1,000 fluorescence Abs_{730}^{-1} [AU] – EYFP	[114]
P*cpc560*	Native	Constitutive	NA	Up to 15% of total soluble proteins – Ter and DldhE	[115]
P*nirA*	Native	Constitutive	NA	~15,000 fluorescence Abs_{750}^{-1} [AU] – EYFP	[105]
P*cpcB*	Native	Constitutive	NA	~50,000 fluorescence Abs_{730}^{-1} [AU] – EYFP	[114]
P*rbcL* variants	Redesigned from *Synechocystis* 6803	Constitutive	NA	1–19-fold – GFPmut3B (Bba_E0040)	[100]
P*psbA2**	Synthetic from *Synechocystis* 6803	Constitutive	NA	6-fold – GFP	[108]

Table 6.1 (continued)

Promoter	Source	Type of expression	Repressor (R)/ inducer (I) amount	Strength – output	Reference
PJ23### library	Synthetic from *E. coli*	Constitutive	NA	~0–25,000 fluorescence Abs_{750}^{-1} [AU] – EYFP	[105]
P*trc*1O	Heterologous from *E. coli*	Constitutive	NA	83-fold – GFPmut3B, 2.4-fold – EFE, ~10,000 fluorescence Abs_{730}^{-1} [AU] – EYFP	[100, 114, 116]
P*trc.x. lacO*	Redesigned from *E. coli*	Constitutive	NA	41-fold – GFP	[108]
P*trc.x. tetO1*	Redesigned from *E. coli*	Constitutive	NA	13-fold – GFP	[108]
P*λcI*	Heterologous from bacteriophage λ	Constitutive	NA	20-fold – GFP	[108]
PT7pol	Orthogonal from bacteriophage T7	Constitutive	NA	0.13-fold – GFP	[108]
P*psbA2*	Native	Light inducible	30 µE m^{-2} s^{-1} (I)	~500 fluorescence Abs_{730}^{-1} [AU] – EYFP	[114]
P*cpcG2*	Native	Green light inducible (CcaS/CcaR)	20 µE m^{-2} s^{-1} (I)	40-fold – GFPuv	[109]
P*cpcG2*	Native	Red light inducible (CcaS#11/ CcaR)	30 µE m^{-2} s^{-1} (I)	22-fold – GFPuv	[117]
P*ompC*	Heterologous from *E. coli*	Dark inducible	NA	>100-fold – EYFP	[118]
P*nrsB*	Native	Nickel inducible	0.5–5 µM Ni^{2+} (I)	350× RT-PCR – *nrsB*, 39-fold – EYFP	[103, 111]
P*nrsD*	Native	Nickel inducible	5 µM Ni^{2+} (I)	14× – EYFP	[111]
P*nrsS*	Native	Nickel inducible	5 µM Ni^{2+} (I)	7× – EYFP	[111]
P*coaT*	Native	Cobalt inducible	3–30 µM Co^{2+} (I)	15× RT-PCR – *coaT*, ~ 0-fold – EYFP	[103, 111]

Table 6.1 (continued)

Promoter	Source	Type of expression	Repressor (R)/ inducer (I) amount	Strength – output	Reference
P*petE*	Native	Copper inducible	0 µM Cu^{2+} (I)	~10,000 fluorescence Abs_{750}^{-1} [AU] – EYFP	[105]
P*ziaA*	Native	Zinc inducible	4–5 µM Zn^{2+} (I)	30× RT-PCR – *ziaA*, ~ 0-fold – EYFP	[103, 111]
P*tac*	Synthetic, hybrid from *E. coli*	LacI repressible, ITPG inducible	1 mM IPTG (I)	24× – GFP	[119]
P*trc*1O	Heterologous from *E. coli*	LacI repressible, IPTG inducible	2 mM IPTG (I)	1.6-fold – GFPmut3B (Bba_E0040)	[100]
P*trc*2O	Redesigned from *E. coli*	LacI repressible, IPTG inducible	2 mM IPTG (I)	4-fold – GFPmut3B (Bba_E0040)	[100]
P*trc.x. lacO*	Redesigned from *E. coli*	LacI repressible, IPTG inducible	1 mM IPTG (I)	2.2-fold – GFP	[108]
PL03	Redesigned from *E. coli*	TetR repressible, aTc inducible	10 µg mL^{-1} aTc (I)	290-fold – EYFP	[110]
P*trc.x. tetO1*	Redesigned from *E. coli*	TetR repressible, aTc inducible	1 µg mL^{-1} aTc (I)	2.3-fold – GFP	[108]
PBAD variant	Redesigned from *E. coli*	Arabinose inducible	5 mM L-arabinose (I)	~50 $fluorescence_{730}^{-1}$ [AU] – EYFP	[118]
P*vanCC*	Redesigned from *Caulobacter crescentus*	VanR repressible, vanillate inducible	2 mM vanillate	16-fold – mVenus	[120]
P*rhaBAD*	Heterologous from *E. coli*	RhaS repressible, rhamnose inducible	1 µg mL^{-1} L-rhamnose (I)	~3,000 fluorescence intensity [AU] – YFP	[121]
P*nirA*	Heterologous from *S. elongatus* 7942	NH_4^+ repressible, NO_3^- inducible	10 µM NH^{4+} (R), 50 µM NO_3 (I)	~1,800 RLU Abs_{750}^{-1} – LuxAB	[122]

Table 6.1 (continued)

Promoter	Source	Type of expression	Repressor (R)/ inducer (I) amount	Strength – output	Reference
***S. elongatus* 7942**					
P*cpcB*	Native	High light repressible, CO_2 inducible	400 µE m^{-2} s^{-1} (R), 0.5% CO_2 (I)	~35,000 fluorescence Abs_{730}^{-1} [AU] – eYFP	[123]
P*trc*	Synthetic from *E. coli*	LacI repressible, ITPG inducible	1 mM IPTG (I)	36-fold – GUS, 24-fold – eYFP	[107, 124]
PT7	Orthogonal from bacteriophage T7	LacI repressible, ITPG inducible	0.01 mM IPTG (I)	6-fold – eYFP	[107]
P*tetA*	Heterologous from *E. coli*	TetR repressible, aTc inducible	100 nM aTc (I)	19-fold – GFP	[107]
P*BAD*	Heterologous from *E. coli*	Arabinose inducible	2 g L^{-1} L-arabinose (I)	~ 3,000 fluorescence Abs_{730}^{-1} [AU] – mtGFP	[125]
P*rbc*	Native	CO_2 repressible	0.5% CO_2 (R)	~4,000 fluorescence Abs_{730}^{-1} [AU] – eYFP	[123]
***Synechococcus* 7002**					
PA#### library	Native	Constitutive	NA	2–30-fold – Ypet	[126]
P*isiAB*	Native	Iron inducible	100 nM Fe (I)	2-fold – LuxAB	[127]
P*cpcB* library	Redesigned from *Synechocystis* 6803	LacI repressible, IPTG inducible	1 mM IPTG (I)	48-fold – YFP	[106]
P*EZtet*	Synthetic from *Synechocystis* 6803	TetR repressible, aTc inducible	1 µg mL^{-1} aTc (I)	32-fold – GFP	[128]
P*smtA*$_{7942}$	Heterologous from *S. elongatus* 7942	*smtB*$_{7942}$ repressible, zinc inducible	60 µM Zn^{2+} (I)	19-fold – YFP	[129]

NA – not applicable.

6.3.2 Ribosome binding sites

RBS are key features in the initiation of translation (Box: 6.2, Figure 6.3B), a process that starts with the binding of the ribosome to the Shine–Dalgarno (SD) sequence, present in the RBS at the 5′ end of a mRNA. The efficiency of the RBS to drive translation depends on the sequence-embedded context that dictates the distance between the SD sequence and the start codon (AUG), and the possible formation of secondary structures or interaction of RNA-binding proteins. The vast majority of studies performed in cyanobacteria involving the heterologous expression of genes, or the overexpression of native ones, used the RBS originally present in the sequence. The knowledge on RBS efficiency is scarce, making it difficult to anticipate the rate of protein synthesis when designing a synthetic device. A genomic comparison of SD sequences in 30 prokaryotic genomes was performed to unveil the role of these sequences in translation initiation and protein expression levels [130]. Based on this work, Heidorn et al. [37] designed an RBS sequence that is complementary to the anti-SD sequence (present in the ribosomes) of *Synechocystis* 6803, and termed it RBS*. The RBS* together with three BioBrick RBS – BBa_B0030, BBa_B0032 and BBa_B0034 – were characterized in this cyanobacterium and in *E. coli*. The RBS efficiency in *Synechocystis* was determined to be RBS* > B0030 > B0032 ~ B0034 while for *E. coli* the relative efficiency was found to be B0034 > B0030 > RBS* > B0032, thus reinforcing that the performance of parts is dependent on the organism's genomic context [37]. These RBS were included in a set of 11, together with other BioBrick RBS and native RBS sequences from *psbA2*, *rbcL* and *rnpB* genes, for further characterization [111]. RBS efficiencies were determined using two different constructs varying the promoter (P*petE* and P*psbA2*S) and the reporter (enhanced yellow fluorescent protein (EYFP) and mTagBFP) used; the 11 RBS showed a dynamic range in terms of expression strength with similar results for the two reporters tested, with the exception of BBa_B0035 and RBS* [111]. In addition, 20 native RBS were characterized in *Synechocystis* 6803 revealing that sequence embedded context and the RBS sequence length are determinant for protein expression, since no EYFP fluorescence was detected when using nine of the RBS tested [114]. An effort to develop synthetic RBS for different cyanobacteria using *in silico* modeling methods has been made in the last years [67, 106, 116, 131]. A synthetic RBS sequence was designed, considering *S. elongatus* 7942 as reference organism, and the expression of two different reporters was found to increase when the synthetic RBS was tested in four different cyanobacteria (*S. elongatus* 7942, *Synechocystis* 6803, *Nostoc* 7120 and *Leptolyngbya* LB0902) [67]. A set of 10 synthetic RBS was developed for *Synechococcus* 7002 using the RBS library calculator, having a predicted 213-fold range of translation initiation rate. However, the translation rates obtained empirically correlated poorly with the predictions providing only a 30-fold translation range [106]. Synthetic RBS libraries were also developed for *Synechocystis* 6803. Wang et al. [116] designed and constructed a library of 13 RBS based on the

previously described synthetic RBSv4. A complementary approach to the RBS prediction software was used by using design principles established to optimize RBS sequences in *E.coli* [132]. Therefore, using these principles, the RBSv4 sequence and length was modified as well as the spacer between the SD sequence and the ATG codon. The resulting 13 RBS were tested in *Synechocystis* 6803 and, a 254% increase in expression of the target protein was obtained using RBSv33 [116]. In addition, Thiel et al. [131] performed the systematic characterization of additional RBS in *Synechocystis* 6803, including cyanobacterial native and synthetic elements previously developed for *E. coli*. The RBS tested displayed a wide dynamic range of translation efficiencies that were shown to be dependent on downstream gene sequence. Different online prediction tools were used to identify factors underlying the reporter-protein-dependent RBS efficiency. However, the RNAfold [133] and mfold [134] algorithms did not identify any unfavorable interactions at the sequence level, while prediction by the RBS calculator [135] and untranslated region (UTR) designer [136] were significantly different from the empirical results [131]. The usefulness of these tools may be limited in cyanobacteria, as the software was primarily developed for *E. coli*, however, they may still be useful tools when designing libraries from scratch [116]. Alternative strategies have been developed to prevent interactions between the UTR and coding sequences that undermine the translation process. The bicistronic design involves two cistrons or genes of interest (GOI), the first of which consists of a short coding sequence (up to 20 amino acids) that harbors the RBS for the second GOI embedded in its 3′ end. The sequence of the first GOI is optimized for transcription/translation initiation and ensures the high expression of the second GOI that is the target gene [137]. This design architecture was applied to a toxin/antitoxin system meant for *Synechocystis* 6803 showing promising results, and was successfully used for the expression of two heterologous hydrogenases in this cyanobacterium [138].

6.3.3 RNA-based regulation

Numerous RNA-based regulation mechanisms have been described including riboregulators, riboswitches and small RNAs, the last two classes have been extensively studied due to its preponderant roles. Nevertheless, in the frame of SB, riboswitches and riboregulators have been the focus of attention and are reviewed below.

6.3.3.1 Riboswitches

Bacterial riboswitches are usually located in the 5′ UTR of an mRNA; these structures are comprised of an aptamer or ligand-binding domain and a regulatory domain or expression platform. The ligand can be a metabolite or a metal that binds to the aptamer and stabilizes this structure causing the conformational change and

further activation of the expression platform, thus mediating gene expression (Figure 6.4) [139, 140].

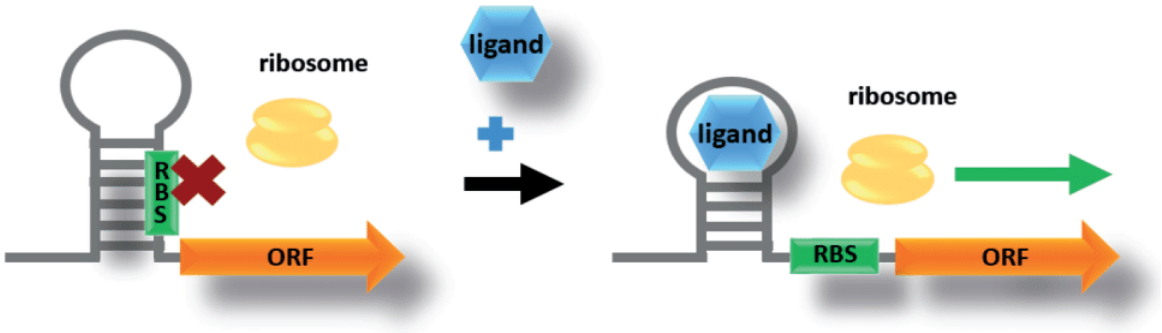

Figure 6.4: Schematic representation of the mechanism of regulation by an ON-riboswitch. A hairpin structure is formed in the 5' end of the mRNA, sequestering the RBS. Upon addition of the ligand (*e.g.* metabolite or metal) the riboswitch conformation is changed, exposing the RBS thus enabling translation initiation.

More than 20 riboswitch–ligand pairs have been identified including thiamin, flavin mononucleotide (FMN), *S*-adenosylmethionine, lysine, guanine/adenine and glycine. However, many of these molecules are not suitable to be used in genetic tools since they are important metabolites or can be cytotoxic [140]. The use of the theophylline-dependent riboswitch has been explored in cyanobacteria; in this system, the aptamer domain forms a hairpin sequestering the RBS and, upon addition of theophylline, the RBS is released and transcript translation is enabled. Nakahira et al. [141] tested three synthetic theophylline-dependent riboswitches (previously developed for *E. coli*) in *S. elongatus* 7942. The expression of luciferase was shown to increase between 33- and 190-fold in presence of theophylline, and dose-dependent expression could be observed between 0 and 2 mM, allowing the fine-tuning of expression [141]. The use of synthetic theophylline-dependent riboswitches was validated in *Synechocystis* sp. strain WHSyn, *Nostoc* 7120 and *Leptolyngbya* LB0902 using the YFP reporter [66]. The riboswitch showing the highest fold increase in luciferase expression in *S. elongatus* 7942, riboswitch E*, was also tested in *Synechocystis* 6803 demonstrating that GFP expression could be detected with a 6-fold increase between 0.1 and 1 mM of theophylline [142]. In addition, this riboswitch was also validated as a tool for the control of translation in *S. elongatus* 2973 showing low leakage levels and a linear response to increasing concentrations of theophylline with a protein increase up to 100-fold [143]. In this work, two other riboswitches responding to theophylline (*theo/yitJ*) and adenine (*xpt(C74U)/metE*) were also shown to be functional in *S. elongatus* 2973. In the presence of ligands, these riboswitches work as transcription inhibitors and the response was demonstrated to be dose-dependent, with a 50% repression of transcription in the presence of 2 mM of theophylline or adenine (increasing up to 80% upon addition of 5 mM of the ligands). Additionally, a cobalamin

transcriptional OFF-riboswitch was identified in *Synechococcus* sp. strain PCC 73109 and validated in *Synechococcus* 7002, showing a significant translation inhibition in the presence of 4 μg L^{-1} of cobalamin [144].

6.3.3.2 Riboregulators

Riboregulators can be used in the regulation of translation. These tools are composed by two independent RNA fragments: the *trans*-activating RNA (taRNA) and *cis*-repressed RNA (crRNA). Upon transcription, the crRNA sequence forms a loop structure in the 5′ UTR of the mRNA of interest, interfering with the respective RBS and leading to translation repression. When the taRNA is expressed, it targets the crRNA causing an alteration in the loop structure that activates translation (Figure 6.5) [145].

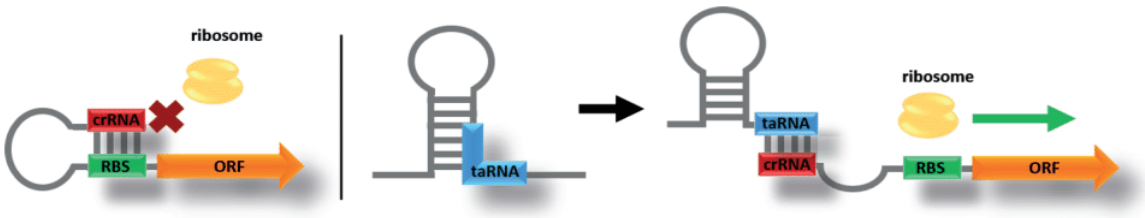

Figure 6.5: Schematic representation of the mechanism of regulation by a riboregulator. The *cis*-repressed RNA (crRNA) sequence forms a loop structure in the 5′ UTR of the mRNA of interest, sequestering the respective RBS. The *trans*-activating RNA (taRNA) binds to the crRNA leaving the RBS exposed, which activates translation.

The first riboregulators designed for *Synechocystis* 6803 were based on the riboregulator crR12/trR12 previously developed for *E. coli* [146, 147]. The RBS present in the crR12 was replaced by the RBS* and additional mismatches were introduced in the stem region of the crRNA to allow high activation in presence of the taRNA and low background transcription in its absence. Following this strategy, two riboregulators were generated – crR*1/trR*1 and crR*2/trR*2 – and tested in *E. coli*. The crR*2/trR*2 riboregulator showed the highest ON/OFF ratio in *E. coli*, and was subsequently tested in *Synechocystis* 6803 also showing to be an effective tool in the regulation of translation in this cyanobacterium [147]. This riboregulator was further improved using a rational design approach based on RNA secondary structure and prediction of hybridization using free-energy values [148]. Using this approach, the crR*4/trR*4 riboregulator was developed and a 51-fold induction in translation was detected in *Synechocystis* 6803, a significant improvement compared to the 19-fold induction observed with crR*2/trR*2. The addition of two AA nucleotides in the 3′ end of the crR*4 sequence led to an increase in RBS accessibility upon crR4*/trR*4 hybridization, which resulted in an improvement of the fold induction to 78 [148].

A tool for the attenuation of translation was developed for *Synechococcus* 7002; this system is based on the *E. coli* IS10 RNA-IN/OUT regulator. When expressed, the small RNA or RNA-OUT will target the RNA-IN present in 5′ UTR of the mRNA reducing translation of the target gene by 70% [128].

6.3.4 Degradation tags

Degradation tags are used as post-transcriptional tools to control protein levels by reducing their stability. These tags are based on the small stable RNA A (*ssrA*) from *E. coli* that works a rescue system: when problems occur in protein translation, the ssRA adds a 11 codon degradation tag and a stop codon to the mRNA, enabling the detachment of the ribosome and targeting the incomplete protein to degradation by proteases. Keiler and Sauer [149] reported that alterations in the final three amino acids of the C-terminal peptide to AAV, ASV, LVA and LAA affect protein stability differently, resulting in different protein half-life. The degradation tags available in the BioBricks – ASV (BBa_E0436), AAV (BBa_E0434) and LVA (BBa_E0432) – were characterized in *Synechocystis* 6803. The stability of the EYFP was evaluated after 48 h revealing that all tags are functional, with the LVA tag having the highest impact in reduction of protein stability followed by the AAV and ASV [100]. Landry et al. [150] generated a collection of C-terminal protein degradation tags based on the consensus for *ssrA* tag sequences determined using the information from 71 cyanobacterial genomes. The collection is comprised of native cyanobacterial and *E. coli* tags and its variants, and was tested in *Synechocystis* 6803 using EYFP as a reporter. The assessment revealed that EYFP fusion with the developed tags resulted in a fluorescence reduction ranging from 50% to 99% [150].

6.3.5 Reporter proteins

Characterization of synthetic parts, devices and circuits often requires a reporter system that enables the detection of an output signal correlated with expression, interaction or localization of a protein. Ideally, the system should not implicate destruction of the biological sample or require additional inputs and it should be easy to detect, with high sensitivity allowing the detection of low signal levels. Bioluminescent assays have been extensively used in cyanobacteria, namely, the luciferase-based systems that use luciferin as substrate generating light as a product [151]. These reporter systems generate dim signals that make them highly quantitative and extremely useful for real time reporting due to the short half-life of its components [152]. In comparison, fluorescent proteins generate signals with higher brightness making them more suitable for subcellular localization or cell-sorting purposes. The use of these reporters in cyanobacteria can be difficult due to autofluorescence of the

photosynthetic pigments that limits the use of red fluorophores [153]. Nevertheless, fluorescent proteins emitting light in other wavelengths are available and, for example, the cerulean (blue), GFPmut3b mutant of the green fluorescent protein and EYFP have been used in cyanobacteria [100]. New variants and fluorophores have been developed by increasing solubility (super folder variants), brightness or photostability [34, 154]. In addition, the use of degradation tags to reduce the half-life of the reporter proteins can increase the range of applications [155]. Bacterial luciferases and traditional fluorescent proteins require oxygen to work properly, thus their use is not recommended under oxygen-depleted conditions as happens during dark cycles [82]. FMN-based fluorescent protein that works under anaerobic conditions was already used for the development of an oxygen sensor in *Synechocystis* 6803 [156].

6.3.6 Terminators

Transcriptional terminators can be used to insulate a synthetic device or circuit preventing cross talk between this device/circuit and the genetic elements in the vicinity. There are two main types of terminators: (i) the Rho-dependent, which require the Rho protein for unwinding the RNA–DNA hybrid and thus preventing RNA elongation and (ii) the intrinsic or Rho-independent, which it relies on the formation of a hairpin loop secondary structure in the nascent RNA strand that once formed leads to the dissociation of the elongation complex. In the latter, termination is intrinsic to the nucleotide sequence of the RNA composed by an adenosine-rich tract (A-tract) located upstream the loop that includes a 4–18 bp GC-rich stem and 3–5 bp loop nucleotides followed by a 6–8 bp highly conserved uracil-rich tract (U-tract) [157].

So far, no Rho homologues have been found in cyanobacterial genomes. An analysis of the RNA-folding energetics near stop codons in *Synechocystis* 6803, did not indicate the formation of hairpin loop structures at these sites, suggesting that this is not a predominant mechanism in this cyanobacterium [158, 159]. The same observation was not confirmed in *S. elongatus* 7942 with the analysis of the RNA free energies suggesting the formation of discrete stem loop structures closer to the 3′ end of genes [159]. A few terminator sequences have been used in cyanobacteria, including the native RuBisCO terminator, the *rrnB* terminator (*E. coli*), the T7 terminator and the BioBrick double terminators *rrnBT1-T7TE* (BBa_B0015) [160]. Four other terminators retrieved from BioBrick registry, including the artificial terminator BBa_B1006, the *rrnC* terminator (*E. coli*, BBa_B0052) and its reverse sequence (BBa_B0062), and the reverse sequence from terminator *rrnBT1* (BBa_B0010) were used to insulate a synthetic multiple cloning site included in vectors targeting five *Synechocystis* 6803 genome *loci* [161]. In this work, the successful insulation of GFP generator device integrated into five chromosome *loci* was demonstrated. More recently, the systematic evaluation of two libraries of terminators was performed in *Synechocystis* 6803 [114, 162]. One of the sets included the *rrnB* terminator and seven

native elements, and the results showed that none of the terminators were able to completely abolish transcription of the reporter, not even the strong *E. coli rrnB* terminator. The performance of these elements showed a 10-fold variation, with the *psbC* terminator showing the highest efficiency [114]. Kelly et al. [162] characterized a set of 19 Rho-independent terminators including synthetic, heterologous (*E. coli* and bacteriophage) and one native element. From this set, 11 revealed to be strong transcriptional terminators, as negligible fluorescence levels were registered during the course of the experiments (96 h). Four of these terminators were further validated showing that they can be used for the insulation of a synthetic device (YFP generator) from its genomic context [162].

6.3.7 Replicative plasmids, integrative plasmids and neutral sites

These tools are essential for the genetic manipulation of microorganisms, serving as vehicles for the introduction of exogenous DNA into cells. For this purpose, replicative or integrative plasmids can be used depending on stability or type of application required. In general, replicative plasmids are used for fast generation of transformants. These shuttle vectors can harbor broad-host range replicons that allow its replication in different organism or can have specific replicons, usually isolated from endogenous plasmids that function in a restricted number of organisms. The replicative plasmids available for cyanobacteria are limited, in particular the broad-host range type, most of which are derived from the RSF1010 [37, 160]. In the last decade, an effort has been made in the development of new plasmids with a modular organization to facilitate standardization and envisaging the cloning and characterization of parts and devices. The pPMQAK1 was the first BioBrick compatible replicative plasmid developed for cyanobacteria, which was validated for *Synechocystis* 6803, *Nostoc* 7120 and *Nostoc punctiforme* [100]. The development of additional self-replicating vectors based on native cyanobacterial plasmids such as pANS from *S. elongatus* 7942 and, pCA2.4, pCB2.4 and pCC5.2 from *Synechocystis* 6803 was also reported [114, 163, 164]. The new plasmids exhibit interesting new features such as the ability to replicate in other hosts (e.g., *E.coli* or *Nostoc* 7120), long-term maintenance in absence of selective pressure, high-copy number or stable co-existence with RSF1010-based plasmids. In addition, the use of replicative vectors from the modular SEVA system based on the RSF1010 and RK2 origins of replication was also validated in *Synechocystis* 6803 [108, 113, 165].

For long-term stable integration of exogenous DNA, integrative or suicide plasmids are used, which are unable to replicate in the host and so the DNA they carry must integrate before the plasmid is eliminated. Integration vectors can be used for the targeted insertion of the DNA and thus must harbor recombination arms homologous to the DNA sequences flanking the site targeted for integration. If a single

recombination event occurs, it leads to the integration of the whole plasmid whereas a double recombination event will result in the replacement of the target *locus* by the DNA construct present between homologous regions. The efficiency of DNA integration varies with the size of the flanking regions and it was also shown to be strain dependent [37]. Since cyanobacteria usually harbor multiple copies of the chromosome or of the native plasmids, the generation of mutants is a time-consuming task since the introduction of the mutation in all genome copies will require several segregation steps under increasing selective pressure.

The increasing complexity of synthetic designs will eventually require several integration sites to accommodate different devices in a given chassis. The disruption of these *loci* should not have any effect on the viability or phenotypic traits of the chassis, and thus are termed neutral sites [166]. In the last decades, a few integration sites have been used in cyanobacteria, presuming their neutrality without any extensive characterization [167–170]. The identification of neutral sites, located either in the chromosome or in the native plasmids, was recently performed in *Synechocystis*, *S. elongatus* 7942 and *Synechococcus* 7002 [107, 161, 171–173]. Ng et al. [171] report the characterization of three neutral sites in *Synechocystis* 6803, one targeting the native plasmid pCC5.2 and two in the chromosome. The integration of EYFP in these *loci* revealed that expression from the plasmid was 14-fold higher compared to the chromosome, and in the latter expression levels obtained for both sites was equivalent [171]. Five additional chromosomal neutral sites were identified and validated in *Synechocystis* 6803; the characterization included an evaluation of the sites neutrality and showed that the sites are equivalent in terms of expression [161]. Moreover, the plasmids targeting these neutral sites include a multiple cloning site compatible with the BioBrick system and includes double terminators that guarantee the insulation of the synthetic devices. Three chromosomal neutral sites were validated in *Synechococcus* 7002; the integration of a kanamycin resistance cassette in these *loci* had a minor impact in the chassis fitness and, in addition, integrative vectors compatible with the BioBrick system were developed [172]. Envisaging the expansion of the neutral sites set available for this cyanobacterium, the identification of 51 putative genome neutral sites was performed based on genomic and transcriptomics data [173]. This work also reported the validation of a site located in the intergenic sequence between two neutral sites as a suitable region to be used for the efficient integration of synthetic devices.

Modular systems for the construction of plasmids dedicated to cyanobacteria have been developed. Similar to the pSEVA system [165], the CYANO-VECTOR web server (http://golden.ucsd.edu/CyanoVECTOR) can be used for the *in silico* design of replicative (narrow or broad range) or integrative plasmids and, in addition, several selection markers and expression or reporter cassettes can be selected [67]. This system was tested in several cyanobacterial strains, such as *Nostoc* 7120, *Leptolyngbya* BL0902, *Synechocystis* 6803, *Synechocystis* WHSyn, *S. elongatus* 7942, *Synechococcus* 7002. An additional SB platform for expression in *S. elongatus* 7942 was developed, simplifying the

construction of SyneBrick vectors that include replicative and integrative vectors harboring different antibiotic resistance cassettes and expression systems [107]. More recently, a cloning suite for cyanobacteria – the CyanoGate – was developed based on the standardized modular cloning system – MoClo, previously developed for plants [113]. Besides the construction of different vectors for the expression and integration of DNA, this cloning suite envisages the design and construction of multigene expression system based on the MoClo syntax. The system was tested and validated using the model *Synechocystis* 6803 and the fast-growing *S. elongatus* 2973.

6.3.8 Generation of markerless knockout mutants

For decades, the generation of knockout mutants in cyanobacteria was mainly carried out by homologous recombination. The generation of markerless mutants through this process requires two rounds of transformation, in the first round a double selection cassette usually harboring an antibiotic resistance and a counter-selection marker replaces the gene to be deleted and, transformants are selected screening for the antibiotic resistance phenotype. In the second round, the selection cassette is replaced by the flanking regions of the gene previously deleted based on the counter-selection method [174]. The counter-selection method more commonly used in cyanobacteria involves the *sacB* gene (conferring sensitivity to sucrose), even though other systems based on the *mazF* toxin, *rps12* mutation, and *aaS*, *acsA* or *nblA* knockouts have been described for *Synechocystis* 6803, *S. elongatus* 7942 and 2973 and *Synechococcus* 7002 [56, 175–178].

Recent techniques for genome editing such as, zinc fingers (ZFNs), transcription activator-like effector nucleases (TALENs) and CRISPR/CRISPR-associated protein (Cas) rely on native or engineered nucleases for the introduction of strand breaks at specific sites in the genome [179]. However, the use of ZFNs and TALENs in bacteria was limited due to the restricted target specificity and customized engineering required by these techniques. On the other hand, CRISPR/Cas (see Chapter 2) has rapidly become popular for cyanobacterial engineering by drastically reducing the time needed to obtain mutants and allowing the manipulation of several genes at the same time [51]. Briefly, the CRISPR/Cas method is able to target a nuclease to a specific site in a very precise manner determined by the single-guide RNA (sgRNA) that has a complementary sequence to the target DNA site. The sgRNA assembles with the Cas9 or Cas12a (Cpf1) to form an effector complex and, depending on the CRISPR system, this complex has different requirements to be active. The CRISPR/Cas9 requires two separate RNA sequences, the crRNA that encodes the guide sequence and a trans-activating crRNA (tacrRNA) whereas the CRISPR/Cas12a (Cpf1) system

requires a single crRNA [34]. After the double-stranded cleavage of the genome, the DNA repair system known as homology-directed repair is induced and, if an appropriate repair template is provided, specific mutations or deletions can be introduced in the target site. The CRISPR/Cas system can also be used as tool for regulation of gene expression, the CRISPR interference (CRISPRi) methodology uses a variant of the Cas9 – the deficient or dead Cas9 (dCas9) – that maintains the ability to bind the target DNA with the sgRNA but is unable to cleave DNA. Yao et al. [50] used CRISPRi to repress *gfp* expression, to inhibit the production of polyhydroxybutyrate and glycogen, and inhibit simultaneously four aldehyde reductases/dehydrogenase in *Synechocystis* 6803. CRISPRi was used again for gene repression in this cyanobacterium leading to an increase in the production of fatty alcohols and *n*-butanol [180, 181]. This methodology has also been extended to other cyanobacterial strains, including *Synechococcus* 7002, *S. elongatus* 7942 and *Nostoc* 7120 [75, 182, 183]. More recently, an inducible CRISPRi library including 10,498 clones for *Synechocystis* 6803 was generated, enabling system-wide analysis of gene essentiality and function [184]. This pooled library was used to explore increased L-lactate production and tolerance, demonstrating the potential for screening mutants with improved industrial phenotypes. The use of the CRISPR/Cas9 system for gene knockout and knock-in was first demonstrated in *S. elongatus* 7942, deleting the *glgC* and introducing the *gltA* and *ppc* genes that resulted in an increased succinate production [185]. Moreover, a Cas9-based tool was used for the deletion of 3 native plasmids of *Synechocystis* 6803 [186].

The Cas9 protein revealed to be toxic in *S. elongatus* 2973 but this hurdle was overcome by the conditional expression of this protein [56]. An alternative system using the Cas12a (Cpf1) was successfully used for genome editing in *Nostoc* 7120, *Synechocystis* 6803, *S. elongatus* 7942, displaying no signs of toxicity [187, 188]. Recently, the CRISPRi methodology using the deficient or dead Cas12a – dCas12a was also applied to *S. elongatus* 7942, *S. elongatus* 2973 [189, 190]. In addition, the development of reversibly induced CRISPRi system aiming at knocking down and recovering the expression of target genes was reported for *Synechocystis* 6803 [191]. For more detailed reviews on genome editing technologies, see for example, Lin et al. [192], Ng et al. [193] and Zhang et al. [194].

6.4 Using a SB approach for industrial biotechnology

Cyanobacteria are continuously being engineered to produce compounds with varied chemical properties and with potential uses as biofuels, pharmaceuticals, feed and food supplements, plastic precursors, among others. Several studies have shown

that it is possible not only to optimize native cyanobacterial production pathways by redirecting metabolic fluxes towards the product of interest, but also to use cyanobacteria as hosts of heterologous biosynthetic pathways. In this context, multiple metabolic engineering approaches have been described but those using a SB-based design are more limited. In Table 6.2, we present a selection of compounds that have been produced by various cyanobacterial strains using such principles, as to illustrate the potential of combining the metabolic plasticity of cyanobacteria with this consolidated discipline.

Table 6.2: Selection of works describing engineering of cyanobacteria with a SB-based design for the production of various types of compounds.

Strain	Product	Production rate or capacity	Reference
Cyanothece 7425	Limonene	0.6–1.0 mg L^{-1}	[195]
Nostoc 7120	Ammonium	200 µM in 4 days	[182]
Nostoc 7120	Cryptomaldamide	15.3 mg g^{-1} (DCW) in 3 weeks	[196]
Synechococcus 7002	Mannitol	0.1 g L^{-1}	[197]
S. elongatus 2973	Lytic polysaccharide monooxygenase	779 µg L^{-1}	[198]
S. elongatus 2973	Indole–isonitrile biosynthetic intermediates and hapalindoles H and 12-*epi*-hapalindole U	0.75–3 mg L^{-1}	[199]
S. elongatus 2973 (in a consortium with *E. coli*)	3-Hydroxypropionic acid	68.29 mg L^{-1}	[200]
S. elongatus 7942	Sucrose	36.1 mg L^{-1} h^{-1}	[201]
S. elongatus 7942 (in a consortium with *Halomonas boliviensis*)	Polyhydroxybutyrate	28.3 mg L^{-1} day^{-1}	[202]
S. elongatus 7942 (in a consortium with *E. coli*)	Polyhydroxybutyrate	0.3 mg L^{-1} in 7 days	[203]
S. elongatus 7942 (in a consortium with *Pseudomonas putida*)	Polyhydroxyalkanoates	23.8 mg L^{-1} d^{-1}	[204]
S. elongatus 7942	3-Hydroxybutyrate	1.22 g L^{-1} in 28 days	[205]

Table 6.2 (continued)

Strain	Product	Production rate or capacity	Reference
S. elongatus 7942	Limonene	0.0763 mg L^{-1} OD^{-1} day^{-1}	[206]
S. elongatus 7942	1-Butanol	14.5 mg L^{-1} in 7 days	[207]
S. elongatus 7942	Isobutyraldehyde	450 mg L^{-1} in 6 days	[208]
S. elongatus 7942	2,3-Butanediol	761 mg L^{-1} in 48 h	[209]
Synechocystis 6803	Lactate	0.0058 mmol g^{-1} (DCW) h^{-1}	[210]
Synechocystis 6803	3-Hydroxybutyrate	533.4 mg L^{-1} in 21 days	[211]
Synechocystis 6803	Squalene	0.67 mg $OD_{750}{}^{-1}$ L^{-1}	[212]
Synechocystis 6803	Manoyl oxide	0.45 mg g^{-1} (DCW)	[213]
Synechocystis 6803	Isoprene	2.8 mg g^{-1} (DCW)	[214]
Synechocystis 6803	Ethanol	160 mg L^{-1} in 8 days	[111]
Synechocystis 6803	Ethanol	200 mg L^{-1} in 7 days	[215]
Synechocystis 6803	Isobutanol	3 mg L^{-1} $OD_{750}{}^{-1}$ in 6 days	[216]
Synechocystis 6803	Alkanes	77.1 mg g^{-1} (DCW)	[217]
Synechocystis 6803	1-Octanol and 1-decanol	80 mg g^{-1} (DCW)	[218]
Synechocystis 6803	2,3-Butanediol	6.5 mmol L^{-1} in 29 days	[219]
Synechocystis 6803	Shinorine	2.37 mg g^{-1} (DCW)	[220]
Synechocystis 6803	Mannitol	>5 µM for 12 days	[221]

DCW – dry cell weight.

6.5 Current limitations and future perspectives

In the last years, significant developments in cyanobacterial SB have been reported demonstrating the potential to use these photoautotrophic bacteria as chassis. Research has focused in the use of the model cyanobacteria but recently the array of prospective chassis has increased. The isolation and characterization of more robust and fast-growing strains embraces the new model of chassis with optimal performances in different scenarios thus leaving behind the paradigm of the universal chassis. The continuous survey of novel cyanobacterial biodiversity will certainly contribute to the discovery of new strains with attractive characteristics. In addition, the exponential increase in the number of sequenced cyanobacterial genomes available and the developments in the generation of genome-scale metabolic models has enabled the rapid establishment of these tools for the fast-growing strains. Nevertheless, the use of these models and the FBA is difficult due to the lack of user-friendly tools. The development of such tools will allow researcher to perform the constraint-based genome-scale analysis with significant contributions for metabolic engineering by the identification of regulatory hotspots, potential bottlenecks, gene knockouts and knock-ins. Future developments in genome streamlining and synthesis will also contribute to improve or generate new chassis with customized performances for specific purposes.

A significant number of SB tools have been developed and characterized already enabling the implementation of successful metabolic engineering strategies. Still there are important gaps that need to be filled namely the development of efficient inducible systems for the control of gene expression. For some of the currently available inducible systems, like the IPTG- and the aTc-regulated, high levels of repression have been achieved but, in most cases, the levels of derepression are very modest. The rational design of regulatory parts has been significantly hampered by the lack of predictive tools, which aid in the design of parts such as promoters and RBS. Moreover, these strategies can generate a high number of variants, therefore requiring high-throughput methodologies for their evaluation. Single-cell strategies have been developed using polyhydroxybutyrate, L-lactate or resorufin as reporters. Further refinements in these methodologies may decrease costs and thus increase their applicability in the future. The development and evaluation of libraries of parts and its variants might facilitate a better understanding of complex phenotypes related to the sequence-embedded context that has a deep impact on the performance of RBS and promoter/RBS preventing behavior predictability. The issues related to rational design of parts is significantly delaying the development of logic gate-based regulation that provides higher-level functions required by complex circuits.

Polyploidy is a significant aspect affecting the genetic manipulation of cyanobacteria that turns transformation into a time-consuming process. The recent developments in genome editing techniques based on the CRISPR/Cas system promise to revolutionize the generation of mutants in cyanobacteria. Nevertheless, polyploidy

goes hand in hand with gene dosage, a criterion that must be considered in the design of strategies. For this reason, it is important to further study the polyploidy phenomenon in cyanobacteria since it will affect the performance of synthetic devices and circuits that are integrated in the chromosome or the native plasmids.

Future advances regarding the abovementioned aspect and others, such as optimization of large-scale cultivation and downstream processing, and the development of efficient cost-effective photobioreactors will be determinant for the success of cyanobacteria as effective industrial chassis.

References

[1] Serrano L. Synthetic biology: promises and challenges. Mol Syst Biol. 2007, 3, 158.
[2] Vermeire T, Epstein M, Hartemann P, Prokovya A, Farre ER, Martinez LM, et al. Opinion on synthetic biology I – Definition. European Commission, Directorate-General for Health and Food Safety; 2014.
[3] Endy D. Foundations for engineering biology. Nature. 2005, 438(7067), 449–453.
[4] Andrianantoandro E, Basu S, Karig DK, Weiss R. Synthetic biology: new engineering rules for an emerging discipline. Mol Syst Biol. 2006, 2, 2006.0028.
[5] Boyle PM, Silver PA. Parts plus pipes: synthetic biology approaches to metabolic engineering. Metab Eng. 2012, 14(3), 223–232.
[6] Purnick PE, Weiss R. The second wave of synthetic biology: from modules to systems. Nat Rev Mol Cell Biol. 2009, 10(6), 410–422.
[7] Knight T. Idempotent Vector Design for Standard Assembly of Biobricks. Cambridge, MA, MIT, 2003.
[8] Anderson J, Dueber JE, Leguia M, Wu GC, Goler JA, Arkin AP, et al. BglBricks: a flexible standard for biological part assembly. J Biol Eng. 2010, 4(1), 1.
[9] Raik. The BioBricks Foundation:Standards/Technical/Formats 2008 [updated april 2012. Available from: https://openwetware.org/wiki/The_BioBricks_Foundation:Standards/Technical/Formats.
[10] Gibson DG, Young L, Chuang RY, Venter JC, Hutchison III CA, Smith HO. Enzymatic assembly of DNA molecules up to several hundred kilobases. Nat Methods. 2009, 6, 343.
[11] Engler C, Gruetzner R, Kandzia R, Marillonnet S. Golden gate shuffling: a one-pot DNA shuffling method based on type IIs restriction enzymes. PLoS ONE. 2009, 4(5), e5553.
[12] Engler C, Kandzia R, Marillonnet S. A one pot, one step, precision cloning method with high throughput capability. PLoS ONE. 2008, 3(11), e3647.
[13] Weber E, Engler C, Gruetzner R, Werner S, Marillonnet S. A modular cloning system for standardized assembly of multigene constructs. PLoS ONE. 2011, 6(2), e16765.
[14] Pollak B, Cerda A, Delmans M, Álamos S, Moyano T, West A, et al. Loop assembly: a simple and open system for recursive fabrication of DNA circuits. New Phytol. 2019, 222(1), 628–640.
[15] Rettberg R. Standards/Assembly/Type IIS 2019 [updated june 2021. Available from: http://parts.igem.org/Help:Standards/Assembly/Type_IIS.
[16] iGem Foundation. International genetically engineered machine competition 2015 [updated january 2019. Available from: https://igem.org/Competition.
[17] Rettberg R. Registry of Standard Biological Parts 2008 [updated 29 june. Available from: http://parts.igem.org/Main_Page.

[18] Chi H, Wang X, Shao Y, Qin Y, Deng Z, Wang L, et al. Engineering and modification of microbial chassis for systems and synthetic biology. Synth Syst Biotechnol. 2019, 4(1), 25–33.
[19] Fraser CM, Gocayne JD, White O, Adams MD, Clayton RA, Fleischmann RD, et al. The minimal gene bomplement of *Mycoplasma genitalium*. Science. 1995, 270(5235), 397–404.
[20] Glass JI, Assad-Garcia N, Alperovich N, Yooseph S, Lewis MR, Maruf M, et al. Essential genes of a minimal bacterium. Proc Natl Acad Sci U.S.A. 2006, 103(2), 425–430.
[21] Gibson DG, Glass JI, Lartigue C, Noskov VN, Chuang RY, Algire MA, et al. Creation of a bacterial cell controlled by a chemically synthesized genome. Science. 2010, 329(5987), 52–56.
[22] Hutchison CA, Chuang RY, Noskov VN, Assad-Garcia N, Deerinck TJ, Ellisman MH, et al. Design and synthesis of a minimal bacterial genome. Science. 2016, 351(6280), aad6253.
[23] Adams BL. The next generation of synthetic biology chassis: moving synthetic biology from the laboratory to the field. ACS Synth Biol. 2016, 5(12), 1328–1330.
[24] Gu Y, Xu X, Wu Y, Niu T, Liu Y, Li J, et al. Advances and prospects of *Bacillus subtilis* cellular factories: from rational design to industrial applications. Metab Eng. 2018, 50, 109–121.
[25] Gong Z, Nielsen J, Zhou YJ. Engineering robustness of microbial cell factories. Biotechnol J. 2017, 12(10), 1700014.
[26] Vickers CE, Williams TC, Peng B, Cherry J. Recent advances in synthetic biology for engineering isoprenoid production in yeast. Curr Opin Chem Biol. 2017, 40, 47–56.
[27] Dai Z, Liu Y, Guo J, Huang L, Zhang X. Yeast synthetic biology for high-value metabolites. FEMS Yeast Res. 2015, 15(1), 1–11.
[28] Li M, Borodina I. Application of synthetic biology for production of chemicals in yeast *Saccharomyces cerevisiae*. FEMS Yeast Res. 2014, 15(1), 1–12.
[29] Zhu L, Zhu Y, Zhang Y, Li Y. Engineering the robustness of industrial microbes through synthetic biology. Trends Microbiol. 2012, 20(2), 94–101.
[30] Westfall PJ, Pitera DJ, Lenihan JR, Eng D, Woolard FX, Regentin R, et al. Production of amorphadiene in yeast, and its conversion to dihydroartemisinic acid, precursor to the antimalarial agent artemisinin. Proc Natl Acad Sci U.S.A. 2012, 109(3), 111–118.
[31] Xiong W, Cano M, Wang B, Douchi D, Yu J. The plasticity of cyanobacterial carbon metabolism. Curr Opin Chem Biol. 2017, 41, 12–19.
[32] Al-Haj L, Lui YT, Abed RMM, Gomaa MA, Purton S. Cyanobacteria as chassis for industrial biotechnology: progress and prospects. Life. 2016, 6(4), 42.
[33] Vavitsas K, Crozet P, Hamborg Vinde M, Davies F, Lemaire SD, Vickers CE. The synthetic biology toolkit for photosynthetic microorganisms. Plant Physiol. 2019, 181, 14–27.
[34] Santos-Merino M, Singh AK, Ducat DC. New applications of synthetic biology tools for cyanobacterial metabolic engineering. Front Bioeng Biotechnol. 2019, 7, 33.
[35] Lopo M, Navarro E, Montagud A, Cunha I, Zille A, Córdoba PF, et al. Experimental and modelling analysis of *Synechocystis* sp. PCC 6803 growth. J Mol Microbiol Biotechnol. 2012, 22(2), 71–82.
[36] Yu J, Liberton M, Cliften PF, Head RD, Jacobs JM, Smith RD, et al. *Synechococcus elongatus* UTEX 2973, a fast growing cyanobacterial chassis for biosynthesis using light and CO_2. Sci Rep. 2015, 5, 8132.
[37] Heidorn T, Camsund D, Huang HH, Lindberg P, Oliveira P, Stensjö K, et al. Synthetic biology in cyanobacteria: engineering and analyzing novel functions. Methods Enzymol. 2011, 497, 539–579.
[38] Berla BM, Pakrasi HB. Upregulation of plasmid genes during stationary phase in *Synechocystis* sp. strain PCC 6803, a cyanobacterium. Appl Environ Microbiol. 2012, 78(15), 5448–5451.

[39] Labarre J, Chauvat F, Thuriaux P. Insertional mutagenesis by random cloning of antibiotic resistance genes into the genome of the cyanobacterium *Synechocystis* strain PCC 6803. J Bacteriol. 1989, 171(6), 3449–3457.
[40] Zerulla K, Ludt K, Soppa J. The ploidy level of *Synechocystis* sp. PCC 6803 is highly variable and is influenced by growth phase and by chemical and physical external parameters. Microbiology. 2016, 162(5), 730–739.
[41] Kaneko T, Sato S, Kotani H, Tanaka A, Asamizu E, Nakamura Y, et al. Sequence analysis of the genome of the unicellular cyanobacterium *Synechocystis* sp. strain PCC 6803. II. Sequence determination of the entire genome and assignment of potential protein-coding regions. DNA Res. 1996, 3(3), 109–136.
[42] Barrios-Llerena ME, Chong PK, Gan CS, Snijders APL, Reardon KF, Wright PC. Shotgun proteomics of cyanobacteria – Applications of experimental and data-mining techniques. Brief Funct Genomics. 2006, 5(2), 121–132.
[43] Schmitt Jr. WA, Stephanopoulos G. Prediction of transcriptional profiles of *Synechocystis* PCC 6803 by dynamic autoregressive modeling of DNA microarray data. Biotechnol Bioeng. 2003, 84(7), 855–863.
[44] Ow SY, Wright PC. Current trends in high throughput proteomics in cyanobacteria. FEBS Lett. 2009, 583(11), 1744–1752.
[45] Suzuki I, Simon WJ, Slabas AR. The heat shock response of *Synechocystis* sp. PCC 6803 analysed by transcriptomics and proteomics. J Exp Bot. 2006, 57(7), 1573–1578.
[46] Zhang Z, Pendse ND, Phillips KN, Cotner JB, Khodursky A. Gene expression patterns of sulfur starvation in *Synechocystis* sp. PCC 6803. BMC Genomics. 2008, 9(1), 344.
[47] Schwarz D, Orf I, Kopka J, Hagemann M. Recent applications of metabolomics toward cyanobacteria. Metabolites. 2013, 3(1), 72–100.
[48] Marraccini P, Bulteau S, Cassier-Chauvat C, Mermet-Bouvier P, Chauvat F. A conjugative plasmid vector for promoter analysis in several cyanobacteria of the genera *Synechococcus* and *Synechocystis*. Plant Mol Biol. 1993, 23(4), 905–909.
[49] Grigorieva G, Shestakov S. Transformation in the cyanobacterium *Synechocystis* sp. 6803. FEMS Microbiol Lett. 1982, 13(4), 367–370.
[50] Yao L, Cengic I, Anfelt J, Hudson EP. Multiple gene repression in cyanobacteria using CRISPRi. ACS Synth Biol. 2016, 5(3), 207–212.
[51] Behler J, Vijay D, Hess WR, Akhtar MK. CRISPR-based technologies for metabolic engineering in cyanobacteria. Trends Biotechnol. 2018, 36(10), 996–1010.
[52] Cohen SE, Golden SS. Circadian rhythms in cyanobacteria. Microbiol Mol Biol Rev. 2015, 79(4), 373–385.
[53] Golden SS, Ishiura M, Johnson CH, Kondo T. Cyanobacterial circadian rhythms. Annu Rev Plant Physiol Plant Mol Biol. 1997, 48(1), 327–354.
[54] Shestakov SV, Khyen NT. Evidence for genetic transformation in blue-green alga *Anacystis nidulans*. Mol Genet Genomics. 1970, 107(4), 372–375.
[55] Tsinoremas NF, Kutach AK, Strayer CA, Golden SS. Efficient gene transfer in *Synechococcus* sp. strains PCC 7942 and PCC 6301 by interspecies conjugation and chromosomal recombination. J Bacteriol. 1994, 176(21), 6764–6768.
[56] Wendt KE, Ungerer J, Cobb RE, Zhao H, Pakrasi HB. CRISPR/Cas9 mediated targeted mutagenesis of the fast growing cyanobacterium *Synechococcus elongatus* UTEX 2973. Microb Cell Fact. 2016, 15(1), 115.
[57] Delaye L, González-Domenech CM, Garcillán-Barcia MP, Peretó J, De La Cruz F, Moya A. Blueprint for a minimal photoautotrophic cell: Conserved and variable genes in *Synechococcus elongatus* PCC 7942. BMC Genomics. 2011, 12, 25.

[58] Kumar K, Mella-Herrera RA, Golden JW. Cyanobacterial heterocysts. Cold Spring Harb Perspect Biol. 2010, 2(4), a000315.
[59] Xu X, Elhai J, Wolk CP. Transcriptional and developmental responses by *Anabaena* to deprivation of fixed nitrogen In: Herrero A, Flores E, editors, The Cyanobacteria: Molecular Biology, Genomics and Evolution. Norfolk, UK, Caister Academic Press, 2008, 383–422.
[60] Callahan SM, Buikema WJ. The role of HetN in maintenance of the heterocyst pattern in *Anabaena* sp. PCC 7120. Mol Microbiol. 2001, 40(4), 941–950.
[61] Stebegg R, Wurzinger B, Mikulic M, Schmetterer G. Chemoheterotrophic growth of the cyanobacterium *Anabaena* sp. strain PCC 7120 dependent on a functional cytochrome *c* oxidase. J Bacteriol. 2012, 194(17), 4601–4607.
[62] Wolk CP, Vonshak A, Kehoe P, Elhai J. Construction of shuttle vectors capable of conjugative transfer from *Escherichia coli* to nitrogen-fixing filamentous cyanobacteria. Proc Natl Acad Sci U.S.A. 1984, 81(5), 1561–1565.
[63] Thiel T, Poo H. Transformation of a filamentous cyanobacterium by electroporation. J Bacteriol. 1989, 171(10), 5743–5746.
[64] Kaneko T, Nakamura Y, Wolk CP, Kuritz T, Sasamoto S, Watanabe A, et al. Complete genomic sequence of the filamentous nitrogen-fixing cyanobacterium *Anabaena* sp. strain PCC 7120. DNA Res. 2001, 8(5), 205–213.
[65] Taton A, Lis E, Adin DM, Dong G, Cookson S, Kay SA, et al. Gene transfer in *Leptolyngbya* sp. strain BL0902, a cyanobacterium suitable for production of biomass and bioproducts. PLoS ONE. 2012, 7(1), e30901.
[66] Ma AT, Schmidt CM, Golden JW. Regulation of gene expression in diverse cyanobacterial species by using theophylline-responsive riboswitches. Appl Environ Microbiol. 2014, 80(21), 6704–6713.
[67] Taton A, Unglaub F, Wright NE, Zeng WY, Paz-Yepez J, Brahamsha B, et al. Broad-host-range vector system for synthetic biology and biotechnology in cyanobacteria. Nucleic Acids Res. 2014, 42(17), e136.
[68] Ludwig M, Bryant DA. *Synechococcus* sp. strain PCC 7002 transcriptome: acclimation to temperature, salinity, oxidative stress, and mixotrophic growth conditions. Front Microbiol. 2012, 3:, 354.
[69] Jaiswal D, Sengupta A, Sohoni S, Sengupta S, Phadnavis AG, Pakrasi HB, et al. Genome features and biochemical characteristics of a robust, fast growing and naturally transformable cyanobacterium *Synechococcus elongatus* PCC 11801 isolated from India. Sci Rep. 2018, 8(1), 16632.
[70] Nomura CT, Sakamoto T, Bryant DA. Roles for heme–copper oxidases in extreme high-light and oxidative stress response in the cyanobacterium *Synechococcus* sp. PCC 7002. Arch Microbiol. 2006, 185(6), 471–479.
[71] Batterton JC, Van Baalen C. Growth responses of blue-green algae to sodium chloride concentration. Archiv für Mikrobiologie. 1971, 76(2), 151–165.
[72] Kopka J, Schmidt S, Dethloff F, Pade N, Berendt S, Schottkowski M, et al. Systems analysis of ethanol production in the genetically engineered cyanobacterium *Synechococcus* sp. PCC 7002. Biotechnol Biofuels. 2017, 10(1), 56.
[73] Stevens SE, Porter RD. Transformation in *Agmenellum quadruplicatum*. Proc Natl Acad Sci U.S.A. 1980, 77(10), 6052–6056.
[74] Frigaard NU, Sakuragi Y, Bryant DA. Gene inactivation in the cyanobacterium *Synechococcus* sp. PCC 7002 and the green sulfur bacterium *Chlorobium tepidum* using *in vitro* made DNA constructs and natural transformation In: Carpentier R, editor, Photosynthesis research protocols. Totowa, NJ, Humana Press, 2004, 325–340.

[75] Gordon GC, Korosh TC, Cameron JC, Markley AL, Begemann MB, Pfleger BF. CRISPR interference as a titratable, *trans*-acting regulatory tool for metabolic engineering in the cyanobacterium *Synechococcus* sp. strain PCC 7002. Metab Eng. 2016, 38, 170–179.
[76] Li T, Zhao J, Zhao C, Liu Z, Zhao F, Marquardt J, et al. *Synechococcus* sp. PCC 7002 genome assembly Genebank 2008 [cited 2019. Available from: https://www.ncbi.nlm.nih.gov/assembly/GCF_000019485.1/.
[77] Ungerer J, Lin PC, Chen HY, Pakrasi HB. Adjustments to photosystem stoichiometry and electron transfer proteins are key to the remarkably fast growth of the cyanobacterium *Synechococcus elongatus* UTEX 2973. mBio. 2018, 9(1), e02327–17.
[78] Ungerer J, Wendt KE, Hendry JI, Maranas CD, Pakrasi HB. Comparative genomics reveals the molecular determinants of rapid growth of the cyanobacterium *Synechococcus elongatus* UTEX 2973. Proc Natl Acad Sci U.S.A. 2018, 115(50), 11761–11770.
[79] Mueller TJ, Ungerer JL, Pakrasi HB, Maranas CD. Identifying the metabolic differences of a fast-growth phenotype in *Synechococcus* UTEX 2973. Sci Rep. 2017, 7, 41569.
[80] Mehta K, Jaiswal D, Nayak M, Prasannan CB, Wangikar PP, Srivastava S. Elevated carbon dioxide levels lead to proteome-wide alterations for optimal growth of a fast-growing cyanobacterium, *Synechococcus elongatus* PCC 11801. Sci Rep. 2019, 9(1), 6257.
[81] Jaiswal D, Sengupta A, Sengupta S, Madhu S, Pakrasi HB, Wangikar PP. A novel cyanobacterium *Synechococcus elongatus* PCC 11802 has distinct genomic and metabolomic characteristics compared to its neighbor PCC 11801. Sci Rep. 2020, 10(1), 191.
[82] Berla BM, Saha R, Immethun CM, Maranas CD, Moon TS, Pakrasi HB. Synthetic biology of cyanobacteria: Unique challenges and opportunities. Front Microbiol. 2013, 4, 246.
[83] Fu P. Genome-scale modeling of *Synechocystis* sp. PCC 6803 and prediction of pathway insertion. J Chem Technol Biotechnol. 2009, 84(4), 473–483.
[84] Montagud A, Navarro E, Fernandez De Cordoba P, Urchueguia JF, Patil KR. Reconstruction and analysis of genome-scale metabolic model of a photosynthetic bacterium. BMC Syst Biol. 2010, 4, 156.
[85] Montagud A, Zelezniak A, Navarro E, De Cordoba PF, Urchueguia JF, Patil KR. Flux coupling and transcriptional regulation within the metabolic network of the photosynthetic bacterium *Synechocystis* sp. PCC 6803. Biotechnol J. 2011, 6(3), 330–342.
[86] Knoop H, Gründel M, Zilliges Y, Lehmann R, Hoffmann S, Lockau W, et al. Flux balance analysis of cyanobacterial metabolism: The metabolic network of *Synechocystis* sp. PCC 6803. PLoS Comput Biol. 2013, 9(6), e1003081.
[87] Nogales J, Gudmundsson S, Knight EM, Palsson BO, Thiele I. Detailing the optimality of photosynthesis in cyanobacteria through systems biology analysis. Proc Natl Acad Sci U.S.A. 2012, 109(7), 2678–2683.
[88] Joshi CJ, Peebles CAM, Prasad A. Modeling and analysis of flux distribution and bioproduct formation in *Synechocystis* sp. PCC 6803 using a new genome-scale metabolic reconstruction. Algal Res. 2017, 27, 295–310.
[89] Gopalakrishnan S, Pakrasi HB, Maranas CD. Elucidation of photoautotrophic carbon flux topology in *Synechocystis* PCC 6803 using genome-scale carbon mapping models. Metab Eng. 2018, 47, 190–199.
[90] Triana J, Montagud A, Siurana M, Fuente D, Urchueguía A, Gamermann D, et al. Generation and evaluation of a genome-scale metabolic network model of *Synechococcus elongatus* PCC 7942. Metabolites. 2014, 4(3), 680–698.
[91] Broddrick JT, Rubin BE, Welkie DG, Du N, Mih N, Diamond S, et al. Unique attributes of cyanobacterial metabolism revealed by improved genome-scale metabolic modeling and essential gene analysis. Proc Natl Acad Sci U.S.A. 2016, 113(51), 8344–8353.

[92] Malatinszky D, Steuer R, Jones PR. A comprehensively curated genome-scale two-cell model for the heterocystous cyanobacterium *Anabaena* sp. PCC 7120. Plant Physiol. 2017, 173(1), 509–523.
[93] Henry CS, DeJongh M, Best AA, Frybarger PM, Linsay B, Stevens RL. High-throughput generation, optimization and analysis of genome-scale metabolic models. Nat Biotechnol. 2010, 28, 977–982.
[94] Hamilton JJ, Reed JL. Identification of functional differences in metabolic networks using comparative genomics and constraint-based models. PLoS ONE. 2012, 7(4), e34670.
[95] Vu TT, Stolyar SM, Pinchuk GE, Hill EA, Kucek LA, Brown RN, et al. Genome-scale modeling of light-driven reductant partitioning and carbon fluxes in diazotrophic unicellular cyanobacterium *Cyanothece* sp. ATCC 51142. PLoS Comput Biol. 2012, 8(4), e1002460.
[96] Vu TT, Hill EA, Kucek LA, Konopka AE, Beliaev AS, Reed JL. Computational evaluation of *Synechococcus* sp. PCC 7002 metabolism for chemical production. Biotechnol J. 2013, 8(5), 619–630.
[97] Hendry JI, Prasannan CB, Joshi A, Dasgupta S, Wangikar PP. Metabolic model of *Synechococcus* sp. PCC 7002: Prediction of flux distribution and network modification for enhanced biofuel production. Bioresour Technol. 2016, 213, 190–197.
[98] Qian X, Kim MK, Kumaraswamy GK, Agarwal A, Lun DS, Dismukes GC. Flux balance analysis of photoautotrophic metabolism: Uncovering new biological details of subsystems involved in cyanobacterial photosynthesis. Biochim Biophys Acta Bioenerg. 2017, 1858(4), 276–287.
[99] Mueller TJ, Berla BM, Pakrasi HB, Maranas CD. Rapid construction of metabolic models for a family of Cyanobacteria using a multiple source annotation workflow. BMC Syst Biol. 2013, 7(1), 142.
[100] Huang HH, Camsund D, Lindblad P, Heidorn T. Design and characterization of molecular tools for a synthetic biology approach towards developing cyanobacterial biotechnology. Nucleic Acids Res. 2010, 38(8), 2577–2593.
[101] Imamura S, Asayama M. Sigma factors for cyanobacterial transcription. Gene Regul Syst Bio. 2009, 3, 65–87.
[102] Hook-Barnard IG, Hinton DM. Transcription initiation by mix and match elements: flexibility for polymerase binding to bacterial promoters. Gene Regul Syst Bio. 2007, 1, 275–293.
[103] Peca L, Kos PB, Vass I. Characterization of the activity of heavy metal-responsive promoters in the cyanobacterium *Synechocystis* PCC 6803. Acta Biol Hung. 2007, 58, 11–22.
[104] Cardinale S, Arkin AP. Contextualizing context for synthetic biology – Identifying causes of failure of synthetic biological systems. Biotechnol J. 2012, 7(7), 856–866.
[105] Camsund D, Heidorn T, Lindblad P. Design and analysis of LacI-repressed promoters and DNA-looping in a cyanobacterium. J Biol Eng. 2014, 8(1), 4.
[106] Markley AL, Begemann MB, Clarke RE, Gordon GC, Pfleger BF. Synthetic biology toolbox for controlling gene expression in the cyanobacterium *Synechococcus* sp. strain PCC 7002. ACS Synth Biol. 2015, 4(5), 595–603.
[107] Kim WJ, Lee SM, Um Y, Sim SJ, Woo HM. Development of SyneBrick vectors as a synthetic biology platform for gene expression in *Synechococcus elongatus* PCC 7942. Front Plant Sci. 2017, 8, 293.
[108] Ferreira EA, Pacheco CC, Pinto F, Pereira J, Lamosa P, Oliveira P, et al. Expanding the toolbox for *Synechocystis* sp. PCC 6803: Validation of replicative vectors and characterization of a novel set of promoters. Synth Biol. 2018, 3(1), ysy014.
[109] Abe K, Miyake K, Nakamura M, Kojima K, Ferri S, Ikebukuro K, et al. Engineering of a green-light inducible gene expression system in *Synechocystis* sp. PCC 6803. Microb Biotechnol. 2014, 7(2), 177–183.

[110] Huang HH, Lindblad P. Wide-dynamic-range promoters engineered for cyanobacteria. J Biol Eng. 2013, 7(1), 10.
[111] Englund E, Liang F, Lindberg P. Evaluation of promoters and ribosome binding sites for biotechnological applications in the unicellular cyanobacterium *Synechocystis* sp. PCC 6803 Sci Rep. 2016, 6, 36640.
[112] Till P, Toepel J, Bühler B, Mach RL, Mach-Aigner AR. Regulatory systems for gene expression control in cyanobacteria. Appl Microbiol Biotechnol. 2020, 104(5), 1977–1991.
[113] Vasudevan R, Gale GAR, Schiavon AA, Puzorjov A, Malin J, Gillespie MD, et al. CyanoGate: A modular cloning suite for engineering cyanobacteria based on the plant MoClo syntax. Plant Physiol. 2019, 180(1), 39–55.
[114] Liu D, Pakrasi HB. Exploring native genetic elements as plug-in tools for synthetic biology in the cyanobacterium *Synechocystis* sp. PCC 6803. Microb Cell Fact. 2018, 17(1), 48.
[115] Zhou J, Zhang H, Meng H, Zhu Y, Bao G, Zhang Y, et al. Discovery of a super-strong promoter enables efficient production of heterologous proteins in cyanobacteria. Sci Rep. 2014, 4, 4500.
[116] Wang B, Eckert C, Maness PC, Yu J. A genetic toolbox for modulating the expression of heterologous genes in the cyanobacterium *Synechocystis* sp. PCC 6803. ACS Synth Biol. 2018, 7(1), 276–286.
[117] Kobayashi S, Nakajima M, Asano R, Ferreira EA, Abe K, Tamagnini P, et al. Application of an engineered chromatic acclimation sensor for red-light-regulated gene expression in cyanobacteria. Algal Res. 2019, 44, 101691.
[118] Immethun CM, DeLorenzo DM, Focht CM, Gupta D, Johnson CB, Moon TS. Physical, chemical, and metabolic state sensors expand the synthetic biology toolbox for *Synechocystis* sp. PCC 6803. Biotechnol Bioeng. 2017, 114(7), 1561–1569.
[119] Albers SC, Gallegos VA, Peebles CA. Engineering of genetic control tools in *Synechocystis* sp. PCC 6803 using rational design techniques. J Biotechnol. 2015, 216, 36–46.
[120] Behle A, Saake P, Germann AT, Dienst D, Axmann IM. Comparative dose–response analysis of inducible promoters in cyanobacteria. ACS Synth Biol. 2020, 9(4), 843–855.
[121] Kelly CL, Taylor GM, Hitchcock A, Torres-Mendez A, Heap JT. A rhamnose-inducible system for precise and temporal control of gene expression in cyanobacteria. ACS Synth Biol. 2018, 7(4), 1056–1066.
[122] Ivanikova NV, McKay RML, Bullerjahn GS. Construction and characterization of a cyanobacterial bioreporter capable of assessing nitrate assimilatory capacity in freshwaters. Limnol Oceanogr: methods. 2005, 3(2), 86–93.
[123] Sengupta A, Sunder AV, Sohoni SV, Wangikar PP. Fine-tuning native promoters of *Synechococcus elongatus* PCC 7942 to develop a synthetic toolbox for heterologous protein expression. ACS Synth Biol. 2019, 8(5), 1219–1223.
[124] Geerts D, Bovy A, De Vrieze G, Borrias M, Weisbeek P. Inducible expression of heterologous genes targeted to a chromosomal platform in the cyanobacterium *Synechococcus* sp. PCC 7942. Microbiology. 1995, 141(4), 831–841.
[125] Cao YQ, Li Q, Xia PF, Wei LJ, Guo N, Li JW, et al. AraBAD based toolkit for gene expression and metabolic robustness improvement in *Synechococcus elongatus*. Sci Rep. 2017, 7(1), 18059.
[126] Ruffing AM, Jensen TJ, Strickland LM. Genetic tools for advancement of *Synechococcus* sp. PCC 7002 as a cyanobacterial chassis. Microb Cell Fact. 2016, 15(1), 190.
[127] Boyanapalli R, Bullerjahn GS, Pohl C, Croot PL, Boyd PW, McKay RM. Luminescent whole-cell cyanobacterial bioreporter for measuring Fe availability in diverse marine environments. Appl Environ Microbiol. 2007, 73(3), 1019–1024.
[128] Zess EK, Begemann MB, Pfleger BF. Construction of new synthetic biology tools for the control of gene expression in the cyanobacterium *Synechococcus* sp. strain PCC 7002. Biotechnol Bioeng. 2016, 113(2), 424–432.

[129] Perez AA, Gajewski JP, Ferlez BH, Ludwig M, Baker CS, Golbeck JH, et al. Zn^{2+}-inducible expression platform for *Synechococcus* sp. strain PCC 7002 based on the *smtA* Promoter/Operator and *smtB* Repressor. Appl Environ Microbiol. 2017, 83(3), e02491–16.
[130] Ma J, Campbell A, Karlin S. Correlations between Shine-Dalgarno sequences and gene features such as predicted expression levels and operon structures. J Bacteriol. 2002, 184(20), 5733–5745.
[131] Thiel K, Mulaku E, Dandapani H, Nagy C, Aro E-M, Kallio P. Translation efficiency of heterologous proteins is significantly affected by the genetic context of RBS sequences in engineered cyanobacterium *Synechocystis* sp. PCC 6803. Microb Cell Fact. 2018, 17(1), 34.
[132] Makrides SC. Strategies for achieving high-level expression of genes in *Escherichia coli*. Microbiol Rev. 1996, 60(3), 512–538.
[133] Lorenz R, Bernhart SH, Höner Zu Siederdissen C, Tafer H, Flamm C, Stadler PF, et al. ViennaRNA Package 2.0. Algorithms Mol Biol. 2011, 6(1), 26.
[134] Zuker M. Mfold web server for nucleic acid folding and hybridization prediction. Nucleic Acids Res. 2003, 31(13), 3406–3415.
[135] Salis HM, Mirsky EA, Voigt CA. Automated design of synthetic ribosome binding sites to control protein expression. Nat Biotechnol. 2009, 27, 946–950.
[136] Seo SW, Yang JS, Cho HS, Yang J, Kim SC, Park JM, et al. Predictive combinatorial design of mRNA translation initiation regions for systematic optimization of gene expression levels. Sci Rep. 2014, 4, 4515.
[137] Mutalik VK, Guimaraes JC, Cambray G, Lam C, Christoffersen MJ, Mai QA, et al. Precise and reliable gene expression via standard transcription and translation initiation elements. Nat Methods. 2013, 10, 354–360.
[138] Lindblad P, Fuente D, Borbe F, Cicchi B, Conejero JA, Couto N, et al. CyanoFactory, a European consortium to develop technologies needed to advance cyanobacteria as chassis for production of chemicals and fuels. Algal Res. 2019, 41, 101510.
[139] Hallberg ZF, Su Y, Kitto RZ, Hammond MC. Engineering and *in vivo* applications of riboswitches. Annu Rev Biochem. 2017, 86(1), 515–539.
[140] Sun T, Li S, Song X, Diao J, Chen L, Zhang W. Toolboxes for cyanobacteria: recent advances and future direction. Biotechnol Adv. 2018, 36(4), 1293–1307.
[141] Nakahira Y, Ogawa A, Asano H, Oyama T, Tozawa Y. Theophylline-dependent riboswitch as a novel genetic tool for strict regulation of protein expression in cyanobacterium *Synechococcus elongatus* PCC 7942. Plant Cell Physiol. 2013, 54(10), 1724–1735.
[142] Ohbayashi R, Akai H, Yoshikawa H, Hess WR, Watanabe S. A tightly inducible riboswitch system in *Synechocystis* sp. PCC 6803. J Gen Appl Microbiol. 2016, 62(3), 154–159.
[143] Li S, Sun T, Xu C, Chen L, Zhang W. Development and optimization of genetic toolboxes for a fast-growing cyanobacterium *Synechococcus elongatus* UTEX 2973. Metab Eng. 2018, 48, 163–174.
[144] Pérez AA, Liu Z, Rodionov DA, Li Z, Bryant DA. Complementation of cobalamin auxotrophy in *Synechococcus* sp. strain PCC 7002 and validation of a putative cobalamin riboswitch *in vivo*. J Bacteriol. 2016, 198(19), 2743–2752.
[145] Ueno K, Tsukakoshi K, Ikebukuro K. Riboregulator elements as tools to engineer gene expression in cyanobacteria. Appl Microbiol Biotechnol. 2018, 102(18), 7717–7723.
[146] Isaacs FJ, Dwyer DJ, Ding C, Pervouchine DD, Cantor CR, Collins JJ. Engineered riboregulators enable post-transcriptional control of gene expression. Nat Biotechnol. 2004, 22(7), 841–847.
[147] Abe K, Sakai Y, Nakashima S, Araki M, Yoshida W, Sode K, et al. Design of riboregulators for control of cyanobacterial *Synechocystis* protein expression. Biotechnol Lett. 2014, 36(2), 287–294.

[148] Sakamoto I, Abe K, Kawai S, Tsukakoshi K, Sakai Y, Sode K, et al. Improving the induction fold of riboregulators for cyanobacteria. RNA Biol. 2018, 15(3), 353–358.
[149] Keiler KC, Sauer RT. Sequence determinants of C-terminal substrate recognition by the Tsp protease. Journal of Biol Chem. 1996, 271(5), 2589–2593.
[150] Landry BP, Stöckel J, Pakrasi HB. Use of degradation tags to control protein levels in the cyanobacterium *Synechocystis* sp. strain PCC 6803. Appl Environ Microbiol. 2013, 79(8), 2833–2835.
[151] Noguchi T, Golden S Bioluminescent and fluorescent reporters in circadian rhythm studies [Internet]: regents of the University of California; 2017. Podcast. Available from: http://ccb.ucsd.edu/the-bioclock-studio/education-resources/reporter-review/ReporterReviewPDF.pdf
[152] Ghim CM, Lee SK, Takayama S, Mitchell RJ. The art of reporter proteins in science: past, present and future applications. BMB Rep. 2010, 43(7), 451–460.
[153] Liu BR, Huang YW, Lee HJ. Mechanistic studies of intracellular delivery of proteins by cell-penetrating peptides in cyanobacteria. BMC Microbiol. 2013, 13(1), 57.
[154] Liauw P, Kannchen D, Gasper R, Dyczmons-Nowaczyk N, Nowaczyk MM, Hofmann E. Cloning, expression, crystallization and preliminary X-ray studies of a superfolder GFP fusion of cyanobacterial Psb32. Acta Crystallogr Sect F. 2015, 71(4), 409–413.
[155] Rodriguez EA, Campbell RE, Lin JY, Lin MZ, Miyawaki A, Palmer AE, et al. The growing and glowing toolbox of fluorescent and photoactive proteins. Trends Biochem Sci. 2017, 42(2), 111–129.
[156] Immethun CM, Ng KM, DeLorenzo DM, Waldron-Feinstein B, Lee Y-C, Moon TS. Oxygen-responsive genetic circuits constructed in *Synechocystis* sp. PCC 6803. Biotechnol Bioeng. 2016, 113(2), 433–442.
[157] Peters JM, Vangeloff AD, Landick R. Bacterial transcription terminators: the RNA 3′-end chronicles. J Mol Biol. 2011, 412(5), 793–813.
[158] Ramey CJ, Barón-Sola Á, Aucoin HR, Boyle NR. Genome engineering in cyanobacteria: where we are and where we need to go. ACS Synth Biol. 2015, 4(11), 1186–1196.
[159] Vijayan V, Jain IH, O'Shea EK. A high resolution map of a cyanobacterial transcriptome. Genome Biol. 2011, 12(5), R47.
[160] Wang B, Wang J, Zhang W, Meldrum DR. Application of synthetic biology in cyanobacteria and algae. Front Microbiol. 2012, 3, 344.
[161] Pinto F, Pacheco CC, Oliveira P, Montagud A, Landels A, Couto N, et al. Improving a *Synechocystis*-based photoautotrophic chassis through systematic genome mapping and validation of neutral sites. DNA Res. 2015, 22(6), 425–437.
[162] Kelly CL, Taylor GM, Šatkutė A, Dekker L, Heap JT. Transcriptional terminators allow leak-free chromosomal integration of genetic constructs in cyanobacteria. Microorganisms. 2019, 7(8), 263.
[163] Chen Y, Taton A, Go M, London RE, Pieper LM, Golden SS, et al. Self-replicating shuttle vectors based on pANS, a small endogenous plasmid of the unicellular cyanobacterium *Synechococcus elongatus* PCC 7942. Microbiology. 2016, 162(12), 2029–2041.
[164] Jin H, Wang Y, Idoine A, Bhaya D. Construction of a shuttle vector using an endogenous plasmid from the cyanobacterium *Synechocystis* sp. PCC 6803. Front Microbiol. 2018, 9, 1662.
[165] Silva-Rocha R, Martínez-García E, Calles B, Chavarría M, Arce-Rodríguez A, De Las Heras A, et al. The Standard European Vector Architecture (SEVA): a coherent platform for the analysis and deployment of complex prokaryotic phenotypes. Nucleic Acids Res. 2013, 41(D1), 666–675.
[166] Clerico EM, Ditty JL, Golden SS. Specialized Techniques for Site-Directed Mutagenesis in Cyanobacteria. In: Rosato E, editor, Circadian Rhythms: Methods and Protocols. Methods in Molecular Biology. Vol. 362, Totowa, Humana Press, 2007, 155–171.
[167] Williams JGK. Construction of specific mutations in photosystem II photosynthetic reaction center by genetic engineering methods in *Synechocystis* 6803. Methods Enzymol. 1988, 167, 766–778.

[168] Burnap RL, Qian M, Shen JR, Inoue Y, Sherman LA. Role of disulfide linkage and putative intermolecular binding residues in the stability and binding of the extrinsic manganese-stabilizing protein to the photosystem II reaction center. Biochemistry-Us. 1994, 33(46), 13712–13718.
[169] Aoki R, Goto T, Fujita Y. A heme oxygenase isoform is essential for aerobic growth in the cyanobacterium *Synechocystis* sp. PCC 6803: modes of differential operation of two isoforms/enzymes to adapt to low oxygen environments in cyanobacteria. Plant Cell Physiol. 2011, 52(10), 1744–1756.
[170] Niederholtmeyer H, Wolfstädter BT, Savage DF, Silver PA, Way JC. Engineering cyanobacteria to synthesize and export hydrophilic products. Appl Environ Microbiol. 2010, 76(11), 3462–3466.
[171] Ng AH, Berla BM, Pakrasi HB. Fine-tuning of photoautotrophic protein production by combining promoters and neutral sites in the cyanobacterium *Synechocystis* sp. strain PCC 6803. Appl Environ Microbiol. 2015, 81(19), 6857–6863.
[172] Vogel AIM, Lale R, Hohmann-Marriott MF. Streamlining recombination-mediated genetic engineering by validating three neutral integration sites in *Synechococcus* sp. PCC 7002. J Biol Eng. 2017, 11(1), 19.
[173] Wang M, Luan G, Lu X. Systematic identification of a neutral site on chromosome of *Synechococcus* sp. PCC 7002, a promising photosynthetic chassis strain. J Biotechnol. 2019, 295:, 37–40.
[174] Ruffing AM. Engineered cyanobacteria: teaching an old bug new tricks. Bioeng Bugs. 2011, 2(3), 136–149.
[175] Cheah YE, Albers SC, Peebles CAM. A novel counter-selection method for markerless genetic modification in *Synechocystis* sp. PCC 6803. Biotechnol Prog. 2013, 29(1), 23–30.
[176] Kojima K, Keta S, Uesaka K, Kato A, Takatani N, Ihara K, et al. A simple method for isolation and construction of markerless cyanobacterial mutants defective in acyl-acyl carrier protein synthetase. Appl Microbiol Biotechnol. 2016, 100(23), 10107–10113.
[177] Matsuoka M, Takahama K, Ogawa T. Gene replacement in cyanobacteria mediated by a dominant streptomycin-sensitive *rps12* gene that allows selection of mutants free from drug resistance markers. Microbiology. 2001, 147(8), 2077–2087.
[178] Begemann MB, Zess EK, Walters EM, Schmitt EF, Markley AL, Pfleger BF. An organic acid based counter selection system for cyanobacteria. PLoS ONE. 2013, 8(10), e76594.
[179] Sengupta A, Pakrasi HB, Wangikar PP. Recent advances in synthetic biology of cyanobacteria. Appl Microbiol Biotechnol. 2018, 102(13), 5457–5471.
[180] Kaczmarzyk D, Cengic I, Yao L, Hudson EP. Diversion of the long-chain acyl-ACP pool in *Synechocystis* to fatty alcohols through CRISPRi repression of the essential phosphate acyltransferase PlsX. Metab Eng. 2018, 45, 59–66.
[181] Shabestary K, Anfelt J, Ljungqvist E, Jahn M, Yao L, Hudson EP. Targeted repression of essential genes to arrest growth and increase carbon partitioning and biofuel titers in cyanobacteria. ACS Synth Biol. 2018, 7(7), 1669–1675.
[182] Higo A, Isu A, Fukaya Y, Ehira S, Hisabori T. Application of CRISPR interference for metabolic engineering of the heterocyst-forming multicellular cyanobacterium *Anabaena* sp. PCC 7120. Plant Cell Physiol. 2017, 59(1), 119–127.
[183] Huang CH, Shen CR, Li H, Sung LY, Wu MY, Hu YC. CRISPR interference (CRISPRi) for gene regulation and succinate production in cyanobacterium *S. elongatus* PCC 7942. Microb Cell Fact. 2016, 15(1), 196.
[184] Yao L, Shabestary K, Björk SM, Asplund-Samuelsson J, Joensson HN, Jahn M, et al. Pooled CRISPRi screening of the cyanobacterium *Synechocystis* sp. PCC 6803 for enhanced industrial phenotypes. Nat Commun. 2020, 11(1), 1666.

[185] Li H, Shen CR, Huang CH, Sung LY, Wu MY, Hu YC. CRISPR-Cas9 for the genome engineering of cyanobacteria and succinate production. Metab Eng. 2016, 38, 293–302.
[186] Xiao Y, Wang S, Rommelfanger S, Balassy A, Barba-Ostria C, Gu P, et al. Developing a Cas9-based tool to engineer native plasmids in *Synechocystis* sp. PCC 6803. Biotechnol Bioeng. 2018, 115(9), 2305–2314.
[187] Ungerer J, Pakrasi HB. Cpf1 is a versatile tool for CRISPR genome editing across diverse species of cyanobacteria. Sci Rep. 2016, 6, 39681.
[188] Niu TC, Lin GM, Xie LR, Wang ZQ, Xing WY, Zhang JY, et al. Expanding the potential of CRISPR-Cpf1-based genome editing technology in the cyanobacterium *Anabaena* PCC 7120. ACS Synth Biol. 2019, 8(1), 170–180.
[189] Choi SY, Woo HM. CRISPRi-dCas12a: a dCas12a-mediated CRISPR interference for repression of multiple genes and metabolic engineering in cyanobacteria. ACS Synth Biol. 2020, 9(9), 2351–2361.
[190] Knoot CJ, Biswas S, Pakrasi HB. Tunable repression of key photosynthetic processes using Cas12a CRISPR interference in the fast-growing cyanobacterium *Synechococcus* sp. UTEX 2973. ACS Synth Biol. 2020, 9(1), 132–143.
[191] Liu D, Johnson VM, Pakrasi HB. A reversibly induced CRISPRi system targeting Photosystem II in the cyanobacterium *Synechocystis* sp. PCC 6803. ACS Synth Biol. 2020, 9(6), 1441–1449.
[192] Lin W-R, Tan S-I, Hsiang -C-C, Sung P-K, Ng IS. Challenges and opportunity of recent genome editing and multi-omics in cyanobacteria and microalgae for biorefinery. Bioresour Technol. 2019, 291, 121932.
[193] Ng IS, Keskin BB, Tan S-I. A critical review of genome editing and synthetic biology applications in metabolic engineering of microalgae and cyanobacteria. Biotechnol J. 2020, 15(8), 1900228.
[194] Zhang Y-T, Jiang J-Y, Shi T-Q, Sun X-M, Zhao Q-Y, Huang H, et al. Application of the CRISPR/Cas system for genome editing in microalgae. Appl Microbiol Biotechnol. 2019, 103(8), 3239–3248.
[195] Chenebault C, Diaz-Santos E, Kammerscheit X, Görgen S, Ilioaia C, Streckaite S, et al. A genetic toolbox for the new model cyanobacterium *Cyanothece* PCC 7425: a case study for the photosynthetic production of limonene. Front Microbiol. 2020, 11, 2335.
[196] Taton A, Ecker A, Diaz B, Moss NA, Anderson B, Reher R, et al. Heterologous expression of cryptomaldamide in a cyanobacterial host. ACS Synth Biol. 2020, Article ASAP.
[197] Madsen MA, Semerdzhiev S, Amtmann A, Tonon T. Engineering mannitol biosynthesis in *Escherichia coli* and *Synechococcus* sp. PCC 7002 using a green algal fusion protein. ACS Synth Biol. 2018, 7(12), 2833–2840.
[198] Russo DA, Zedler JAZ, Wittmann DN, Möllers B, Singh RK, Batth TS, et al. Expression and secretion of a lytic polysaccharide monooxygenase by a fast-growing cyanobacterium. Biotechnol Biofuels. 2019, 12(1), 74.
[199] Knoot CJ, Khatri Y, Hohlman RM, Sherman DH, Pakrasi HB. Engineered production of hapalindole alkaloids in the cyanobacterium *Synechococcus* sp. UTEX 2973. ACS Synth Biol. 2019, 8(8), 1941–1951.
[200] Zhang L, Chen L, Diao J, Song X, Shi M, Zhang W. Construction and analysis of an artificial consortium based on the fast-growing cyanobacterium *Synechococcus elongatus* UTEX 2973 to produce the platform chemical 3-hydroxypropionic acid from CO_2. Biotechnol Biofuels. 2020, 13(1), 82.
[201] Ducat DC, Avelar-Rivas JA, Way JC, Silver PA. Rerouting carbon flux to enhance photosynthetic productivity. Appl Environ Microbiol. 2012, 78(8), 2660–2668.
[202] Weiss TL, Young EJ, Ducat DC. A synthetic, light-driven consortium of cyanobacteria and heterotrophic bacteria enables stable polyhydroxybutyrate production. Metab Eng. 2017, 44, 236–245.

[203] Hays SG, Yan LLW, Silver PA, Ducat DC. Synthetic photosynthetic consortia define interactions leading to robustness and photoproduction. J Biol Eng. 2017, 11(1), 4.
[204] Löwe H, Hobmeier K, Moos M, Kremling A, Pflüger-Grau K. Photoautotrophic production of polyhydroxyalkanoates in a synthetic mixed culture of *Synechococcus elongatus cscB* and *Pseudomonas putida cscAB*. Biotechnol Biofuels. 2017, 10(1), 190.
[205] Ku JT, Lan EI. A balanced ATP driving force module for enhancing photosynthetic biosynthesis of 3-hydroxybutyrate from CO_2. Metab Eng. 2018, 46, 35–42.
[206] Wang X, Liu W, Xin C, Zheng Y, Cheng Y, Sun S, et al. Enhanced limonene production in cyanobacteria reveals photosynthesis limitations. Proc Natl Acad Sci U.S.A. 2016, 113(50), 14225–14230.
[207] Lan EI, Liao JC. Metabolic engineering of cyanobacteria for 1-butanol production from carbon dioxide. Metab Eng. 2011, 13(4), 353–363.
[208] Atsumi S, Higashide W, Liao JC. Direct photosynthetic recycling of carbon dioxide to isobutyraldehyde. Nat Biotechnol. 2009, 27, 1177.
[209] Kanno M, Atsumi S. Engineering an obligate photoautotrophic cyanobacterium to utilize glycerol for growth and chemical production. ACS Synth Biol. 2017, 6(1), 69–75.
[210] Angermayr SA, Paszota M, Hellingwerf KJ. Engineering a cyanobacterial cell factory for production of lactic acid. Appl Environ Microbiol. 2012, 78(19), 7098–7106.
[211] Wang B, Pugh S, Nielsen DR, Zhang W, Meldrum DR. Engineering cyanobacteria for photosynthetic production of 3-hydroxybutyrate directly from CO_2. Metab Eng. 2013, 16, 68–77.
[212] Englund E, Pattanaik B, Ubhayasekera SJK, Stensjö K, Bergquist J, Lindberg P. Production of squalene in *Synechocystis* sp. PCC 6803. PLoS ONE. 2014, 9(3), e90270.
[213] Englund E, Andersen-Ranberg J, Miao R, Hamberger B, Lindberg P. Metabolic engineering of *Synechocystis* sp. PCC 6803 for production of the plant diterpenoid manoyl oxide. ACS Synth Biol. 2015, 4(12), 1270–1278.
[214] Englund E, Shabestary K, Hudson EP, Lindberg P. Systematic overexpression study to find target enzymes enhancing production of terpenes in *Synechocystis* PCC 6803, using isoprene as a model compound. Metab Eng. 2018, 49, 164–177.
[215] Liang F, Englund E, Lindberg P, Lindblad P. Engineered cyanobacteria with enhanced growth show increased ethanol production and higher biofuel to biomass ratio. Metab Eng. 2018, 46, 51–59.
[216] Miao R, Liu X, Englund E, Lindberg P, Lindblad P. Isobutanol production in *Synechocystis* PCC 6803 using heterologous and endogenous alcohol dehydrogenases. Metab Eng Commun. 2017, 5, 45–53.
[217] Yunus IS, Wichmann J, Wördenweber R, Lauersen KJ, Kruse O, Jones PR. Synthetic metabolic pathways for photobiological conversion of CO_2 into hydrocarbon fuel. Metab Eng. 2018, 49, 201–211.
[218] Yunus IS, Jones PR. Photosynthesis-dependent biosynthesis of medium chain-length fatty acids and alcohols. Metab Eng. 2018, 49, 59–68.
[219] Savakis PE, Angermayr SA, Hellingwerf KJ. Synthesis of 2,3-butanediol by *Synechocystis* sp. PCC 6803 via heterologous expression of a catabolic pathway from lactic acid- and enterobacteria. Metabolic Eng. 2013, 20, 121–130.
[220] Yang G, Cozad MA, Holland DA, Zhang Y, Luesch H, Ding Y. Photosynthetic production of sunscreen shinorine using an engineered cyanobacterium. ACS Synth Biol. 2018, 7(2), 664–671.
[221] Wu W, Du W, Gallego RP, Hellingwerf KJ, Van Der Woude AD, Branco Dos Santos F. Using osmotic stress to stabilize mannitol production in *Synechocystis* sp. PCC6803. Biotechnol Biofuels. 2020, 13(1), 117.

Chapter III. Expanding the toolbox for *Synechocystis* sp. PCC 6803: validation of replicative vectors and characterization of a novel set of promoters

Work published in:

Ferreira, E. A., Pacheco, C. C., Pinto, F., Pereira, J., Lamosa, P., Oliveira, P., Kirov, B., Jaramillo, A., & Tamagnini, P. (2018). Expanding the toolbox for *Synechocystis* sp. PCC 6803: validation of replicative vectors and characterization of a novel set of promoters. *Synthetic Biology, 3*(1), ysy014. https://doi.org/10.1093/synbio/ysy014.

Synthetic Biology, 2018, 3(1): ysy014

doi: 10.1093/synbio/ysy014
Advance Access Publication Date: 8 August 2018
Research article

Expanding the toolbox for *Synechocystis* sp. PCC 6803: validation of replicative vectors and characterization of a novel set of promoters

Eunice A. Ferreira[1,2,3,†], Catarina C. Pacheco[1,2,†], Filipe Pinto[1,2,4,5], José Pereira[1,2], Pedro Lamosa[6], Paulo Oliveira[1,2], Boris Kirov[7,8,9], Alfonso Jaramillo[7,10,11], and Paula Tamagnini[1,2,12,*]

[1]i3S – Instituto de Investigação e Inovação em Saúde Universidade do Porto, 4200-135 Porto, Portugal, [2]IBMC – Instituto de Biologia Molecular e Celular Universidade do Porto, 4200-135 Porto, Portugal, [3]ICBAS – Instituto de Ciências Biomédicas Abel Salazar Universidade do Porto, 4050-313 Porto, Portugal, [4]School of Biological Sciences, University of Edinburgh, Edinburgh EH9 3FF, UK, [5]Centre for Synthetic and Systems Biology, University of Edinburgh, Edinburgh EH9 3FF, UK, [6]Instituto de Tecnologia Química e Biológica António Xavier, ITQB NOVA, 2780-157 Oeiras, Portugal, [7]CNRS-UMR8030 Laboratoire iSSB and Université Paris-Saclay and Université d'Évry and CEA DRF, IG, Genoscope, Évry, 91000 France, [8]ANP - Faculty of Automatics, TU – Sofia, Sofia, Bulgaria, [9]BioInfoTech Lab - RDIC, Sofia Tech Park, Sofia, Bulgaria, [10]Warwick Integrative Synthetic Biology Centre and School of Life Sciences, University of Warwick, CV4 7AL Coventry, UK, [11]Institute for Integrative Systems Biology (I2SysBio) University of Valencia-CSIC, 46980 Paterna, Spain and [12]Faculdade de Ciências, Departamento de Biologia, Universidade do Porto, 4169-007 Porto, Portugal

*Corresponding author: E-mail: pmtamagn@ibmc.up.pt

†The authors wish it to be known that, in their opinion, the first two authors should be regarded as Joint First Authors.

Abstract

Cyanobacteria are promising 'low-cost' cell factories since they have minimal nutritional requirements, high metabolic plasticity and can use sunlight and CO_2 as energy and carbon sources. The unicellular *Synechocystis* sp. PCC 6803, already considered the 'green' *Escherichia coli*, is the best studied cyanobacterium but to be used as an efficient and robust photoautotrophic chassis it requires a customized and well-characterized toolbox. In this context, we evaluated the possibility of using three self-replicative vectors from the Standard European Vector Architecture (SEVA) repository to transform *Synechocystis*. Our results demonstrated that the presence of the plasmid does not lead to an evident phenotype or hindered *Synechocystis* growth, being the vast majority of the cells able to retain the replicative plasmid even in the absence of selective pressure. In addition, a set of heterologous and redesigned promoters were characterized exhibiting a wide range of activities compared to the reference P_{rnpB}, three of which could be efficiently repressed. As a proof-of-concept, from the expanded toolbox, one promoter was selected and assembled with the *ggpS* gene [encoding one of the proteins involved in the synthesis of the native compatible solute glucosylglycerol (GG)] and the synthetic device was introduced into *Synechocystis* using one of the SEVA plasmids. The presence of this device restored the production of the GG in a *ggpS* deficient mutant validating the functionality of the tools/device developed in this study.

Submitted: 29 November 2017; **Received (in revised form):** 27 July 2018; **Accepted:** 30 July 2018

Key words: cyanobacteria; promoters; pSEVA plasmids; *Synechocystis*; synthetic toolbox.

1. Introduction

Cyanobacteria are photoautotrophic organisms with simple nutritional requirements due to their ability to use sunlight and CO_2 as energy and carbon sources (1). The unicellular *Synechocystis* sp. PCC 6803 (hereafter *Synechocystis*) was the first photosynthetic organism to have its genome sequenced (2) and rapidly became the model strain for cyanobacteria. Moreover, the large amount of data generated over the last decades allowed the construction of genome-scale metabolic models (3, 4) leading to this organism being recognized as the 'green' *Escherichia coli* (5). Nevertheless, the vast majority of the available synthetic biology tools have been developed for heterotrophic chassis like *E. coli* or *Saccharomyces cerevisiae* (6, 7), and most of the regulatory elements characterized in *E. coli* function rather poorly or not at all in cyanobacteria (8, 9). Consequently, a considerable effort has been placed on the design and construction of efficient, predictable and easy-to-use molecular tools for cyanobacteria (8, 10–14). Within this context, native promoters such as P_{psbA2}, P_{nrsB} or the 'super strong' $P_{cpcG560}$ have been previously used to drive gene expression for specialty chemicals production (11, 15, 16). These promoters have the obvious advantage of responding to environmental signals that cells are used to integrate and modulate (17, 18). Nevertheless, the predictability of the system is compromised since these promoters are not insulated from the organism's regulatory networks (often involving multiple poorly understood control mechanisms), which represents a clear disadvantage for the design of genetic circuits. Chemical-induced promoters have an additional drawback due to the difficulty of removing the inducer from the culture, resulting in a continuous gene control. In metal-induced promoters, the metal can be actively pumped out of the cells, being a restraint when a strong inducible system is required (11). In contrast, light-inducible promoters do not require the addition of a specific molecule but its regulation is confined to specific growth conditions e.g. wavelength and light intensity (12, 19). In this context, the rational design of heterologous promoters has been used as a strategy to increase insulation and obtain more efficient promoters, with several attempts to engineer the well-described systems regulated by TetR or LacI e.g. replacing bases between the -10 box and the transcription start site or changing the distance between -10 and -35 boxes (10, 20). Although some improvements have been achieved there are still limitations for the available systems and room for expanding the cyanobacterial toolbox. The implementation of synthetic devices/circuits into the chassis also presents its challenges. While replicative vectors allow a faster generation/assessment of the mutants, integrative ones ensure long-term stability (21). The availability of replicative vectors for cyanobacterial synthetic biology applications is still scarce (8, 21), while a set of integrative plasmids targeting *Synechocystis* chromosomal neutral sites were recently developed and validated by us and others (13, 22). Cyanobacteria are promising cell factories that have already been engineered to be used as sustainable platforms to produce a variety of value-added compounds such as ethylene, sugars and biofuels (23–25). Therefore, the development and validation of a cyanobacterial synthetic biology toolbox is of the utmost importance to render processes more efficient and economically viable. With this purpose, we validated the use of three Standard European Vector Architecture (SEVA) replicative plasmids in *Synechocystis*, developed a novel set of heterologous/redesigned promoters and, as a proof-of-concept, used some of these tools to bypass the native control of the compatible solute glucosylglycerol (GG) synthesis.

2. Materials and methods

2.1 Chemicals and reagents

The chemicals anhydrotetracycline hydrochloride (aTc, Sigma-Aldrich), Isopropyl β-D-1-thiogalactopyranoside (IPTG, lactose analog, BioVectra Inc.), lactose (Merck Millipore), *N*-(β-ketocaproyl)-L-homoserine lactone (AHL, 3OC6HSL, Santa Cruz Biotech.), and L-arabinose (Sigma-Aldrich) were used. All other chemicals and reagents were purchased from ThermoFisher Scientific or Sigma-Aldrich.

2.2 Organisms and culture conditions

Wild-type and mutants of the cyanobacterium *Synechocystis* sp. PCC 6803 substrain Kazusa (26, 27) (obtained from the Pasteur Culture Collection, Paris, France) were maintained in Erlenmeyer flasks batch cultures with BG11 medium (28) at 30°C with rotary shaking (100 rpm) under a 12 h light/12 h dark regimen. Light intensity was 20 μE/m^2/s in all experiments and cosine-corrected irradiance was measured using a Dual Solar/Electric Quantum Meter (Spectrum Technologies, Inc.). For solid BG11, the medium was supplemented with 1.5% (wt/vol) noble agar (Difco), 0.3% (wt/vol) sodium thiosulfate and 10 mM TES-KOH buffer, pH 8.2. For the selection and maintenance of mutants, BG11 medium was supplemented with kanamycin (Km, 10–500 μg/ml), chloramphenicol (Cm, 10–20 μg/ml) or streptomycin and spectinomycin (Sp and Sm, 1.5 μg/ml each).

For cloning purposes, *E. coli* strains DH5α (Stratagene) or TOP10 (ThermoFisher Scientific) were used. Cells were grown at 37°C in LB medium (29), supplemented with Amp (100 μg/ml), Km (50 μg/ml), Cm (34 μg/ml) or Sm (50 μg/ml).

2.3 Synthetic promoters design

The synthetic T7 promoter variants used in this study ($P_{T7.1.x.lacO}$, $P_{T7.2.x.lacO}$ and $P_{T7.3.x.lacO}$) were based on three existing variants of the T7 RNA polymerase promoter sequence containing single nucleotide substitutions—$P_{T7.1}$, $P_{T7.2}$ and $P_{T7.3}$ (30, 31) and on Novagen® pET expression vectors. The existing variants were redesigned including the *lacO* operator sequence originating the $P_{T7.1.x.lacO}$, $P_{T7.2.x.lacO}$ and $P_{T7.3.x.lacO}$ promoters (for more details see Figure 5a and Table 1).

The other novel synthetic promoters were based on the well-characterized hybrid promoter P_{trc} (33) that was redesigned replacing the existing *lacO* sequence by other operators and/or including additional operators such as, the *lacOid*, *tetO* or $araI_1$ half-site (for more details see Figure 5b and Table 1). All the synthetic promoters are flanked by the prefix and suffix sequences of the BioBrick RFC[10] standard and were synthesized and cloned into pJ201 vector (DNA 2.0, Inc.).

2.4 DNA devices assembly

All DNA constructs were generated following the standard assembly protocol, and the BioBrick DNA parts used were

Table 1. List of parts used in this study

Designation	Plasmid	Description	References/sources
P_{rnpB}	pSB1A2	Promote—reference for promoter strength	(8)
$P_{T7.1.x.lacO}$	pJ201	Promoter variant 1 based on P_{T7} with a single mutation and containing a *lacO* operator	This study
$P_{T7.2.x.lacO}$	pJ201	Promoter variant 2 based on P_{T7} with a single mutation and containing a *lacO* operator	This study
$P_{T7.3.x.lacO}$	pJ201	Promoter variant 3 based on P_{T7} with a single mutation and containing a *lacO* operator	This study
P_{psbA2*}	pJ201	Promoter based on *Synechocystis* native P_{psbA2} promoter	(13)
P_{tacI}	pJ201	Hybrid promoter containing a *lacO* operator	(32)
$P_{trc.x.lacO}$	pJ201	Synthetic promoter containing two *lacO* operators	This study
$P_{trc.x.araO}$	pJ201	Synthetic promoter containing an *araO* operator	This study
$P_{trc.x.tetO1}$	pJ201	Synthetic promoter containing a *tetO* operator	This study
$P_{trc.x.tetO2}$	pJ201	Synthetic promoter containing a modified *tetO* operator	This study
ggpS	pSB1A2	*Synechocystis*' native *ggpS* gene	This study
$P_{\lambda cI}$	pSB1A2	BioBrick promoter	Part: BBa_R0051
P_{luxR}	pSB1A2	BioBrick promoter	Part: BBa_R0062
P_{T7pol}	pSB1AK8	BioBrick promoter	Part: BBa_I712074
P_{araC}	pSB1A2	BioBrick promoter	Part: BBa_R0080
P_{BADwt}	pSB1A3	BioBrick promoter	Part: BBa_I13453
GFP generator	pSB1A2	GFP transcriptional unit (RBS, CDS and double terminator)	Part: BBa_E0240
RBS	pSB1A2	Ribosome binding site	Part: BBa_B0030
T7pol	pSB1C3	RNA polymerase from phage T7	Part: BBa_K145001
cI	pSB1A2	Regulator	Part: BBa_C0051
lacI	pSB1A2	Regulator	Part: BBa_C0012
tetR	pSB1C3	Regulator	Part: BBa_C0040
araC	pSB1C3	Regulator	Part: BBa_C0080
luxR	pSB1A2	Regulator	Part: BBa_C0062

obtained from the Registry of Standard Biological Parts (Table 1). Briefly, to test promoter constitutive expression, the GFP generator (part BBa_E0240 that comprises the RBS BBa_B0032, the coding sequence for GFP BBa_E0040, and the double terminator BBa_B0015) was excised from the delivery plasmid with XbaI and PstI and cloned downstream each promoter (plasmids digested with SpeI and PstI). To test the promoters' regulated expression, the *lacI*, *tetR*, *cI*, *luxR* or *araC* regulators' ORFs were cloned under regulation of the constitutive promoter P_{rnpB} and the RBS BBa_B0030. The ORFs were excised with XbaI and PstI and cloned in the plasmid containing the promoter, previously digested with SpeI and PstI. Subsequently, the devices containing the promoter and GFP were excised with EcoRI and SpeI and cloned upstream of the respective P_{rnpB}:: regulator assembly (plasmid digested with EcoRI and XbaI). For the T7 polymerase (T7pol), a similar assembly was performed.

For generation of the GG device used in the proof of concept, the *ggpS* ORF was amplified by PCR using *Synechocystis* genomic DNA as template with primers flanked by the BioBrick prefix or suffix (see Supplementary Table S1). Amplification was performed using Phusion high-fidelity DNA polymerase (Thermo Scientific), according to the manufacturer's instructions. The PCR product was purified using the NZYGelpure kit (NZYTech), digested with XbaI and PstI and cloned downstream of $P_{trc.x.lacO}$ and BBa_B0030 RBS (plasmid digested with SpeI and PstI).

All the generated constructions were transferred to pSEVA251 or pSEVA351 shuttle vectors (obtained from the 'Standard European Vector Architecture' repository) (34) and the construct harboring the RNA polymerase from phage T7 (P_{rnpB}::T7pol) was cloned into the pSN15K vector (13). The correct assembly of the generated constructs was confirmed by PCR, restriction analysis and sequencing (STAB VIDA).

2.5 Generation of the *Synechocystis ggpS* deletion mutant

The construction of integrative plasmids for the deletion of the *ggpS* gene was performed as described previously (35). Briefly, the plasmids were based on pGEM-T® Easy (Promega) and contain the *Synechocystis* chromosomal regions flanking the *ggpS* gene. The 5′- and 3′-flanking regions were amplified from the cyanobacterium's genome using *Pfu* DNA polymerase and the primer pairs 5-O/5-I and 3-O/3-I (Supplementary Table S1), respectively. Subsequently, the purified PCR fragments were fused by 'overlap PCR' using primers 5-O/3-O and 80 ng of each amplicon (Supplementary Table S1). The resulting product was purified and cloned into the vector pGEM-T® Easy, according to the manufacturer's instructions, originating the pGDggpS plasmid. A selection cassette, containing the *nptII* gene (conferring resistance to neomycin and kanamycin), obtained from the plasmid pK18mobsacB (36), was cloned in the *Age*I restriction site of pGDggpS using the T4 DNA ligase to generate the plasmid pGDggpS.K (Table 2). All the constructs were confirmed by DNA sequencing (STAB VIDA).

For the generation of the Δ*ggpS* mutant, *Synechocystis* was transformed via natural transformation based on the procedure described previously (37). Briefly, *Synechocystis* was grown in standard conditions to an $OD_{730} \approx 0.5$. Cells were harvested by centrifugation (10 min at 3850 *g*) and resuspended in BG11 to a final $OD_{730} \approx 2.5$. The pGDggpS.K plasmid was incubated for 5 h with 500 µl of those cells (final plasmid DNA concentration of 20 µg/ml), in light and at 25°C. Cells were then spread onto Immobilon™-NC membranes (0.45 µm pore size, 82 mm, Millipore) resting on solid BG11 plates, grown in standard growth conditions and transferred to selective plates after 24 h (Km, 10 µg/ml). Transformants were observed after 2 weeks. For complete segregation, Km-resistant colonies were grown at increasing Km concentrations (25 and 50 µg/ml), then transferred to liquid medium and the antibiotic concentration was

Table 2. List of plasmids used to transform *Synechocystis*

Designation	Plasmid	Description	References/sources
pGDggpS.K	pGEM-T® Easy	pGEM-T easy vector containing the kanamycin resistance cassette flanked by the two regions for double homologous recombination on the *ggpS locus*	This study
pSEVA251	pSEVA251	Replicative plasmid/shuttle vector, Km^R, *ori* RSF1010	(34)
pSEVA351	pSEVA351	Replicative plasmid/shuttle vector, Cm^R, *ori* RSF1010	(34)
pSEVA451	pSEVA451	Replicative plasmid/shuttle vector, Sp^R/Sm^R, *ori* RSF1010	(34)
P_{rnpB}::*gfp*	pSEVA251/pSEVA351	GFP generator (Part: BBa_E0240) under the control of the native constitutive promoter P_{rnpB}	(8)
$P_{\lambda cI}$::*gfp*	pSEVA251	GFP generator (Part: BBa_E0240) under the control of the $P_{\lambda cI}$ promoter (Part: BBa_ R0051)	This study
$P_{\lambda cI}$::*gfp*-P_{rnpB}::*cI*	pSEVA251	GFP generator (Part: BBa_E0240) under the control of the $P_{\lambda cI}$ promoter (Part: BBa_ R0051), upstream of the CI regulator coding region (Part: BBa_ C0051) under the control of the native P_{rnpB} and the BBa_B0030 RBS	This study
P_{araC}::*gfp*	pSEVA251	GFP generator (Part: BBa_E0240) under the control of the P_{araC} promoter (Part: BBa_ R0080)	This study
P_{araC}::*gfp* P_{rnpB}::*araC*	pSEVA251	GFP generator (Part: BBa_E0240) under the control of the P_{araC} promoter (Part: BBa_R0080), upstream of the AraC regulator coding sequence (Part: BBa_C0080) under the control of the native P_{rnpB} and the BBa_B0030 RBS	This study
P_{luxR}::*gfp*	pSEVA251	GFP generator (Part: BBa_E0240) under the control of the P_{luxR} promoter (Part: BBa_ R0062)	This study
P_{luxR}::*gfp*-P_{rnpB}::luxR	pSEVA251	GFP generator (Part: BBa_E0240) under the control of the P_{luxR} promoter (Part: BBa_R0062), upstream of the LuxR regulator coding sequence (Part: BBa_C0062) under the control of the native P_{rnpB} and the BBa_B0030 RBS	This study
P_{BADwt}::*gfp*	pSEVA251	GFP generator (Part: BBa_E0240) under the control of the P_{BADwt} promoter (Part: BBa_ I13453)	This study
P_{BADwt}::*gfp* P_{rnpB}::*araC*	pSEVA251	GFP generator (Part: BBa_E0240) under the control of the P_{BADwt} promoter (Part: BBa_I13453) upstream of the AraC regulator coding sequence (Part: BBa_C0080) under the control of the native P_{rnpB} and the BBa_B0030 RBS	This study
P_{T7pol}::*gfp*-P_{rnpB}::T7pol	pSEVA251	GFP generator (Part: BBa_E0240) under the control of the P_{T7pol} promoter (Part: BBa_I712074), upstream of the T7 polymerase coding sequence (Part: BBa_K145001) under the control of the native P_{rnpB} and the BBa_B0030 RBS	This study
P_{rnpB}::T7pol	pSN15K	T7 polymerase under the control of the native constitutive promoter P_{rnpB} and the BBa_B0030 RBS	This study
$P_{T7.1.x.lacO}$::*gfp*	pSEVA351	GFP generator (Part: BBa_E0240) under the control of the $P_{T7.1.x.lacO}$ variant	This study
$P_{T7.2.x.lacO}$::*gfp*	pSEVA351	GFP generator (Part: BBa_E0240) under the control of the $P_{T7.2.x.lacO}$ variant	This study
$P_{T7.3.x.lacO}$::*gfp*	pSEVA351	GFP generator (Part: BBa_E0240) under the control of the $P_{T7.3.x.lacO}$ variant	This study
$P_{T7.1.x.lacO}$::*gfp*-P_{rnpB}::*lacI*	pSEVA351	GFP generator (Part: BBa_E0240) under the control of the $P_{T7.1.x.lacO}$ variant upstream of the LacI regulator coding region (Part: BBa_C0012) under the control of the native P_{rnpB} and the BBa_B0030 RBS	This study
$P_{T7.2.x.lacO}$::*gfp*-P_{rnpB}::*lacI*	pSEVA351	GFP generator (Part: BBa_E0240) under the control of the $P_{T7.2.x.lacO}$ variant upstream of the LacI regulator coding region (Part: BBa_C0012) under the control of the native P_{rnpB} and the BBa_B0030 RBS	This study
$P_{T7.3.x.lacO}$:: *gfp*-P_{rnpB}:: *lacI*	pSEVA351	GFP generator (Part: BBa_E0240) under the control of the $P_{T7.3.x.lacO}$ variant upstream of the LacI regulator coding region (Part: BBa_C0012) under the control of the native P_{rnpB} and the BBa_B0030 RBS	This study
P_{tacI}::*gfp*	pSEVA251	GFP generator (Part: BBa_E0240) under the control of the hybrid promoter P*tacI*	(32)
$P_{trc.x.tetO1}$::*gfp*	pSEVA251	GFP generator (Part: BBa_E0240) under the control of the synthetic promoter $P_{trc.x.tetO1}$	This study
$P_{trc.x.tetO1}$::*gfp*-P_{rnpB}::*tetR*	pSEVA251	GFP generator (Part: BBa_E0240) under the control of the synthetic promoter $P_{trc.x.tetO1}$, upstream of the TetR regulator coding region (Part: BBa_C0040) under the control of the native P_{rnpB} and the BBa_B0030 RBS	This study
$P_{trc.x.araO}$::*gfp*	pSEVA251	GFP generator (Part: BBa_E0240) under the control of the synthetic promoter $P_{trc.x.araO}$	This study

Table 2. (continued)

Designation	Plasmid	Description	References/sources
$P_{trc.x.araO}$::*gfp*-P_{rnpB}::*araC*	pSEVA251	GFP generator (Part: BBa_E0240) under the control of the synthetic promoter $P_{trc.x.araO}$, upstream of the AraC regulator coding region (Part: BBa_C0080) under the control of the native P_{rnpB} and the BBa_B0030 RBS	This study
$P_{trc.x.tetO2}$::*gfp*	pSEVA251	GFP generator (Part: BBa_E0240) under the control of the synthetic promoter $P_{trc.x.tetO2}$	This study
$P_{trc.x.tetO2}$::*gfp*-P_{rnpB}::*tetR*	pSEVA251	GFP generator (Part: BBa_E0240) under the control of the synthetic promoter $P_{trc.x.tetO2}$, upstream of the TetR regulator coding region (Part: BBa_C0040) under the control of the native P_{rnpB} and the BBa_B0030 RBS	This study
$P_{trc.x.lacO}$::*gfp*	pSEVA251	GFP generator (Part: BBa_E0240) under the control of the synthetic promoter $P_{trc.x.lacO}$	This study
$P_{trc.x.lacO}$::*gfp*-P_{rnpB}::*lacI*	pSEVA251	GFP generator (Part: BBa_E0240) under the control of the synthetic promoter $P_{trc.x.lacO}$, upstream of the LacI regulator coding region(Part: BBa_C0012) under the control of the native P_{rnpB} and the BBa_B0030 RBS	This study
P_{psbA2*}::*gfp*	pSEVA251	GFP generator (Part: BBa_E0240) under the control of the modified *psbA2* promoter (P_{psbA2*})	(13)
$P_{trc.x.lacO}$::*ggpS*	pSEVA351	Native *ggpS* coding region under the control of the synthetic promoter $P_{trc.x.lacO}$ and the BBa_B0030 RBS	This study

increased up to 500 μg/ml. The full segregation of the mutant was confirmed by Southern blot with a probe covering the 5′ flanking region of the *ggpS* gene labeled with digoxigenin using the DIG DNA labeling kit (Roche Molecular Biochemicals) and following the manufacturer's instructions. The Southern blot was carried out using the *Synechocystis* strains gDNA (4 μg) that was digested with *Ava*II Fast-Digest® for 45 min at 37°C, followed by an agarose gel electrophoresis. The remaining protocol was performed according to the DIG High Prime DNA Detection Starter kit (Roche Molecular Biochemicals) instructions. The final results were observed with a ChemiDoc™ XRS+ Imager (Bio-Rad).

2.6 *Synechocystis* transformation and mutants/transformants confirmation

The three replicative plasmids pSEVA251 (Km^R), pSEVA351 (Cm^R) and pSEVA451 (Sp/Sm^R), as well as the derived plasmids (listed in Table 2) were introduced into *Synechocystis* by electroporation, adapting the protocol previously described (38). Briefly, *Synechocystis* cultures were grown at 25°C under a continuous light regimen until an $OD_{730} \approx 0.5$ was reached. Cells were collected by centrifugation at 4190 *g* for 10 min and washed three times with 10 ml of 1 mM 4-(2-hydroxyethyl)-1-piperazineethanesulfonic (HEPES) acid buffer, pH 7.5. The cells were then suspended in 1 ml of HEPES buffer and 60 μL aliquots were mixed with 1 μg of plasmid DNA (eluted in water) and electroporated using a Gene Pulser™ (Bio-Rad). The capacitor was set to 25 μF and the resistor to 400 Ω, for a time constant of 9 ms with an electric field of 12 kV/cm. Immediately after the electric pulse, cells were transferred to 400 μL of fresh BG11 medium and spread onto Immobilon-NC membranes (0.45 μm pore size, 82 mm, Merck Millipore) resting on solid BG11 plates incubated at 25°C, under a 16 h light/8 h dark regimen for 24 h. Then, the membranes were transferred to solid BG11 plates supplemented with the appropriate antibiotic and incubated in the same conditions described above. Colonies were observed after 1–2 weeks.

The integrative plasmid pSN15K (Km^R) and the pSEVA replicative plasmids were introduced into *Synechocystis* by natural transformation, as described previously (37). Additionally, the replicative plasmid pSEVA451 was introduced into *Synechocystis* by conjugation, as described previously (39).

The presence of replicative plasmids or mutant segregation was confirmed by PCR using specific primers (Supplementary Table S1). For this purpose, *Synechocystis* DNA was extracted using 2 ml of culture that were centrifuged at 14 100 *g* for 3 min and washed with 1 ml of distilled water. Then, cell pellet was resuspended in 200 μL of distilled water and, 1 μL of RNase solution (20 mg/ml, Sigma) and 0.1 g of 0.2 mm-diameter glass beads (acid washed, Sigma) were added. Cells were disrupted by two cycles of vortexing for 1 min with incubation on ice for 1 min in between. Subsequently, the mixture was centrifuged at 14 100 *g* for 2 min, and the DNA containing supernatant was transferred to a new tube. The PCR reaction mixtures (20 μl) were setup using GoTaq® G2 Flexi DNA Polymerase (Promega), according to manufacturer's instructions, and 2 μl of DNA containing supernatant.

2.7 Growth experiments

Synechocystis cells (wild-type and mutants harboring pSEVA251, pSEVA351 and pSEVA451) were inoculated into 25 ml of BG11 medium in 50 ml Erlenmeyer flasks to an initial $OD_{730} \approx 0.5$, and grown in batch cultures at 30°C, 100 rpm, under a 12 h light (20 $\mu E/m^2/s$)/12 h dark regimen or continuous light (non-enriched air). Cell growth was monitored by measuring the OD_{730} for a 16 days period. All the growth experiments were performed in the absence of selective pressure and included three biological replicates with technical duplicates.

For the halotolerance growth experiments, pre-cultures of *Synechocystis* wild-type (WT), Δ*ggpS* mutant and the complemented Δ*ggpS* mutant (Δ*ggpS*_GG device) were inoculated in BG11 medium (supplemented with 10 μg/ml Cm and/or 25 μg/ml Km, when appropriate), and grown in an orbital shaker (150 rpm), at 30°C under a 12 h light (25 $\mu E/m^2/s$)/12 h dark regimen (non-enriched air). The cultures were grown until an $OD_{730} \approx 2$ was reached and, subsequently diluted in fresh BG11 medium without antibiotic to a final $OD_{730} \approx 0.5$. Fifty milliliter of

the dilution were transferred to 100 ml Erlenmeyer flasks (previously sterilized) containing NaCl, providing the cultures with the following final NaCl concentrations: 0, 3, 5 and 7% (w/v). These cultures were maintained in the same conditions as the pre-cultures and growth was monitored as described above. Each experiment was performed in triplicate.

2.8 Flow cytometry analysis

Cells of *Synechocystis* wild-type and mutants harboring pSEVA251, pSEVA251 P_{rnpB}::*gfp* and pSEVA251 $P_{trc.x.lacO}$::*gfp* were cultivated in liquid BG11 medium without or with kanamycin (Km, 25 μg/ml) under a 12 h light (20 μE/m^2/s)/12 h dark regimen as described above (Section 2.7). At Days 0, 4, 9 and 16 of cultivation, cells were diluted to $OD_{730} \approx 0.1$ and 50 000 events *per* sample were acquired after cell debris exclusion [forward scatter (FSC) versus side scatter (SSC) plot] using a FACSCalibur™ flow cytometer (BD Biosciences). FSC, SSC and GFP fluorescence signal (acquired in the FL1 channel) were plotted in a logarithmic scale, and data were analyzed with Cellquest software. Average GFP fluorescence signal and cell population percentages from three biological replicates with technical duplicates were calculated using the FlowJo® software vX10.0.7. Fluorescence signal of wild-type cells and cells harboring pSEVA251 were used as negative controls to establish the GFP+ gates that allow discriminating the cell population that emits GFP fluorescence (GFP+ cells).

2.9 GFP fluorescence analysis

For the evaluation of constitutive or regulated expression, cultures of *Synechocystis* carrying the promoter or promoter + regulator devices were grown to a final $OD_{730} \approx 1$ in 25 ml flasks, under continuous light at 30°C. The cultures were diluted to a final $OD_{730} \approx 0.5$ and 200 μL aliquots were distributed in Nunc™ MicroWell™ 96-Well Optical-Bottom Plates (Thermo Fisher Scientific). For regulated expression experiments, the inducers were used in the following final concentrations: 1, 2 or 20 mM IPTG; 2 or 5 mM lactose; 1 nM, 1 μM or 1 mM AHL; 0.2% or 1% (wt/vol) L-arabinose and 1, 2 or 10 μg/ml aTc. For the latter, a control was performed growing cells in 1% (vol/vol) ethanol since the aTc stock was prepared in 50% (vol/vol) ethanol. The 96-wells plates were incubated at 30°C under continuous light, with the exception of experiments using aTc that were maintained in the dark and cells were grown in mixotrophic conditions, adding glucose to a final concentration of 5 mM and providing a daily light pulse during the measurement procedure (10–15 min). Each experiment was repeated three times, including three technical replicates and the measurements were carried out in duplicate 0, 24, 48 and 72 h after plate setup. GFP fluorescence and OD_{790} were detected using the Synergy 2 Multi-Mode Microplate Reader and the Gen5™ software (BioTek Instruments, Inc.). For fluorescence detection, an excitation filter of 485/20 nm and an emission filter of 528/20 nm were used (sensibility set for 110). For data analysis, the background fluorescence and absorbance of the BG11 medium was subtracted from the values obtained for the samples and, the fluorescence values were normalized by optical density. Then, the normalized fluorescence obtained for the cells harboring the empty plasmids were subtracted from the normalized fluorescence of all samples.

2.10 Confocal microscopy

Synechocystis cells harboring the pSEVA251 or the promoter::GFP generator devices were inoculated in 20 ml of BG11 medium to a final $OD_{730} \approx 0.5$ and grown under continuous light at 30°C until an $OD_{730} \approx 1.0$ was reached. Five microliter of each culture were added to 20 μL of 1% (wt/vol) low-melting point agarose beds (dissolved in BG11 medium) and covered with a coverslip. The cultures were observed using a Leica TCS SP5 confocal microscope (Leica Microsystems). Initially, the microscopy settings were adjusted in order to minimize the autofluorescence of *Synechocystis* wild-type harboring the pSEVA251 and were the same throughout the experiment: GFP emission (collected between 500 and 540 nm) was observed when cells were exposed to a laser beam at 488 nm, and cyanobacterial autofluorescence was collected between 640 and 680 nm after excitation at 633 nm. Images were analyzed with the Leica Application Suite X software (Leica Microsystems).

2.11 SDS-PAGE and western blot

To confirm the presence of the LacI in *Synechocystis* LacI-expressing strains, cell-free extracts were obtained by sonication as described by Pinto *et al.* (13) from *Synechocystis* wild-type and mutants harboring pSEVA251, pSEVA251 $P_{trc.x.lacO}$::*gfp*-P_{rnpB}::*lacI*, pSEVA351, pSEVA351 $P_{T7.1.x.lacO}$::*gfp*-P_{rnpB}::*lacI*, $P_{T7.2.x.lacO}$::*gfp*-P_{rnpB}::*lacI* and $P_{T7.3.x.lacO}$::*gfp*-P_{rnpB}::*lacI* with the T7 RNA polymerase under the control of P_{rnpB} and RBS BBa_B0030 integrated into the chromosomal neutral site N15. Samples were denaturated in reducing SDS sample buffer for 6 min at 95°C and later separated by electrophoresis on 12% (wt/vol) SDS-polyacrylamide gels. The proteins were visualized with colloidal Coomassie Brilliant Blue (Sigma) or blotted onto nitrocellulose membrane pore size 0.45 μm (Amersham™ Protan™, GE Healthcare). Western blots were performed using the rabbit anti-LacI polyclonal antibody (Abnova) and the HRP-conjugated goat anti-rabbit IgG antibody (Sigma). The blot was developed using Clarity™ Western ECL Substrate (Bio-Rad) on a ChemiDoc™ XRS+ Imager (Bio-Rad). In this experiment, three independent biological replicates were performed.

2.12 Transcription analysis by RT-qPCR

Pre-cultures of *Synechocystis* wild-type and the mutant harboring the pSEVA351 $P_{trc.x.lacO}$::*ggpS* (GG device) were grown at 30°C, with rotary shaking (150 rpm), under a 12 h light/12 h dark regimen, until an $OD_{730} \approx 2$ was reached. Subsequently, cultures were diluted in 50 ml of fresh BG11 medium supplemented or not with 3% (wt/vol) NaCl to a final $OD_{730} \approx 0.5$. One-hundred milliliter of culture were collected 3 days post-inoculation ($OD_{730} \approx 1$), centrifuging cells for 10 min at 3850 *g*, pellets were treated with RNAprotect Bacteria Reagent (Qiagen) according to instructions and stored at −80°C. Total RNA was extracted using the TRIzol® Reagent (Ambion) in combination with the Purelink™ RNA Mini Kit (Ambion). Briefly, the cells were disrupted in TRIzol containing 0.2 g of 0.2 mm-diameter glass beads (acid washed, Sigma) using FastPrep®-24 (MP Biomedicals), the following extraction steps included the On-column PureLink® DNase treatment. All steps were performed according to the manufacturer's instructions except DNase treatment, in which a 90 min incubation period at 25°C was used. RNA was quantified on a NanoDrop ND-1000 spectrophotometer (NanoDrop Technologies, Inc.) and the quality and integrity was checked using the Experion™ RNA StdSens Analysis Kit (Bio-Rad). The absence of genomic DNA contamination was checked by PCR, in reaction mixtures containing: 0.5 U of GoTaq® G2 Flexi DNA Polymerase (Promega), 1x Green GoTaq Flexi buffer, 200 μM of each deoxyribonucleotide triphosphate (dNTP), 1.5 mM $MgCl_2$,

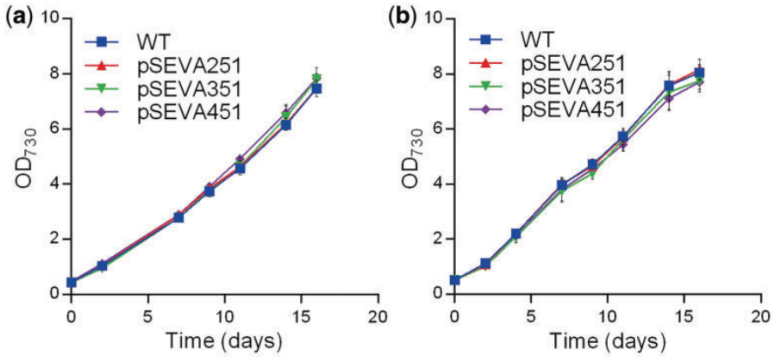

Figure 1. Growth curves of *Synechocystis* wild-type (WT) and mutants harboring the replicative plasmids pSEVA251, pSEVA351 and pSEVA451. Cultures were grown at 30°C with rotary shaking (100 rpm) under (**a**) 12 h light (20 μE/m^2/s)/12 h dark or (**b**) continuous light (20 μE/m^2/s). Growth was monitored by measuring optical density at 730 nm (OD_{730}). Error bars correspond to standard deviations from three biological replicates with technical duplicates.

0.25 μM of each rnpB primer (Supplementary Table S1) and 1 μl total RNA. The PCR profile was: 2 min at 95°C followed by 25 cycles of 30 s at 95°C, 30 s at 56°C and 30 s at 72°C and a final extension at 72°C for 7 min. The PCR reactions were run on agarose gel electrophoresis.

For cDNA synthesis, 1 μg of total RNA was transcribed with the iScript™ Reverse Transcription Supermix for RT-qPCR (Bio-Rad) in a final volume of 20 μl, following the manufacturer's instructions. A control PCR was performed using 1 μl of cDNA as template and the same reaction conditions and PCR program described above. Five-fold standard dilutions of the cDNAs were made (1/5, 1/25, 1/125 and 1/625) and stored at −20°C.

RT-qPCRs were performed as described in Pinto *et al.* (35) using 2 μl of template cDNA (dilution 1/25) and the primers pairs are listed in Supplementary Table S1. The genes 16S, *petB* and *rnpB* were validated as reference genes for data normalization using the geNorm application included in the qbase$^+$ software v3.1 (Biogazelle). All RT-qPCR parameters in these experiments were in agreement with the MIQE (minimum information for publication of quantitative real-time PCR experiments) guidelines. RT-qPCR data from three biological replicates and three technical replicates were analyzed using the IQ5™ Optical System Software v2.1 (Bio-Rad).

2.13 Compatible solutes detection

Pre-cultures of *Synechocystis* wild-type, Δ*ggpS* mutant and the complemented Δ*ggpS* mutant harboring the pSEVA351 $P_{trc.x.lacO}$::*ggpS* (GG device), were grown as described for the RT-qPCR experiments. Five hundred milliliter of culture were cultivated in presence or absence of 3% (wt/vol) NaCl (distributed in ten 50 ml cultures). Three days after inoculation ($OD_{730} \approx 1$) cells were harvested as described in Santos *et al.* (40) with modifications. Cell cultures were centrifuged at 4470 *g* for 10 min at room temperature and the supernatant discarded. Cells were washed adding 100 ml of cold deionized water or 3% (wt/vol) NaCl solution (identical to the growth medium). Centrifugation was repeated and the cell pellet was suspended in 20 ml of the respective solution. Two 1 ml aliquots were removed for protein quantification, centrifuged and stored at −20°C until further use. The remaining cell suspension was centrifuged at 4°C and the cell pellet was stored at −20°C. Ethanol-chloroform extraction of solutes was performed according to Santos *et al.* (40) with adaptations. Briefly, cell pellets were suspended in 50 ml of 80% (vol/vol) ethanol and the cell suspension was transferred to a 250 ml round flask containing a magnetic stir bar. The flask was then connected to a coil condenser (circulating cold water), and the flask was heated in a boiling water bath with stirring for 10 min. The suspension was transferred to a 50 ml tube and centrifuged at 8000 *g* for 10 min at RT. The supernatant was kept in a clean 250 ml round flask and the pellet suspended again in 50 ml of 80% (vol/vol) ethanol for a new extraction; this step was repeated three times. The remainder protocol was performed as described. Detection, identification and quantification of compatible solutes were carried out by Proton NMR (ITQB magnetic resonance center, CERMAX).

2.14 Statistical analysis

The statistical analysis was performed by means of a one-way ANOVA, using GraphPad Prism v6.01 (GraphPad software Inc.).

3. Results and discussion

For the efficient use of the unicellular cyanobacterium *Synechocystis* sp. PCC 6803 as a photoautotrophic chassis, a well-characterized portfolio of tools/biological parts is mandatory. Therefore, three SEVA replicative plasmids and an array of heterologous and redesigned promoters were tested in this organism.

3.1 SEVA plasmids

The SEVA repository (http://seva.cnb.csic.es/) comprises plasmids that are formed by three variable modules—cargo, replication origin and antibiotic marker—separated by three permanent regions, the T_0 and T_1 terminators and the *oriT* conjugation origin (34). In this study, the vectors that include the default multiple cloning site, the RSF1010 broad-host-range replicon, and the antibiotic markers conferring resistance to kanamycin (pSEVA251), chloramphenicol (pSEVA351) or spectinomycin/streptomycin (pSEVA451), were tested. The plasmids were successfully transformed into *Synechocystis* by three different methods: natural transformation, electroporation and conjugation (data not shown). Transformation was confirmed by the acquisition of resistance to the respective antibiotic, by PCR, and by further sequencing of the respective fragment. The presence of the plasmid did not lead to an evident phenotype or hinder *Synechocystis* mutants' growth compared to the wild-type (Figure 1). The replication of these vectors in the cyanobacterium was expected since RSF1010 is the origin of replication present in most of the self-replicating plasmids currently used to

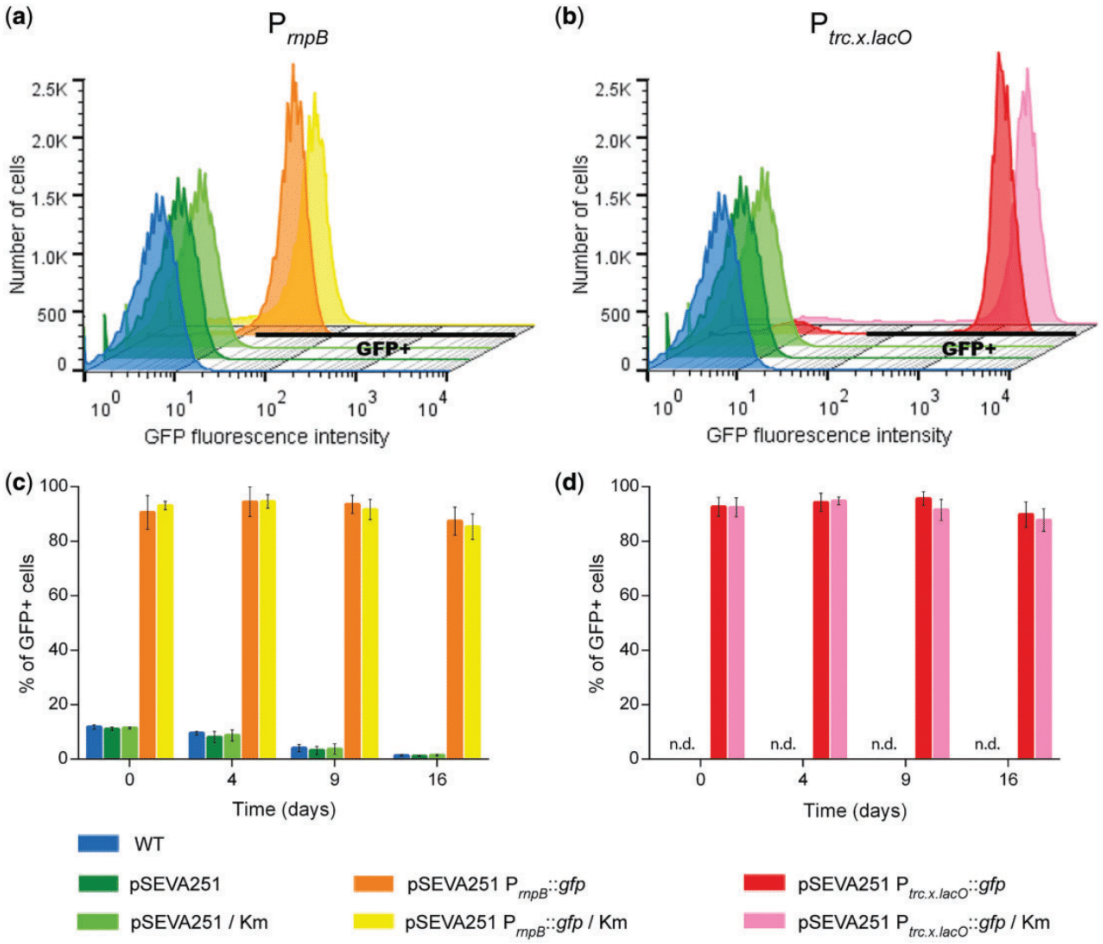

Figure 2. Flow cytometry analysis of GFP fluorescence intensity in cells of *Synechocystis* wild-type (WT) and *Synechocystis* mutants harboring the empty plasmid pSEVA251 or the GFP generator BBa_E0240 under the control of two different promoters P_{rnpB} (reference promoter) and $P_{trc.x.lacO}$ (later characterized in this study)—pSEVA251 P_{rnpB}::*gfp* (**a** and **c**) or pSEVA251 $P_{trc.x.lacO}$::*gfp* (**b** and **d**). The cells were grown in BG11 without or with kanamycin (Km). Histograms of GFP fluorescence intensities acquired in FL1 channel show the establishment of the GFP+ gates (black solid line) in *Synechocystis* mutants harboring the promoter P_{rnpB} (a) or $P_{trc.x.lacO}$ (b) to evaluate the percentage of GFP+ cells (c and d). Histograms are representative of fluorescence intensity of cells analyzed after 16 days of cultivation; the error bars correspond to standard deviations from three biological replicates with technical duplicates. n.d. indicates non-detectable percentage of GFP+ cells for the WT and the strains harboring empty plasmid (d).

transform *Synechocystis* [e.g. pAWG1.1 (41) or pPMQAK1 (8)]. In comparison with these vectors that are over 8 kb (8), the pSEVAs are relatively small (pSEVA251: 5275 bp, pSEVA351: 5120 bp and pSEVA451: 5334 bp), making handling and transference easier. In addition, the possibility to use electroporation reduces the amount of DNA and time required to transform *Synechocystis* cells and the transformant colonies are obtained faster (about 1 week compared to at least 2 weeks for natural transformation and 4 weeks for conjugation).

To evaluate the capacity of the *Synechocystis* mutants to retain the replicative plasmid pSEVA251 during cultivation in medium without the selective pressure, a flow cytometry analysis was performed. Cells transformed with the empty vector pSEVA251, or with the same vector containing the GFP generator BBa_E0240 under the control of either P_{rnpB} (8) (the cyanobacterial reference promoter) or $P_{trc.x.lacO}$ (one of the redesigned promoters characterized in this study, see Section 3.3) (for details see Figure 3a), were grown in BG11 medium with or without Km. The mean GFP fluorescence intensity in cells of *Synechocystis* harboring the $P_{trc.x.lacO}$ was 34-fold higher compared to the cells harboring the P_{rnpB} (Figure 2a and b). The results also showed that the percentage of cells emitting fluorescence in the GFP detecting channel determined by the GFP+ gates (hereafter named GFP+ cells) was similar for the two promoters tested (~92%, Figure 2c and d). In addition, the percentage of GFP+ cells cultivated in medium with selective pressure was not significantly different from that of cells grown in medium without antibiotic (Figure 2c and d). These results were further confirmed by observing the cells with a confocal microscope. Overall, it is possible to determine that at least 90% of the cells grown for 16 days without selective pressure were able to retain the replicative plasmid, and that this

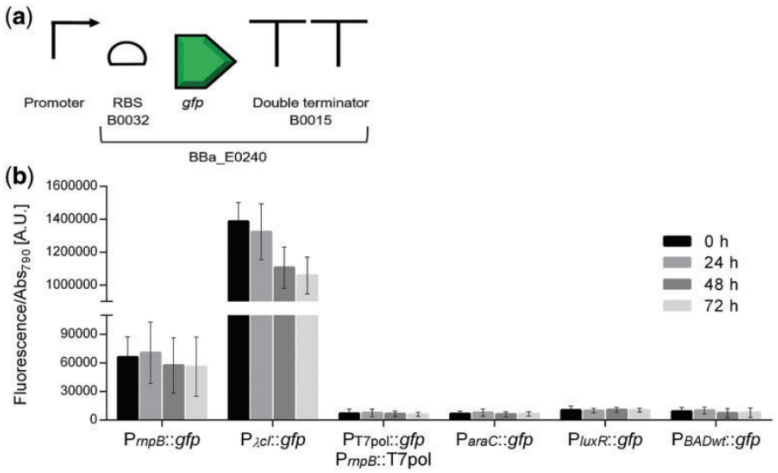

Figure 3. Characterization of heterologous promoters in *Synechocystis*. (**a**) Schematic representation of the promoters and the GFP generator (BBa_E0240) assembly. (**b**) Normalized GFP fluorescence of *Synechocystis* cultures harboring the $P_{\lambda cI}$, P_{T7pol}, P_{araC}, P_{luxR} and P_{BADwt} promoters. Measurements were performed up to three days (0, 24, 48 and 72 h) and the fluorescence was normalized to Abs_{790}. Fluorescence of the control strain harboring the pSEVA251 was subtracted from each sample. Error bars correspond to standard deviations from three biological replicates with technical triplicates (measured in duplicate). P_{rnpB}::*gfp* was included for comparison purposes.

flow cytometry methodology can accurately be used to follow the fraction of the population that keeps carrying a replicative plasmid for a given period of time.

3.2 Heterologous promoters

A set of heterologous promoters well described and routinely used in *E. coli* either from bacterial origin (P_{luxR}, P_{araC} and P_{BADwt}) or bacteriophage-derived ($P_{\lambda cI}$ and P_{T7pol}) were characterized in *Synechocystis*. For this purpose, the promoters were assembled with the GFP generator BBa_E0240 (Figure 3a), subsequently each module was transferred to pSEVA251 and transformed into *Synechocystis* by electroporation. For promoter characterization, GFP expression was determined by measuring fluorescence of the cultures and normalizing it to cell density. The promoter of the RNase P gene (P_{rnpB}) was used as reference (8).

The heterologous promoters P_{T7pol}, P_{araC}, P_{luxR} and P_{BADwt} exhibited lower activity compared to the reference promoter P_{rnpB} (Figure 3b), supporting earlier observations that promoters with strong activity in *E. coli* may perform differently in cyanobacteria (8). Beyond the genomic context, the transcriptional machinery of *Synechocystis* has several differences compared to *E. coli*, namely the RNA polymerase subunits (42). In contrast, 20-fold higher fluorescence levels were detected when $P_{\lambda cI}$ was used. This result can be explained by the high similarity of the $P_{\lambda cI}$-10 and -35 consensus boxes with the cyanobacterial type I promoters (42). Nevertheless, Huang *et al.* (8) reported no activity for this promoter (referred to as P_R) in *Synechocystis*, using two different fluorescence detection systems. The only difference between our constructs and those of Huang *et al.* (8) is the RBS (here BBa_B0032 was used, while Huang *et al.* (8) used BBa_B0034). However, this should not have any influence on the output since it has been reported that these RBS have similar translation efficiencies in *Synechocystis* (43).

To evaluate whether the P_{araC}, P_{BADwt}, P_{luxR} and $P_{\lambda cI}$ promoters could be regulated in *Synechocystis*, the genes encoding the respective regulatory proteins (*araC*—BBa_C0080; *luxR*—BBa_C0062 or *cI*—BBa_C0051) were cloned under the control of P_{rnpB} with a strong RBS (BBa_B0030) and placed downstream of the respective promoter::*gfp* assembly (Figure 4a). The AraC regulated promoters, P_{araC} and P_{BADwt} were not repressed in presence of the protein, probably due to the absence of the $araO_2$ operator region that has been shown to be essential for promoter repression in *E. coli* (44, 45). For the P_{BADwt}, the presence of the AraC regulatory protein led to a 6-fold increase in GFP fluorescence independently of the presence of L-arabinose (Supplementary Figure S1). In the native system, the P_{BADwt} is induced by the binding of an AraC dimer to the $araI_1$ and $araI_2$ operators in an L-arabinose dependent manner (46). However, our results indicate that in *Synechocystis* AraC binds to the $araI_1$ and $araI_2$ operators in the absence of L-arabinose, as previously suggested for *E. coli* (47) and that can be explained by the high affinity of AraC to these operators. The P_{luxR} promoter from *Vibrio fischeri* promotes weak constitutive expression of downstream genes and can be induced by the binding of LuxR complexed with signaling molecules from the acyl-homoserine lactone class (AHLs) (48). In *Synechocystis*, an 8-fold increase in fluorescence was observed in presence of LuxR compared to constitutive levels (Supplementary Figure S2), and the induction was shown to be independent of AHLs. Similarly, in *E. coli*, it was shown that backwards transcription from the P_{luxR} can occur by binding of the LuxR to the promoter in the absence of AHLs (49). The regulated expression of the heterologous $P_{\lambda cI}$ promoter was also tested in *Synechocystis*. The presence of the CI protein in the system resulted in 99% repression compared to constitutive levels (Figure 4b), displaying a similar behavior to the previously reported (50). A tight and stable repression was registered during the 3 days of the experiment demonstrating that $P_{\lambda cI}$, together with the regulating protein CI can be used to efficiently control transcription. Therefore, regulation of CI expression levels would allow the implementation of a controlled circuit using the $P_{\lambda cI}$ promoter.

3.3 Redesigned promoters

In addition to the heterologous promoters, the use of orthogonal regulatory parts based on the T7 RNA polymerase promoter was also explored. For this purpose, three existing variants of the

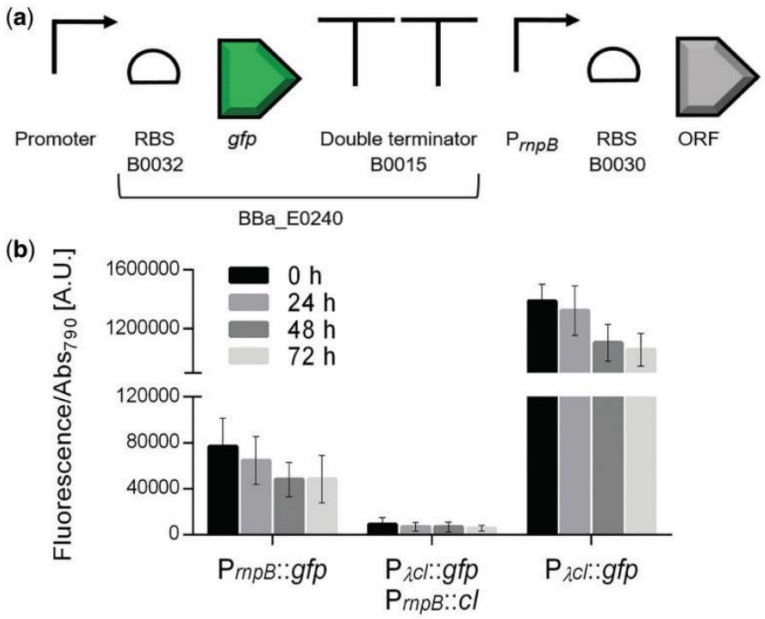

Figure 4. Characterization of the $P_{\lambda cI}$ regulated expression in *Synechocystis*. (**a**) Schematic representation of the promoter GFP generator (BBa_E0240) assembly followed by P_{rnpB}::ORF encoding the regulatory protein. (**b**) Normalized GFP fluorescence of *Synechocystis* cultures harboring the promoter $P_{\lambda cI}$ in presence ($P_{\lambda cI}$::*gfp*-P_{rnpB}::*cI*) or in absence ($P_{\lambda cI}$::*gfp*) of the CI repressor. Measurements were performed up to three days (0, 24, 48 and 72 h) and the fluorescence was normalized to Abs_{790}. The fluorescence of the control strain harboring the pSEVA251 was subtracted from each sample. Error bars correspond to standard deviations from three biological replicates with technical triplicates (measured in duplicate). P_{rnpB}::*gfp* was included for comparison purposes.

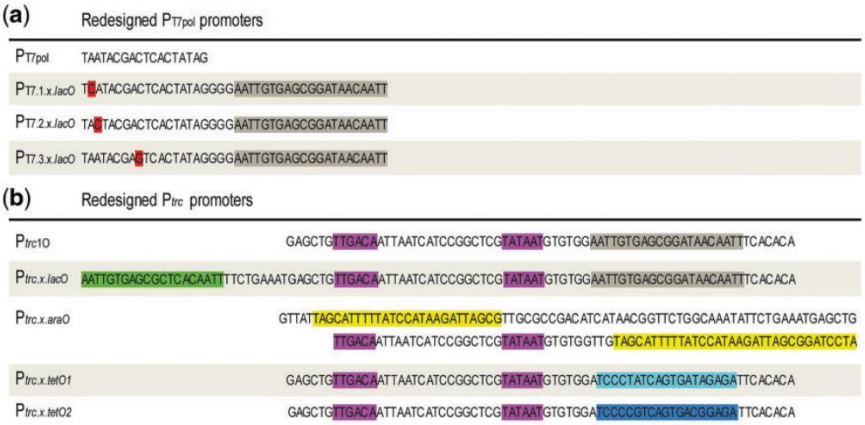

Figure 5. Redesigned promoter sequences. (**a**) Promoter sequences of $P_{T7.1.x.lacO}$, $P_{T7.2.x.lacO}$ and $P_{T7.3.x.lacO}$. The mutations are highlighted in red and the *lacO* operator in gray. The P_{T7pol} original promoter sequence was included for comparison purposes. (**b**) Promoter sequences of $P_{trc.x.lacO}$, $P_{trc.x.araO}$, $P_{trc.x.tetO1}$ and $P_{trc.x.tetO2}$. The predicted -35 and -10 boxes are highlighted in purple, the *lacO* operator in gray, the *lacO*id operator in green, the *araO* operators in yellow, the *tetO* operator in light blue and the modified *tetO* operator in dark blue. The P_{trc1O} original sequence was included for comparison purposes.

P_{T7pol}, differing only in one nucleotide (meant to obtain promoters with different strengths) (30, 31), and based on Novagen® pET expression vectors, were redesigned to include an operator region for the LacI regulator originating the $P_{T7.1.x.lacO}$, $P_{T7.2.x.lacO}$ and $P_{T7.3.x.lacO}$ promoters (Figure 5a, for details see Table 1).

These redesigned T7 promoters were assembled with the GFP generator BBa_E0240 (depicted in Figure 3a, see also Section 2.4), cloned in pSEVA351 and transformed into a *Synechocystis* mutant with the T7 RNA polymerase under the control of the P_{rnpB} and RBS BBa_B0030 integrated into the chromosomal neutral site N15 (13).

All the redesigned P_{T7pol} variants showed lower GFP expression levels compared to the reference promoter P_{rnpB}; while the comparison of the expression levels of the variants with the P_{T7pol} revealed significant differences for $P_{T7.2.x.lacO}$ and $P_{T7.3.x.lacO}$, P-value <0.0001 (Figure 6). Furthermore, our results showed that the GFP expression levels driven by the P_{T7pol} were similar when the T7 polymerase was integrated into the genome (Figure 6, P_{T7pol}::*gfp*) or in a self-replicating plasmid (see

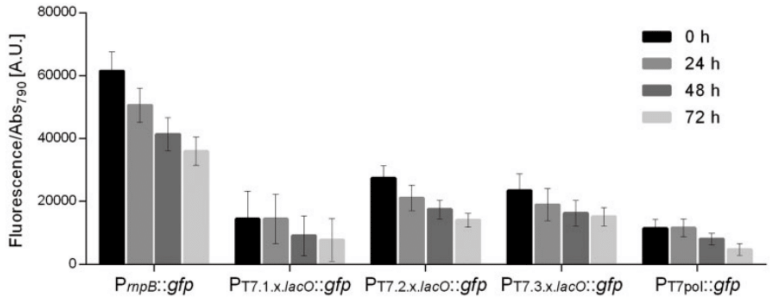

Figure 6. Characterization of the P_{T7pol} and redesigned P_{T7pol} promoter variants in *Synechocystis* constitutively expressing the T7 polymerase. Normalized GFP fluorescence of *Synechocystis* cultures harboring the P_{T7pol}, $P_{T7.1.x.lacO}$, $P_{T7.2.x.lacO}$ and $P_{T7.3.x.lacO}$. Measurements were performed up to three days (0, 24, 48 and 72 h) and the fluorescence was normalized to Abs_{790}. The fluorescence of the control strain harboring the pSEVA251 was subtracted from each sample. Error bars correspond to standard deviations from three biological replicates with technical triplicates (measured in duplicate). P_{rnpB}::*gfp* was included for comparison purposes.

Figure 3, P_{T7pol}::*gfp*-P_{rnpB}::T7pol). The regulation of these promoters by the LacI protein was also tested. The Lac repressor from *E. coli* is one of the most well-characterized transcription factors and is orthogonal to cyanobacteria (51), hence a low risk of cross-talking was expected. However, the results revealed that the redesigned P_{T7pol} variants were not repressed in the presence of the co-expressed LacI (data not shown). The presence of LacI, in the cells harboring the three variants was confirmed by western blot (Supplementary Figure S3), implying that the lack of repression was not due to the lack of the regulatory protein. One possible explanation is that LacI is not binding to the operator region. The lack of repression was also observed in P_{tacI} (data not shown), a hybrid promoter that contains the -35 sequence from P_{trp} (tryptophan operon promoter from *E. coli*) and the P_{lacUV5} sequence that includes the -10 box and the *lacO* operator (32). Interestingly, Huang *et al.* (8) reported LacI-mediated repression of the P_{trc1O} promoter, which differs from the P_{tacI} only in the spacer size between the -35 and -10 boxes, with 17 bp instead of 16 bp. This change in the core promoter also influenced the constitutive expression levels: P_{tacI} is 17-fold stronger than P_{rnpB}, while P_{trc1O} is 83-fold stronger (8). From the promoters characterized in *Synechocystis* and referred herein, the P_{trc1O} is the strongest and was, therefore, redesigned including the operator sequences for the regulatory proteins LacI, AraC and TetR (promoter sequences shown in Figure 5b). The constitutive GFP expression driven by the redesigned promoters $P_{trc.x.tetO1}$, $P_{trc.x.araO}$, $P_{trc.x.tetO2}$ and $P_{trc.x.lacO}$ was evaluated being respectively 13-, 14-, 21- and 41-fold stronger than the one registered for P_{rnpB} (Figure 7a). However, the strength of the promoters was lower than expected since the core promoter from the P_{trc1O} was maintained in these elements. The fluorescence of *Synechocystis* cells harboring the constructs with the promoters P_{rnpB}, $P_{trc.x.tetO2}$ and $P_{trc.x.lacO}$ was also analyzed by confocal microscopy, showing that the fluorescence signal was evenly distributed within the cells (Figure 7b). Moreover, differences in GFP expression driven by the three promoters could be readily observed (Figure 7b) and are consistent with the differences in promoter strength previously determined (Figure 7a).

The regulated expression of the redesigned promoters based on P_{trc1O} was also evaluated, cloning the genes encoding the regulatory proteins LacI, AraC or TetR downstream of the respective promoter::*gfp* assembly, in a similar approach to that described for the heterologous promoters (Figure 4a). The promoter $P_{trc.x.lacO}$ was designed to include a second *lac* operator—the *lacO*id that has a modified sequence known to increase its affinity to the LacI in *E. coli*—16 bp upstream of the -35 box (52). In *Synechocystis*, characterization of the $P_{trc.x.lacO}$ promoter in the presence of LacI, revealed a 97% reduction in fluorescence compared to constitutive levels (Figure 8). This is in agreement with previous work in *E. coli* demonstrating that the presence of two spatially separated LacI-binding operators in phase can confer a tight repression of P_{lac} through the formation of a DNA loop (53). In *Synechocystis*, similar repression levels were obtained for a P_{lac} based promoter with two *lacO*id operators separated by 50 bp (51), the same distance between the operators of the $P_{trc.x.lacO}$. In *E. coli*, the LacI mediated repression can be reverted in presence of isopropyl β-D-1-thiogalactopyranoside (IPTG) or lactose. Therefore, the derepression of the $P_{trc.x.lacO}$ by IPTG was tested in *Synechocystis*. Three days (72 h) after the addition of 1 or 2 mM of IPTG, the expression levels increased 2.2-fold compared to repression conditions (-IPTG) (Figure 8). However, increasing the IPTG concentration up to 20 mM or using lactose did not increase the efficiency of derepression, which could be due to: high amounts of LacI, tight repression by DNA looping, high affinity of the *lacO*id operator and/or lack of an import system for IPTG or lactose. This limited derepression was also previously reported by Huang *et al.* (8) Recently, the permeability of *Synechocystis* to small organic nutrients was shown to be >20-fold lower than that of *E. coli* (54), which could account for the poor promoter derepression response to IPTG. Nevertheless, the introduction of the *E. coli*'s lactose permease (*lacY*) in *Synechocystis* did not result in increased levels of derepression (20).

$P_{trc.x.araO}$ was designed to be efficiently repressed by the AraC. For this purpose, two $araI_1$ half-sites from the *E. coli*'s P_{BAD} promoter (55) were included. However, only a 15% reduction in fluorescence was observed in the presence of AraC compared to the constitutive levels (data not shown), which may be due to the inefficient formation of the DNA loop using two $araI_1$ operator regions. This is unexpected, since the 111 bp distance between the centers of the $araI_1$ operators should be sufficient to enable the formation of the DNA loop through the binding of the AraC homodimer, and also, the operators should be in phase since 11.1 bp is the periodicity of P_{BAD} repression (45).

Finally, the P_{trc} promoter was redesigned replacing the original operator sequence by the *tetO* operator that was included 8 bp downstream of the -10 box – $P_{trc.x.tetO1}$. In *Synechocystis*, evaluation of the expression regulated by TetR revealed a significant repression with 89% reduction in fluorescence compared to constitutive levels (Supplementary Figure S4). The derepression of this promoter using anhydrotetracycline hydrochloride (aTc) was tested, and a 2.3-fold increase in GFP expression levels was

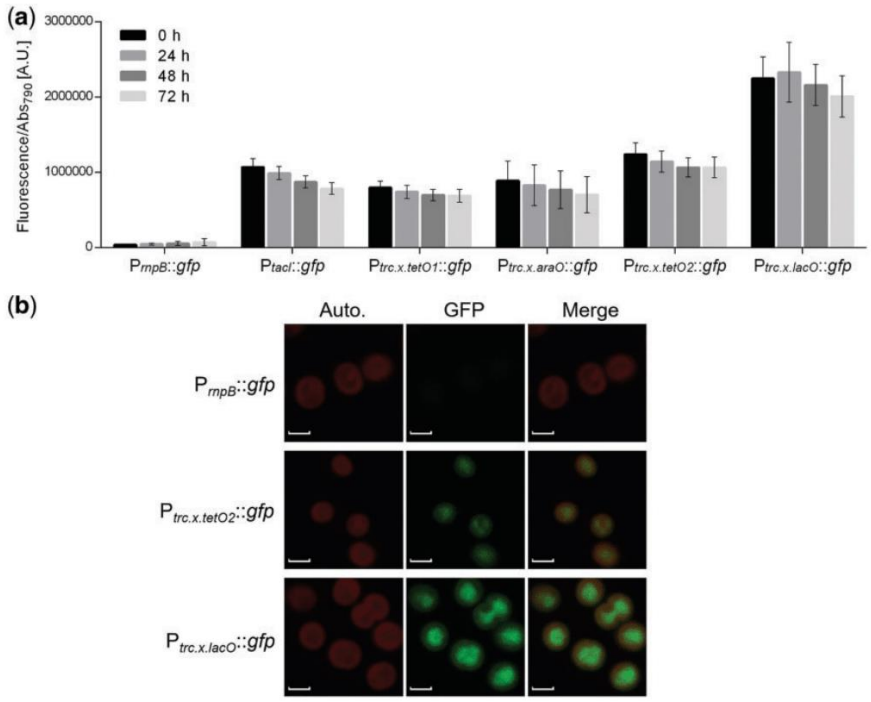

Figure 7. Characterization of the hybrid P_{tacI} and the redesigned *trc* promoters in *Synechocystis*. (**a**) Normalized GFP fluorescence of *Synechocystis* cultures harboring the P_{tacI}, $P_{trc.x.tetO1}$, $P_{trc.x.araO}$, $P_{trc.x.tetO2}$ and $P_{trc.x.lacO}$. Measurements were performed up to three days (0, 24, 48 and 72 h) and the fluorescence was normalized to Abs_{790}. The fluorescence of the control strain harboring the pSEVA251 was subtracted from each sample. Error bars correspond to standard deviations from three biological replicates with technical triplicates (measured in duplicate). P_{rnpB}::*gfp* was included for comparison purposes. (**b**) Confocal micrographs of *Synechocystis* cells harboring the P_{rnpB}, $P_{trc.x.tetO2}$ or $P_{trc.x.lacO}$ promoters assembled with the GFP generator. Autofluorescence is depicted in the left column, GFP signal in the middle column and the merged signals in the right column. Scale bar, 2 μm.

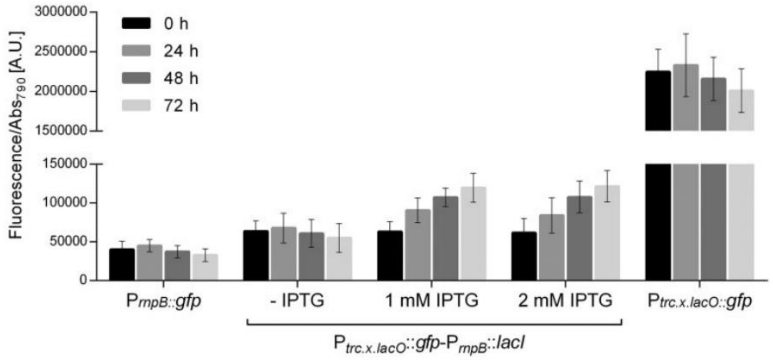

Figure 8. Characterization of the regulated expression of the $P_{trc.x.lacO}$ in *Synechocystis*. Normalized GFP fluorescence was determined for cell cultures harboring the redesigned *trc* promoter and expressing the LacI repressor ($P_{trc.x.lacO}$::*gfp*-P_{rnpB}::*lacI*) without (-) or with addition (1 or 2 mM) of IPTG. Measurements were performed up to three days (0, 24, 48 and 72 h) and the fluorescence was normalized to Abs_{790}. The fluorescence of the control strain harboring the pSEVA251 was subtracted from each sample. Error bars correspond to standard deviations from three biological replicates with technical triplicates (measured in duplicate). Data from P_{rnpB}::*gfp* and $P_{trc.x.lacO}$::*gfp* were included for comparison purposes.

registered 72 h after the addition of 1 μg/ml aTc, compared to repression conditions (-aTc) (Supplementary Figure S4). Increasing the aTc concentration up to 10 μg/ml did not result in higher derepression levels (data not shown), which cannot be related to the light-sensitivity of aTc (10) since these experiments were conducted in the dark. However, the use of aTc was previously demonstrated to derepress TetR regulated promoters but this occurred in the presence of two operator regions (56) instead of the single operator used in this study. The presence of two operators seems to be essential to regulate the system. A second version of a TetR regulated P_{trc} promoter was designed harboring a modified *tetO* operator that differs from the original sequence in four nucleotides (57). When tested in *Synechocystis*, the $P_{trc.x.tetO2}$ was not repressed in the presence of TetR (data not shown), which is in agreement with the results obtained in *E. coli* (57).

Another promoter tested in this study was P_{psbA2*}, a synthetic regulatory element based on one of the strongest *Synechocystis* native promoters (P_{psbA2}) from which the elements for light dependent regulation were removed (13). The functionality of the P_{psbA2*} was previously demonstrated in *Synechocystis* (13), and its characterization here revealed that it is 6-fold stronger than the reference promoter P_{rnpB} (Supplementary Figure S5).

3.4 The expanded toolbox at work: restoring the production of a compatible solute

From the set of novel and validated molecular tools described above, the synthetic constitutive promoter $P_{trc.x.lacO}$ was used in the assembly of a synthetic device meant to restore the production the compatible solute GG in a *Synechocystis* deletion mutant (Δ*ggpS*). Compatible solutes are low molecular weight organic molecules that can be accumulated intracellularly without interfering with essential processes or metabolism and allow the organism to cope with environmental stresses such as temperature, salt or drought (58). *Synechocystis* is a moderately halotolerant cyanobacterium that is known to produce sucrose and GG as major compatible solutes (58). GG is synthesized via the glucosylglycerol-phosphate synthase (GgpS) and glucosylglycerol-phosphate phosphatase (GgpP) pathway (58). The synthetic GG producing device, including the *ggpS* ORF preceded by $P_{trc.x.lacO}$ and the strong RBS BBa_B0030 (Supplementary Figure S6a), was cloned in pSEVA351 and transformed into *Synechocystis* Δ*ggpS* via electroporation.

The growth of *Synechocystis* wild-type (WT), the Δ*ggpS* mutant, and the complemented Δ*ggpS* mutant (Δ*ggpS*_GG device) in BG11 medium containing 0, 3 or 5% (wt/vol) NaCl was monitored (Supplementary Figure S6b). The results suggest that, in absence of salt, the presence of the GG device imposes a metabolic burden due to increased *ggpS* gene transcription (Supplementary Figure S7). However, in the presence of 3% (wt/vol) NaCl no significant differences between the three strains were observed, while with 5% (wt/vol) NaCl the growth of the Δ*ggpS* mutant complemented with the GG device is similar to the wild-type, pointing out to the functionality of our device/tools.

In addition, the transcript levels of *ggpS* and *ggpP* were analyzed by RT-qPCR (Supplementary Figure S7). As shown in Supplementary Figure S7, cultivation of *Synechocystis* wild-type in medium supplemented with NaCl leads to an increase in relative transcript levels of both *ggpS* and *ggpP*, in agreement with previous studies (59, 60). In the Δ*ggpS* mutant, the transcription profile of *ggpP* was similar to the one exhibited by the wild-type. When the Δ*ggpS* mutant is complemented by the introduction of the GG device, a 45-fold increase in transcription could be observed for *ggpS* in 5% (wt/vol) NaCl compared to the wild-type, clearly demonstrating the functionality of the synthetic GG device at the transcriptional level.

Moreover, the presence of salt-stress related compatible solutes was evaluated using H-NMR (Supplementary Figure S8). In the wild-type, GG is detected only in presence of salt while glutamate is present independently of the stress. As expected, GG was not detected in the Δ*ggpS* mutant, but since sucrose and glutamate could be detected under 3% (wt/vol) NaCl, and the Δ*ggpS* mutant was able to grow similarly to the wild-type, we postulate that sucrose and glutamate can compensate for the absence of GG. The complementation of the Δ*ggpS* mutant with the GG device restored the production of this compatible solute in presence of NaCl (Supplementary Figure S8, lower right panel). This salt-dependent synthesis of GG is in agreement with previous works, showing that the GgpS enzyme is inhibited by electrostatic interaction with nucleic acids and that its activation occurs only in the presence of salt (60, 61). Thus, the synthetic GG device assembled using the promoters developed herein was shown to be fully functional.

4. Conclusions

In this study, we expanded the synthetic biology toolbox for the photoautotrophic cyanobacterial chassis *Synechocystis* sp. PCC 6803: three self-replicating plasmids available at the SEVA repository were validated and 13 heterologous and redesigned promoters based on P_{T7pol} and P_{trc} were characterized, exhibiting a wide range of activities varying from ∼0.13- to ∼41-fold compared to P_{rnpB}. From this set of promoters, three could be efficiently repressed ($P_{λcI}$, $P_{trc.x.lacO}$ and $P_{trc.x.tetO1}$). Derepression of the LacI- and TetR-regulated redesigned promoters using IPTG or aTc was also shown, although a modest effect (about ∼2-fold increase) was observed. This study constitutes a solid basis for the development and implementation of more efficient and tightly regulated elements required by applications using cyanobacteria as cell factories. Moreover, the tools developed and presented here allowed the assembly of a synthetic module with *ggpS* gene and its introduction into the *chassis*—a *Synechocystis ggpS* deficient mutant, restoring the production of the compatible solute GG.

SUPPLEMENTARY DATA

Supplementary data are available at SYNBIO online.

Acknowledgements

The authors wish to thank the Parasite Disease group (i3S/IBMC) for the use of Synergy 2 Multi-Mode Microplate Reader. We are also grateful to Prof. Helena Santos and Sara Rebelo (ITQB, Universidade Nova de Lisboa) for the collaboration and technical assistance regarding compatible solutes extraction and quantification, and Prof. Peter Lindblad (Uppsala University) for providing the initial aliquot of the anti-LacI polyclonal antibody.

Funding

European Commission through the 7th Framework Programme FP7-ENERGY-2012-1-2STAGE-308518 project CyanoFactory [308518] and 6th Framework Programme EU FP6-NEST-2005-Path-SYN project BioModularH2 [043340]; National Portuguese Funds through FCT—Fundação para a Ciência e a Tecnologia scholarships SFRH/BD/117508/2016 (E.A.F.), SFRH/BD/36378/2007 (F.P.), SFRH/BPD/64095/2009 (C.C.P.) and SFRH/BPD/74894/2010 (P.O.) and by the FCT Investigator Programme (IF/00256/2015) (P.O.); and by project NORTE-01-0145-FEDER-000012—Structured Programme on Bioengineering Therapies for Infectious Diseases and Tissue Regeneration, supported by Norte Portugal Regional Operational Programme (NORTE 2020), under the PORTUGAL 2020 Partnership Agreement, through the European Regional Development Fund (ERDF).

Conflict of interest statement. None declared.

References

1. Knoll,A.H. (2008) Cyanobacteria and earth history. In: FG Flores and A Herrero (eds). *The Cyanobacteria: Molecular Biology, Genomics, and Evolution*. Caister Academic Press, Norfolk, UK, pp. 1–19.
2. Kaneko,T., Sato,S., Kotani,H., Tanaka,A., Asamizu,E., Nakamura,Y., Miyajima,N., Hirosawa,M., Sugiura,M., Sasamoto,S. et al. (1996) Sequence analysis of the genome of the unicellular cyanobacterium *Synechocystis* sp. strain PCC 6803. II. Sequence determination of the entire genome and assignment of potential protein-coding regions. *DNA Res.*, 3, 109–136.
3. Montagud,A., Zelezniak,A., Navarro,E., de Córdoba,P.F., Urchueguía,J.F. and Patil,K.R. (2011) Flux coupling and transcriptional regulation within the metabolic network of the photosynthetic bacterium *Synechocystis* sp. PCC 6803. *Biotechnol. J.*, 6, 330–342.
4. Fu,P. (2009) Genome-scale modeling of *Synechocystis* sp. PCC 6803 and prediction of pathway insertion. *J. Chem. Technol. Biotechnol.*, 84, 473–483.
5. Branco dos Santos,F., Du,W. and Hellingwerf,K.J. (2014) *Synechocystis*: not just a plug-bug for CO_2, but a green *E. coli*. *Front. Bioeng. Biotechnol.*, 2,
6. Tsai,C.-S., Kwak,S., Turner,T.L. and Jin,Y.-S. (2015) Yeast synthetic biology toolbox and applications for biofuel production. *FEMS Yeast Res.*, 15, 1–15.
7. Xu,P., Vansiri,A., Bhan,N. and Koffas,M.A.G. (2012) ePathBrick: a synthetic biology platform for engineering metabolic pathways in *E. coli*. *ACS Synth. Biol.*, 1, 256–266.
8. Huang,H.-H., Camsund,D., Lindblad,P. and Heidorn,T. (2010) Design and characterization of molecular tools for a Synthetic Biology approach towards developing cyanobacterial biotechnology. *Nucleic Acids Res.*, 38, 2577–2593.
9. Cardinale,S. and Arkin,A.P. (2012) Contextualizing context for synthetic biology—identifying causes of failure of synthetic biological systems. *Biotechnol. J.*, 7, 856–866.
10. Huang,H.-H. and Lindblad,P. (2013) Wide-dynamic-range promoters engineered for cyanobacteria. *J. Biol. Eng.*, 7, 10.
11. Englund,E., Liang,F. and Lindberg,P. (2016) Evaluation of promoters and ribosome binding sites for biotechnological applications in the unicellular cyanobacterium *Synechocystis* sp. PCC 6803. *Sci. Rep.*, 6, 36640.
12. Immethun,C.M., DeLorenzo,D.M., Focht,C.M., Gupta,D., Johnson,C.B. and Moon,T.S. (2017) Physical, chemical, and metabolic state sensors expand the synthetic biology toolbox for *Synechocystis* sp. PCC 6803. *Biotechnol. Bioeng.*, 114, 1561–1569.
13. Pinto,F., Pacheco,C.C., Oliveira,P., Montagud,A., Landels,A., Couto,N., Wright,P.C., Urchueguía,J.F. and Tamagnini,P. (2015) Improving a *Synechocystis*-based photoautotrophic chassis through systematic genome mapping and validation of neutral sites. *DNA Res.*, 22, 425–437.
14. Liu,D. and Pakrasi,H.B. (2018) Exploring native genetic elements as plug-in tools for synthetic biology in the cyanobacterium *Synechocystis* sp. PCC 6803. *Microb. Cell Fact.* 17, 48.
15. Lindberg,P., Park,S. and Melis,A. (2010) Engineering a platform for photosynthetic isoprene production in cyanobacteria, using *Synechocystis* as the model organism. *Metab. Eng.*, 12, 70–79.
16. Zhou,J., Zhang,H., Meng,H., Zhu,Y., Bao,G., Zhang,Y., Li,Y. and Ma,Y. (2015) Discovery of a super-strong promoter enables efficient production of heterologous proteins in cyanobacteria. *Sci. Rep.*, 4, 4500.
17. Peca,L., Kós,P. and Vass,I. (2007) Characterization of the activity of heavy metal-responsive promoters in the cyanobacterium *Synechocystis* PCC 6803. *Acta Biol. Hung.*, 58, 11–22.
18. Muramatsu,M. and Hihara,Y. (2007) Coordinated high-light response of genes encoding subunits of photosystem I is achieved by AT-rich upstream sequences in the cyanobacterium *Synechocystis* sp. strain PCC 6803. *J. Bacteriol.*, 189, 2750–2758.
19. Abe,K., Miyake,K., Nakamura,M., Kojima,K., Ferri,S., Ikebukuro,K. and Sode,K. (2014) Engineering of a green-light inducible gene expression system in *Synechocystis* sp. PCC 6803. *Microb. Biotechnol.*, 7, 177–183.
20. Albers,S.C., Gallegos,V.A. and Peebles,C.A.M. (2015) Engineering of genetic control tools in *Synechocystis* sp. PCC 6803 using rational design techniques. *J. Biotechnol.*, 216, 36–46.
21. Taton,A., Unglaub,F., Wright,N.E., Zeng,W.Y., Paz-Yepes,J., Brahamsha,B., Palenik,B., Peterson,T.C., Haerizadeh,F., Golden,S.S. et al. (2014) Broad-host-range vector system for synthetic biology and biotechnology in cyanobacteria. *Nucleic Acids Res.*, 42, e136.
22. Ng,A.H., Berla,B.M. and Pakrasi,H.B. (2015) Fine-tuning of photoautotrophic protein production by combining promoters and neutral sites in the cyanobacterium *Synechocystis* sp. strain PCC 6803. *Appl. Environ. Microbiol.*, 81, 6857–6863.
23. Ducat,D.C., Way,J.C. and Silver,P.A. (2011) Engineering cyanobacteria to generate high-value products. *Trends Biotechnol.*, 29, 95–103.
24. Lindblad,P., Lindberg,P., Oliveira,P., Stensjö,K. and Heidorn,T. (2012) Design, engineering, and construction of photosynthetic microbial cell factories for renewable solar fuel production. *Ambio*, 41, 163–168.
25. Wang,B., Wang,J., Zhang,W. and Meldrum,D.R. (2012) Application of synthetic biology in cyanobacteria and algae. *Front. Microbiol.*, 3,
26. Kanesaki,Y., Shiwa,Y., Tajima,N., Suzuki,M., Watanabe,S., Sato,N., Ikeuchi,M. and Yoshikawa,H. (2012) Identification of substrain-specific mutations by massively parallel whole-genome resequencing of *Synechocystis* sp. PCC 6803. *DNA Res.*, 19, 67–79.
27. Trautmann,D., Voss,B., Wilde,A., Al-Babili,S. and Hess,W.R. (2012) Microevolution in cyanobacteria: re-sequencing a motile substrain of *Synechocystis* sp. PCC 6803. *DNA Res.*, 19, 435–448.
28. Stanier,R.Y., Kunisawa,R., Mandel,M. and Cohen-Bazire,G. (1971) Purification and properties of unicellular blue-green algae (order Chroococcales). *Bacteriol. Rev.*, 35, 171–205.
29. Sambrook,J. and Russel,D. (2001) *Molecular Cloning: A Laboratory Manual*, 3rd ed. Cold Spring Harbor Laboratory Press, Cold Spring Harbor, New York, USA.
30. Imburgio,D., Rong,M., Ma,K. and McAllister,W.T. (2000) Studies of promoter recognition and start site selection by T7 RNA polymerase using a comprehensive collection of promoter variants. *Biochemistry*, 39, 10419–10430.
31. Diaz,G.A., Raskin,C.A. and McAllister,W.T. (1993) Hierarchy of base-preference in the binding domain of the bacteriophage T7 promoter. *J. Mol. Biol.*, 229, 805–811.
32. de Boer,H.A., Comstock,L.J. and Vasser,M. (1983) The *tac* promoter: a functional hybrid derived from the *trp* and *lac* promoters. *Proc. Natl. Acad. Sci. U. S. A.*, 80, 21–25.
33. Brosius,J., Erfle,M. and Storella,J. (1985) Spacing of the -10 and -35 regions in the *tac* promoter. Effect on its *in vivo* activity. *J. Biol. Chem.*, 260, 3539–3541.
34. Silva-Rocha,R., Martínez-García,E., Calles,B., Chavarría,M., Arce-Rodríguez,A., de las Heras,A., Páez-Espino,A.D.,

Durante-Rodríguez,G., Kim,J., Nikel,P.I. et al. (2013) The Standard European Vector Architecture (SEVA): a coherent platform for the analysis and deployment of complex prokaryotic phenotypes. *Nucleic Acids Res.*, 41, D666–D675.

35. Pinto,F., Pacheco,C.C., Ferreira,D., Moradas-Ferreira,P. and Tamagnini,P. (2012) Selection of suitable reference genes for RT-qPCR analyses in cyanobacteria. *PLoS One*, 7, e34983.
36. Schäfer,A., Tauch,A., Jäger,W., Kalinowski,J., Thierbach,G. and Pühler,A. (1994) Small mobilizable multi-purpose cloning vectors derived from the *Escherichia coli* plasmids pK18 and pK19: selection of defined deletions in the chromosome of *Corynebacterium glutamicum*. *Gene*, 145, 69–73.
37. Williams,J.G. (1988) Construction of specific mutations in photosystem II photosynthetic reaction center by genetic engineering methods in *Synechocystis* 6803. *Methods Enzymol.*, 167, 766–778.
38. Ludwig,A., Heimbucher,T., Gregor,W., Czerny,T. and Schmetterer,G. (2008) Transformation and gene replacement in the facultatively chemoheterotrophic, unicellular cyanobacterium *Synechocystis* sp. PCC 6714 by electroporation. *Appl. Microbiol. Biotechnol.*, 78, 729–735.
39. Elhai,J. and Wolk,C.P. (1988) Conjugal transfer of DNA to cyanobacteria. *Methods Enzymol.*, 167, 747–754.
40. Santos,H., Lamosa,P. and Borges,N. (2006) Characterization and quantification of compatible solutes in (hyper)thermophilic microorganisms. In: Rainey FA and Oren A (eds.) *Methods in Microbiology*. Academic Press, Amsterdam, Netherlands, pp. 173–199.
41. Dyczmons,N.G. (2006) Expression and regulation of membrane proteins: special focus on cytochrome bd-oxidase from *Synechocystis* sp. PCC 6803, *Ph. D. Thesis. Ruhr-Universität Bochum*, Bochum, Germany.
42. Camsund,D. and Lindblad,P. (2014) Engineered transcriptional systems for cyanobacterial biotechnology. *Front. Bioeng. Biotechnol.*, 2, 40.
43. Heidorn,T., Camsund,D., Huang,H.-H., Lindberg,P., Oliveira,P., Stensjö,K. and Lindblad,P. (2011) Synthetic biology in cyanobacteria: engineering and analyzing novel functions. *Methods Enzymol.*, 497, 539–579.
44. Hamilton,E.P. and Lee,N. (1988) Three binding sites for AraC protein are required for autoregulation of *araC* in *Escherichia coli*. *Proc. Natl. Acad. Sci. U. S. A.*, 85, 1749–1753.
45. Lee,D.H. and Schleif,R.F. (1989) *In vivo* DNA loops in *araCBAD*: size limits and helical repeat. *Proc. Natl. Acad. Sci. U. S. A.*, 86, 476–480.
46. Lee,N., Francklyn,C. and Hamilton,E.P. (1987) Arabinose-induced binding of AraC protein to *araI2* activates the *araBAD* operon promoter. *Proc. Natl. Acad. Sci. U. S. A.*, 84, 8814–8818.
47. Schleif,R. (2010) AraC protein, regulation of the L-arabinose operon in *Escherichia coli*, and the light switch mechanism of AraC action. *FEMS Microbiol. Rev.*, 34, 779–796.
48. Nasser,W. and Reverchon,S. (2007) New insights into the regulatory mechanisms of the LuxR family of quorum sensing regulators. *Anal. Bioanal. Chem.*, 387, 381–390.
49. Pearson,B., Lau,K.H., DeLoache,W., Penumetcha,P., Rinker,V.G., Allen,A., Cool,R., Feeney,E., Igo,J., Eckdahl,T.T. et al. (2011) Bacterial hash function using DNA-based XOR logic reveals unexpected behavior of the *luxR* promoter. *Interdiscip. Bio Central*, 3, 1.
50. Lewis,D., Le,P., Zurla,C., Finzi,L. and Adhya,S. (2011) Multilevel autoregulation of λ repressor protein CI by DNA looping in *vitro*. *Proc. Natl. Acad. Sci. U. S. A.*, 108, 14807–14812.
51. Camsund,D., Heidorn,T. and Lindblad,P. (2014) Design and analysis of LacI-repressed promoters and DNA-looping in a cyanobacterium. *J. Biol. Eng.*, 8, 4.
52. Müller,J., Oehler,S. and Müller-Hill,B. (1996) Repression of *lac* promoter as a function of distance, phase and quality of an auxiliary *lac* operator. *J. Mol. Biol.*, 257, 21–29.
53. Schleif,R. (1992) DNA looping. *Annu. Rev. Biochem.*, 61, 199–223.
54. Kowata,H., Tochigi,S., Takahashi,H. and Kojima,S. (2017) Outer membrane permeability of cyanobacterium *Synechocystis* sp. strain PCC 6803: studies of passive diffusion of small organic nutrients reveal the absence of classical porins and intrinsically low permeability. *J. Bacteriol.*, 199, e00371–e00317.
55. Seabold,R.R. and Schleif,R.F. (1998) Apo-AraC actively seeks to loop. *J. Mol. Biol.*, 278, 529–538.
56. Yao,L., Cengic,I., Anfelt,J. and Hudson,E.P. (2016) Multiple gene repression in cyanobacteria using CRISPRi. *ACS Synth. Biol.*, 5, 207–212.
57. Krueger,M., Scholz,O., Wisshak,S. and Hillen,W. (2007) Engineered Tet repressors with recognition specificity for the *tetO*-4C5G operator variant. *Gene*, 404, 93–100.
58. Hagemann,M. (2013) Genomics of salt acclimation: synthesis of compatible solutes among cyanobacteria. In: CC-C Franck Chauvat (ed.). *Advances in Botanical Research*. Academic Press, Amsterdam, Netherlands, pp. 27–55.
59. ——, Richter,S. and Mikkat,S. (1997) The *ggtA* gene encodes a subunit of the transport system for the osmoprotective compound glucosylglycerol in *Synechocystis* sp. strain PCC 6803. *J. Bacteriol.*, 179, 714–720.
60. Marin,K., Huckauf,J., Fulda,S. and Hagemann,M. (2002) Salt-dependent expression of glucosylglycerol-phosphate synthase, involved in osmolyte synthesis in the cyanobacterium *Synechocystis* sp. strain PCC 6803. *J. Bacteriol.*, 184, 2870–2877.
61. Novak,J.F., Stirnberg,M., Roenneke,B. and Marin,K. (2011) A novel mechanism of osmosensing, a salt-dependent protein-nucleic acid interaction in the cyanobacterium *Synechocystis* species PCC 6803. *J. Biol. Chem.*, 286, 3235–3241.

Supporting Information

Expanding the toolbox for *Synechocystis* sp. PCC 6803: Validation of replicative vectors and characterization of a novel set of promoters

Eunice A. Ferreira[1,2,3,†], Catarina C. Pacheco[1,2,†], Filipe Pinto[1,2,a], José Pereira[1,2], Pedro Lamosa[4], Paulo Oliveira[1,2], Boris Kirov[5,b], Alfonso Jaramillo[5,6,7], and Paula Tamagnini[1,2,8,*]

[1]i3S – Instituto de Investigação e Inovação em Saúde, Universidade do Porto, 4200-135 Porto, Portugal. [2]IBMC – Instituto de Biologia Molecular e Celular, Universidade do Porto, 4200-135 Porto, Portugal. [3]ICBAS – Instituto de Ciências Biomédicas Abel Salazar, Universidade do Porto, 4050-313 Porto, Portugal. [4]Instituto de Tecnologia Química e Biológica António Xavier, ITQB NOVA, 2780-157 Oeiras, Portugal. [5]CNRS-UMR8030, Laboratoire iSSB and Université Paris-Saclay and Université d'Évry and CEA, DRF, IG, Genoscope, Évry 91000, France. [6]Warwick Integrative Synthetic Biology Centre and School of Life Sciences, University of Warwick, CV4 7AL, Coventry, UK. [7]Institute for Integrative Systems Biology (I2SysBio), University of Valencia-CSIC, 46980 Paterna, Spain. [8]Faculdade de Ciências, Departamento de Biologia, Universidade do Porto, 4169-007 Porto, Portugal.

[*]Corresponding author: Rua Alfredo Allen, 208, 4200-135 Porto, Portugal. Tel: +351 220 408 800. E-mail address: pmtamagn@ibmc.up.pt

[†]The first two authors are joint first authors.

Present Addresses: [a]School of Biological Sciences, University of Edinburgh, Edinburgh EH9 3FF, UK. Centre for Synthetic and Systems Biology, University of Edinburgh, Edinburgh EH9 3FF, UK. [b]ANP - Faculty of Automatics, TU – Sofia, Sofia, Bulgaria. BioInfoTech Lab - RDIC, Sofia Tech Park, Sofia, Bulgaria.

Contents

Supplementary Figures

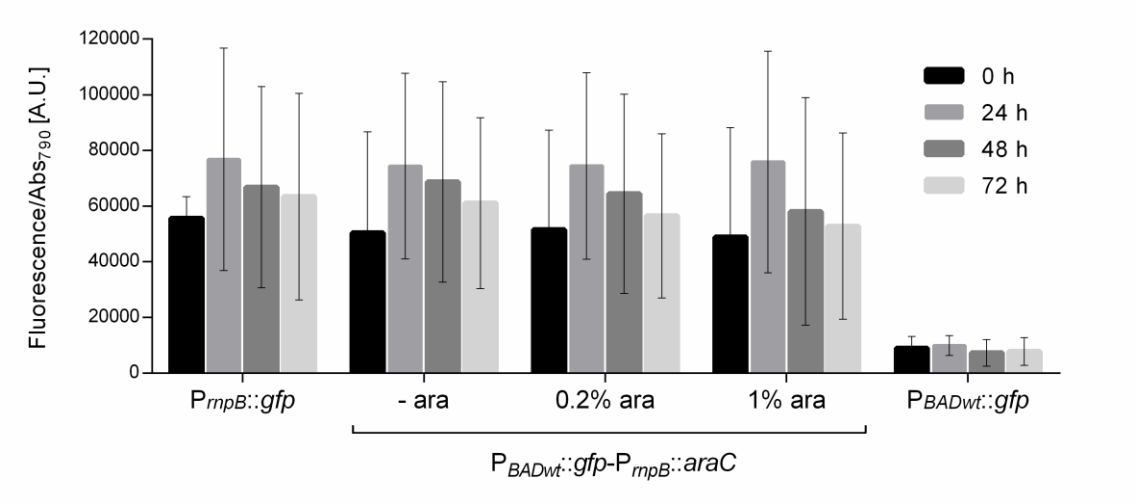

Figure S1. Characterization of the regulated expression of the P_{BADwt} in *Synechocystis*. Normalized GFP fluorescence was determined for cell cultures harboring the promoter and expressing the AraC (P_{BADwt}::*gfp*-P_{rnpB}::*araC*) without (-) or with addition [0.2% or 1% (wt/vol)] of L-arabinose. Measurements were performed up to three days (0, 24, 48 and 72 h) and the fluorescence was normalized to Abs_{790}. The fluorescence of the control strain harboring the pSEVA251 was subtracted from each sample. Error bars correspond to standard deviations from three biological replicates with technical triplicates (measured in duplicate). Data from P_{rnpB}::*gfp* and P_{BADwt}::*gfp* were included for comparison purposes.

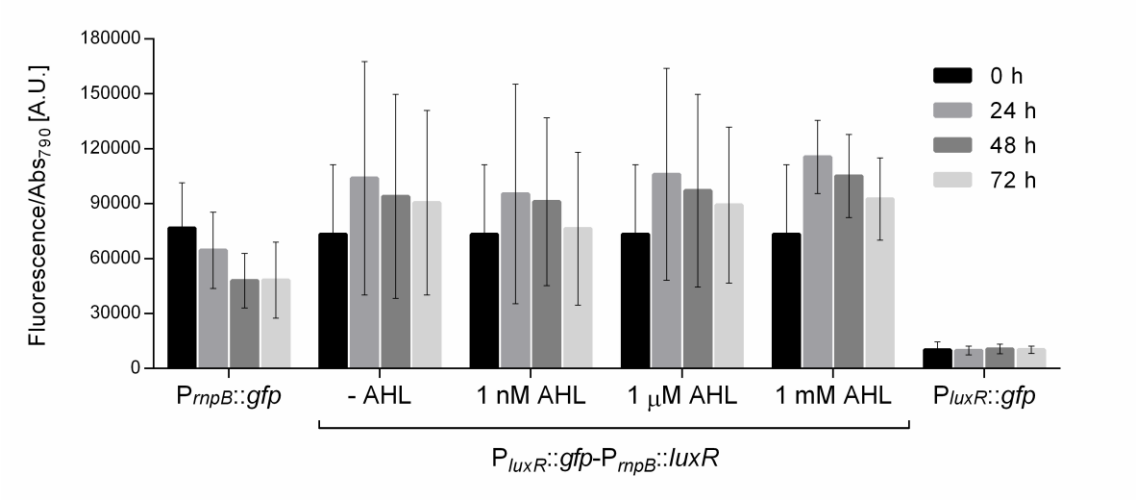

Figure S2. Characterization of the regulated expression of the P_{luxR} in *Synechocystis*. Normalized GFP fluorescence was determined for cell cultures harboring the promoter and expressing the LuxR (P_{luxR}::*gfp*-P_{rnpB}::*luxR*) without (-) or with addition (1 nM, 1 µM or 1 mM) of AHL. Measurements were performed up to three days (0, 24, 48 and 72 h) and the fluorescence was normalized to Abs_{790}. The fluorescence of the control strain harboring the pSEVA251 was subtracted from each sample. Error bars correspond to standard deviations from three biological replicates with technical triplicates (measured in duplicate). Data from P_{rnpB}::*gfp* and P_{luxR}::*gfp* were included for comparison purposes.

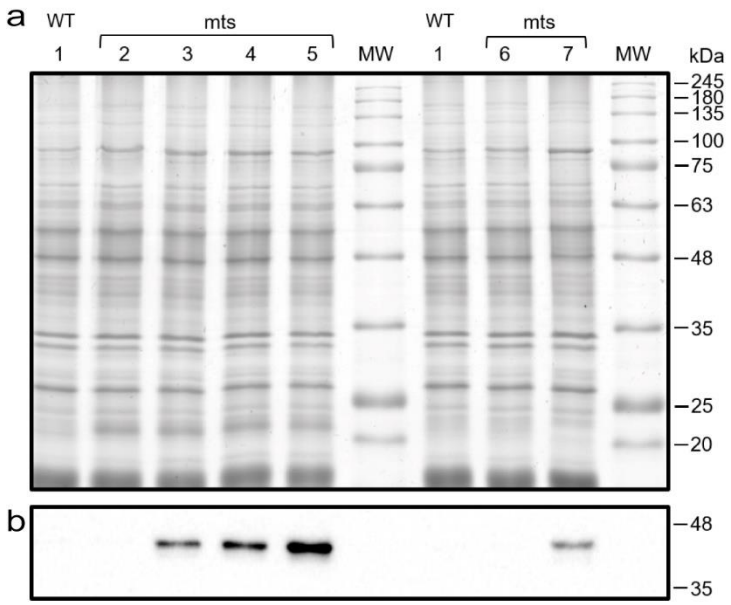

Figure S3. SDS-PAGE and SDS-PAGE/Western blot of *Synechocystis* wild-type (WT) and mutant strains (mts). 10 µg of cell-free protein extracts of *Synechocystis* wild-type (1) and *Synechocystis* mutants harboring pSEVA351 (2), pSEVA351 $P_{T7.1.x.lacO}$::*gfp*-P_{rnpB}::*lacI* (3), $P_{T7.2.x.lacO}$::*gfp*-P_{rnpB}::*lacI* (4) and $P_{T7.3.x.lacO}$::*gfp*-P_{rnpB}::*lacI* (5) with the T7 RNA polymerase under the control of the P_{rnpB} and RBS BBa_B0030 integrated into the chromosomal neutral site N15, pSEVA251 (6) and pSEVA251 $P_{trc.x.lacO}$::*gfp*-P_{rnpB}::*lacI* (7) were separated on a 12% SDS-PAGE, and visualized using Coomassie Brilliant Blue (a) or blotted onto nitrocellulose membrane (b). For the detection of LacI, the nitrocellulose membrane was incubated with the rabbit anti-LacI polyclonal antibody (Abnova) and the HRP-conjugated goat anti-rabbit IgG antibody (Sigma). The molecular weight (MW) of the NZYColour Protein Marker II (NZYTech) bands are indicated on the right. A single peptide, with the LacI expected molecular weight (~38 kDa), was detected in four mutant strains (b). The results are representative of three independent biological replicates.

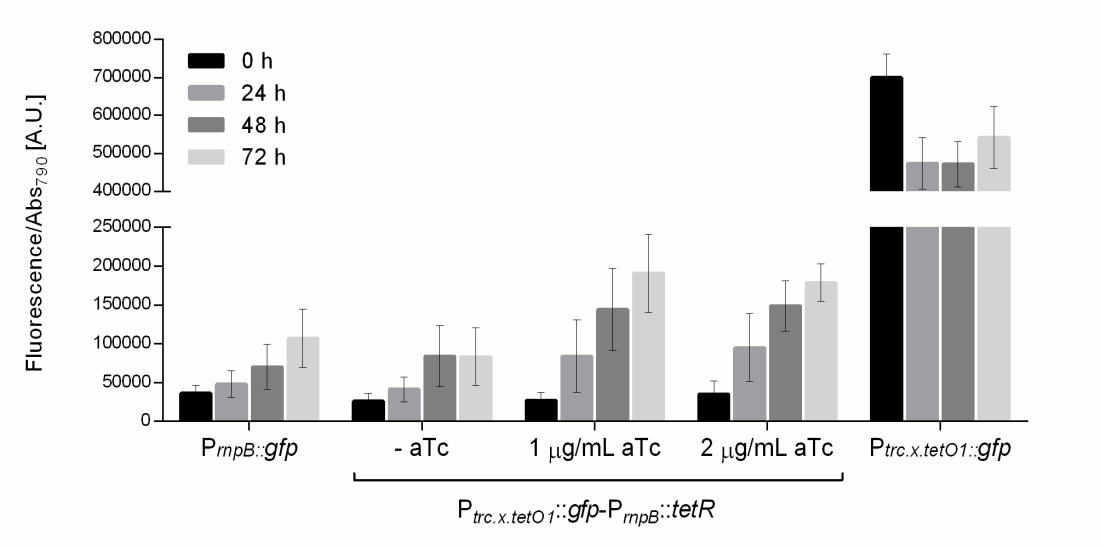

Figure S4. Characterization of the regulated expression of the $P_{trc.x.tetR1}$ in *Synechocystis*. Normalized GFP fluorescence was determined for cell cultures harboring the redesigned *trc* promoter and expressing the TetR repressor ($P_{trc.x.tetO1}$::*gfp*-P_{rnpB}::*tetR*) without (-) or with addition (1 µg/mL or 2 µg/mL) of aTc. Measurements were performed up to three days (0, 24, 48 and 72 h) and the fluorescence was normalized to Abs_{790}. The fluorescence of the control strain harboring the pSEVA251 was subtracted from each sample. Error bars correspond to standard deviations from three biological replicates with technical triplicates (measured in duplicate). Data from P_{rnpB}::*gfp* and $P_{trc.x.tetO1}$::*gfp* were included for comparison purposes.

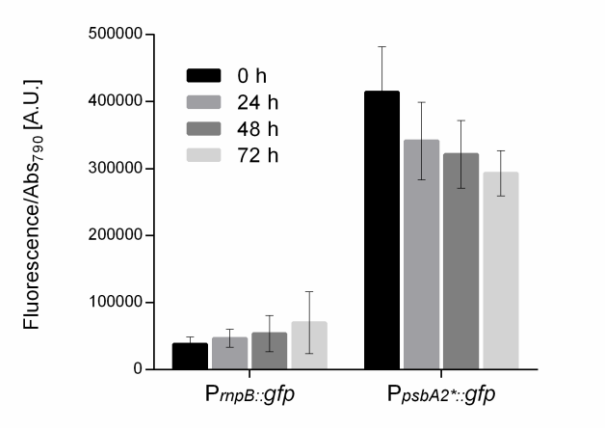

Figure S5. Characterization of the promoter P_{psbA2*} in *Synechocystis*. Normalized GFP fluorescence of *Synechocystis* cultures harboring the P_{psbA2*}. Measurements were performed up to three days (0, 24, 48 and 72 h) and the fluorescence was normalized to Abs_{790}. The fluorescence of the control strain harboring the pSEVA251 was subtracted from each sample. Error bars correspond to standard deviations from three biological replicates with technical triplicates (measured in duplicate). P_{rnpB}::*gfp* was included for comparison purposes.

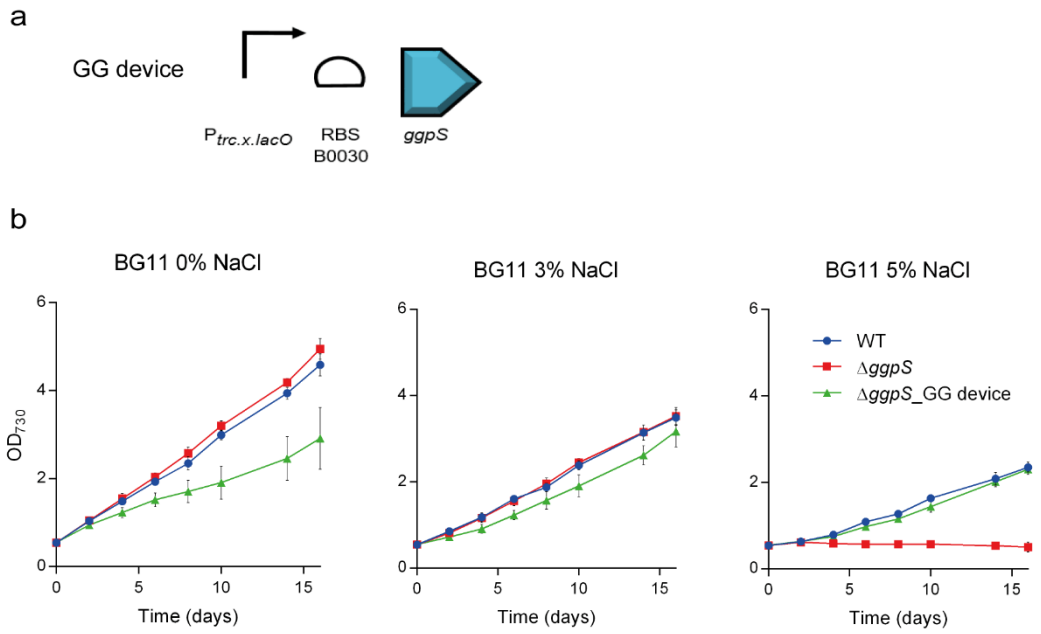

Figure S6. Complementation of a *Synechocystis* Δ*ggpS* mutant with a synthetic device meant to restore the production of glucosylglycerol (GG). (a) Schematic representation of the GG device. (b) Growth curves of *Synechocystis* wild-type (WT), Δ*ggpS* mutant and the complemented Δ*ggpS* mutant (Δ*ggpS*_GG device). The cells were grown in BG11, or BG11 supplemented with 3% or 5% (wt/vol) NaCl. Cultures were incubated at 30 ºC with orbital shaking (150 rpm) under a 12 h light (25 µE/m^2/s) / 12 h dark regimen. Growth was monitored by measuring optical density at 730 nm (OD_{730}) every two days for a 16-days period. Error bars correspond to standard deviations from three biological replicates with technical duplicates.

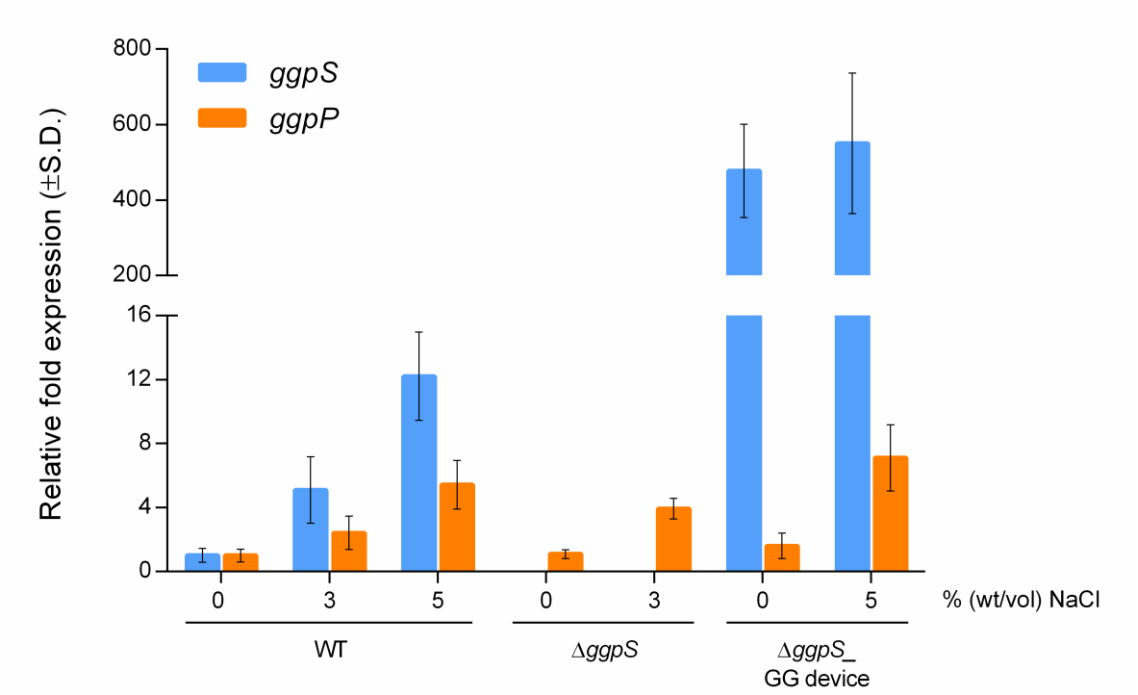

Figure S7. Analysis of *ggpS* and *ggpP* transcript levels by RT-qPCR. Cultures of *Synechocystis* wild-type (WT), the Δ*ggpS* mutant and the Δ*ggpS* mutant harboring GG device (Δ*ggpS*_GG device) were grown in BG11 medium supplemented with 0, 3 or 5% (wt/vol) NaCl. The relative fold expression is normalized for the wild-type at 0% (wt/vol) NaCl and the *rnpB*, *petB* and 16S were used as reference genes. Error bars correspond to standard deviations from three biological replicates with technical triplicates.

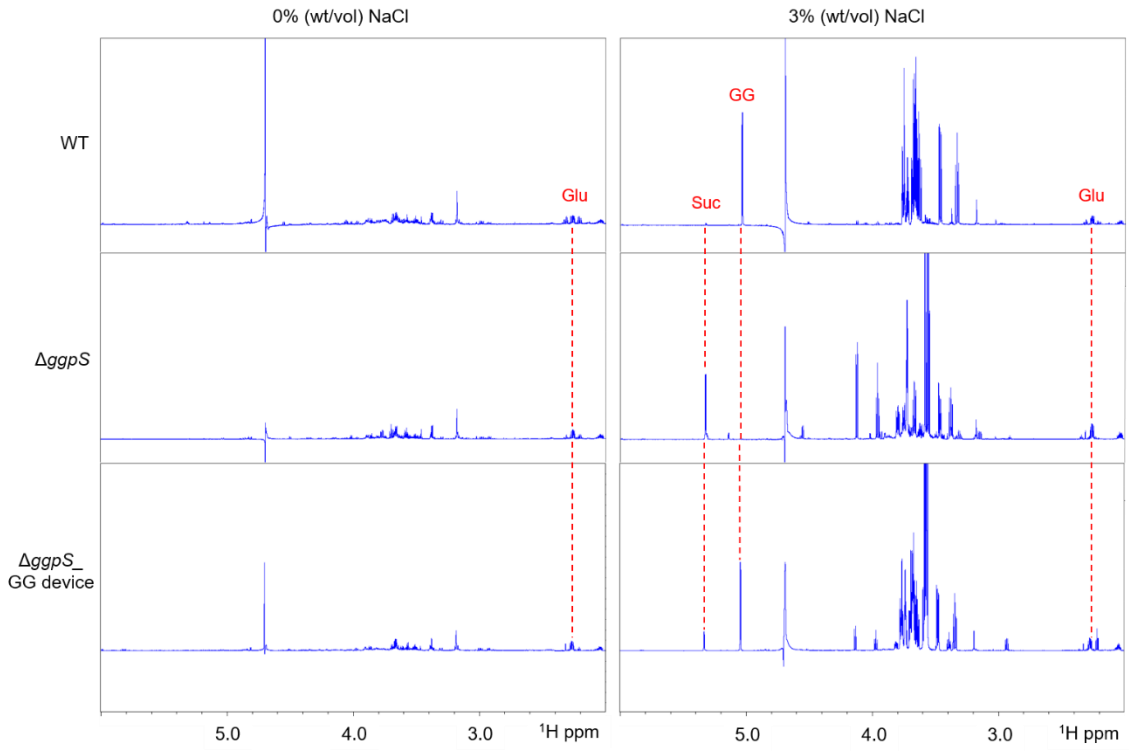

Figure S8. Proton NMR spectra of *Synechocystis* cell extracts for the detection of the compatible solutes glutamate (Glu), sucrose (Suc), and glucosylglycerol (GG). Cell extracts were obtained from *Synechocystis* wild-type (WT), Δ*ggpS* mutant and the complemented Δ*ggpS* mutant (Δ*ggpS*_GG device) cultures grown in BG11 [0% (wt/vol) NaCl] – left pannel, or BG11 supplemented with NaCl [3% (wt/vol) NaCl] – right panel. Spectra were acquired at 25 °C on an AVANCE III 800 spectrometer (Bruker) using a four channel inverse detection probe head with solvent presaturation of the extracts. Dashed red lines label one representative ressonance of Glu, Suc and GG.

Supplementary Table

Table S1. List of primers used in this study.

Primer name	Sequence*	T_a (°C)**	Purpose	Reference/ Source
pJ201F (pTF***)	CTCGAAAATAATAAAGGGAAAATCAG	51	Confirmation of constructs in pJ201	DNA2.0, Inc.
pJ201R (pTR***)	TGGTAGTGTGGGGACTC			DNA2.0, Inc.
GFP.F	TCTTGTTGAATTAGATGGTG	51	Confirmation of constructs with the GFP generator	This work
GFP.R	TGTGAGTTATAGTTGTATTCC			
VF2	TGCCACCTGACGTCTAAGAA	55	Confirmation of constructs in BioBrick plasmids	http://parts.igem.org/Part:BBa_G00100
VR	ATTACCGCCTTTGAGTGAGC			http://parts.igem.org/Part:BBa_G00101
PS1	AGGGCGGCGGATTTGTCC	60	Confirmation of constructs in pSEVA vectors	[1]
PS2	GCGGCAACCGAGCGTTC			
ggpS.5-O	GCTGGCTCGAGAACACCGTAGGGCAGGGAATAGGTC	60	Generation of the Δ*ggpS* mutant / Southern probe	This work
ggpS.5-I	GATTACAACCGGTTGTAATCACGGCTAATGCACCCGACTTCCCGGAACCCAAGTTAATTC			
ggpS.3-O	CTGGCTTTAACCCTGTCGAGGGAACCATCATAG	60	Generation of the Δ*ggpS* mutant	"
ggpS.3-I	GATTACAACCGGTTGTAATCGTGGTCGGCGGATGGTAACCAAATAACCATTGTC			
BBa_ggpS.F	GTTTCTTCGAATTCGCGGCCGCTTCTAGATGAACTC	60	Amplification of *ggpS* in the BioBrick format	"
BBa_ggpS.R	ATCCCTTGTGATCCTTTACGTTTCTTCCTGCAGCGGCCGCTACTAGTATTATTACATTTGGGGGGGCTCTCCCAGTACC			
ggpP.FI	ATTACAAACGGGCATTGAAGC	56	RT-qPCR	"
ggpP.RI	TGTCCGATTGTGATAGTAACG			
ggpS.FI	CGTGGGCACCAATCCGGCAAATATC	56	RT-qPCR	

ggpS.RI	GGTTAGTCAACACCGCATCGGGTAG			
rnpBF1	CGTTAGGATAGTGCCACAG	56	RT-qPCR	*2*
rnpBR1	CGCTCTTACCGCACCTTTG			
SpetB1F	CCTTCGCCTCTGTCCAATAC	56	RT-qPCR	*2*
SpetB1R	TAGCATTACACCCACAACCC			
BD16SF1	CACACTGGGACTGAGACAC	56	RT-qPCR	*2*
BD16SR1	CTGCTGGCACGGAGTTAG			
PrnpB.F	ACAGCGGCCTATGGCTCTAATC		Confirmation of constructs with P_{rnpB}	This work

*Restriction enzyme recognition sites are underlined
**T_a – annealing temperature
***DNA2.0 original primer names

References

Pinto, F., Pacheco, C. C., Ferreira, D., Moradas-Ferreira, P., & Tamagnini, P. (2012). Selection of suitable reference genes for RT-qPCR analyses in cyanobacteria. *PLoS One, 7*, e34983.

Silva-Rocha, R., Martínez-García, E., Calles, B., Chavarría, M., Arce-Rodríguez, A., de las Heras, A., Páez-Espino, A. D., Durante-Rodríguez, G., Kim, J., Nikel, P. I., Platero, R., & de Lorenzo, V. (2013). The Standard European Vector Architecture (SEVA): a coherent platform for the analysis and deployment of complex prokaryotic phenotypes. *Nucleic Acids Res, 41*, D666-D675.

ysy014_suppl_data.zip

ysy014_Fasta file

```
>PrnpB
TTCAATGCGGTCCAATACCTCCCCTGCCCAACTGGGTAAGCTCGCGGCTCCACTGAGTAA
TACAGACAAGGCTAAACAGGCAAATTTTTTCATTGGTCAACTCCTAGCACCAATTTCCCA
AGACTACGGAGGGGGCAATGAAGTTTCAATTAATTGGGGTCACAAACCACAGCGGCCTAT
GGCTCTAATCAATGGCACACTAGAAAAA

>PT7.1.x.lacO
TCATACGACTCACTATAGGGGAATTGTGAGCGGATAACAATTCC

>PT7.2.x.lacO
TACTACGACTCACTATAGGGGAATTGTGAGCGGATAACAATTCC

>PT7.3.x.lacO
TAATACGAGTCACTATAGGGGAATTGTGAGCGGATAACAATTCC

>PpsbA2*
AGCTTTACAAAACTCTCATTAATCCTTTAGACTAAGTTTAGTCAGTTCCAATCTG

>PtacI
GAGCTGTTGACAATTAATCATCGGCTCGTATAATGTGTGGAATTGTGCGCGGATAACAAT
TTCACAC

>Ptrc.x.lacO
AATTGTGAGCGCTCACAATTTTCTGAAATGAGCTGTTGACAATTAATCATCCGGCTCGTA
TAATGTGTGGAATTGTGAGCGGATAACAATTTCACACA

>Ptrc.x.araO
GTTATTAGCATTTTTATCCATAAGATTAGCGTTGCGCCGACATCATAACGGTTCTGGCAA
ATATTCTGAAATGAGCTGTTGACAATTAATCATCCGGCTCGTATAATGTGTGGTTGTAGC
ATTTTTATCCATAAGATTAGCGGATCCTA

>Ptrc.x.tetO1
GAGCTGTTGACAATTAATCATCCGGCTCGTATAATGTGTGGATCCCTATCAGTGATAGAG
ATTCACACA

>Ptrc.x.tetO2
GAGCTGTTGACAATTAATCATCCGGCTCGTATAATGTGTGGATCCCCGTCAGTGACGGAG
ATTCACACA

>ggpS
ATGAATTCATCCCTTGTGATCCTTTACCACCGTGAGCCCTACGACGAAGTTAGGGAAAAT
GGCAAAACGGTGTATCGAGAGAAAAAGAGTCCCAACGGGATTTTGCCCACCCTCAAAAGT
TTTTTTGCCGATGCGGAACAGAGCACCTGGGTCGCATGGAAACAGGTTTCGCCGAAGCAA
AAGGATGATTTTCAGGCGGATATGTCCATTGAAGGCCTTGGCGATCGTTGTACGGTGCGC
CGGGTGCCCCTGACGGCGGAGCAGGTAAAAAACTTCTATCACATCACTTCCAAGGAAGCC
TTTTGGCCCATTCTCCACTCTTTCCCCTGGCAGTTCACCTACGATTCTTCTGATTGGGAT
AATTTTCAGCACATTAACCGCTTATTTGCCGAGGCGGCCTGTGCCGATGCCGATGACAAT
GCATTGTTTTGGGTCCACGACTATAACCTCTGGTTAGCGCCCCTTTACATTCGTCAGCTC
AAGCCCAACGCCAAGATTGCCTTTTTCCACCACACCCCCTTCCCCAGCGTTGATATTTTC
AATATTTTGCCCTGGCGGGAGGCGATCGTAGAAAGCTTGCTGGCCTGTGATCTCTGTGGT
TTTCATATTCCCCGCTACGTAGAAAATTTTGTCGCCGTGGCCCGTAGTCTCAAGCCGGTG
GAAATCACCAGACGGGTTGTGGTAGACCAAGCCTTTACCCCCTACGGTACGGCCCTGGCG
```

GAACCGGAACTCACCACCCAGTTGCGTTATGGCGATCGCCTCATTAACCTCGATGCGTTT
CCCGTGGGCACCAATCCGGCAAATATCCGGGCGATCGTGGCCAAAGAAAGTGTGCAACAA
AAAGTTGCTGAAATTAAACAAGATTTAGGCGGTAAGAGGCTAATTGTTTCCGCTGGGCGG
GTGGATTACGTGAAGGGCACCAAGGAAATGTTGATGTGCTATGAACGTCTACTGGAGCGT
CGCCCCGAATTGCAGGGGGAAATTAGCCTGGTAGTCCCCGTAGCCAAGGCCGCTGAGGGA
ATGCGTATTTATCGCAACGCCCAAAACGAAATTGAACGACTGGCAGGGAAAATTAACGGT
CGCTTTGCCAAACTGTCCTGGACACCAGTGATGCTGTTCACCTCTCCTTTAGCCTATGAG
GAGCTCATTGCCCTGTTCTGTGCCGCCGACATTGCCTGGATCACTCCCCTGCGGGATGGG
CTAAACCTGGTGGCTAAGGAGTATGTGGTGGCTAAAAATGGCGAAGAAGGAGTTCTGATC
CTCTCGGAATTTGCCGGTTGTGCGGTGGAACTACCCGATGCGGTGTTGACTAACCCCTAC
GCTTCCAGCCGTATGGACGAATCCATTGACCAGGCCCTGGCCATGGACAAAGACGAACAG
AAAAAACGCATGGGGAGAATGTACGCCGCCATTAAGCGTTACGACGTTCAACAATGGGCC
AATCACCTACTGCGGGAAGCCTACGCCGATGTGGTACTGGGAGAGCCCCCCCAAATGTAG

>PlambdacI
TAACACCGTGCGTGTTGACTATTTTACCTCTGGCGGTGATAATGGTTGC

>PluxR
ACCTGTAGGATCGTACAGGTTTACGCAAGAAAATGGTTTGTTATAGTCGAATAAA

>PT7pol
TAATACGACTCACTATAGGGAATACAAGCTACTTGTTCTTTTTGCA

>ParaC
GCGTAACAAAAGTGTCTATAATCACGGCAGAAAAGTCCACATTGATTATTTGCACGGCGT
CACACTTTGCTATGCCATAGCATTTTTATCCATAAGATTAGCGGATCCTACCTGACGCTT
TTTATCGCAACTCTCTACTGTTTCTCCAT

>GFPgenerator
TCACACAGGAAAGTACTAGATGCGTAAAGGAGAAGAACTTTTCACTGGAGTTGTCCCAAT
TCTTGTTGAATTAGATGGTGATGTTAATGGGCACAAATTTTCTGTCAGTGGAGAGGGTGA
AGGTGATGCAACATACGGAAAACTTACCCTTAAATTTATTTGCACTACTGGAAAACTACC
TGTTCCATGGCCAACACTTGTCACTACTTTCGGTTATGGTGTTCAATGCTTTGCGAGATA
CCCAGATCATATGAAACAGCATGACTTTTTCAAGAGTGCCATGCCCGAAGGTTATGTACA
GGAAAGAACTATATTTTTCAAAGATGACGGGAACTACAAGACACGTGCTGAAGTCAAGTT
TGAAGGTGATACCCTTGTTAATAGAATCGAGTTAAAAGGTATTGATTTTAAAGAAGATGG
AAACATTCTTGGACACAAATTGGAATACAACTATAACTCACACAATGTATACATCATGGC
AGACAAACAAAAGAATGGAATCAAAGTTAACTTCAAAATTAGACACAACATTGAAGATGG
AAGCGTTCAACTAGCAGACCATTATCAACAAAATACTCCAATTGGCGATGGCCCTGTCCT
TTTACCAGACAACCATTACCTGTCCACACAATCTGCCCTTTCGAAAGATCCCAACGAAAA
GAGAGACCACATGGTCCTTCTTGAGTTTGTAACAGCTGCTGGGATTACACATGGCATGGA
TGAACTATACAAATAATAATACTAGAGCCAGGCATCAAATAAAACGAAAGGCTCAGTCGA
AAGACTGGGCCTTTCGTTTTATCTGTTGTTTGTCGGTGAACGCTCTCTACTAGAGTCACA
CTGGCTCACCTTCGGGTGGGCCTTTCTGCGTTTATA

>RBS
ATTAAAGAGGAGAAA

>T7pol
ATGAACACGATTAACATCGCTAAGAACGACTTCTCTGACATCGAACTGGCTGCTATCCCG
TTCAACACTCTGGCTGACCATTACGGTGAGCGTTTAGCTCGCGAACAGTTGGCCCTTGAG
CATGAGTCTTACGAGATGGGTGAAGCACGCTTCCGCAAGATGTTTGAGCGTCAACTTAAA
GCTGGTGAGGTTGCGGATAACGCTGCCGCCAAGCCTCTCATCACTACCCTACTCCCTAAG
ATGATTGCACGCATCAACGACTGGTTTGAGGAAGTGAAAGCTAAGCGCGGCAAGCGCCCG
ACAGCCTTCCAGTTCCTGCAAGAAATCAAGCCGGAAGCCGTAGCGTACATCACCATTAAG
ACCACTCTGGCTTGCCTAACCAGTGCTGACAATACAACCGTTCAGGCTGTAGCAAGCGCA

ATCGGTCGGGCCATTGAGGACGAGGCTCGCTTCGGTCGTATCCGTGACCTTGAAGCTAAG
CACTTCAAGAAAAACGTTGAGGAACAACTCAACAAGCGCGTAGGGCACGTCTACAAGAAA
GCATTTATGCAAGTTGTCGAGGCTGACATGCTCTCTAAGGGTCTACTCGGTGGCGAGGCG
TGGTCTTCGTGGCATAAGGAAGACTCTATTCATGTAGGAGTACGCTGCATCGAGATGCTC
ATTGAGTCAACCGGAATGGTTAGCTTACACCGCCAAAATGCTGGCGTAGTAGGTCAAGAC
TCTGAGACTATCGAACTCGCACCTGAATACGCTGAGGCTATCGCAACCCGTGCAGGTGCG
CTGGCTGGCATCTCTCCGATGTTCCAACCTTGCGTAGTTCCTCCTAAGCCGTGGACTGGC
ATTACTGGTGGTGGCTATTGGGCTAACGGTCGTCGTCCTCTGGCGCTGGTGCGTACTCAC
AGTAAGAAAGCACTGATGCGCTACGAAGACGTTTACATGCCTGAGGTGTACAAAGCGATT
AACATTGCGCAAAACACCGCATGGAAAATCAACAAGAAAGTCCTAGCGGTCGCCAACGTA
ATCACCAAGTGGAAGCATTGTCCGGTCGAGGACATCCCTGCGATTGAGCGTGAAGAACTC
CCGATGAAACCGGAAGACATCGACATGAATCCTGAGGCTCTCACCGCGTGGAAACGTGCT
GCCGCTGCTGTGTACCGCAAGGACAAGGCTCGCAAGTCTCGCCGTATCAGCCTTGAGTTC
ATGCTTGAGCAAGCCAATAAGTTTGCTAACCATAAGGCCATCTGGTTCCCTTACAACATG
GACTGGCGCGGTCGTGTTTACGCTGTGTCAATGTTCAACCCGCAAGGTAACGATATGACC
AAAGGACTGCTTACGCTGGCGAAAGGTAAACCAATCGGTAAGGAAGGTTACTACTGGCTG
AAAATCCACGGTGCAAACTGTGCGGGTGTCGATAAGGTTCCGTTCCCTGAGCGCATCAAG
TTCATTGAGGAAAACCACGAGAACATCATGGCTTGCGCTAAGTCTCCACTGGAGAACACT
TGGTGGGCTGAGCAAGATTCTCCGTTCTGCTTCCTTGCGTTCTGCTTTGAGTACGCTGGG
GTACAGCACCACGGCCTGAGCTATAACTGCTCCCTTCCGCTGGCGTTTGACGGGTCTTGC
TCTGGCATCCAGCACTTCTCCGCGATGCTCCGAGATGAGGTAGGTGGTCGCGCGGTTAAC
TTGCTTCCTAGTGAAACCGTTCAGGACATCTACGGGATTGTTGCTAAGAAAGTCAACGAG
ATTCTACAAGCAGACGCAATCAATGGGACCGATAACGAAGTAGTTACCGTGACCGATGAG
AACACTGGTGAAATCTCTGAGAAAGTCAAGCTGGGCACTAAGGCACTGGCTGGTCAATGG
CTGGCTTACGGTGTTACTCGCAGTGTGACTAAGCGTTCAGTCATGACGCTGGCTTACGGG
TCCAAAGAGTTCGGCTTCCGTCAACAAGTGCTGGAAGATACCATTCAGCCAGCTATTGAT
TCCGGCAAGGGTCTGATGTTCACTCAGCCGAATCAGGCTGCTGGATACATGGCTAAGCTG
ATTTGGGAATCTGTGAGCGTGACGGTGGTAGCTGCGGTTGAAGCAATGAACTGGCTTAAG
TCTGCTGCTAAGCTGCTGGCTGCTGAGGTCAAAGATAAGAAGACTGGAGAGATTCTTCGC
AAGCGTTGCGCTGTGCATTGGGTAACTCCTGATGGTTTCCCTGTGTGGCAGGAATACAAG
AAGCCTATTCAGACGCGCTTGAACCTGATGTTCCTCGGTCAGTTCCGCTTACAGCCTACC
ATTAACACCAACAAAGATAGCGAGATTGATGCACACAAACAGGAGTCTGGTATCGCTCCT
AACTTTGTACACAGCCAAGACGGTAGCCACCTTCGTAAGACTGTAGTGTGGGCACACGAG
AAGTACGGAATCGAATCTTTTGCACTGATTCACGACTCCTTCGGTACCATTCCGGCTGAC
GCTGCGAACCTGTTCAAAGCAGTGCGCGAAACTATGGTTGACACATATGAGTCTTGTGAT
GTACTGGCTGATTTCTACGACCAGTTCGCTGACCAGTTGCACGAGTCTCAATTGGACAAA
ATGCCAGCACTTCCGGCTAAAGGTAACTTGAACCTCCGTGACATCTTAGAGTCGGACTTC
GCGTTCGCGTAATAA

>cI
ATGAGCACAAAAAAGAAACCATTAACACAAGAGCAGCTTGAGGACGCACGTCGCCTTAAA
GCAATTTATGAAAAAAAGAAAAATGAACTTGGCTTATCCCAGGAATCTGTCGCAGACAAG
ATGGGGATGGGGCAGTCAGGCGTTGGTGCTTTATTTAATGGCATCAATGCATTAAATGCT
TATAACGCCGCATTGCTTGCAAAAATTCTCAAAGTTAGCGTTGAAGAATTTAGCCCTTCA
ATCGCCAGAGAAATCTACGAGATGTATGAAGCGGTTAGTATGCAGCCGTCACTTAGAAGT
GAGTATGAGTACCCTGTTTTTTCTCATGTTCAGGCAGGGATGTTCTCACCTGAGCTTAGA
ACCTTTACCAAAGGTGATGCGGAGAGATGGGTAAGCACAACCAAAAAAGCCAGTGATTCT
GCATTCTGGCTTGAGGTTGAAGGTAATTCCATGACCGCACCAACAGGCTCCAAGCCAAGC
TTTCCTGACGGAATGTTAATTCTCGTTGACCCTGAGCAGGCTGTTGAGCCAGGTGATTTC
TGCATAGCCAGACTTGGGGGTGATGAGTTTACCTTCAAGAAACTGATCAGGGATAGCGGT
CAGGTGTTTTTACAACCACTAAACCCACAGTACCCAATGATCCCATGCAATGAGAGTTGT
TCCGTTGTGGGGAAAGTTATCGCTAGTCAGTGGCCTGAAGAGACGTTTGGCGCTGCAAAC
GACGAAAACTACGCTTTAGTAGCTTAATAACGCTGATAGTGCTAGTGTAGATCGC

>lacI
ATGGTGAATGTGAAACCAGTAACGTTATACGATGTCGCAGAGTATGCCGGTGTCTCTTAT

CAGACCGTTTCCCGCGTGGTGAACCAGGCCAGCCACGTTTCTGCGAAAACGCGGGAAAAA
GTGGAAGCGGCGATGGCGGAGCTGAATTACATTCCCAACCGCGTGGCACAACAACTGGCG
GGCAAACAGTCGTTGCTGATTGGCGTTGCCACCTCCAGTCTGGCCCTGCACGCGCCGTCG
CAAATTGTCGCGGCGATTAAATCTCGCGCCGATCAACTGGGTGCCAGCGTGGTGGTGTCG
ATGGTAGAACGAAGCGGCGTCGAAGCCTGTAAAGCGGCGGTGCACAATCTTCTCGCGCAA
CGCGTCAGTGGGCTGATCATTAACTATCCGCTGGATGACCAGGATGCCATTGCTGTGGAA
GCTGCCTGCACTAATGTTCCGGCGTTATTTCTTGATGTCTCTGACCAGACACCCATCAAC
AGTATTATTTTCTCCCATGAAGACGGTACGCGACTGGGCGTGGAGCATCTGGTCGCATTG
GGTCACCAGCAAATCGCGCTGTTAGCGGGCCCATTAAGTTCTGTCTCGGCGCGTCTGCGT
CTGGCTGGCTGGCATAAATATCTCACTCGCAATCAAATTCAGCCGATAGCGGAACGGGAA
GGCGACTGGAGTGCCATGTCCGGTTTTCAACAAACCATGCAAATGCTGAATGAGGGCATC
GTTCCCACTGCGATGCTGGTTGCCAACGATCAGATGGCGCTGGGCGCAATGCGCGCCATT
ACCGAGTCCGGGCTGCGCGTTGGTGCGGATATCTCGGTAGTGGGATACGACGATACCGAA
GACAGCTCATGTTATATCCCGCCGTTAACCACCATCAAACAGGATTTTCGCCTGCTGGGG
CAAACCAGCGTGGACCGCTTGCTGCAACTCTCTCAGGGCCAGGCGGTGAAGGGCAATCAG
CTGTTGCCCGTCTCACTGGTGAAAAGAAAAACCACCCTGGCGCCCAATACGCAAACCGCC
TCTCCCCGCGCGTTGGCCGATTCATTAATGCAGCTGGCACGACAGGTTTCCCGACTGGAA
AGCGGGCAGGCTGCAAACGACGAAAACTACGCTTTAGTAGCTTAATAACTCTGATAGTGC
TAGTGTAGATCTC

>tetR
ATGTCCAGATTAGATAAAAGTAAAGTGATTAACAGCGCATTAGAGCTGCTTAATGAGGTC
GGAATCGAAGGTTTAACAACCCGTAAACTCGCCCAGAAGCTAGGTGTAGAGCAGCCTACA
TTGTATTGGCATGTAAAAAATAAGCGGGCTTTGCTCGACGCCTTAGCCATTGAGATGTTA
GATAGGCACCATACTCACTTTTGCCCTTTAGAAGGGGAAAGCTGGCAAGATTTTTTACGT
AATAACGCTAAAAGTTTTAGATGTGCTTTACTAAGTCATCGCGATGGAGCAAAAGTACAT
TTAGGTACACGGCCTACAGAAAAACAGTATGAAACTCTCGAAAATCAATTAGCCTTTTTA
TGCCAACAAGGTTTTTCACTAGAGAATGCATTATATGCACTCAGCGCTGTGGGGCATTTT
ACTTTAGGTTGCGTATTGGAAGATCAAGAGCATCAAGTCGCTAAAGAAGAAAGGGAAACA
CCTACTACTGATAGTATGCCGCCATTATTACGACAAGCTATCGAATTATTTGATCACCAA
GGTGCAGAGCCAGCCTTCTTATTCGGCCTTGAATTGATCATATGCGGATTAGAAAAACAA
CTTAAATGTGAAAGTGGGTCCGCTGCAAACGACGAAAACTACGCTTTAGTAGCTTAATAA
CACTGATAGTGCTAGTGTAGATCAC

>araC
ATGGCTGAAGCGCAAAATGATCCCCTGCTGCCGGGATACTCGTTTAACGCCCATCTGGTG
GCGGGTTTAACGCCGATTGAGGCCAATGGTTATCTCGATTTTTTTATCGACCGACCGCTG
GGAATGAAAGGTTATATTCTCAATCTCACCATTCGCGGTCAGGGGGTGGTGAAAAATCAG
GGACGAGAATTTGTCTGCCGACCGGGTGATATTTTGCTGTTCCCGCCAGGAGAGATTCAT
CACTACGGTCGTCATCCGGAGGCTCGCGAATGGTATCACCAGTGGGTTTACTTTCGTCCG
CGCGCCTACTGGCATGAATGGCTTAACTGGCCGTCAATATTTGCCAATACGGGTTTCTTT
CGCCCGGATGAAGCGCACCAGCCGCATTTCAGCGACCTGTTTGGGCAAATCATTAACGCC
GGGCAAGGGGAAGGGCGCTATTCGGAGCTGCTGGCGATAAATCTGCTTGAGCAATTGTTA
CTGCGGCGCATGGAAGCGATTAACGAGTCGCTCCATCCACCGATGGATAATCGGGTACGC
GAGGCTTGTCAGTACATCAGCGATCACCTGGCAGACAGCAATTTTGATATCGCCAGCGTC
GCACAGCATGTTTGCCTGTCGCCGTCGCGTCTGTCACATCTTTTCCGCCAGCAGTTAGGG
ATTAGCGTCTTAAGCTGGCGCGAGGACCAACGCATCAGCCAGGCGAAGCTGCTTTTGAGC
ACTACCCGGATGCCTATCGCCACCGTCGGTCGCAATGTTGGTTTTGACGATCAACTCTAT
TTCTCGCGAGTATTTAAAAAATGCACCGGGGCCAGCCCGAGCGAGTTCCGTGCCGGTTGT
GAAGAAAAAGTGAATGATGTAGCCGTCAAGTTGTCAGCTGCAAACGACGAAAACTACGCT
TTAGTAGCTTAATAACACTGATAGTGCTAGTGTAGATCAC

>luxR
ATGAAAAACATAAATGCCGACGACACATACAGAATAATTAATAAAATTAAAGCTTGTAGA
AGCAATAATGATATTAATCAATGCTTATCTGATATGACTAAAATGGTACATTGTGAATAT
TATTTACTCGCGATCATTTATCCTCATTCTATGGTTAAATCTGATATTTCAATCCTAGAT

AATTACCCTAAAAAATGGAGGCAATATTATGATGACGCTAATTTAATAAAATATGATCCT
ATAGTAGATTATTCTAACTCCAATCATTCACCAATTAATTGGAATATATTTGAAAACAAT
GCTGTAAATAAAAAATCTCCAAATGTAATTAAAGAAGCGAAAACATCAGGTCTTATCACT
GGGTTTAGTTTCCCTATTCATACGGCTAACAATGGCTTCGGAATGCTTAGTTTTGCACAT
TCAGAAAAAGACAACTATATAGATAGTTTATTTTTACATGCGTGTATGAACATACCATTA
ATTGTTCCTTCTCTAGTTGATAATTATCGAAAAATAAATATAGCAAATAATAAATCAAAC
AACGATTTAACCAAAAGAGAAAAAGAATGTTTAGCGTGGGCATGCGAAGGAAAAAGCTCT
TGGGATATTTCAAAAATATTAGGTTGCAGTGAGCGTACTGTCACTTTCCATTTAACCAAT
GCGCAAATGAAACTCAATACAACAAACCGCTGCCAAAGTATTTCTAAAGCAATTTTAACA
GGAGCAATTGATTGCCCATACTTTAAAAATTAATAACACTGATAGTGCTAGTGTAGATCA
C

pGDggpS.K

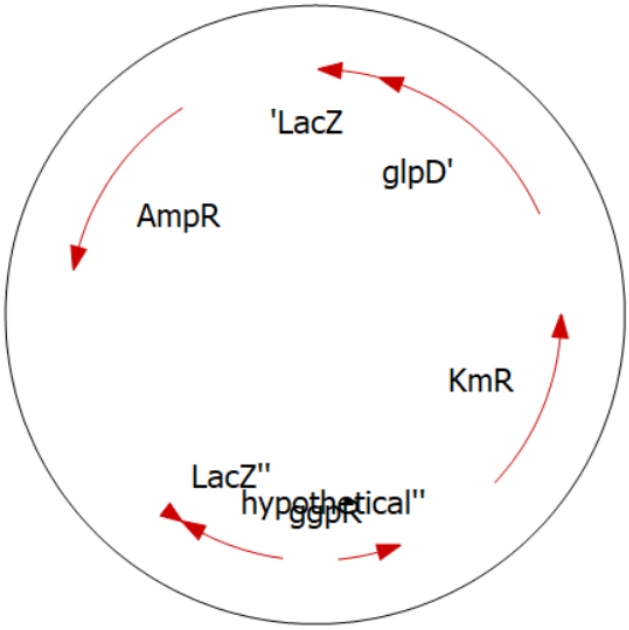

>pGDggpS.K
CACCCGCCGCGCTTAATGCGCCGCTACAGGGCGCGTCCATTCGCCATTCAGGCTGCGCAA
CTGTTGGGAAGGGCGATCGGTGCGGGCCTCTTCGCTATTACGCCAGCTGGCGAAAGGGGG
ATGTGCTGCAAGGCGATTAAGTTGGGTAACGCCAGGGTTTTCCCAGTCACGACGTTGTAA
AACGACGGCCAGTGAATTGTAATACGACTCACTATAGGGCGAATTGGGCCCGACGTCGCA
TGCTCCCGGCCGCCATGGCGGCCGCGGGAATTCGATTCTGGCTTTAACCCTGTCGAGGGA
ACCATCATAGCGGTGGTCCGTGGTGCCAATCAGATATTTACCCAACCAGGGAATGATGAA
ATAGGGCCGTTTATCCACAAACGCTTCCACATATAAGGCTGAAGCGGGGGCTCCAGGGAA
GGGATCCACCACAATATGACTGCCCTTGGTGCCACCAATTTTTCTTTCTTGGACAATGGC
AACGGGTTCTCCCCCTCGATGGGCTAAGCCACAAACTTCATCTACCCAGGGGCCAGTGGT
ATTAATGACGATCGCCTGGGCGCTATTAACAGTAAATTTTTCTCCGCTCAGTTGATCCTG
GCAATGGATGGCGGTAATCAGGTTATTTTCCCCTTTCTCCAACCCCTTCACAGCCACATA
ATTGAGCATGGCCGCCCCGGCCTTTTGGGCCGATAGGGTCACTTCTAAATCTAACCGTTC
CGCATATTCCACCTGGCCGTCAAAATATTGGGCTCCTCCTTTTAAGCCTTTTTTCTCCGC
CGCTCGGAACAGTTGCTGGAACTGTTGGGGGCTTAACATCCTATGGGAAGGGAGGGTTTT
ATCAAAACTGAGGATGTCGTAAAGAATCATGCCCGCCTGAATTTCCCAATAGGCCCGGCT
CGACCAGTCGTACACCGGAATGGTCAACTGGAGGGGCTGGACCAAATGGGGGGCGGTGTG
GAGCAGAACTTCCCGCTCCCGCAGGGATTCCCGCACCAGATTAAATTCAAAATATTCCAG
ATAGCGCAGGCCGCCATGGATTAAGCGGGTGGACCAACTACTCGTACCACTGGCGAAATC
ATCCTTTTCGATCAGGAGGGTTTTTAGGCCCCGTAGGGCTCCGTCCCGGGCCGTGCCAAC
CCCGTTAATGCCTCCCCCAATCACAATTAGGTCATAGGCCGTATTTTGGATTTCTGGGAA
ATTACGCATGGCTGGGTAATGCTCCAATGAGGAATAAATCGTGCAATTGAATGGAAAAAA
GCCCCCTAAACTCTAACTTTGGGCAATTTTTAGGGGGTTTGGACAATGGTTATTTGGTTA
CCATCCGCCGACCACGATTACAACCGGGCGATTTACTTTTCGACCTCATTCTATTAGACT
CTCGTTTGGATTGCAACTGGTCTATTTTCCTCTTTTGTTTGATAGAAAATCATAAAAGGA
TTTGCAGACTACGGGCCTAAAGAACTAAAAAATCTATCTGTTTCTTTTCATTCTCTGTAT
TTTTTATAGTTTCTGTTGCATGGGCATAAAGTTGCCTTTTTAATCACAATTCAGAAAATA
TCATAATATCTCATTTCACTAAATAATAGTGAACGGCAGGTATATGTGATGGGTTAAAAA
GGATCGATCCTCTAGCGAACCCCAGAGTCCCGCTCAGAAGAACTCGTCAAGAAGGCGATA
GAAGGCGATGCGCTGCGAATCGGGAGCGGCGATACCGTAAAGCACGAGGAAGCGGTCAGC
CCATTCGCCGCCAAGCTCTTCAGCAATATCACGGGTAGCCAACGCTATGTCCTGATAGCG

GTCCGCCACACCCAGCCGGCCACAGTCGATGAATCCAGAAAAGCGGCCATTTTCCACCAT
GATATTCGGCAAGCAGGCATCGCCATGGGTCACGACGAGATCCTCGCCGTCGGGCATCCG
CGCCTTGAGCCTGGCGAACAGTTCGGCTGGCGCGAGCCCCTGATGCTCTTCGTCCAGATC
ATCCTGATCGACAAGACCGGCTTCCATCCGAGTACGTGCTCGCTCGATGCGATGTTTCGC
TTGGTGGTCGAATGGGCAGGTAGCCGGATCAAGCGTATGCAGCCGCCGCATTGCATCAGC
CATGATGGATACTTTCTCGGCAGGAGCAAGGTGAGATGACAGGAGATCCTGCCCCGGCAC
TTCGCCCAATAGCAGCCAGTCCCTTCCCGCTTCAGTGACAACGTCGAGCACAGCTGCGCA
AGGAACGCCCGTCGTGGCCAGCCACGATAGCCGCGCTGCCTCGTCTTGGAGTTCATTCAG
GGCACCGGACAGGTCGGTCTTGACAAAAAGAACCGGGCGCCCCTGCGCTGACAGCCGGAA
CACGGCGGCATCAGAGCAGCCGATTGTCTGTTGTGCCCAGTCATAGCCGAATAGCCTCTC
CACCCAAGCGGCCGGAGAACCTGCGTGCAATCCATCTTGTTCAATCATGCGAAACGATCC
TCATCCTGTCTCTTGATCAGATCTTGATCCCCTGCGCCATCAGATCCTTGGCGGCAAGAA
AGCCATCCAGTTTACTTTGCAGGGCTTCCCAACCTTACCAGAGGGCGCCCCAGCTGGCAA
TTCCGGTTCGCTTGCTGTCCATAAAACCGCCCAGTCTAGCTATCGCCATGTAAGCCCACT
GCAAGCTACCTGCTTTCTCTTTGCGCTTGCGTTTTCCCTTGTCCAGATAGCCCAGTAGCT
GACATTCACCCGGTTGTAATCACGGCTAATGCACCCGACTTCCCGGAACCCAAGTTAATT
CCCGCCGGGGCATTTTAGTACGTTGAATAAAACTTTTCACCGCTAATATCGGTACAGAAA
AATTGATTACGTCCTGGGCGAGTCCACAGACATCGCGTTCCCCTGTGGGGGCAATTACGG
TAACGGCTCATAAATCTTTGTTAAAGATTACTTAACCCGTCAGTAAAATGCCGTAACACT
AATTACCTTTTCCCCTTACTCCAGAGGAGAACAGCAGCGGCAAGCCACCAATCTCTGGTT
TTTGGAAAGCCGCCCCTGGACTATGGAAAAAGTAGTTACTTGTTAAGTATAGTAACAGAA
AAAGCTTTTCTGGCAAGATTTCTGCTTCTGGAGTTGGGGGTATCCTCTGGAAATTTACCC
GTCGATTGCGGTAAATTCTATTTTTTTTGTTAACCTTAAAACTATTGCCATGGGCAGGGT
AAATTGATTTTTTCTTGTTGTTTGATCCCATTTTCCAGTCTTTTTGACTTCCATTCAGTC
AGGATAATTTTTGCAGTTTTTTTATGGAGTTTTGATAACATTGAGCTTTGCCCCCGGCGA
TCGCCTAGGGATAAACAATAAACGTGTGAACTAATATGCCTGGATTTATCCCTGGATTGA
CATTGTTTTTGCCCCCCTAAGTCAGCAATGACAGAGTTGAAAATCCCTTACTCCCCAGCA
ATTTCAGCTTATTTTGAGCTTATTTTTCAGTATGAAAACATTGAATCGTATCCATCTGGT
CGAAGAAGAAACAGAAAAACTAATGGCTTGGGCCCGGAGTGTCACGGAATCGCCGGAGAA
CTATTTCCAAGCGGCCCGGGAAGTGGTGAAAAAATTGGGGGGCCATTACCAAGGGGATGG
CCTAACCCAAGTGGGATTTTGGGTGCCCCGGTTAGCGGGGGAAGGGGCTTTTACTGAAAA
GTTAATTTACCTAGAGGTGTTTACGCCCCTGGGGGAGATTGATTTCCAAGCGCCGGAACA
AACTGGCTTGTTTCGTTGGGAAAGGATTGAATTGCCGCAACAGGGGGAATTTGTTTGGGC
TGTGCTGTCGGGGATGCGGCCAGGCACCAGAGATCAAGCTGGTTCTTTCTATTGGTTGCG
CTATTACGATTCCATTTTGTCCAACACGTTGGTCATCCGTGATCCCCTGACCTATTCCCT
GCCCTACGGTGTTCTCGACCATATGGGAGAGCTCCCAACGCGTTGGATGCATAGCTTGAG
TATTCTATAGTGTCACCTAAATAGCTTGGCGTAATCATGGTCATAGCTGTTTCCTGTGTG
AAATTGTTATCCGCTCACAATTCCACACAACATACGAGCCGGAAGCATAAAGTGTAAAGC
CTGGGGTGCCTAATGAGTGAGCTAACTCACATTAATTGCGTTGCGCTCACTGCCCGCTTT
CCAGTCGGGAAACCTGTCGTGCCAGCTGCATTAATGAATCGGCCAACGCGCGGGGAGAGG
CGGTTTGCGTATTGGGCGCTCTTCCGCTTCCTCGCTCACTGACTCGCTGCGCTCGGTCGT
TCGGCTGCGGCGAGCGGTATCAGCTCACTCAAAGGCGGTAATACGGTTATCCACAGAATC
AGGGGATAACGCAGGAAAGAACATGTGAGCAAAAGGCCAGCAAAAGGCCAGGAACCGTAA
AAAGGCCGCGTTGCTGGCGTTTTTCCATAGGCTCCGCCCCCCTGACGAGCATCACAAAAA
TCGACGCTCAAGTCAGAGGTGGCGAAACCCGACAGGACTATAAAGATACCAGGCGTTTCC
CCCTGGAAGCTCCCTCGTGCGCTCTCCTGTTCCGACCCTGCCGCTTACCGGATACCTGTC
CGCCTTTCTCCCTTCGGGAAGCGTGGCGCTTTCTCATAGCTCACGCTGTAGGTATCTCAG
TTCGGTGTAGGTCGTTCGCTCCAAGCTGGGCTGTGTGCACGAACCCCCCGTTCAGCCCGA
CCGCTGCGCCTTATCCGGTAACTATCGTCTTGAGTCCAACCCGGTAAGACACGACTTATC
GCCACTGGCAGCAGCCACTGGTAACAGGATTAGCAGAGCGAGGTATGTAGGCGGTGCTAC
AGAGTTCTTGAAGTGGTGGCCTAACTACGGCTACACTAGAAGAACAGTATTTGGTATCTG
CGCTCTGCTGAAGCCAGTTACCTTCGGAAAAAGAGTTGGTAGCTCTTGATCCGGCAAACA
AACCACCGCTGGTAGCGGTGGTTTTTTTGTTTGCAAGCAGCAGATTACGCGCAGAAAAAA
AGGATCTCAAGAAGATCCTTTGATCTTTTCTACGGGGTCTGACGCTCAGTGGAACGAAAA
CTCACGTTAAGGGATTTTGGTCATGAGATTATCAAAAAGGATCTTCACCTAGATCCTTTT
AAATTAAAAATGAAGTTTTAAATCAATCTAAAGTATATATGAGTAAACTTGGTCTGACAG

TTACCAATGCTTAATCAGTGAGGCACCTATCTCAGCGATCTGTCTATTTCGTTCATCCAT
AGTTGCCTGACTCCCCGTCGTGTAGATAACTACGATACGGGAGGGCTTACCATCTGGCCC
CAGTGCTGCAATGATACCGCGAGACCCACGCTCACCGGCTCCAGATTTATCAGCAATAAA
CCAGCCAGCCGGAAGGGCCGAGCGCAGAAGTGGTCCTGCAACTTTATCCGCCTCCATCCA
GTCTATTAATTGTTGCCGGGAAGCTAGAGTAAGTAGTTCGCCAGTTAATAGTTTGCGCAA
CGTTGTTGCCATTGCTACAGGCATCGTGGTGTCACGCTCGTCGTTTGGTATGGCTTCATT
CAGCTCCGGTTCCCAACGATCAAGGCGAGTTACATGATCCCCCATGTTGTGCAAAAAAGC
GGTTAGCTCCTTCGGTCCTCCGATCGTTGTCAGAAGTAAGTTGGCCGCAGTGTTATCACT
CATGGTTATGGCAGCACTGCATAATTCTCTTACTGTCATGCCATCCGTAAGATGCTTTTC
TGTGACTGGTGAGTACTCAACCAAGTCATTCTGAGAATAGTGTATGCGGCGACCGAGTTG
CTCTTGCCCGGCGTCAATACGGGATAATACCGCGCCACATAGCAGAACTTTAAAAGTGCT
CATCATTGGAAAACGTTCTTCGGGGCGAAAACTCTCAAGGATCTTACCGCTGTTGAGATC
CAGTTCGATGTAACCCACTCGTGCACCCAACTGATCTTCAGCATCTTTTACTTTCACCAG
CGTTTCTGGGTGAGCAAAAACAGGAAGGCAAAATGCCGCAAAAAAGGGAATAAGGGCGAC
ACGGAAATGTTGAATACTCATACTCTTCCTTTTTCAATATTATTGAAGCATTTATCAGGG
TTATTGTCTCATGAGCGGATACATATTTGAATGTATTTAGAAAAATAAACAAATAGGGGT
TCCGCGCACATTTCCCCGAAAAGTGCCACCTGATGCGGTGTGAAATACCGCACAGATGCG
TAAGGAGAAAATACCGCATCAGGAAATTGTAAGCGTTAATATTTTGTTAAAATTCGCGTT
AAATTTTTGTTAAATCAGCTCATTTTTTAACCAATAGGCCGAAATCGGCAAAATCCCTTA
TAAATCAAAAGAATAGACCGAGATAGGGTTGAGTGTTGTTCCAGTTTGGAACAAGAGTCC
ACTATTAAAGAACGTGGACTCCAACGTCAAAGGGCGAAAAACCGTCTATCAGGGCGATGG
CCCACTACGTGAACCATCACCCTAATCAAGTTTTTTGGGGTCGAGGTGCCGTAAAGCACT
AAATCGGAACCCTAAAGGGAGCCCCCGATTTAGAGCTTGACGGGGAAAGCCGGCGAACGT
GGCGAGAAAGGAAGGGAAGAAAGCGAAAGGAGCGGGCGCTAGGGCGCTGGCAAGTGTAGC
GGTCACGCTGCGCGTAACCACCA

pSEVA251

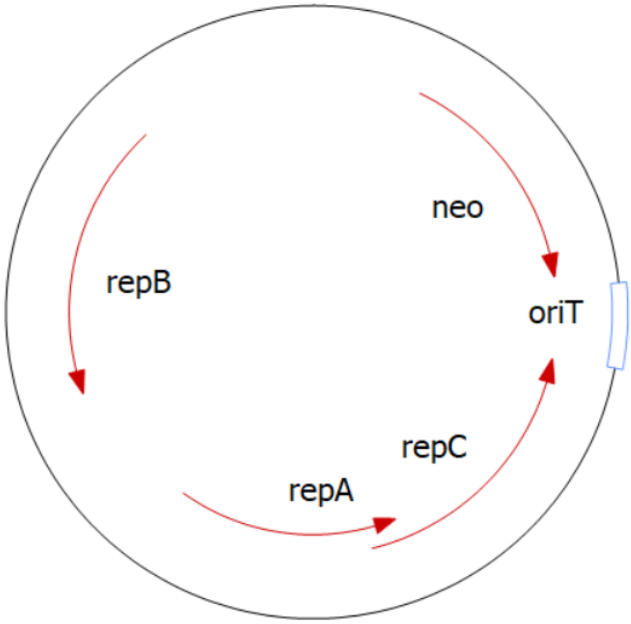

>pSEVA251
TTAATTAAAGCGGATAACAATTTCACACAGGAGGCCGCCTAGGCCGCGGCCGCGCGAATT
CGAGCTCGGTACCCGGGGATCCTCTAGAGTCGACCTGCAGGCATGCAAGCTTGCGGCCGC
GTCGTGACTGGGAAAACCCTGGCGACTAGTCTTGGACTCCTGTTGATAGATCCAGTAATG
ACCTCAGAACTCCATCTGGATTTGTTCAGAACGCTCGGTTGCCGCCGGGCGTTTTTTATT
GGTGAGAATCCAGGGGTCCCCAATAATTACGATTTAAATTTGTGTCTCAAAATCTCTGAT
GTTACATTGCACAAGATAAAAATATATCATCATGAACAATAAAACTGTCTGCTTACATAA
ACAGTAATACAAGGGGTGTTATGAGCCATATTCAGCGTGAAACGAGCTGTAGCCGTCCGC
GTCTGAACAGCAACATGGATGCGGATCTGTATGGCTATAAATGGGCGCGTGATAACGTGG
GTCAGAGCGGCGCGACCATTTATCGTCTGTATGGCAAACCGGATGCGCCGGAACTGTTTC
TGAAACATGGCAAAGGCAGCGTGGCGAACGATGTGACCGATGAAATGGTGCGTCTGAACT
GGCTGACCGAATTTATGCCGCTGCCGACCATTAAACATTTTATTCGCACCCCGGATGATG
CGTGGCTGCTGACCACCGCGATTCCGGGCAAAACCGCGTTTCAGGTGCTGGAAGAATATC
CGGATAGCGGCGAAAACATTGTGGATGCGCTGGCCGTGTTTCTGCGTCGTCTGCATAGCA
TTCCGGTGTGCAACTGCCCGTTTAACAGCGATCGTGTGTTTCGTCTGGCCCAGGCGCAGA
GCCGTATGAACAACGGCCTGGTGGATGCGAGCGATTTTGATGATGAACGTAACGGCTGGC
CGGTGGAACAGGTGTGGAAAGAAATGCATAAACTGCTGCCGTTTAGCCCGGATAGCGTGG
TGACCCACGGCGATTTTAGCCTGGATAACCTGATTTTCGATGAAGGCAAACTGATTGGCT
GCATTGATGTGGGCCGTGTGGGCATTGCGGATCGTTATCAGGATCTGGCCATTCTGTGGA
ACTGCCTGGGCGAATTTAGCCCGAGCCTGCAAAAACGTCTGTTTCAGAAATATGGCATTG
ATAATCCGGATATGAACAAACTGCAATTTCATCTGATGCTGGATGAATTTTTCTAATAAT
TAATTGGACCGCGGTCCGCGCGTTGTCCTTTTCCGCTGCATAACCCTGCTTCGGGGTCAT
TATAGCGATTTTTTCGGTATATCCATCCTTTTTCGCACGATATACAGGATTTTGCCAAAG
GGTTCGTGTAGACTTTCCTTGGTGTATCCAACGGCGTCAGCCGGGCAGGATAGGTGAAGT
AGGCCCACCCGCGAGCGGGTGTTCCTTCTTCACTGTCCCTTATTCGCACCTGGCGGTGCT
CAACGGGAATCCTGCTCTGCGAGGCTGGCCGTAGGCCGGCCTCAGCCTGCCGCCTTGGGC
CGGGTGATGTCGTACTTGCCCGCCGCGAACTCGGTTACCGTCCAGCCCAGCGCGACCAGC
TCCGGCAACGCCTCGCGCACCCGCTGGCGGCGCTTGCGCATGGTCGAACCACTGGCCTCT
GACGGCCAGACATAGCCGCACAAGGTATCTATGGAAGCCTTGCCGGTTTTGCCGGGGTCG
ATCCAGCCACACAGCCGCTGGTGCAGCAGGCGGGCGGTTTCGCTGTCCAGCGCCCGCACC
TCGTCCATGCTGATGCGCACATGCTGGCCGCCACCCATGACGGCCTGCGCGATCAAGGGG
TTCAGGGCCACGTACAGGCGCCCGTCCGCCTCGTCGCTGGCGTACTCCGACAGCAGCCGA
AACCCCTGCCGCTTGCGGCCATTCTGGGCGATGATGGATACCTTCCAAAGGCGCTCGATG

CAGTCCTGTATGTGCTTGAGCGCCCCACCACTATCGACCTCTGCCCCGATTTCCTTTGCC
AGCGCCCGATAGCTACCTTTGACCACATGGCATTCAGCGGTGACGGCCTCCCACTTGGGT
TCCAGGAACAGCCGGAGCTGCCGTCCGCCTTCGGTCTTGGGTTCCGGGCCAAGCACTAGG
CCATTAGGCCCAGCCATGGCCACCAGCCCTTGCAGGATGCGCAGATCATCAGCGCCCAGC
GGCTCCGGGCCGCTGAACTCGATCCGCTTGCCGTCGCCGTAGTCATACGTCACGTCCAGC
TTGCTGCGCTTGCGCTCGCCCCGCTTGAGGGCACGGAACAGGCCGGGGGCCAGACAGTGC
GCCGGGTCGTGCCGGACGTGGCTGAGGCTGTGCTTGTTCTTAGGCTTCACCACGGGGCAC
CCCCTTGCTCTTGCGCTGCCTCTCCAGCACGGCGGGCTTGAGCACCCCGCCGTCATGCCG
CCTGAACCACCGATCAGCGAACGGTGCGCCATAGTTGGCCTTGCTCACACCGAAGCGGAC
GAAGAACCGGCGCTGGTCGTCGTCCACACCCCATTCCTCGGCCTCGGCGCTGGTCATGCT
CGACAGGTAGGACTGCCAGCGGATGTTATCGACCAGTACCGAGCTGCCCCGGCTGGCCTG
CTGCTGGTCGCCTGCGCCCATCATGGCCGCGCCCTTGCTGGCATGGTGCAGGAACACGAT
AGAGCACCCGGTATCGGCGGCGATGGCCTCCATGCGACCGATGACCTGGGCCATGGGGCC
GCTGGCGTTTTCTTCCTCGATGTGGAACCGGCGCAGCGTGTCCAGCACCATCAGGCGGCG
GCCCTCGGCGGCGCGCTTGAGGCCGTCGAACCACTCCGGGGCCATGATGTTGGGCAGGCT
GCCGATCAGCGGCTGGATCAGCAGGCCGTCAGCCACGGCTTGCCGTTCCTCGGCGCTGAG
GTGCGCCCCAAGGGCGTGCAGGCGGTGATGAATGGCGGTGGGCGGGTCTTCGGCGGGCAG
GTAGATCACCGGGCCGGTGGGCAGTTCGCCCACCTCCAGCAGATCCGGCCCGCCTGCAAT
CTGTGCGGCCAGTTGCAGGGCCAGCATGGATTTACCGGCACCACCGGGCGACACCAGCGC
CCCGACCGTACCGGCCACCATGTTGGGCAAAACGTAGTCCAGCGGTGGCGGCGCTGCTGC
GAACGCCTCCAGAATATTGATAGGCTTATGGGTAGCCATTGATTGCCTCCTTTGCAGGCA
GTTGGTGGTTAGGCGCTGGCGGGGTCACTACCCCCGCCCTGCGCCGCTCTGAGTTCTTCC
AGGCACTCGCGCAGCGCCTCGTATTCGTCGTCGGTCAGCCAGAACTTGCGCTGACGCATC
CCTTTGGCCTTCATGCGCTCGGCATATCGCGCTTGGCGTACAGCGTCAGGGCTGGCCAGC
AGGTCGCCGGTCTGCTTGTCCTTTTGGTCTTTCATATCAGTCACCGAGAAACTTGCCGGG
GCCGAAAGGCTTGTCTTCGCGGAACAAGGACAAGGTGCAGCCGTCAAGGTTAAGGCTGGC
CATATCAGCGACTGAAAAGCGGCCAGCCTCGGCCTTGTTTGACGTATAACCAAAGCCACC
GGGCAACCAATAGCCCTTGTCACTTTTGATCAGGTAGACCGACCCTGAAGCGCTTTTTTC
GTATTCCATAAAACCCCCTTCTGTGCGTGAGTACTCATAGTATAACAGGCGTGAGTACCA
ACGCAAGCACTACATGCTGAAATCTGGCCCGCCCCTGTCCATGCCTCGCTGGCGGGGTGC
CGGTGCCCGTGCCAGCTCGGCCCGCGCAAGCTGGACGCTGGGCAGACCCATGACCTTGCT
GACGGTGCGCTCGATGTAATCCGCTTCGTGGCCGGGCTTGCGCTCTGCCAGCGCTGGGCT
GGCCTCGGCCATGGCCTTGCCGATTTCCTCGGCACTGCGGCCCCGGCTGGCCAGCTTCTG
CGCGGCGATAAAGTCGCACTTGCTGAGGTCATCACCGAAGCGCTTGACCAGCCCGGCCAT
CTCGCTGCGGTACTCGTCCAGCGCCGTGCGCCGGTGGCGGCTAAGCTGCCGCTCGGGCAG
TTCGAGGCTGGCCAGCCTGCGGGCCTTCTCCTGCTGCCGCTGGGCCTGCTCGATCTGCTG
GCCAGCCTGCTGCACCAGCGCCGGGCCAGCGGTGGCGGTCTTGCCCTTGGATTCACGCAG
CAGCACCCACGGCTGATAACCGGCGCGGGTGGTGTGCTTGTCCTTGCGGTTGGTGAAGCC
CGCCAAGCGGCCATAGTGGCGGCTGTCGGCGCTGGCCGGGTCGGCGTCGTACTCGCTGGC
CAGCGTCCGGGCAATCTGCCCCCGAAGTTCACCGCCTGCGGCGTCGGCCACCTTGACCCA
TGCCTGATAGTTCTTCGGGCTGGTTTCCACTACCAGGGCAGGCTCCCGGCCCTCGGCTTT
CATGTCATCCAGGTCAAACTCGCTGAGGTCGTCCACCAGCACCAGACCATGCCGCTCCTG
CTCGGCGGGCCTGATATACACGTCATTGCCCTGGGCATTCATCCGCTTGAGCCATGGCGT
GTTCTGGAGCACTTCGGCGGCTGACCATTCCCGGTTCATCATCTGGCCGGTGGTGGCGTC
CCTGACGCCGATATCGAAGCGCTCACAGCCCATGGCCTTGAGCTGTCGGCCTATGGCCTG
CAAAGTCCTGTCGTTCTTCATCGGGCCACCAAGCGATTCCCACACATTATACGAGCCGGA
AGCATAAAGTGTAAAGCCTAGATCCGAAGGATGAGCCGGGCTGAATGATCGACCGAGACA
GGCCCTGCGGGGCTGCACACGCGCCCCCACCCTTCGGGTAGGGGGAAAGGCCGCTAAAGC
GGCTAAAAGCGCTCCAGCGTATTTCTGCGGGGTTTGGTGTGGGGTTTAGCGGGCTTTGCC
CGCCTTTCCCCCTGCCGCGCAGCGGTGGGGCGGTGTGTAGCCTAGCGCAGCGAATAGACC
AGCTATCCGGCCTCTGGCCGGGCATATTGGGCAAGGGCAGCAGCGCCCCACAAGGGCGCT
GATAACCGCGCCTAGTGGATTATTCTTAGATAATCATGGATGGATTTTTCCAACACCCCG
CCAGCCCCCGCCCCTGCTGGGTTTGCAGGTTTGGGGGCGTGACAGTTATTGCAGGGGTTC
GTGACAGTTATTGCAGGGGGGCGTGACAGTTATTGCAGGGGTTCGTGACAGTTAGGGCGC
GCCCAGCTGTCTAGGGCGGCGGATTTGTCCTACTCAGGAGAGCGTTCACCGACAAACAAC
AGATAAAACGAAAGGCCCAGTCTTTCGACTGAGCCTTTCGTTTTATTTGATGCCT

pSEVA351

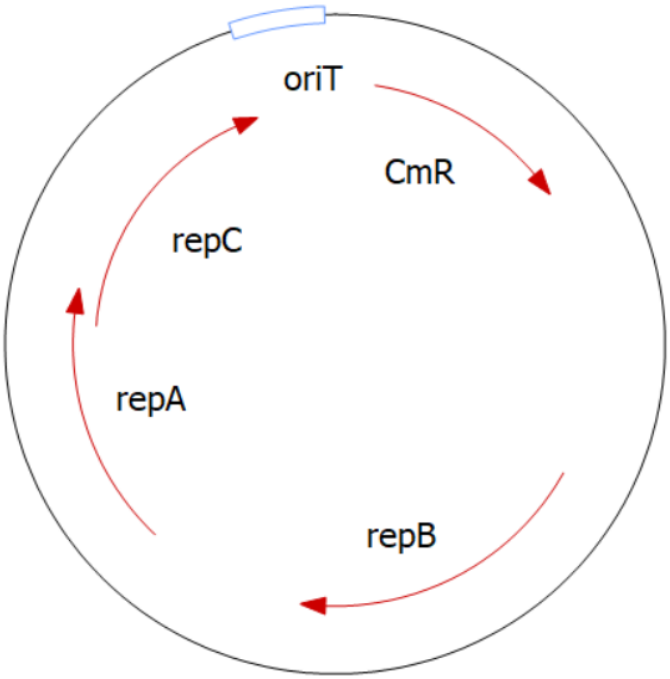

>pSEVA351
AAATTGGCGAAAATGAGACGTTGATCGGCACGTAAGAGGTTCCAACTTTCACCATAATGA
AATAAGATCACTACCGGGCGTATTTTTTGAGTTATCGAGATTTTCAGGAGCTAAGGAAGC
TAAAATGGAGAAAAAAATCACTGGATATACCACCGTTGATATATCCCAATGGCATCGTAA
AGAACATTTTGAGGCATTTCAGTCAGTTGCTCAATGTACCTATAACCAGACCGTTCAGCT
GGATATTACGGCCTTTTTAAAGACCGTAAAGAAAAATAAGCACAAGTTTTATCCGGCCTT
TATTCACATTCTTGCCCGCCTGATGAATGCTCATCCGGAATTTCGTATGGCAATGAAAGA
CGGTGAGCTGGTGATATGGGATAGTGTTCACCCTTGTTACACCGTTTTCCATGAGCAAAC
TGAAACGTTTTCATCGCTCTGGAGTGAATACCACGACGATTTCCGGCAGTTTCTACACAT
ATATTCGCAAGATGTGGCGTGTTACGGTGAAAACCTGGCCTATTTCCCTAAAGGGTTTAT
TGAGAATATGTTTTTCGTCTCAGCCAATCCCTGGGTGAGTTTCACCAGTTTTGATTTAAA
CGTGGCCAATATGGACAACTTCTTCGCCCCCGTTTTCACCATGGGCAAATATTATACGCA
AGGCGACAAGGTGCTGATGCCGCTGGCGATTCAGGTTCATCATGCCGTTTGTGATGGCTT
CCATGTCGGCAGAATGCTTAATGAATTACAACAGTACTGCGATGAGTGGCAGGGCGGGGC
GTAATTTGACTTAAATCGTAATTATTGGGGACCCCTGGATTCTCACCAATAAAAAACGCC
CGGCGGCAACCGAGCGTTCTGAACAAATCCAGATGGAGTTCTGAGGTCATTACTGGATCT
ATCAACAGGAGTCCAAGACTAGTCGCCAGGGTTTTCCCAGTCACGACGCGGCCGCAAGCT
TGCATGCCTGCAGGTCGACTCTAGAGGATCCCCGGGTACCGAGCTCGAATTCGCGCGGCC
GCGGCCTAGGCGGCCTCCTGTGTGAAATTGTTATCCGCTTTAATTAAAGGCATCAAATAA
AACGAAAGGCTCAGTCGAAAGACTGGGCCTTTCGTTTTATCTGTTGTTTGTCGGTGAACG
CTCTCCTGAGTAGGACAAATCCGCCGCCCTAGACAGCTGGGCGCGCCCTAACTGTCACGA
ACCCCTGCAATAACTGTCACGCCCCCCTGCAATAACTGTCACGAACCCCTGCAATAACTG
TCACGCCCCCAAACCTGCAAACCCAGCAGGGGCGGGGGCTGGCGGGGTGTTGGAAAAATC
CATCCATGATTATCTAAGAATAATCCACTAGGCGCGGTTATCAGCGCCCTTGTGGGGCGC
TGCTGCCCTTGCCCAATATGCCCGGCCAGAGGCCGGATAGCTGGTCTATTCGCTGCGCTA
GGCTACACACCGCCCCACCGCTGCGCGGCAGGGGGAAAGGCGGGCAAAGCCCGCTAAACC
CCACACCAAACCCCGCAGAAATACGCTGGAGCGCTTTTAGCCGCTTTAGCGGCCTTTCCC
CCTACCCGAAGGGTGGGGGCGCGTGTGCAGCCCCGCAGGGCCTGTCTCGGTCGATCATTC
AGCCCGGCTCATCCTTCGGATCTAGGCTTTACACTTTATGCTTCCGGCTCGTATAATGTG
TGGGAATCGCTTGGTGGCCCGATGAAGAACGACAGGACTTTGCAGGCCATAGGCCGACAG
CTCAAGGCCATGGGCTGTGAGCGCTTCGATATCGGCGTCAGGGACGCCACCACCGGCCAG

ATGATGAACCGGGAATGGTCAGCCGCCGAAGTGCTCCAGAACACGCCATGGCTCAAGCGG
ATGAATGCCCAGGGCAATGACGTGTATATCAGGCCCGCCGAGCAGGAGCGGCATGGTCTG
GTGCTGGTGGACGACCTCAGCGAGTTTGACCTGGATGACATGAAAGCCGAGGGCCGGGAG
CCTGCCCTGGTAGTGGAAACCAGCCCGAAGAACTATCAGGCATGGGTCAAGGTGGCCGAC
GCCGCAGGCGGTGAACTTCGGGGGCAGATTGCCCGGACGCTGGCCAGCGAGTACGACGCC
GACCCGGCCAGCGCCGACAGCCGCCACTATGGCCGCTTGGCGGGCTTCACCAACCGCAAG
GACAAGCACACCACCCGCGCCGGTTATCAGCCGTGGGTGCTGCTGCGTGAATCCAAGGGC
AAGACCGCCACCGCTGGCCCGGCGCTGGTGCAGCAGGCTGGCCAGCAGATCGAGCAGGCC
CAGCGGCAGCAGGAGAAGGCCCGCAGGCTGGCCAGCCTCGAACTGCCCGAGCGGCAGCTT
AGCCGCCACCGGCGCACGGCGCTGGACGAGTACCGCAGCGAGATGGCCGGGCTGGTCAAG
CGCTTCGGTGATGACCTCAGCAAGTGCGACTTTATCGCCGCGCAGAAGCTGGCCAGCCGG
GGCCGCAGTGCCGAGGAAATCGGCAAGGCCATGGCCGAGGCCAGCCCAGCGCTGGCAGAG
CGCAAGCCCGGCCACGAAGCGGATTACATCGAGCGCACCGTCAGCAAGGTCATGGGTCTG
CCCAGCGTCCAGCTTGCGCGGGCCGAGCTGGCACGGGCACCGGCACCCCGCCAGCGAGGC
ATGGACAGGGGCGGGCCAGATTTCAGCATGTAGTGCTTGCGTTGGTACTCACGCCTGTTA
TACTATGAGTACTCACGCACAGAAGGGGGTTTTATGGAATACGAAAAAAGCGCTTCAGGG
TCGGTCTACCTGATCAAAAGTGACAAGGGCTATTGGTTGCCCGGTGGCTTTGGTTATACG
TCAAACAAGGCCGAGGCTGGCCGCTTTTCAGTCGCTGATATGGCCAGCCTTAACCTTGAC
GGCTGCACCTTGTCCTTGTTCCGCGAAGACAAGCCTTTCGGCCCCGGCAAGTTTCTCGGT
GACTGATATGAAAGACCAAAAGGACAAGCAGACCGGCGACCTGCTGGCCAGCCCTGACGC
TGTACGCCAAGCGCGATATGCCGAGCGCATGAAGGCCAAAGGGATGCGTCAGCGCAAGTT
CTGGCTGACCGACGACGAATACGAGGCGCTGCGCGAGTGCCTGGAAGAACTCAGAGCGGC
GCAGGGCGGGGGTAGTGACCCCGCCAGCGCCTAACCACCAACTGCCTGCAAAGGAGGCAA
TCAATGGCTACCCATAAGCCTATCAATATTCTGGAGGCGTTCGCAGCAGCGCCGCCACCG
CTGGACTACGTTTTGCCCAACATGGTGGCCGGTACGGTCGGGGCGCTGGTGTCGCCCGGT
GGTGCCGGTAAATCCATGCTGGCCCTGCAACTGGCCGCACAGATTGCAGGCGGGCCGGAT
CTGCTGGAGGTGGGCGAACTGCCCACCGGCCCGGTGATCTACCTGCCCGCCGAAGACCCG
CCCACCGCCATTCATCACCGCCTGCACGCCCTTGGGGCGCACCTCAGCGCCGAGGAACGG
CAAGCCGTGGCTGACGGCCTGCTGATCCAGCCGCTGATCGGCAGCCTGCCCAACATCATG
GCCCCGGAGTGGTTCGACGGCCTCAAGCGCGCCGCCGAGGGCCGCCGCCTGATGGTGCTG
GACACGCTGCGCCGGTTCCACATCGAGGAAGAAAACGCCAGCGGCCCCATGGCCCAGGTC
ATCGGTCGCATGGAGGCCATCGCCGCCGATACCGGGTGCTCTATCGTGTTCCTGCACCAT
GCCAGCAAGGGCGCGGCCATGATGGGCGCAGGCGACCAGCAGCAGGCCAGCCGGGGCAGC
TCGGTACTGGTCGATAACATCCGCTGGCAGTCCTACCTGTCGAGCATGACCAGCGCCGAG
GCCGAGGAATGGGGTGTGGACGACGACCAGCGCCGGTTCTTCGTCCGCTTCGGTGTGAGC
AAGGCCAACTATGGCGCACCGTTCGCTGATCGGTGGTTCAGGCGGCATGACGGCGGGGTG
CTCAAGCCCGCCGTGCTGGAGAGGCAGCGCAAGAGCAAGGGGGTGCCCCGTGGTGAAGCC
TAAGAACAAGCACAGCCTCAGCCACGTCCGGCACGACCCGGCGCACTGTCTGGCCCCCGG
CCTGTTCCGTGCCCTCAAGCGGGGCGAGCGCAAGCGCAGCAAGCTGGACGTGACGTATGA
CTACGGCGACGGCAAGCGGATCGAGTTCAGCGGCCCGGAGCCGCTGGGCGCTGATGATCT
GCGCATCCTGCAAGGGCTGGTGGCCATGGCTGGGCCTAATGGCCTAGTGCTTGGCCCGGA
ACCCAAGACCGAAGGCGGACGGCAGCTCCGGCTGTTCCTGGAACCCAAGTGGGAGGCCGT
CACCGCTGAATGCCATGTGGTCAAAGGTAGCTATCGGGCGCTGGCAAAGGAAATCGGGGC
AGAGGTCGATAGTGGTGGGGCGCTCAAGCACATACAGGACTGCATCGAGCGCCTTTGGAA
GGTATCCATCATCGCCCAGAATGGCCGCAAGCGGCAGGGGTTTCGGCTGCTGTCGGAGTA
CGCCAGCGACGAGGCGGACGGGCGCCTGTACGTGGCCCTGAACCCCTTGATCGCGCAGGC
CGTCATGGGTGGCGGCCAGCATGTGCGCATCAGCATGGACGAGGTGCGGGCGCTGGACAG
CGAAACCGCCCGCCTGCTGCACCAGCGGCTGTGTGGCTGGATCGACCCCGGCAAAACCGG
CAAGGCTTCCATAGATACCTTGTGCGGCTATGTCTGGCCGTCAGAGGCCAGTGGTTCGAC
CATGCGCAAGCGCCGCCAGCGGGTGCGCGAGGCGTTGCCGGAGCTGGTCGCGCTGGGCTG
GACGGTAACCGAGTTCGCGGCGGGCAAGTACGACATCACCCGGCCCAAGGCGGCAGGCTG
AGGCCGGCCTACGGCCAGCCTCGCAGAGCAGGATTCCCGTTGAGCACCGCCAGGTGCGAA
TAAGGGACAGTGAAGAAGGAACACCCGCTCGCGGGTGGGCCTACTTCACCTATCCTGCCC
GGCTGACGCCGTTGGATACACCAAGGAAAGTCTACACGAACCCTTTGGCAAAATCCTGTA
TATCGTGCGAAAAAGGATGGATATACCGAAAAAATCGCTATAATGACCCCGAAGCAGGGT
TATGCAGCGGAAAAGGACAACGCGCGGACCG

pSEVA451

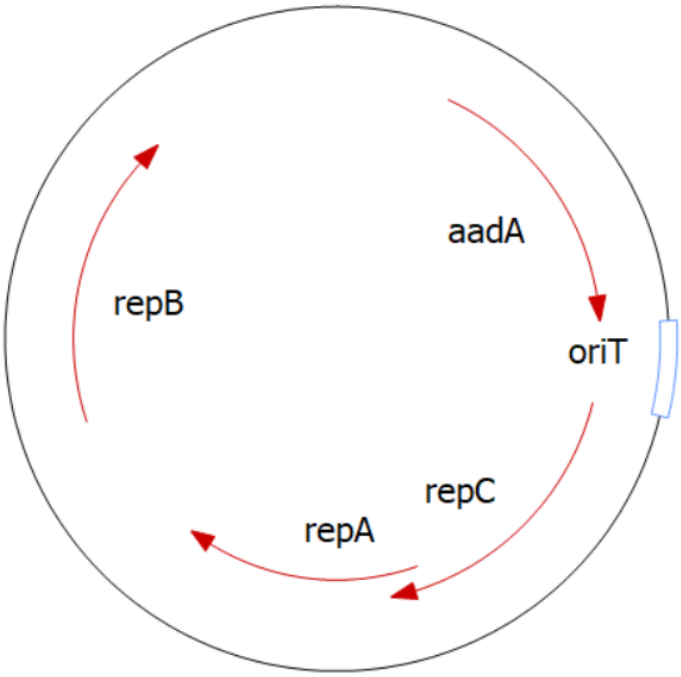

>pSEVA451
TTAATTAAAGCGGATAACAATTTCACACAGGAGGCCGCCTAGGCCGCGGCCGCGCGAATT
CGAGCTCGGTACCCGGGGATCCTCTAGAGTCGACCTGCAGGCATGCAAGCTTGCGGCCGC
GTCGTGACTGGGAAAACCCTGGCGACTAGTCTTGGACTCCTGTTGATAGATCCAGTAATG
ACCTCAGAACTCCATCTGGATTTGTTCAGAACGCTCGGTTGCCGCCGGGCGTTTTTTATT
GGTGAGAATCCAGGGGTCCCCAATAATTACGATTTACGTATTTAAATGAACCTTGACCGA
ACGCAGCGGTGGTAACGGCGCAGTGGCGGTTTTCATGGCTTGTTATGACTGTTTTTTTGG
GGTACAGTCTATGCCTCGGGCATCCAAGCAGCAAGCGCGTTACGCCGTGGGTCGATGTTT
GATGTTATGGAGCAGCAACGATGTTACGCAGCAGGGCAGTCGCCCTAAAACAAAGTTAAA
CATCATGAGGGAAGCGGTGATCGCCGAAGTATCGACTCAACTATCAGAGGTAGTTGGCGT
CATCGAGCGCCATCTCGAACCGACGTTGCTGGCCGTACATTTGTACGGCTCCGCAGTGGA
TGGCGGCCTGAAGCCACACAGTGATATTGATTTGCTGGTTACGGTGACCGTAAGGCTTGA
TGAAACAACGCGGCGAGCTTTGATCAACGACCTTTTGGAAACTTCGGCTTCCCCTGGAGA
GAGCGAGATTCTCCGCGCTGTAGAAGTCACCATTGTTGTGCACGACGACATCATTCCGTG
GCGTTATCCAGCTAAGCGCGAACTGCAATTTGGAGAATGGCAGCGCAATGACATTCTTGC
AGGTATCTTCGAGCCAGCCACGATCGACATTGATCTGGCTATCTTGCTGACAAAAGCAAG
AGAACATAGCGTTGCCTTGGTAGGTCCAGCGGCGGAGGAACTCTTTGATCCGGTTCCTGA
ACAGGATCTATTTGAGGCGCTAAATGAAACCTTAACGCTATGGAACTCGCCGCCCGACTG
GGCTGGCGATGAGCGAAATGTAGTGCTTACGTTGTCCCGCATTTGGTACAGCGCAGTAAC
CGGCAAAATCGCGCCGAAGGATGTCGCTGCCGACTGGGCAATGGAGCGCCTGCCGGCCCA
GTATCAGCCCGTCATACTTGAAGCTAGACAGGCTTATCTTGGACAAGAAGAAGATCGCTT
GGCCTCGCGCGCAGATCAGTTGGAAGAATTTGTCCACTACGTGAAAGGCGAGATCACCAA
GGTAGTCGGCAAATAAGACAATTGTCCTTTTCCGCTGCATAACCCTGCTTCGGGGTCATT
ATAGCGATTTTTTCGGTATATCCATCCTTTTTCGCACGATATACAGGATTTTGCCAAAGG
GTTCGTGTAGACTTTCCTTGGTGTATCCAACGGCGTCAGCCGGGCAGGATAGGTGAAGTA
GGCCCACCCGCGAGCGGGTGTTCCTTCTTCACTGTCCCTTATTCGCACCTGGCGGTGCTC
AACGGGAATCCTGCTCTGCGAGGCTGGCCGTAGGCCGGCCTCAGCCTGCCGCCTTGGGCC
GGGTGATGTCGTACTTGCCCGCCGCGAACTCGGTTACCGTCCAGCCCAGCGCGACCAGCT
CCGGCAACGCCTCGCGCACCCGCTGGCGGCGCTTGCGCATGGTCGAACCACTGGCCTCTG
ACGGCCAGACATAGCCGCACAAGGTATCTATGGAAGCCTTGCCGGTTTTGCCGGGGTCGA

TCCAGCCACACAGCCGCTGGTGCAGCAGGCGGGCGGTTTCGCTGTCCAGCGCCCGCACCT
CGTCCATGCTGATGCGCACATGCTGGCCGCCACCCATGACGGCCTGCGCGATCAAGGGGT
TCAGGGCCACGTACAGGCGCCCGTCCGCCTCGTCGCTGGCGTACTCCGACAGCAGCCGAA
ACCCCTGCCGCTTGCGGCCATTCTGGGCGATGATGGATACCTTCCAAAGGCGCTCGATGC
AGTCCTGTATGTGCTTGAGCGCCCCACCACTATCGACCTCTGCCCCGATTTCCTTTGCCA
GCGCCCGATAGCTACCTTTGACCACATGGCATTCAGCGGTGACGGCCTCCCACTTGGGTT
CCAGGAACAGCCGGAGCTGCCGTCCGCCTTCGGTCTTGGGTTCCGGGCCAAGCACTAGGC
CATTAGGCCCAGCCATGGCCACCAGCCCTTGCAGGATGCGCAGATCATCAGCGCCCAGCG
GCTCCGGGCCGCTGAACTCGATCCGCTTGCCGTCGCCGTAGTCATACGTCACGTCCAGCT
TGCTGCGCTTGCGCTCGCCCCGCTTGAGGGCACGGAACAGGCCGGGGGCCAGACAGTGCG
CCGGGTCGTGCCGGACGTGGCTGAGGCTGTGCTTGTTCTTAGGCTTCACCACGGGGCACC
CCCTTGCTCTTGCGCTGCCTCTCCAGCACGGCGGGCTTGAGCACCCCGCCGTCATGCCGC
CTGAACCACCGATCAGCGAACGGTGCGCCATAGTTGGCCTTGCTCACACCGAAGCGGACG
AAGAACCGGCGCTGGTCGTCGTCCACACCCCATTCCTCGGCCTCGGCGCTGGTCATGCTC
GACAGGTAGGACTGCCAGCGGATGTTATCGACCAGTACCGAGCTGCCCCGGCTGGCCTGC
TGCTGGTCGCCTGCGCCCATCATGGCCGCGCCCTTGCTGGCATGGTGCAGGAACACGATA
GAGCACCCGGTATCGGCGGCGATGGCCTCCATGCGACCGATGACCTGGGCCATGGGGCCG
CTGGCGTTTTCTTCCTCGATGTGGAACCGGCGCAGCGTGTCCAGCACCATCAGGCGGCGG
CCCTCGGCGGCGCGCTTGAGGCCGTCGAACCACTCCGGGGCCATGATGTTGGGCAGGCTG
CCGATCAGCGGCTGGATCAGCAGGCCGTCAGCCACGGCTTGCCGTTCCTCGGCGCTGAGG
TGCGCCCCAAGGGCGTGCAGGCGGTGATGAATGGCGGTGGGCGGGTCTTCGGCGGGCAGG
TAGATCACCGGGCCGGTGGGCAGTTCGCCCACCTCCAGCAGATCCGGCCCGCCTGCAATC
TGTGCGGCCAGTTGCAGGGCCAGCATGGATTTACCGGCACCACCGGGCGACACCAGCGCC
CCGACCGTACCGGCCACCATGTTGGGCAAAACGTAGTCCAGCGGTGGCGGCGCTGCTGCG
AACGCCTCCAGAATATTGATAGGCTTATGGGTAGCCATTGATTGCCTCCTTTGCAGGCAG
TTGGTGGTTAGGCGCTGGCGGGGTCACTACCCCCGCCCTGCGCCGCTCTGAGTTCTTCCA
GGCACTCGCGCAGCGCCTCGTATTCGTCGTCGGTCAGCCAGAACTTGCGCTGACGCATCC
CTTTGGCCTTCATGCGCTCGGCATATCGCGCTTGGCGTACAGCGTCAGGGCTGGCCAGCA
GGTCGCCGGTCTGCTTGTCCTTTTGGTCTTTCATATCAGTCACCGAGAAACTTGCCGGGG
CCGAAAGGCTTGTCTTCGCGGAACAAGGACAAGGTGCAGCCGTCAAGGTTAAGGCTGGCC
ATATCAGCGACTGAAAAGCGGCCAGCCTCGGCCTTGTTTGACGTATAACCAAAGCCACCG
GGCAACCAATAGCCCTTGTCACTTTTGATCAGGTAGACCGACCCTGAAGCGCTTTTTTCG
TATTCCATAAAACCCCCTTCTGTGCGTGAGTACTCATAGTATAACAGGCGTGAGTACCAA
CGCAAGCACTACATGCTGAAATCTGGCCCGCCCCTGTCCATGCCTCGCTGGCGGGGTGCC
GGTGCCCGTGCCAGCTCGGCCCGCGCAAGCTGGACGCTGGGCAGACCCATGACCTTGCTG
ACGGTGCGCTCGATGTAATCCGCTTCGTGGCCGGGCTTGCGCTCTGCCAGCGCTGGGCTG
GCCTCGGCCATGGCCTTGCCGATTTCCTCGGCACTGCGGCCCCGGCTGGCCAGCTTCTGC
GCGGCGATAAAGTCGCACTTGCTGAGGTCATCACCGAAGCGCTTGACCAGCCCGGCCATC
TCGCTGCGGTACTCGTCCAGCGCCGTGCGCCGGTGGCGGCTAAGCTGCCGCTCGGGCAGT
TCGAGGCTGGCCAGCCTGCGGGCCTTCTCCTGCTGCCGCTGGGCCTGCTCGATCTGCTGG
CCAGCCTGCTGCACCAGCGCCGGGCCAGCGGTGGCGGTCTTGCCCTTGGATTCACGCAGC
AGCACCCACGGCTGATAACCGGCGCGGGTGGTGTGCTTGTCCTTGCGGTTGGTGAAGCCC
GCCAAGCGGCCATAGTGGCGGCTGTCGGCGCTGGCCGGGTCGGCGTCGTACTCGCTGGCC
AGCGTCCGGGCAATCTGCCCCCGAAGTTCACCGCCTGCGGCGTCGGCCACCTTGACCCAT
GCCTGATAGTTCTTCGGGCTGGTTTCCACTACCAGGGCAGGCTCCCGGCCCTCGGCTTTC
ATGTCATCCAGGTCAAACTCGCTGAGGTCGTCCACCAGCACCAGACCATGCCGCTCCTGC
TCGGCGGGCCTGATATACACGTCATTGCCCTGGGCATTCATCCGCTTGAGCCATGGCGTG
TTCTGGAGCACTTCGGCGGCTGACCATTCCCGGTTCATCATCTGGCCGGTGGTGGCGTCC
CTGACGCCGATATCGAAGCGCTCACAGCCCATGGCCTTGAGCTGTCGGCCTATGGCCTGC
AAAGTCCTGTCGTTCTTCATCGGGCCACCAAGCGATTCCCACACATTATACGAGCCGGAA
GCATAAAGTGTAAAGCCTAGATCCGAAGGATGAGCCGGGCTGAATGATCGACCGAGACAG
GCCCTGCGGGGCTGCACACGCGCCCCCACCCTTCGGGTAGGGGGAAAGGCCGCTAAAGCG
GCTAAAAGCGCTCCAGCGTATTTCTGCGGGGTTTGGTGTGGGGTTTAGCGGGCTTTGCCC
GCCTTTCCCCCTGCCGCGCAGCGGTGGGGCGGTGTGTAGCCTAGCGCAGCGAATAGACCA
GCTATCCGGCCTCTGGCCGGGCATATTGGGCAAGGGCAGCAGCGCCCCACAAGGGCGCTG
ATAACCGCGCCTAGTGGATTATTCTTAGATAATCATGGATGGATTTTTCCAACACCCCGC

CAGCCCCCGCCCCTGCTGGGTTTGCAGGTTTGGGGGCGTGACAGTTATTGCAGGGGTTCG
TGACAGTTATTGCAGGGGGGCGTGACAGTTATTGCAGGGGTTCGTGACAGTTAGGGCGCG
CCCAGCTGTCTAGGGCGGCGGATTTGTCCTACTCAGGAGAGCGTTCACCGACAAACAACA
GATAAAACGAAAGGCCCAGTCTTTCGACTGAGCCTTTCGTTTTATTTGATGCCT

pSN15K

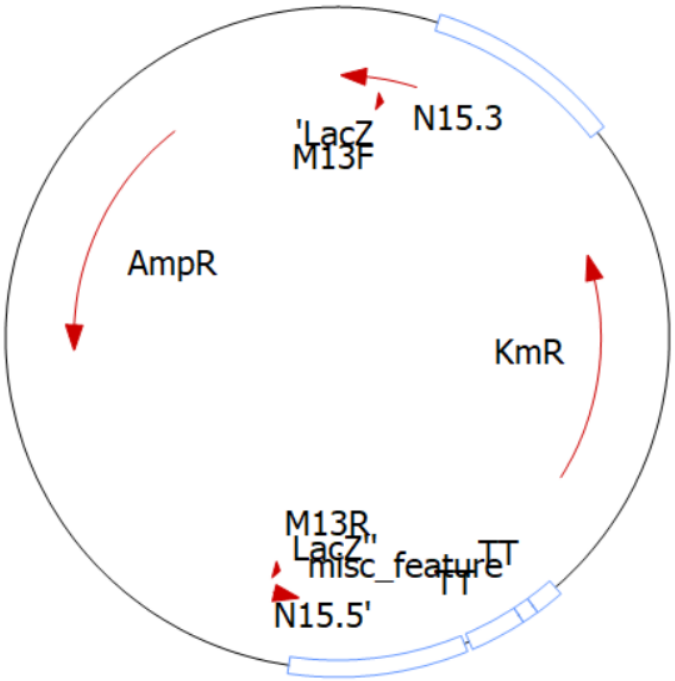

>pSN15K
CACCCGCCGCGCTTAATGCGCCGCTACAGGGCGCGTCCATTCGCCATTCAGGCTGCGCAA
CTGTTGGGAAGGGCGATCGGTGCGGGCCTCTTCGCTATTACGCCAGCTGGCGAAAGGGGG
ATGTGCTGCAAGGCGATTAAGTTGGGTAACGCCAGGGTTTTCCCAGTCACGACGTTGTAA
AACGACGGCCAGTGAATTGTAATACGACTCACTATAGGGCGAATTGGGCCCGACGTCGCA
TGCTCCCGGCCGCCATGGCGGCCGCGGGAATTCGATTCTAAACTTACGGCATTGGCATCA
ACGGGAGCCACCGTCGGAGTAGGGGAAGTAACAACGGGGGAACTGGTATTGGTGGGCAAA
ATTTTTACTAGCCATTGATTCCATTGGGGCAGATTGAACGCTCCCAACCACCAAAGTCCC
CCTAATACAACGACAGAACTAAATAACAGGAAAAAAGGAATCCAAGGAGTTACCCCTCTT
TTATGGGATGGAACTTCATCGACATTAAAGGTGGGAGGGGGAGGAGGCAATGGGGACAAT
GGTGGTCCAGAAAAGGAAGGTGGCTCCGACGTCAAGGCAACGGGACATCCACAGGATTCA
CAGAAACGAACCTGGGGGCTAAGGCGGTTGCCACAATTAGTACAAAAAACGGGAGTAGTC
ATAGGTGAAAACCCCGACTATAGAATTAGAAAAATTTAACTTTTTATCCGAATTTTATTC
GTCCATGTTCCCCAAATAACTATCAAAATAATTGGAAAAATTAAATTATTTGGTCGTTGG
TCACCGCTCCCTAAAGACCTGGCCATTGTAAAGAGATTACACCCGGGCGATTTACTTTTC
GACCTCATTCTATTAGACTCTCGTTTGGATTGCAACTGGTCTATTTTCCTCTTTTGTTTG
ATAGAAAATCATAAAAGGATTTGCAGACTACGGGCCTAAAGAACTAAAAAATCTATCTGT
TTCTTTTCATTCTCTGTATTTTTTATAGTTTCTGTTGCATGGGCATAAAGTTGCCTTTTT
AATCACAATTCAGAAAATATCATAATATCTCATTTCACTAAATAATAGTGAACGGCAGGT
ATATGTGATGGGTTAAAAAGGATCGATCCTCTAGCGAACCCCAGAGTCCCGCTCAGAAGA
ACTCGTCAAGAAGGCGATAGAAGGCGATGCGCTGCGAATCGGGAGCGGCGATACCGTAAA
GCACGAGGAAGCGGTCAGCCCATTCGCCGCCAAGCTCTTCAGCAATATCACGGGTAGCCA
ACGCTATGTCCTGATAGCGGTCCGCCACACCCAGCCGGCCACAGTCGATGAATCCAGAAA
AGCGGCCATTTTCCACCATGATATTCGGCAAGCAGGCATCGCCATGGGTCACGACGAGAT
CCTCGCCGTCGGGCATCCGCGCCTTGAGCCTGGCGAACAGTTCGGCTGGCGCGAGCCCCT
GATGCTCTTCGTCCAGATCATCCTGATCGACAAGACCGGCTTCCATCCGAGTACGTGCTC
GCTCGATGCGATGTTTCGCTTGGTGGTCGAATGGGCAGGTAGCCGGATCAAGCGTATGCA
GCCGCCGCATTGCATCAGCCATGATGGATACTTTCTCGGCAGGAGCAAGGTGAGATGACA

GGAGATCCTGCCCCGGCACTTCGCCCAATAGCAGCCAGTCCCTTCCCGCTTCAGTGACAA
CGTCGAGCACAGCTGCGCAAGGAACGCCCGTCGTGGCCAGCCACGATAGCCGCGCTGCCT
CGTCTTGGAGTTCATTCAGGGCACCGGACAGGTCGGTCTTGACAAAAAGAACCGGGCGCC
CCTGCGCTGACAGCCGGAACACGGCGGCATCAGAGCAGCCGATTGTCTGTTGTGCCCAGT
CATAGCCGAATAGCCTCTCCACCCAAGCGGCCGGAGAACCTGCGTGCAATCCATCTTGTT
CAATCATGCGAAACGATCCTCATCCTGTCTCTTGATCAGATCTTGATCCCCTGCGCCATC
AGATCCTTGGCGGCAAGAAAGCCATCCAGTTTACTTTGCAGGGCTTCCCAACCTTACCAG
AGGGCGCCCCAGCTGGCAATTCCGGTTCGCTTGCTGTCCATAAAACCGCCCAGTCTAGCT
ATCGCCATGTAAGCCCACTGCAAGCTACCTGCTTTCTCTTTGCGCTTGCGTTTTCCCTTG
TCCAGATAGCCCAGTAGCTGACATTCACCCGGGAAAAAAAAACCCCGCCCCTGACAGGGC
GGGGTTTTTTTTCAGATAAAAAAAATCCTTAGCTTTCGCTAAGGATGATTTCTGCAATTG
GCGGCCGCTTCTAGAATGCACTAGTAGCGGCCGCTGCAGTCCGGCAAAAAAACGGGCAAG
GTGTCACCACCCTGCCCTTTTTCTTTAAAACCGAAAAGATTACTTCGCGTTGGAGAGCGT
TCACCGACAAACAACAGATAAAACGAAAGGCCCAGTCTTTCGACTGAGCCTTTCGTTTTA
TTTGATGCCTGGTACCGGGTGTAATCCATTGGGCACGAGAGTTAGTAAGGCAGTGGCAAT
TAATAGAGGCTTATGGTTGATTCGCATTGTTTTGCTCCTGAAATTTTCGGCAAATACAAA
TACTTCGCTCTTCTAGCCCTATTAACCATTTTAACGACAAATTGATGGGGCAACGATTAA
CAAATAATGAATAAATTTTATGTTTTTCAAGATGAAAATTTGAAAATTTGATTTCCTTAT
ATTTCTACTATAGAAGACTAATACAATTAGATCTAAAATTTGCAAGTATAAAAATCAGCA
AATAGTTATATTGTTAATAATTCAATGACCCAATAACTCGTACTGTTATCTACGTGGTGA
AAGCCAAAAAGACGAACAGTTTAGCCTCCTCCTCCTCGGCGATCGCCAAGCGAAATGTCA
TGGGAGATGTTCAGATTGAGCATTTTTTTCTAAAAGCCCTTGCTAAAACAAACCACATGT
GCAGGGTGTCCCCGATGTTGACTAAATTCAGCGGCTCGACCATATGGGAGAGCTCCCAAC
GCGTTGGATGCATAGCTTGAGTATTCTATAGTGTCACCTAAATAGCTTGGCGTAATCATG
GTCATAGCTGTTTCCTGTGTGAAATTGTTATCCGCTCACAATTCCACACAACATACGAGC
CGGAAGCATAAAGTGTAAAGCCTGGGGTGCCTAATGAGTGAGCTAACTCACATTAATTGC
GTTGCGCTCACTGCCCGCTTTCCAGTCGGGAAACCTGTCGTGCCAGCTGCATTAATGAAT
CGGCCAACGCGCGGGGAGAGGCGGTTTGCGTATTGGGCGCTCTTCCGCTTCCTCGCTCAC
TGACTCGCTGCGCTCGGTCGTTCGGCTGCGGCGAGCGGTATCAGCTCACTCAAAGGCGGT
AATACGGTTATCCACAGAATCAGGGGATAACGCAGGAAAGAACATGTGAGCAAAAGGCCA
GCAAAAGGCCAGGAACCGTAAAAAGGCCGCGTTGCTGGCGTTTTTCCATAGGCTCCGCCC
CCCTGACGAGCATCACAAAAATCGACGCTCAAGTCAGAGGTGGCGAAACCCGACAGGACT
ATAAAGATACCAGGCGTTTCCCCCTGGAAGCTCCCTCGTGCGCTCTCCTGTTCCGACCCT
GCCGCTTACCGGATACCTGTCCGCCTTTCTCCCTTCGGGAAGCGTGGCGCTTTCTCATAG
CTCACGCTGTAGGTATCTCAGTTCGGTGTAGGTCGTTCGCTCCAAGCTGGGCTGTGTGCA
CGAACCCCCCGTTCAGCCCGACCGCTGCGCCTTATCCGGTAACTATCGTCTTGAGTCCAA
CCCGGTAAGACACGACTTATCGCCACTGGCAGCAGCCACTGGTAACAGGATTAGCAGAGC
GAGGTATGTAGGCGGTGCTACAGAGTTCTTGAAGTGGTGGCCTAACTACGGCTACACTAG
AAGAACAGTATTTGGTATCTGCGCTCTGCTGAAGCCAGTTACCTTCGGAAAAAGAGTTGG
TAGCTCTTGATCCGGCAAACAAACCACCGCTGGTAGCGGTGGTTTTTTTGTTTGCAAGCA
GCAGATTACGCGCAGAAAAAAAGGATCTCAAGAAGATCCTTTGATCTTTTCTACGGGGTC
TGACGCTCAGTGGAACGAAAACTCACGTTAAGGGATTTTGGTCATGAGATTATCAAAAAG
GATCTTCACCTAGATCCTTTTAAATTAAAAATGAAGTTTTAAATCAATCTAAAGTATATA
TGAGTAAACTTGGTCTGACAGTTACCAATGCTTAATCAGTGAGGCACCTATCTCAGCGAT
CTGTCTATTTCGTTCATCCATAGTTGCCTGACTCCCCGTCGTGTAGATAACTACGATACG
GGAGGGCTTACCATCTGGCCCCAGTGCTGCAATGATACCGCGAGACCCACGCTCACCGGC
TCCAGATTTATCAGCAATAAACCAGCCAGCCGGAAGGGCCGAGCGCAGAAGTGGTCCTGC
AACTTTATCCGCCTCCATCCAGTCTATTAATTGTTGCCGGGAAGCTAGAGTAAGTAGTTC
GCCAGTTAATAGTTTGCGCAACGTTGTTGCCATTGCTACAGGCATCGTGGTGTCACGCTC
GTCGTTTGGTATGGCTTCATTCAGCTCCGGTTCCCAACGATCAAGGCGAGTTACATGATC
CCCCATGTTGTGCAAAAAAGCGGTTAGCTCCTTCGGTCCTCCGATCGTTGTCAGAAGTAA
GTTGGCCGCAGTGTTATCACTCATGGTTATGGCAGCACTGCATAATTCTCTTACTGTCAT
GCCATCCGTAAGATGCTTTTCTGTGACTGGTGAGTACTCAACCAAGTCATTCTGAGAATA
GTGTATGCGGCGACCGAGTTGCTCTTGCCCGGCGTCAATACGGGATAATACCGCGCCACA
TAGCAGAACTTTAAAAGTGCTCATCATTGGAAAACGTTCTTCGGGGCGAAAACTCTCAAG
GATCTTACCGCTGTTGAGATCCAGTTCGATGTAACCCACTCGTGCACCCAACTGATCTTC

AGCATCTTTTACTTTCACCAGCGTTTCTGGGTGAGCAAAAACAGGAAGGCAAAATGCCGC
AAAAAAGGGAATAAGGGCGACACGGAAATGTTGAATACTCATACTCTTCCTTTTTCAATA
TTATTGAAGCATTTATCAGGGTTATTGTCTCATGAGCGGATACATATTTGAATGTATTTA
GAAAAATAAACAAATAGGGGTTCCGCGCACATTTCCCCGAAAAGTGCCACCTGATGCGGT
GTGAAATACCGCACAGATGCGTAAGGAGAAAATACCGCATCAGGAAATTGTAAGCGTTAA
TATTTTGTTAAAATTCGCGTTAAATTTTTGTTAAATCAGCTCATTTTTTAACCAATAGGC
CGAAATCGGCAAAATCCCTTATAAATCAAAAGAATAGACCGAGATAGGGTTGAGTGTTGT
TCCAGTTTGGAACAAGAGTCCACTATTAAAGAACGTGGACTCCAACGTCAAAGGGCGAAA
AACCGTCTATCAGGGCGATGGCCCACTACGTGAACCATCACCCTAATCAAGTTTTTTGGG
GTCGAGGTGCCGTAAAGCACTAAATCGGAACCCTAAAGGGAGCCCCCGATTTAGAGCTTG
ACGGGGAAAGCCGGCGAACGTGGCGAGAAAGGAAGGGAAGAAAGCGAAAGGAGCGGGCGC
TAGGGCGCTGGCAAGTGTAGCGGTCACGCTGCGCGTAACCACCA

Chapter IV. Heterologous production of glycine betaine using *Synechocystis* sp. PCC 6803-based chassis lacking native compatible solutes

Work published in:

Ferreira, E. A., Pacheco, C. C., Rodrigues, J. S., Pinto, F., Lamosa, P., Fuente, D., Urchueguía, J., & Tamagnini, P. (2022) Heterologous production of glycine betaine using *Synechocystis* sp. PCC 6803-based chassis lacking native compatible solutes. *Frontiers in Bioengineering and Biotechnology*, *9*:821075. https://doi.org/10.3389/fbioe.2021.821075.

frontiers in Bioengineering and Biotechnology

ORIGINAL RESEARCH
published: 07 January 2022
doi: 10.3389/fbioe.2021.821075

Heterologous Production of Glycine Betaine Using *Synechocystis* sp. PCC 6803-Based Chassis Lacking Native Compatible Solutes

Eunice A. Ferreira[1,2,3], *Catarina C. Pacheco*[1,2], *João S. Rodrigues*[1,2,4†], *Filipe Pinto*[1,2], *Pedro Lamosa*[5], *David Fuente*[6], *Javier Urchueguía*[6] *and Paula Tamagnini*[1,2,4*]

[1]*I3S—Instituto de Investigação e Inovação em Saúde, Universidade do Porto, Porto, Portugal,* [2]*IBMC—Instituto de Biologia Molecular e Celular, Universidade do Porto, Porto, Portugal,* [3]*ICBAS—Instituto de Ciências Biomédicas Abel Salazar, Universidade do Porto, Porto, Portugal,* [4]*Departamento de Biologia, Faculdade de Ciências, Universidade do Porto, Porto, Portugal,* [5]*Instituto de Tecnologia Química e Biológica António Xavier, ITQB NOVA, Oeiras, Portugal,* [6]*Instituto de Aplicaciones de las Tecnologías de la Información y de las Comunicaciones Avanzadas, Universitat Politècnica de València, València, Spain*

OPEN ACCESS

Edited by:
Shota Atsumi,
University of California, Davis, United States

Reviewed by:
Xuefeng Lu,
Qingdao Institute of Bioenergy and Bioprocess Technology (CAS), China
Jianping Yu,
National Renewable Energy Laboratory (DOE), United States
Weiwen Zhang,
Tianjin University, China

***Correspondence:**
Paula Tamagnini
pmtamagn@ibmc.up.pt

†Present Address:
João S. Rodrigues,
Department of Chemistry—Ångström, Uppsala University, Uppsala, Sweden

Specialty section:
This article was submitted to Synthetic Biology, a section of the journal Frontiers in Bioengineering and Biotechnology

Received: *23 November 2021*
Accepted: *15 December 2021*
Published: *07 January 2022*

Citation:
Ferreira EA, Pacheco CC, Rodrigues JS, Pinto F, Lamosa P, Fuente D, Urchueguía J and Tamagnini P (2022) Heterologous Production of Glycine Betaine Using Synechocystis *sp. PCC 6803-Based Chassis Lacking Native Compatible Solutes. Front. Bioeng. Biotechnol. 9:821075. doi: 10.3389/fbioe.2021.821075*

Among compatible solutes, glycine betaine has various applications in the fields of nutrition, pharmaceuticals, and cosmetics. Currently, this compound can be extracted from sugar beet plants or obtained by chemical synthesis, resulting in low yields or high carbon footprint, respectively. Hence, in this work we aimed at exploring the production of glycine betaine using the unicellular cyanobacterium *Synechocystis* sp. PCC 6803 as a photoautotrophic chassis. *Synechocystis* mutants lacking the native compatible solutes sucrose or/and glucosylglycerol—Δ*sps*, Δ*ggpS*, and Δ*sps*Δ*ggpS*—were generated and characterized. Under salt stress conditions, the growth was impaired and accumulation of glycogen decreased by ~50% whereas the production of compatible solutes and extracellular polymeric substances (capsular and released ones) increased with salinity. These mutants were used as chassis for the implementation of a synthetic device based on the metabolic pathway described for the halophilic cyanobacterium *Aphanothece halophytica* for the production of the compatible solute glycine betaine. Transcription of ORFs comprising the device was shown to be stable and insulated from *Synechocystis'* native regulatory network. Production of glycine betaine was achieved in all chassis tested, and was shown to increase with salinity. The introduction of the glycine betaine synthetic device into the Δ*ggpS* background improved its growth and enabled survival under 5% NaCl, which was not observed in the absence of the device. The maximum glycine betaine production [64.29 µmol/gDW (1.89 µmol/mg protein)] was reached in the Δ*ggpS* chassis grown under 3% NaCl. Taking into consideration this production under seawater-like salinity, and the identification of main key players involved in the carbon fluxes, this work paves the way for a feasible production of this, or other compatible solutes, using optimized *Synechocystis* chassis in a pilot-scale.

Keywords: compatible solutes, cyanobacteria, glycine betaine, glucosylglycerol, salt stress, sucrose, *Synechocystis*, synthetic biology

Abbreviations: CPS, capsular polysaccharides; CS, compatible solutes; DW, dry weight; EPS, extracellular polymeric substances; FW, fresh weight; GB, glycine betaine; GG, glucosylglycerol; NMR, nuclear magnetic resonance; RPS, released polysaccharides; RT-qPCR, reverse transcription quantitative PCR.

INTRODUCTION

Microorganisms can cope with environmental stresses such as temperature, salinity or drought via the production of compatible solutes (CS)—low-molecular weight organic compounds highly soluble in water that can accumulate intracellularly up to molar concentrations, without interfering with the cell metabolism (Klähn and Hagemann, 2011). CS belong to different chemical classes including sugars (e.g., sucrose, trehalose), polyols (e.g., glycerol, sorbitol), heterosides (e.g., glucosylglycerol, floridoside), and amino acids or their derivatives (e.g., proline, glutamate, glycine betaine, ectoine) (Kirsch et al., 2019). Glycine betaine (or *N*,*N*,*N*-trimethylglycine) is an ubiquitous solute that can be found in bacteria, plants and mammals, being mostly synthesized by the two-step oxidation of choline to betaine aldehyde and subsequently to glycine betaine (Landfald and Strøm, 1986; Grossman and Hebert, 1989; Rathinasabapathi et al., 1997). Later on, the synthesis of glycine betaine *via* a three-step methylation of glycine was described in extremely halophilic bacteria (Nyyssola et al., 2000; Waditee et al., 2003). This biosynthetic pathway involves two *N*-methyltransferases: the glycine-sarcosine-*N*-methyltransferase (GSMT) that catalyzes the methylation of glycine and sarcosine, and the dimethylglycine-*N*-methyltransferase (DMT) that converts dimethylglycine to glycine betaine. This CS has a strong stabilizing effect on biomolecules, by maintaining their structure and function (Guinn et al., 2011; Stadmiller et al., 2017), and thus conferring drought-, osmo- and thermo-protection to cells (Caldas et al., 1999; Holmström et al., 2000; Cleland et al., 2004; You et al., 2019). Moreover, glycine betaine plays an important physiological role as methyl group donor with beneficial stress-mitigating effects in humans (Lever and Slow, 2010; Day and Kempson, 2016), and up-regulating antioxidant defense systems in plants (Rady et al., 2018; Sun et al., 2020). Due to these interesting properties, glycine betaine is a value-added compound with applications in human nutrition, animal feed, agriculture, pharmaceuticals, and cosmetics (Eklund et al., 2005; Lever and Slow, 2010; Nsimba et al., 2010; Cholewa et al., 2014; Day and Kempson, 2016; Dikilitas et al., 2020). Most of the commercially available glycine betaine is extracted from sugar beets (*Beta vulgaris*) (Heikkila et al., 1982), resulting in relatively low yields and rendering this organic production an expensive process. Alternatively, glycine betaine can be produced by chemical synthesis, but this process, although cheaper, has a high environmental impact increasing the carbon footprint (DuPont, 2015; Kar et al., 2015). A more sustainable and cost-effective production is highly desirable, and thus cyanobacteria emerge as promising chassis for the production of compatible solutes and other products of interest. Their photoautotrophic metabolism enables the sequestration and conversion of atmospheric CO_2 into organic compounds using sunlight and water as energy and electron sources, respectively (Knoll, 2008; Ananya and Ahmad, 2014). Therefore, they are being increasingly studied to be used as solar-powered cell factories for many biotechnological applications including the production of e.g., alcohols, alkanes, hydrogen, sugars, and terpenoids (Hays and Ducat, 2015; Lindblad, 2018; Sadvakasova et al., 2020; Wang et al., 2020; Rodrigues and Lindberg, 2021). Among cyanobacteria, the unicellular *Synechocystis* sp. PCC 6803 (hereafter *Synechocystis*) is the best studied strain, and the vast array of data generated over the past decades allowed the construction of genome-scale metabolic models to predict system's behavior (Montagud et al., 2010; Montagud et al., 2011; Joshi et al., 2017; Gopalakrishnan et al., 2018). Moreover, various molecular and synthetic biology tools are now available for the genetic manipulation and engineering of this particular cyanobacterial strain (Huang et al., 2010; Heidorn et al., 2011; Pinto et al., 2015; Pacheco et al., 2021). *Synechocystis* is a freshwater strain and thus moderately halotolerant, relying on the biosynthesis of the compatible solutes sucrose, glutamate and glucosylglycerol to maintain the osmotic pressure under stress conditions (Klähn and Hagemann, 2011; Iijima et al., 2020).

In this study, *Synechocystis* knockout mutants in the biosynthetic pathways producing the main native compatible solutes sucrose or/and glucosylglycerol were generated to serve as chassis for the production of value-added compounds. The genome-scale metabolic model *i*Syn811 was used to simulate the production rates of different heterologous CS and the highest rate was predicted for glycine betaine. As a proof-of-concept, we explored the production of this compatible solute using our *Synechocystis*-based chassis. For this purpose, a synthetic device based on the biosynthetic gene cluster from the halophilic cyanobacterium *Aphanothece halophytica* was constructed and introduced in the different chassis. Besides showing the production of glycine betaine and validating the functionality of the synthetic device, the characterization of the strains contributes to a better understanding of the mechanisms used by the cells to maintain homeostasis and cope with different levels of salinity.

MATERIALS AND METHODS

Reagents and Enzymes

The media components and other reagents were obtained from Fisher Scientific (United States), Merck (Germany) or Sigma Aldrich (United States), and noble agar from Difco (United States). All DNA-modifying enzymes and polymerases were purchased from Thermo Fisher Scientific (United States) and Promega (United States), and standard molecular biology kits were obtained from NZY Tech (Portugal). The Sanger sequencing and oligo synthesis services were provided by STAB VIDA, Lda (Portugal).

Organisms and Culture Conditions

Wild-type and mutants of the unicellular, non-motile cyanobacterium *Synechocystis* sp. PCC 6803 substrain GT-Kazusa (Kanesaki et al., 2012; Trautmann et al., 2012)

(obtained from the Pasteur Culture Collection, France) were maintained in Erlenmeyer flasks batch cultures with BG11 medium (Stanier et al., 1971) at 30°C with orbital shaking (150 rpm) under a 12 h light/12 h dark regimen. Light intensity was 25 μE/m^2/s in all experiments and Cosine-corrected irradiance was measured using a Dual Solar/Electric Quantum Meter (Spectrum Technologies, Inc., United States). For solid BG11, the medium was supplemented with 1.5% (wt/vol) noble agar, 0.3% (wt/vol) sodium thiosulfate and 10 mM TES-KOH buffer, pH 8.2 (Stanier et al., 1971). For the selection and maintenance of mutants, BG11 medium was supplemented with chloramphenicol (Cm, 10–20 μg/ml). For cloning purposes, *E. coli* strains DH5α and XL1-blue were used. Cells were grown at 37°C in LB medium (Sambrook and Russel, 2001), supplemented with kanamycin (Km, 50 μg/ml) or Cm (34 μg/ml).

DNA and RNA Extraction

Cyanobacterial genomic DNA (gDNA) extraction was performed according to the procedure described previously (Tamagnini et al., 1997). For RNA extraction, 50 ml of *Synechocystis* culture at OD_{730} ≈ 1 was centrifuged for 10 min at 4,470 *g*; cell pellets were treated with RNAprotect Bacteria Reagent (Qiagen, Germany) according to instructions, and stored at −80°C. RNA was extracted using the TRIzol® Reagent (Ambion) according to the method described previously (Leitão et al., 2006) with the following adaptations: the cells were disrupted using a FastPrep®-24 (MP Biomedicals) in 2 cycles of 1 min at 4.0 m/s and the RNA samples were treated with 1 U of RQ1 RNase-Free DNase (Promega) according to manufacturer's instructions.

Glycine Betaine Device: Design, DNA Synthesis, and Assembly

The synthetic construction for the synthesis of glycine betaine (Ahbet) was designed based on *gsmt* (encoding the glycine-sarcosine-*N*-methyltransferase) and *dmt* (encoding the dimethylglycine-*N*-methyltransferase) Open Reading Frames (ORFs) from the cyanobacterium *Aphanothece halophytica*, and the *metX* (*sll0927*, encoding *S*-adenosyl-methionine synthase) ORF from *Synechocystis*. All the ORF sequences were codon optimized for *Synechocystis* using the Gene Designer 2.0 software (DNA 2.0, Inc., United States), restriction sites incompatible with the BioBrick™ standard RFC [10] were eliminated and double stop codons included. Each ORF is preceded by the BioBrick™ (BB) ribosome binding site (RBS) BBa_B0030 and the double terminator BBa_B0015 was included after the *metX* ORF. In addition, the synthetic construction is flanked by the prefix and suffix sequences of the BB RFC [10] standard. All the BB sequences were retrieved from the Registry of Standard Biological Parts (parts.igem.org). Subsequently, the sequence of the glycine betaine synthetic construction flanked by the BB prefix, the double terminator and BB suffix was synthesized and cloned into *Sma*I digested pBluescript II SK(-) (Epoch Life Science, Inc., United States).

To construct the glycine betaine device, the synthesized Ahbet construct was assembled with the synthetic promoter $P_{trc.x.lacO,}$ previously characterized in *Synechocystis* (Ferreira et al., 2018). For this purpose, the Ahbet was PCR-amplified from the plasmid pBSK with the pUC primers (Additional file 1: **Supplementary Table S4**), using Phusion high-fidelity DNA polymerase, according to the manufacturer's instructions. The PCR product was purified using NZYGelpure kit, digested with *Xba*I and *Pst*I and cloned downstream of $P_{trc.x.lacO}$ in the pJ201 plasmid (digested with *Spe*I and *Pst*I, and dephosphorylated). The generated $P_{trc.x.lacO}$::Ahbet device was excised from the pJ201 plasmid with *Xba*I and *Spe*I, and transferred to pSEVA351 shuttle vector (Silva-Rocha et al., 2013), digested with *Xba*I. The pSEVA351 was obtained from the "Standard European Vector Architecture" repository and is comprised by the broad-host-range replicon RSF1010 and the chloramphenicol antibiotic marker. The assembly and transfer of the synthetic device was confirmed by PCR, restriction analysis and Sanger sequencing.

Construction of Integrative Plasmids for the Generation of CS Mutants

The construction of integrative plasmids for the knockout of *ggpS* (glucosylglycerol-phosphate synthase) and *sps* (sucrose-phosphate synthase) genes was performed as described previously (Pinto et al., 2012). Briefly, the plasmids were based on pGEM-T® Easy (Promega, United States) and contain the *Synechocystis* chromosomal regions flanking the *ggpS* or the *sps* gene. The 5′- and 3′-flanking regions were amplified from the cyanobacterium's genome using *Pfu* DNA polymerase and the primer pairs 5-O/5-I and 3-O/3-I (Additional file 1: **Supplementary Table S4**), respectively. Subsequently, the purified PCR fragments were fused by Overlap Extension PCR using primers 5-O/3-O and 80 ng of each amplicon. The resulting product was purified and cloned into the vector pGEM-T® Easy, according to the manufacturer's instructions, originating the pGDggpS, and the pGDsps plasmids (**Table 1**). A selection cassette, containing the *nptII* gene (conferring resistance to neomycin and kanamycin) and the *sacB* gene (conferring sensitivity to sucrose), was PCR amplified from the plasmid pK18mobsacB (Schafer et al., 1994) with specific primers (Additional file 1: **Supplementary Table S4**). The amplicon was then cloned into the *Age*I/*Sma*I restriction site of pGDggpS or pGDsps plasmids, generating the pGDggpS.KS and the pGDsps.KS plasmids, respectively (**Table 1**). All constructs were confirmed by sequencing.

Generation of *Synechocystis* CS Knockout Mutants

Synechocystis was transformed based on the protocol described by Williams (1988) with modifications. *Synechocystis* cultures were grown under standard conditions to an OD_{730} ≈ 0.5. Cells were harvested by centrifugation at 3,850 *g* for 10 min; and then resuspended in BG11 to a final OD_{730} ≈ 2.5. A 500 μL aliquot of these cells was used (per transformation) and incubated with

TABLE 1 | List of plasmids used to transform *Synechocystis*.

Designation	Plasmid	Description	Reference/ Source
$P_{trc.x.lacO}$:: Ahbet	pSEVA351	Ahbet synthetic construction under the control of the $P_{trc.x.lacO}$ promoter	This study
pGDggpS	pGEM-T® Easy	pGEM-T easy vector containing the two regions for double homologous recombination targeting the *ggpS locus*	Ferreira et al. (2018)
pGDggpS.KS	pGEM-T® Easy	pGEM-T easy vector containing the *nptII* and *sacB* genes flanked by the two regions for double homologous recombination targeting the *ggpS locus*	This study
pGDsps	pGEM-T® Easy	pGEM-T easy vector containing the two regions for double homologous recombination targeting the *sps locus*	This study
pGDsps.KS	pGEM-T® Easy	pGEM-T easy vector containing the *nptII* and *sacB* genes flanked by the two regions for double homologous recombination targeting the *sps locus*	This study

purified pGDggpS.KS or pGDsps.KS plasmids, at a final DNA concentration of 20 μg/ml, for 5 h in light at 30°C. Cells were then spread onto Immobilon™-NC membranes (0.45 μm pore size, 82 mm, Millipore, United States) resting on solid BG11 plates, incubated at 25°C under low light, and transferred to selective solid BG11 plates supplemented with 10 μg/mL km after 24 h. Transformants were observed after 1–2 weeks. For complete segregation, Km-resistant colonies were streaked on BG11 plates with increasing Km concentrations (up to 500 μg/ml), and finally transferred into liquid medium. Mutants were then tested for sucrose sensitivity and confirmed by PCR and Southern blot (for details see below). Subsequently, to remove the selection markers from the insertion mutants, cells were transformed as described above with the pGDggpS or the pGDsps plasmids, and the mutants were selected on solid BG11 containing 10% (wt/vol) sucrose. These mutants were also screened for Km-sensitivity. The double mutant Δ*sps*Δ*ggpS* was generated by deleting the *ggpS* gene from the Δ*sps* background following the abovementioned protocol. The full segregation of the mutants was confirmed by PCR using GoTaq® G2 Flexi DNA Polymerase, together with specific primers (Additional file 1: **Supplementary Table S4**), according to manufacturer's instructions. Mutant segregation was also confirmed by Southern blots that were performed using 4 μg of genomic DNA of the wild-type and mutants, digested with *Mun*I (wild-type, Δ*sps.KS*, Δ*sps*, Δ*ggpS.KS*, and Δ*ggpS*), and *Ava*II (wild-type, Δ*sps*Δ*ggpS.KS*, and Δ*sps*Δ*ggpS*). The DNA fragments were separated by electrophoresis on a 1% (wt/vol) agarose gel and blotted onto Hybond™-N membrane (GE Healthcare, United States). Probes covering the 5′ flanking region of the *ggpS* or 3′ flanking region of the *sps* genes were amplified by PCR (using primers indicated in Additional file 1: **Supplementary Table S4**), and labeled using the DIG DNA labelling kit (Roche Diagnostics GmbH, Germany), according to the manufacturer's instructions. Hybridization was performed overnight at 65°C, and digoxigenin-labelled probes were detected by chemiluminescence using CPD-star (Roche) in a Chemi Doc™ XRS+ Imager (Bio-Rad, United States).

Introduction of the Glycine Betaine Synthetic Device Into *Synechocystis*

The pSEVA351 plasmid containing the synthetic device $P_{trc.x.lacO}$::Ahbet (**Table 1**; sequence provided in **Supplementary Datasheet S2**) was introduced into *Synechocystis* by electroporation following the protocol described previously (Ferreira et al., 2018). The presence of the synthetic device was confirmed in *Synechocystis* transformants by PCR using specific primers (Additional file 1: **Supplementary Table S4**), as described by Ferreira et al. (2018).

Growth Experiments

Pre-cultures of *Synechocystis* wild-type and mutants were inoculated in BG11 medium (supplemented with 10 μg/ml Cm, when appropriate) and grown in an orbital shaker (150 rpm), at 30°C under a 12 h light (25 μE/m^2/s)/12 h dark regimen. The cultures were grown to an $OD_{730} \approx 2$ and, subsequently, diluted in fresh BG11 medium without antibiotic to a final $OD_{730} \approx 0.5$. Fifty milliliters of the dilution were transferred to 100 ml Erlenmeyer flasks without NaCl or containing 3, 5, or 7% (wt/vol) NaCl (510, 860, and 1,200 mM NaCl, respectively), previously sterilized. These cultures were maintained in the same conditions as the pre-cultures and growth was monitored for at least 16 days, by measuring the optical density at 730 nm (OD_{730}) and determining the chlorophyll *a* (chl *a*) content as described by Meeks and Castenholz (1971). All the growth experiments included, at least, three biological replicates with technical duplicates.

Total Carbohydrate Content, Released and Capsular Polysaccharides Measurements

Total carbohydrate content and RPS were determined as previously described (Mota et al., 2013). Briefly, 10 ml of culture samples were dialyzed (12–14 kDa molecular weight cutoff; CelluSepT4, Orange Scientific) against at least 10 volumes of distilled water, 3 or 5% (wt/vol) NaCl solutions (identical to the growth medium), for at least 24 h. One milliliter of the collected sample was used to spectrophotometrically quantify the total carbohydrate content by the phenol-sulfuric acid method (Dubois et al., 1956), whereas 5 ml of the dialyzed sample was centrifuged at 3,857 *g* for 10 min at RT, and the cell-free supernatant was used to determine the RPS. For CPS quantification, the procedure was performed as described previously (Pereira et al., 2019). Five milliliters of

dialyzed cultures were centrifuged at 3,857 *g* for 10 min at RT, the cell pellet was resuspended in water and boiled for 15 min. After centrifugation as described previously, the cell-free supernatant was used for CPS measurement by the phenol-sulfuric acid method (Dubois et al., 1956). Total carbohydrate content, RPS and CPS were normalized by chl *a* content. All experiments included, at least, three biological replicates with technical triplicates.

Glycogen Extraction and Quantification

Glycogen extraction was performed as described previously (Ernst et al., 1984). Ten milliliters of cell culture were collected 1 h after the transition between the dark and the light phase. Samples were centrifuged, and the cell pellets suspended in 100 µL of distilled water and 400 µL of 30% (wt/vol) KOH was added. The mixture was incubated at 100°C for 90 min and then quickly cooled on ice. Six hundred µL of ice-cold absolute ethanol were added, and the mixture was incubated on ice for 2 h. The mixture was centrifuged for 5 min at maximum speed and 4°C. The supernatant was discarded, and the isolated glycogen was washed three times with 500 µL of ice-cold absolute ethanol and dried at 60°C. Glycogen quantification was performed by the phenol-sulfuric acid method (Dubois et al., 1956), and normalized by chl *a* content. Experiments included, at least, three biological replicates with technical triplicates.

Optical Microscopy

Cultures of *Synechocystis* wild-type (WT) and the Δ*sps* mutant were grown in BG11 or BG11 supplemented with 5% (wt/vol) NaCl as stated above (initial $OD_{730} \approx 0.5$). Four days after inoculation, cells were stained with 0.5% (wt/vol) of Alcian Blue (in 3% (vol/vol) acetic acid) in 1:1 (culture:dye) ratio. This mixture was added to 10 µL of 1% (wt/vol) low-melting point agarose beds (dissolved in BG11 medium) and covered with a coverslip. The preparations were observed using the light microscope Olympus DP25 Camera software Cell B.

Transcription Analysis by RT-qPCR

After extraction (for details see above), RNA concentration and purity (the ratios A_{260}/A_{280} and A_{260}/A_{230}) were measured using a NanoDrop ND-1000 spectrophotometer (NanoDrop Technologies, Inc., United States). The quality and integrity of the RNA samples was also inspected in 1% (wt/vol) agarose gel performed by standard protocols using TAE buffer. The absence of genomic DNA contamination was checked by PCR, in reaction mixtures containing 0.5 U of GoTaq® G2 Flexi DNA Polymerase, 1x Green GoTaq Flexi buffer, 200 µM of each dNTP, 1.5 mM $MgCl_2$, 0.25 µM of each rnpB primer (Additional file 1: **Supplementary Table S4**), and 200 ng of total RNA. The PCR profile was: 5 min at 95°C followed by 25 cycles of 20 s at 95°C, 20 s at 56°C and 20 s at 72°C, and a final extension at 72°C for 5 min. The PCR reactions were run on 1% (wt/vol) agarose gel as described above. For cDNA synthesis, 1 µg of total RNA was transcribed with the iScript™ Reverse Transcription Supermix for RT-qPCR (Bio-Rad) in a final volume of 20 µL, following the manufacturer's instructions. A control PCR was performed using 1 µL of cDNA as a template, the BD16S primers (Additional file 1: **Supplementary Table S4**), and the same reaction conditions and PCR program described above. Five-fold standard dilutions of the cDNAs were made (1/5, 1/25, 1/125, and 1/625) and stored at −20°C. RT-qPCRs were performed on Hard-Shell 384-Well PCR Plates (thin wall, skirted, clear/white) covered with Microseal® B adhesive seal (Bio-Rad). The reactions (10 µL) were manually assembled and contained 0.125 µM of each primer (Additional file 1: **Supplementary Table S4**), 5 µL of iTaq™ Universal SYBR® Green Supermix (Bio-Rad) and 1 µL of template cDNA (dilution 1/5). The PCR protocol used was: 3 min at 95°C followed by 45 cycles of 30 s at 95°C, 30 s at 56°C, and 30 s at 72°C. In the end, a melting curve analysis of the amplicons (10 s cycles between 55 and 95°C with a 0.5°C increment per cycle) was conducted. Standard dilutions of the cDNA were used to check the relative efficiency and quality of primers, and negative controls (no template cDNA) included (for more details on RT-qPCR parameters see Additional file 1: **Supplementary Table S5**). RT-qPCRs were performed with three biological replicates and technical triplicates of each cDNA sample in the CFX384 Touch™ Real-Time PCR Detection System (Bio-Rad). The data obtained were analyzed using the Bio-Rad CFX Maestro™ 1.1 software, implementing an efficiency-corrected delta Cq method (ΔCq). This method was used since the target genes *gsmt*, *dmt*, and *metX* were validated as reference genes using the reference gene selection tool available in the Maestro™ software. For this reason, the relative expression of the targets is represented instead of the usual relative normalized expression. Statistical analysis was performed using a one-way ANOVA using the same software, and tests were considered significant if $p < 0.05$. The amplicon sizes were checked by agarose gel electrophoresis, and the DNA sequence was confirmed by Sanger sequencing. These experiments were compliant with the MIQE guidelines (Bustin et al., 2009), to promote the effort for experimental consistency and transparency, and to increase the reliability and integrity of the results obtained.

Compatible Solutes Quantification

Cultures of *Synechocystis* wild-type (WT), the Δ*sps*, Δ*ggpS*, and Δ*sps*Δ*ggpS* mutants and the strains harboring the GB device (WT, Δ*ggpS*, and Δ*sps*Δ*ggpS* backgrounds) were grown in BG11 or BG11 supplemented with 3% or 5% (wt/vol) NaCl, as described above, at an initial $OD_{730} \approx 0.5$. The quantification of the CS—sucrose, glutamate, glucosylglycerol, and glycine betaine—was performed using 500 ml culture (distributed in 50 ml cultures in 100 ml Erlenmeyer flasks). Four days after inoculation, cells were harvested by centrifugation at 4,470 *g* for 10 min at room temperature (RT). In the case of the strains harboring the GB device, the extracellular medium was stored at −80°C, for further lyophilization and CS extraction. Cells were washed using 100 ml of cold distilled water, 3 or 5% (wt/vol) NaCl solutions (identical to the growth medium). Centrifugation was repeated and the cell pellets were resuspended in 50 ml of

the respective solutions. From this suspension, a 0.5 ml aliquot was centrifuged and stored at −20°C to be used later for protein quantification. The remaining cell suspension was centrifuged at 4°C and the cell pellet was stored at −20°C. Ethanol-chloroform extraction of the CS was performed as described in Ferreira et al. (2018) with adaptations. Briefly, cell pellets or lyophilized extracellular medium were suspended in 25 ml of 80% (vol/vol) ethanol and subsequently transferred to a 100 ml round flask containing a magnetic stir bar. The flask was connected to a coil condenser (circulating cold water) and heated at 100°C with stirring, for 10 min. The suspension was transferred to a 50 ml tube and centrifuged at 4,000 *g* for 10 min at RT. The supernatant was stored and the pellet resuspended in 20 ml of 80% (vol/vol) ethanol for a new extraction process. The remainder protocol was performed as described in Santos et al. (2006). Detection, identification and quantification of CS was performed by proton NMR. To that effect, freeze-dried extracts were dissolved in 1 ml of D_2O and a known amount of sodium formate was added to serve as an internal concentration standard. Spectra were acquired at 25°C on a Bruker Avance III 800 spectrometer (Bruker, Rheinstetten, Germany) working at a proton operating frequency of 800.33 MHz, equipped with a 5 mm, three channel, inverse detection cryoprobe TCI-z H&F/C/N with pulse-field gradients. A 3 s soft pulse was applied before the excitation pulse, to pre-saturate the water signal. Spectra were acquired under fully relaxed conditions (flip angle 60°; repetition delay of 60 s) so that the area of the NMR signals was proportional to the amount of the different protons in the sample. Integration of the signals was performed using the tools available in the TopSpin software (Bruker, Rheinstetten, Germany) version 3.6.2. The concentration of CS was expressed as μmol per mg of protein. Protein extracts were obtained by sonication as described by Pinto et al. (2015), and protein quantification was performed using the Bio-Rad Protein Assay. For cell dry weight (DW) determinations, 40 ml of culture at $OD_{730} \approx 1.0$ (or equivalent) was centrifuged at 3,857 *g* for 10 min at RT. Then, the cell pellet was dried at 60°C for 48 h. Experiments included, at least, three biological replicates.

In silico Analysis of CS Production

The genome-scale metabolic model of *Synechocystis*—*i*Syn811 (Montagud et al., 2011) –, was updated to include all the information required for the simulations. The manual curation process started with the addition of the final reaction in the synthesis of sucrose ("spp: H_2O+ sucrose 6-phosphate → phosphate + sucrose"), and also the metabolic precursors and the three reactions required for the synthesis of the heterologous CS, glycine betaine ("GSMT1: *S*-adenosyl-L-methionine + glycine ↔ *S*-adenosyl-L-homocysteine + sarcosine," "GSMT2: *S*-adenosyl-L-methionine + sarcosine ↔ *S*-adenosyl-L-homocysteine + *N*,*N*-dimethylglycine," and "DMT: *S*-adenosyl-L-methionine + *N*,*N*-dimethylglycine ↔ *S*-adenosyl-L-homocysteine + *N*,*N*,*N*-trimethylglycine"). In this process, the nomenclature was corrected and standardized (e.g., "glycerone" to "dihydroxy-acetone" or "GDP-mannose" to "GDP-D-mannose"), and the reversibility of some reactions changed (e.g., "sn-glycerol-3-phosphate → dihydroxy-acetone phosphate" to "sn-glycerol-3-phosphate ↔ dihydroxy-acetone phosphate"). Flux balance analysis (Orth et al., 2010) was performed to the *i*Syn811 genome-scale metabolic reconstruction of *Synechocystis* for the production assessment of four different CS: three heterologous (glycine betaine, ectoine, and mannosylglycerate), and three native (glucosylglycerol, glutamate and sucrose). The MATLAB software, COBRA Toolbox v3.0 (Heirendt et al., 2019) was used for quantitative prediction of cellular and multicellular biochemical networks with constraint-based modelling. Simulations were constrained to match an autotrophic specific growth rate of 0.09/h, which corresponds to a light input of 0.8 mE/gDW/h and to a net carbon flux of 3.4 mmol/gDW/h into the cell, with CO_2 as carbon source. The description of the *i*Syn811 model and further information on the simulation procedure are available in Montagud et al. (2010).

Statistical Analysis

The statistical analysis was performed by means of one- or two-way ANOVAs, using GraphPad Prism v6.01 (GraphPad Software Inc., United States).

RESULTS

Generation of *Synechocystis* Mutants Deficient in the Synthesis of Native Compatible Solutes

The sustainable production of heterologous compatible solutes using *Synechocystis* as a chassis was envisioned in this work. The starting step was the generation of mutants deficient in the production of one or both of the main native compatible solutes, sucrose, or glucosylglycerol (GG). For this purpose, the genes encoding the enzymes involved in the first step of sucrose or/and GG synthesis (*sps* and *ggpS*, respectively), were knockout by double homologous recombination generating the *Synechocystis* markerless mutants Δ*sps*, Δ*ggpS*, and Δ*sps*Δ*ggpS* (for details see *Materials*). The complete segregation of the mutants was confirmed by PCR and Southern blot (Additional file 1: **Supplementary Figures S1, S2**).

Effect of NaCl on the Growth of *Synechocystis* Wild-Type and the CS Deficient Mutants

The growth of the CS deficient mutants under different salinities was analyzed. *Synechocystis* WT and mutants Δ*sps*, Δ*ggpS*, and Δ*sps*Δ*ggpS* were grown in standard BG11 medium or in BG11 supplemented with 3, 5, and 7% (wt/vol) NaCl, corresponding to 510, 860, and 1,200 mM, respectively. The growth was monitored by measuring the OD_{730} and chlorophyll *a* (chl *a*) content (**Figure 1**). In the absence of NaCl, the three mutants exhibited growth similar to the WT

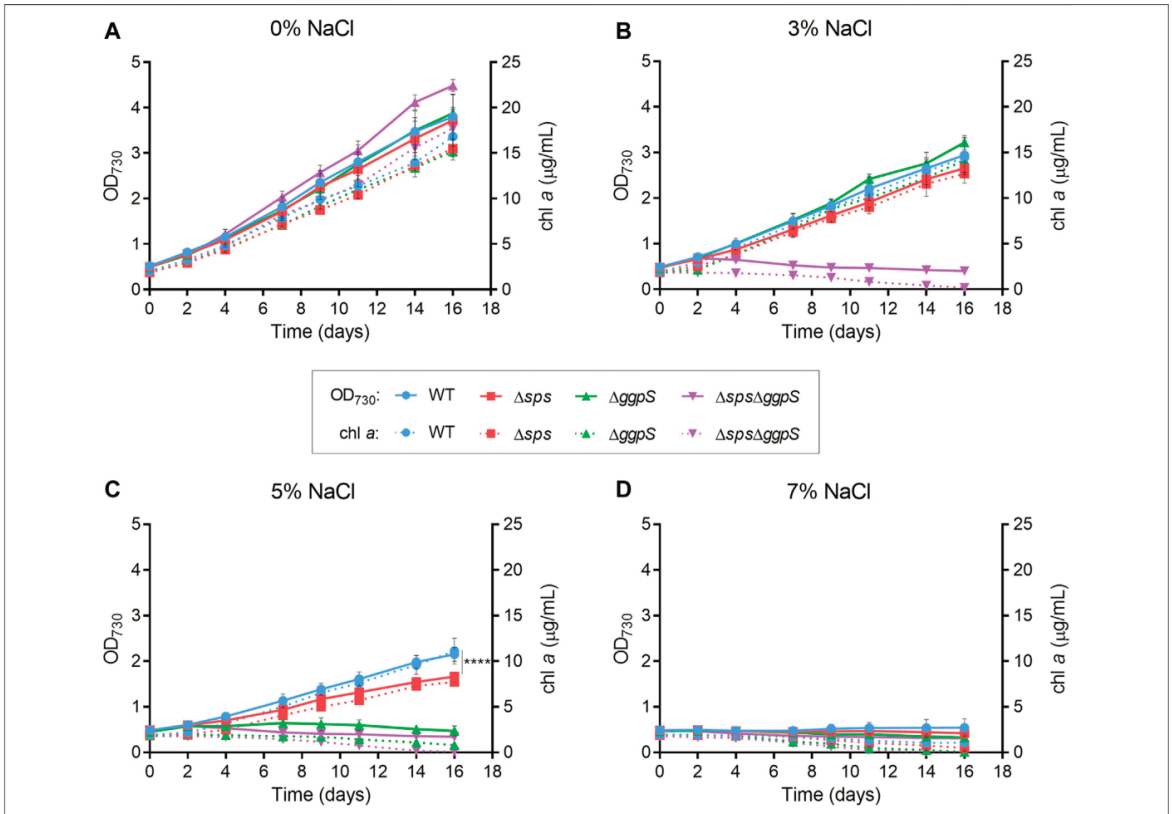

FIGURE 1 | Growth curves of *Synechocystis* wild-type (WT) and Δ*sps*, Δ*ggpS* and Δ*sps*Δ*ggpS* mutants in BG11 **(A)** or BG11 supplemented with 3% **(B)**, 5% **(C)** or 7% **(D)** (wt/vol) NaCl. Cultures were grown at 30°C with orbital shaking (150 rpm) under a 12 h light (25 µE/m^2/s)/12 h dark regimen. Growth was monitored by measuring optical density at 730 nm (OD_{730}), and chlorophyll *a* (chl *a*) (full and dotted lines, respectively). Error bars correspond to standard deviations from at least three biological replicates with technical duplicates. Statistical analysis was performed using a two-way ANOVA, and a significant difference in terms of OD_{730} is identified by **** ($p \leq 0.0001$).

(**Figure 1A**), indicating that the synthesis of sucrose and/or GG is nonessential under standard growth conditions. Nonetheless, challenging the cells with 3% NaCl had clear detrimental effects, with a ~23% growth decrease observed for the WT and CS single mutants Δ*sps* and Δ*ggpS* (**Figure 1B**; Additional file 1: **Supplementary Table S1**). The inactivation of both pathways in the Δ*sps*Δ*ggpS* mutant led to total growth arrest accompanied by a decline in chl *a* content (**Figure 1B**; purple lines and Additional file 1: **Supplementary Table S1**). A more pronounced impact was observed by increasing NaCl to 5%. The Δ*ggpS* could not grow in these conditions, while for the WT and Δ*sps*, a severe growth impairment (~49%) was observed (**Figure 1C**; Additional file 1: **Supplementary Table S1**). The growth of the latter two strains was similar up to day 7 however, after this period, the growth of Δ*sps* slowed down and by day 16 there was a significant difference ($p \leq 0.0001$) compared with the WT. The chl *a* content confirmed these observations (**Figure 1C**; red and blue lines). Further increase in the NaCl concentration to 7% (wt/vol) showed that none of the strains tested could withstand the stress imposed (**Figure 1D**; Additional file 1: **Supplementary Table S1**).

Quantification of CS in *Synechocystis* Wild-Type and the CS Deficient Mutants

The CS content was quantified in *Synechocystis* WT, Δ*sps*, Δ*ggpS*, and Δ*sps*Δ*ggpS* mutants grown in BG11 or BG11 supplemented with NaCl (**Figure 2**), under salinity conditions in which each strain could sustain growth (**Figure 1**). In the WT, CS accumulation increased significantly in a salinity-dependent manner and GG was accumulated in higher amounts followed by glutamate and sucrose (**Figure 2A**). As expected, the two main compatible solutes sucrose and GG could only be detected in the presence of NaCl. The amino acid glutamate was detected in all backgrounds and conditions, and increased more than 1.8-fold in the presence of salinity (significant difference $p \leq 0.01$ for WT in 0 and 5% NaCl). In the Δ*sps*, Δ*ggpS*, and Δ*sps*Δ*ggpS* mutants the absence of sucrose and/or GG production was confirmed

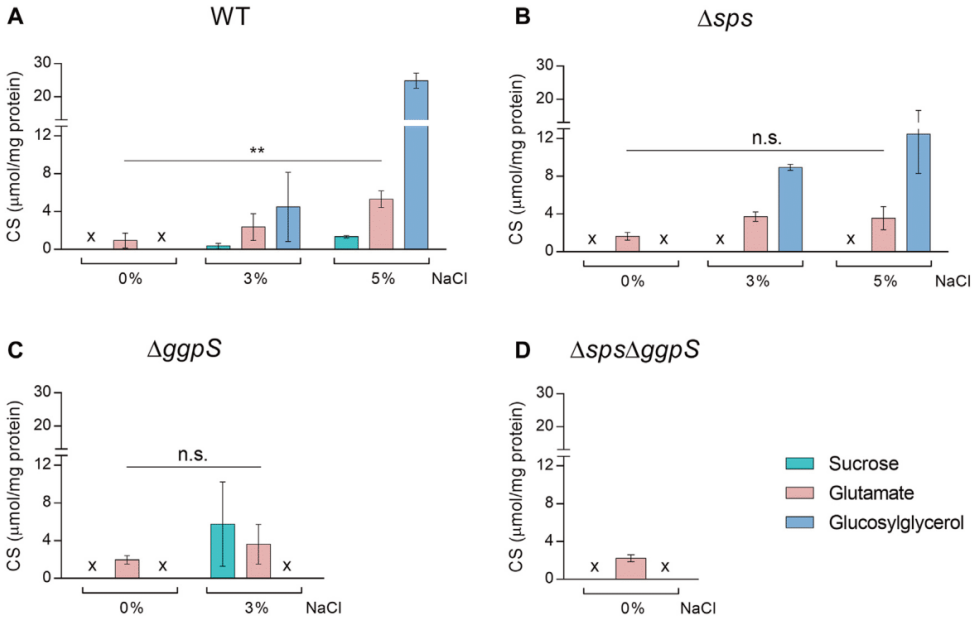

FIGURE 2 | Effect of NaCl on the synthesis of native compatible solutes sucrose, glutamate and glucosylglycerol by *Synechocystis* wild-type (WT) **(A)**, and the Δ*sps* **(B)**, Δ*ggpS* **(C),** and Δ*sps*Δ*ggpS* mutants **(D)**. Cultures were grown in BG11 or BG11 supplemented with 3% or 5% (wt/vol) NaCl, at 30°C with orbital shaking (150 rpm) under a 12 h light (25 µE/m^2/s)/12 h dark regimen, and cells were harvested 4 days after inoculation (initial OD_{730} ≈ 0.5). Compatible solutes were quantified by H-NMR and the results were normalized per mg of protein. x—not detected. Error bars correspond to standard deviations from at least three biological replicates. Statistical analysis was performed using two-way ANOVA. Statistically significant differences are identified: ** ($p \leq 0.01$) and n.s. (not significant).

(**Figures 2B–D**). For the Δ*sps*, a salinity-dependent accumulation of GG was also detected (**Figure 2B**), however, the GG concentration was 50% lower compared with the WT, under 5% NaCl. In contrast, the Δ*ggpS* mutant accumulated 17-fold more sucrose than the WT, under 3% NaCl (**Figure 2C**). All the proton NMR spectra are depicted in Additional file 1: **Supplementary Figure S3**.

Effect of NaCl on Total Carbohydrates, Glycogen, Capsular, and Released Polysaccharides

In addition to the CS pools, the total carbohydrate content was analyzed in *Synechocystis* WT and the CS deficient mutants (**Figure 3A**). Generally, the presence of salinity (3 or 5% NaCl) had no significant impact on the production of total carbohydrates, except for the Δ*sps* mutant that showed some fluctuation when exposed to different salinities (**Figure 3A**; $p \leq 0.05$). To further clarify the carbon distribution in response to salinity, the amount of glycogen as well as the production of extracellular polymeric substances, CPS and RPS, were also determined (**Figures 3B–D**). The presence of NaCl led to a significant decrease in the amount of glycogen in the WT, Δ*sps*, and Δ*ggpS*, with reductions of more than 56%, independent of the salinity concentration and the deletion of one of the CS pathways (**Figure 3B**). In terms of CPS, the opposite effect was observed with a 2.4-fold increase in CPS for the WT and the Δ*sps* at 5%, and a 2.1-fold increase for Δ*ggpS* at 3% NaCl, compared with 0% NaCl (**Figure 3C**). The amount of RPS produced by WT or Δ*ggpS* did not change significantly whereas for the Δ*sps* a 2.5-fold increase was registered under 5% NaCl (**Figure 3D**). Staining the WT and Δ*sps* cultures with Alcian Blue confirmed similar RPS production for the WT under 0 and 5% NaCl, while for the Δ*sps* the accumulation of RPS in 5% NaCl is evident, leading to the formation of cell aggregates (**Figure 3E**; black arrowhead).

In silico Prediction of Production Rates for Native and Heterologous CS Using *Synechocystis* Wild-Type

The genome-scale metabolic model of *Synechocystis*—*i*Syn811 (Montagud et al., 2011)—was updated to include all the information required for calculating CS production rates. The manual curation process started with the addition of the metabolic precursors and the reactions required for CS synthesis. The nomenclature was also corrected and standardized, and the reversibility of some reactions was changed (for more details see the *Materials* section). After the curation of the metabolic model was completed, the COBRA ("The COnstraint-Based Reconstruction and Analysis") Toolbox v3.0 (Heirendt et al., 2019), was used to simulate the compatible solute production rate as a function of *Synechocystis* wild-type growth under autotrophic conditions (**Figure 4**). The results show a linear tradeoff between the cell's

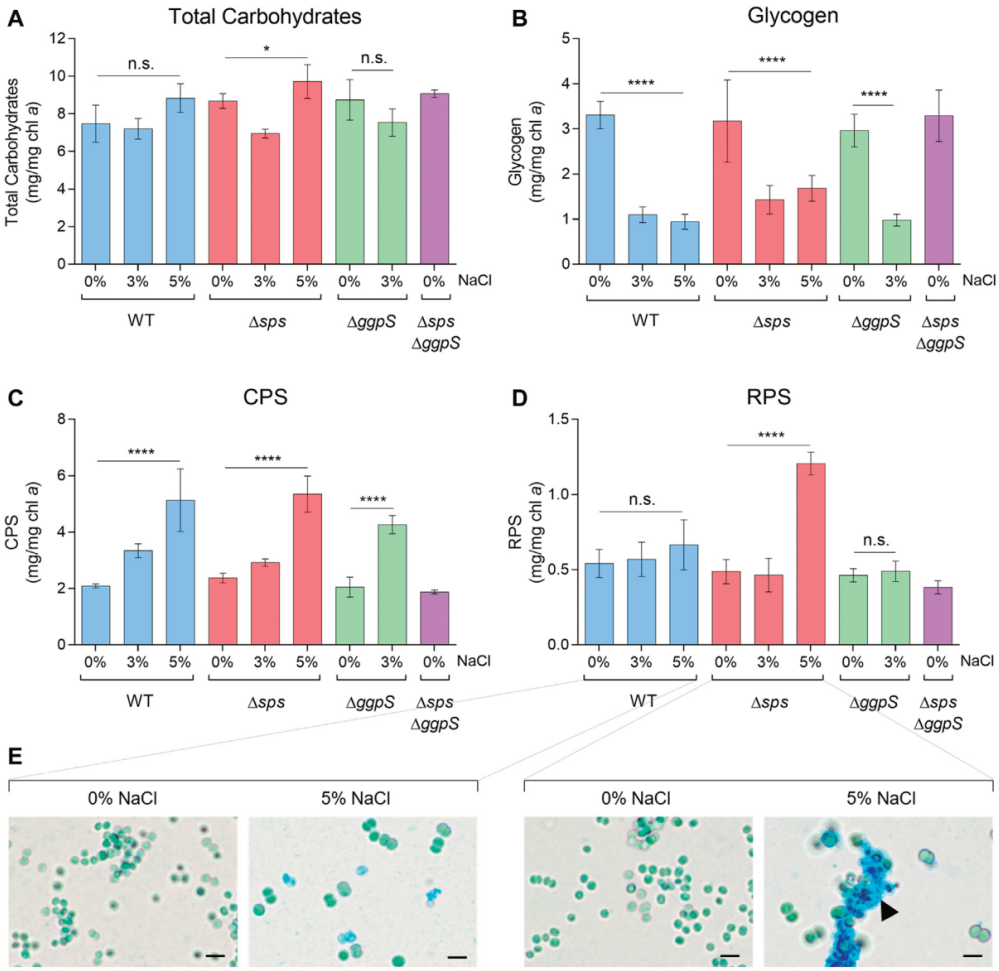

FIGURE 3 | Effect of NaCl on total carbohydrates **(A)**, glycogen **(B)**, CPS—capsular polysaccharides **(C)**, and RPS—released polysaccharides **(D)** produced by *Synechocystis* wild-type (WT) and the Δ*sps*, Δ*ggpS*, and Δ*sps*Δ*ggpS* mutants. Cells were grown in BG11 or BG11 supplemented with 3% or 5% (wt/vol) NaCl, at 30°C with orbital shaking (150 rpm) under a 12 h light (25 μE/m^2/s)/12 h dark regimen for 16 days. Results are expressed as milligrams per milligram of chlorophyll *a* (chl *a*). Error bars correspond to standard deviations from at least three biological replicates, with technical triplicates. Statistical analysis was performed using one-way ANOVA. Statistically significant differences are identified: **** ($p \leq 0.0001$), * ($p \leq 0.05$), and n.s. (not significant). Light micrographs **(E)** of *Synechocystis* WT and Δ*sps* cultures grown in BG11 or BG11 supplemented with 5% NaCl and stained with Alcian Blue; the black arrowhead highlights RPS production by the Δ*sps* mutant under 5% NaCl. Scale bars: 5 μm.

resources toward growth or the production of the different CS. Regarding the production of the native CS, GG, and sucrose impose a higher metabolic burden showing lower *in silico* production rates (0.378 and 0.283 mmol/gDW/h, respectively), compared with glutamate (0.567 mmol/gDW/h). The simulation of the production of heterologous CS glycine betaine (GB) showed the best compromise between growth and production compared with the three native CS, with the highest predicted maximum production rate of 0.680 mmol/gDW/h. In addition to GB, the production rates of other heterologous CS, such as ectoine and mannosylglycerate were also simulated, revealing that the maximum production rate predicted for these two solutes is lower than the obtained for GB (Additional file 1: **Supplementary Figure S4**). Hence, GB was chosen as the heterologous CS to be produced using the *Synechocystis* chassis developed (CS-deficient mutants).

Design and Assembly of the Synthetic Device for the Production of Glycine Betaine

Envisaging the heterologous production of GB, a synthetic device was designed based on the metabolic pathway described for the

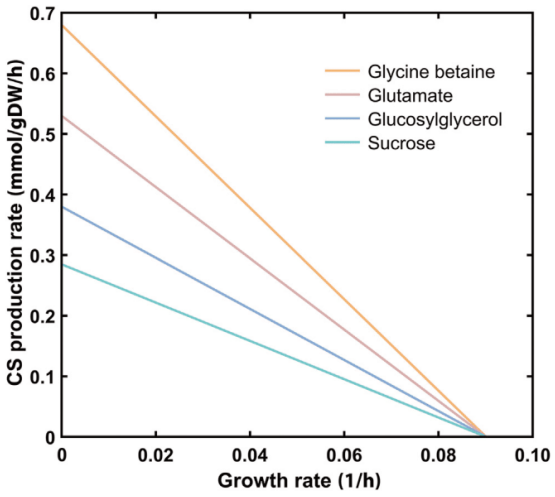

FIGURE 4 | Theoretical productivity of the heterologous compatible solute glycine betaine and the native ones (glutamate, glucosylglycerol, and sucrose), as predicted by the updated version of the genome-scale metabolic model iSyn811. The lines represent the compatible solute production rate as a function of *Synechocystis* wild-type growth under autotrophic conditions.

halophilic cyanobacterium *Aphanothece halophytica* (**Figure 5A**) (Nyyssola et al., 2000; Waditee et al., 2003). This device comprises two Open Reading Frames (ORFs) encoding the enzymes involved in the three-step methylation of glycine to glycine betaine: glycine-sarcosine-*N*-methyltransferase (*gsmt*), and the dimethylglycine-*N*-methyltransferase (*dmt*). In these reactions, *S*-adenosylmethionine (SAM) is the source of methyl groups for the synthesis of GB, and it can be synthesized from L-methionine by the *S*-adenosyl-methionine synthase (MetX) (**Figure 5A**). To prevent the shortage of the SAM precursor, the ORF encoding *Synechocystis'* native MetX (*metX*, *sll0927*) was also included in the device. The sequences of the three ORFs (*gsmt*, *dmt*, and *metX*) were codon-optimized and restriction sites incompatible with the BioBrick standard RFC [10] were eliminated. Subsequently, the ribosome binding site (RBS) BBa_B0030 and double stop codons (TAATAA) were included before and after each ORF, respectively. A double terminator (BBa_B0015) was also included at the end of the synthetic construction (Ahbet). Additionally, the designed DNA sequence was flanked by the prefix and suffix of the BioBrick RFC [10] standard (Canton et al., 2008), enabling the use of the standard assembly method to include the regulatory element (promoter). After DNA synthesis, the Ahbet construction was cloned downstream of the promoter $P_{trc.x.lacO}$, originating the $P_{trc.x.lacO}$::Ahbet synthetic device (hereafter GB device) (**Figure 5B**). The $P_{trc.x.lacO}$ is a constitutive promoter in *Synechocystis*, previously characterized by our group and is 41-fold stronger than the reference cyanobacterial promoter P_{rnpB} (Ferreira et al., 2018).

Effect of the Implementation of the GB Device Into the *Synechocystis* Chassis

The GB synthetic device was implemented into the *Synechocystis* WT and the CS deficient Δ*ggpS* and Δ*sps*Δ*ggpS* chassis described above, using the replicative plasmid pSEVA351. The device was not introduced into

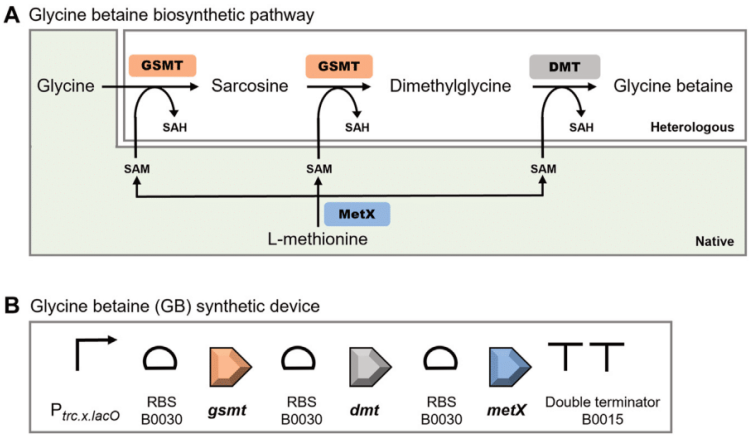

FIGURE 5 | Glycine betaine biosynthetic pathway **(A)** and schematic representation of the glycine betaine (GB) synthetic device for the production of this heterologous compatible solute in *Synechocystis* **(B)**. The glycine betaine biosynthetic pathway comprises the GSMT (glycine-sarcosine-*N*-methyltransferase) and DMT (dimethylglycine-*N*-methyltransferase) from *Aphanothece halophytica* (heterologous), and MetX (*S*-adenosyl-methionine synthase) from *Synechocystis* (native). SAM—*S*-adenosyl-methionine; SAH—*S*-adenosyl-homocysteine. The GB device includes the promoter $P_{trc.x.lacO}$, the ribosomal binding site (RBS) B0030, the open reading frames *gsmt*, *dmt*, and *metX* codon optimized for *Synechocystis*, and the double terminator B0015.

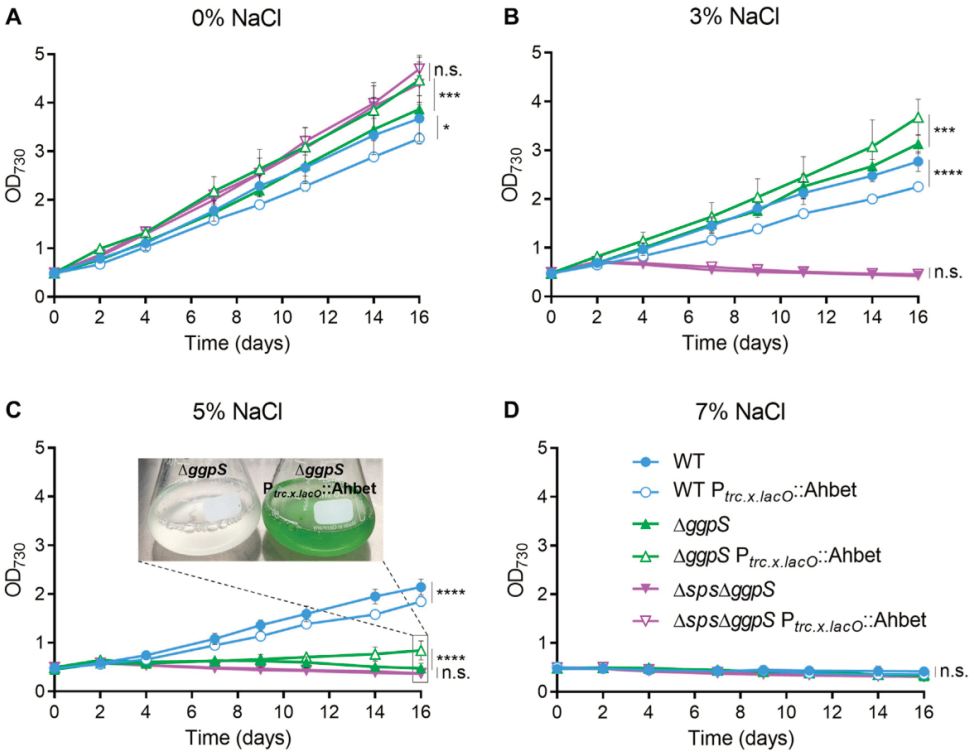

FIGURE 6 | Growth of *Synechocystis* wild-type (WT), Δ*ggpS*, and Δ*sps*Δ*ggpS* without or with the GB device ($P_{trc.x.lacO}$::Ahbet). Cultures were grown in BG11 **(A)** or BG11 supplemented with 3% **(B)**, 5% **(C)**, or 7% **(D)** (wt/vol) NaCl, at 30°C with orbital shaking (150 rpm) under a 12 h light (25 μE/m^2/s)/12 h dark regimen. Growth was monitored by measuring the optical density at 730 nm (OD_{730}). Error bars correspond to standard deviations from at least three biological replicates with technical duplicates. Statistical analysis was performed using two-way ANOVA. Statistically significant differences are identified: **** ($p \leq 0.0001$), *** ($p \leq 0.001$), * ($p \leq 0.05$), and n.s. (not significant). In **Figure 6C**, the liquid cultures of *Synechocystis* Δ*ggpS* **(left)** and Δ*ggpS* $P_{trc.x.lacO}$::Ahbet **(right)**, in BG11 supplemented with 5% NaCl after 16 days of cultivation, are shown.

Δ*sps* since the characterization showed that this mutant is similar to the WT in terms of growth, total carbohydrates, glycogen content and CPS (**Figure 1**, **Figures 3A–C**, respectively). The presence of the GB device in the cells was confirmed by PCR (Additional file 1: **Supplementary Figure S5**), and the growth and chl *a* content of the transformants were monitored in absence/presence of salinity and compared with the respective backgrounds (**Figure 6**; Additional file 1: **Supplementary Figure S6**). As shown in **Figure 6**, the introduction of the synthetic device had distinct effects depending on the genetic background. The implementation of GB device into Δ*ggpS* led to a significant improvement of growth (16%) in BG11 and BG11 supplemented with 3% NaCl (**Figures 6A,B**; green lines), and supported its survival under 5% NaCl (**Figure 6C**; green lines). After 16 days of cultivation under 5% NaCl, the batch culture of Δ*ggpS* showed clear signs of chlorosis/necrosis while the culture of the Δ*ggpS* mutant harboring the GB device remained green (**Figure 6C**; insert). In agreement, the chl *a* content was 0.8 μg/ml and 1.8 μg/ml, respectively (Additional file 1: **Supplementary Figure S6**; green lines). Notably, this survival phenotype was observed for at least 25 days (data not shown). In the WT background the presence of the device had a detrimental effect on growth (~15% decrease) in all conditions tested (**Figure 6**; blue lines). The growth of the double mutant Δ*sps*Δ*ggpS* in the absence of NaCl was not affected by the introduction of the synthetic device (**Figure 6A**; purple lines). Moreover, the mutant harboring the GB device was unable to survive under saline conditions, similarly to what happened to Δ*sps*Δ*ggpS* background (**Figures 6B–D**; purple lines).

Analysis of Transcript Levels in *Synechocystis* Strains Harboring the GB Device

The next step in the characterization of the different *Synechocystis* strains harboring the GB device was the

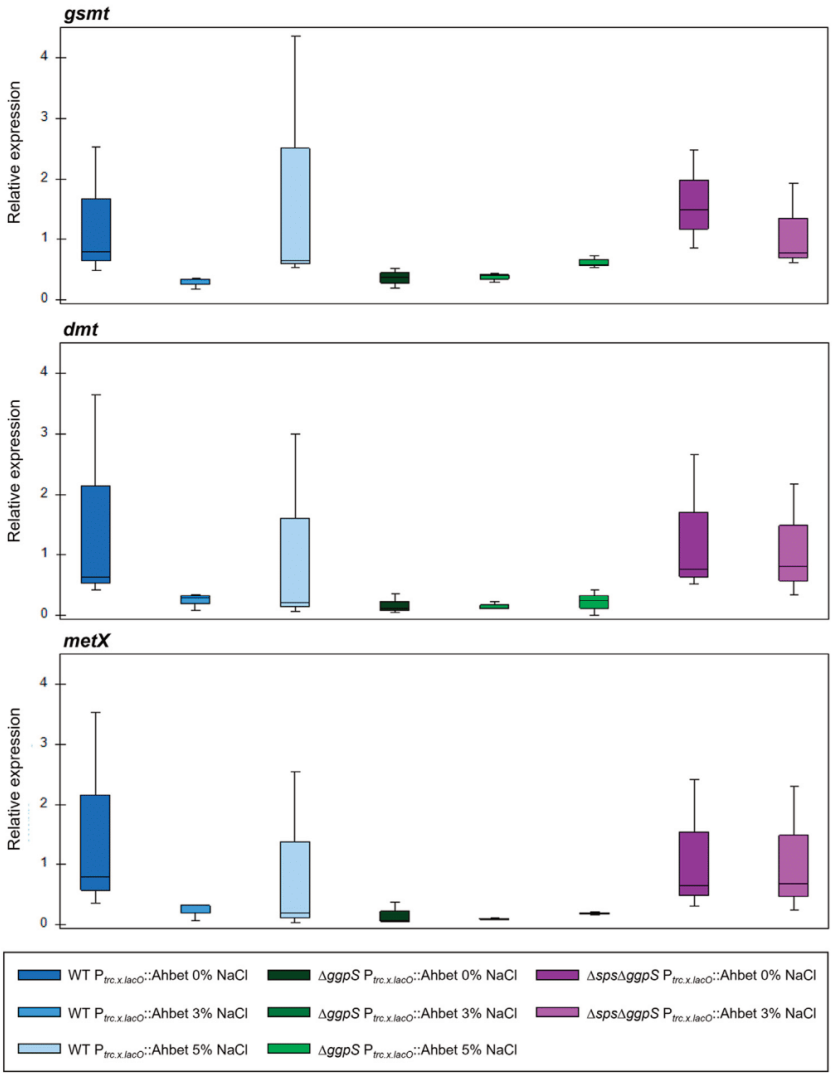

FIGURE 7 | RT-qPCR analysis of *gsmt*, *dmt*, and *metX* relative expression in *Synechocystis* strains (WT, Δ*ggpS*, and Δ*sps*Δ*ggpS*) harboring the GB device. RNA was extracted from cells grown in BG11 or BG11 supplemented with 3 and 5% (wt/vol) NaCl, at 30°C with orbital shaking (150 rpm) under a 12 h light (25 μE/m^2/s)/12 h dark regimen. The box-whisker plots represent the expression of the target genes relative to WT $P_{trc.x.LacO}$::Ahbet in absence of salt (0% NaCl). Data were obtained from three biological replicates and three technical replicates, and the whiskers represent the minimum and maximum non-outlier values in the dataset. One-way ANOVA was performed no significant differences could be detected.

evaluation of the transcript levels of the three ORFs comprised in the device (*gsmt*, *dmt*, and *metX*) by RT-qPCR (for more details see the *Materials* section). As shown in **Figure 7**, the transcripts of the three genes (*gsmt*, *dmt*, and *metX*) were detected in all samples and the relative expression was reasonably stable independently of the background strain. Additionally, the relative expression remained similar under salinity conditions and, even though some variation could be detected, it was not statistically significant (Additional file 1: **Supplementary Table S2**).

Quantification of Native and Heterologous CS in *Synechocystis* Chassis Harboring the GB Device

The CS pool of the different *Synechocystis* strains (WT, Δ*ggpS*, and Δ*sps*Δ*ggpS*) harboring the GB device was analyzed in

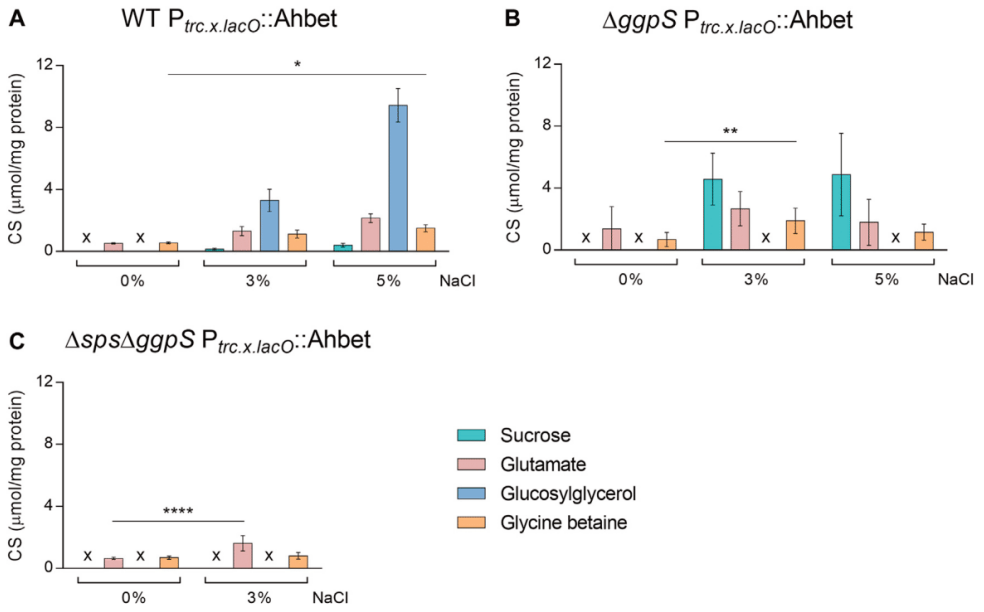

FIGURE 8 | Production of glycine betaine (GB) and native compatible solutes in different *Synechocystis* strains harboring the GB device: WT (wild-type) $P_{trc.x.lacO}$::Ahbet **(A)**, Δ*ggpS* $P_{trc.x.lacO}$::Ahbet **(B)**, and Δ*sps*Δ*ggpS* $P_{trc.x.lacO}$::Ahbet **(C)**. Cultures were grown in BG11 or BG11 supplemented with 3% or 5% (wt/vol) NaCl, at 30°C with orbital shaking (150 rpm) under a 12 h light (25 µE/m^2/s)/12 h dark regimen; and cells were harvested 4 days after inoculation (initial OD_{730} ≈ 0.5). Compatible solutes were quantified by H-NMR and the results were normalized per mg of protein. x—not detected. Error bars correspond to standard deviations from three biological replicates. Statistical analysis was performed using two-way ANOVA. Statistically significant differences are identified: **** ($p \leq 0.0001$), ** ($p \leq 0.01$), and * ($p \leq 0.05$).

absence/presence of NaCl after 4 days of cultivation (**Figure 8**). The results obtained confirmed that the implementation of the pathway for the synthesis of heterologous CS was successful, since glycine betaine could be detected in all strains and conditions analyzed. Under 0 and 3% NaCl, the presence of the GB device in the WT background did not significantly influence the synthesis of native CS and heterologous production of GB is not significantly influenced by salinity. However, under 5% NaCl, there was an impact on the synthesis of glutamate and GG that decreased by 59 and 62%, respectively, and the synthesis of GB increased 2.7-fold compared with 0% NaCl (**Figures 2A**, **8A**). Similarly, the implementation of the device in the Δ*ggpS* did not affect the production of the native CS under 0 and 3% NaCl compared with Δ*ggpS* chassis (**Figures 2C**, **8B**). However, the introduction of the device into the Δ*ggpS* background allowed this strain to survive under 5% NaCl and, therefore the quantification of CS was also performed. The results obtained showed that in Δ*ggpS* $P_{trc.x.lacO}$::Ahbet, besides glycine betaine production, the levels of sucrose and glutamate were similar to the ones observed for 3% NaCl (**Figure 8B**). An analysis of the Δ*ggpS* harboring the GB device after 16 days of cultivation suggested that the production of all CS is maintained for at least 2 weeks of cultivation (Additional file 1: **Supplementary Figure S7**). For the double mutant, the presence of the device led to a significant decrease (71%) of glutamate in the absence of salinity (**Figures 2D**, **8C**). In contrast, under 3% NaCl, there was a 2.5-fold increase in glutamate ($p \leq 0.0001$) compared with 0% NaCl, while the glycine betaine content remained similar (**Figure 8C**). All the proton NMR spectra are depicted in Additional file 1: **Supplementary Figure S8**. Furthermore, the CS quantification was also performed for the extracellular medium, and the results showed that none of the native CS could be detected, while GB was detected in negligible amounts in all strains harboring the device and conditions tested (Additional file 1: **Supplementary Table S3**).

DISCUSSION

The sustainable production of compatible solutes (CS) is essential for pharmaceutical and cosmetic industries. The current microbiological processes have a significant negative impact on the environment, which could be mitigated by the use of photoautotrophic chassis such as cyanobacteria. For the synthesis of heterologous CS in *Synechocystis*, the construction of customized chassis is required and our strategy was to eliminate competing or redundant pathways. Therefore, in this work we have generated three *Synechocystis* mutants deficient in the production of native compatible solutes (namely, sucrose, or/and glucosylglycerol). These strains—Δ*sps*, Δ*ggpS*, and Δ*sps*Δ*ggpS*—were characterized under different salinity concentrations, expanding the knowledge that will allow

further optimization of the chassis for the increased production of heterologous CS, such as glycine betaine (GB). In this context, an updated version of the genome-scale metabolic model of *Synechocystis*—*i*Syn811 (Montagud et al., 2011)—was used to predict the production rates for native and heterologous CS using *Synechocystis* wild-type. The simulations show a linear tradeoff between deviating resources toward cellular growth or toward the production of the solutes. Since energy and carbon uptake are limited, any extra need of ATP or carbon molecules for compatible solute synthesis will impair cell growth. Whether carbon or light uptake is limiting the synthesis of each CS is difficult to predict, since alternative routes with different energetic efficiencies can be simultaneously active under different growth conditions. From the CS evaluated, the predictions indicate that the synthesis of native sucrose, and glucosylglycerol (GG) has a higher impact on cell growth than glutamate or the heterologous solute glycine betaine (GB) (**Figure 4**). The production of sucrose and GG require glucose that drains more cell resources than the reported for the synthesis of an amino acid (Kaleta et al., 2013), such as glutamate or glycine (the latter required for GB production). The results also suggest that the production of GB has a smaller restraining effect on growth than glutamate or other heterologous CS, like ectoine and mannosylglycerate (Additional file 1: **Supplementary Figure S4**).

In parallel, the evaluation of the CS levels of the wild-type and the mutants (Δ*sps*, Δ*ggpS*, and Δ*sps*Δ*ggpS*) confirmed the salt-induced accumulation of sucrose and GG, which is well documented in the literature [for reviews see e.g., Klähn and Hagemann (2011); Hagemann (2013); Kirsch et al. (2019)]. In contrast, glutamate could be detected in the absence and presence of NaCl (**Figure 2**). These results are in agreement with the reported accumulation of this amino acid in *Synechocystis* grown in artificial seawater medium (ASW; 340 mM NaCl), and in BG11 supplemented with 12 mM KCl (Iijima et al., 2015; Iijima et al., 2020).

Previous works have also reported a tradeoff between the pools of different compatible solutes and other carbon sinks, such as glycogen or extracellular polymeric substances (EPS) in cyanobacteria (Du et al., 2013; Baran et al., 2017; Kirsch et al., 2017). In our work, the total carbohydrate content of *Synechocystis* WT and CS-deficient mutants remained unchanged when cells were exposed to NaCl, whereas a significant decrease in glycogen was observed (**Figure 3**). Concomitantly, the accumulation of capsular polysaccharides (CPS) was observed in a salinity-dependent manner and for the strains tested. In line with these observations is the increase in the levels of proteins involved in glycogen degradation, reported when *Synechocystis* cells were grown in ASW medium (Iijima et al., 2015). The protective role of EPS against salt stress was also demonstrated in a *Synechocystis* Δ*sll1581*Δ*slr1875* double mutant, showing that a decrease in CPS content increases NaCl sensitivity (Jittawuttipoka et al., 2013). Altogether, these results strongly suggest that under saline conditions, *Synechocystis* breaks down glycogen and redirects carbon fluxes toward the production of CS and extracellular polysaccharides, promoting cell homeostasis and contributing to cell protection.

From the three *Synechocystis* CS-deficient mutants generated in this work, the Δ*sps* was the only one able to grow in 5% NaCl. We also observed that this mutant's growth gets impaired over time, suggesting that the presence of sucrose is of additional importance for long-term cultivation. Accordingly, a previous work showed that Δ*sps* cells in stationary phase were unable to survive a salt shock, which was not observed for cells in exponential phase; this effect could be prevented by sucrose supplementation (Desplats et al., 2005). Moreover, we show that the absence of sucrose leads to a severe reduction in the accumulation of GG whereas the released polysaccharides (RPS) increase significantly (1.8-fold), implying that extracellular polysaccharides production is crucial for the survival of the Δ*sps* mutant under 5% NaCl. These results also suggest that sucrose role might go beyond osmoprotection, being involved in the regulation of metabolic pathways, e.g., triggering signaling cascades, as it was previously hypothesized by Desplats et al. (2005). For the Δ*ggpS* mutant an increased sucrose level was detected under 3% NaCl, showing that this sugar can sustain *Synechocystis'* survival under sea salt conditions for at least 16 days. Previously (Miao et al., 2003), generated a *Synechocystis* Δ*agp* mutant unable to synthesize ADP-glucose (a precursor required for GG synthesis) that was also shown to accumulate high levels of sucrose and could survive upon a salt shock of 900 mM (5.2% NaCl). Notably, in the latter work and here, the mutant's sucrose levels were similar to GG accumulated in the WT cultivated under the same conditions. Taken together, these studies imply that GG and sucrose can have comparable osmoprotectant capacity when accumulated in similar levels. Additionally, the Δ*sps*Δ*ggpS* mutant was unable to survive in any salt concentration tested and glutamate was the only CS that could be detected. Thus, this amino acid seems to have a minor contribution to the salt acclimation process in *Synechocystis*, similar to what was reported for the halophilic bacterium *Salinibacter ruber* (Oren et al., 2002).

Considering the metabolic model simulation, a synthetic device for the production of glycine betaine (GB) was designed and implemented into the *Synechocystis* wild-type and our customized chassis (CS-deficient mutants). Besides the ORFs required for GB production (*gsmt* and *dmt*) and *metX* (to prevent SAM shortage), this device comprises well-characterized regulatory elements: the synthetic promoter $P_{trc.x.lacO}$ (Ferreira et al., 2018), the RBS BBa_B0030, and the double terminator BBa_B0015. This design ensured the stable constitutive transcription observed for the GB device ORFs, regardless of the chassis or salinity conditions (**Figure 7**), reinforcing that the use of orthogonal regulatory components is crucial to ensure the proper insulation of synthetic devices from the regulatory network of the chassis (Costello and Badran, 2021). Unlike transcription, the synthesis of the solute was not independent of cultivation conditions, and GB levels increased with salinity. In agreement, higher levels of glycine have been reported for *Synechocystis* cells grown in ASW medium compared with those grown in BG11 (Iijima et al., 2015). Since this amino acid is a precursor of GB, the high levels of glycine under salinity conditions most probably favor the synthesis of GB. In addition, glycogen degradation and carbon fluxes redirection

TABLE 2 | Native and heterologous production of glycine betaine *via* the three-step glycine methylation pathway.

Native production

Strain	Salinity (mM)	Production capacity	Cultivation time	Reference
Aphanothece halophytica	2,000	0.06 μmol/mg protein	1 h	Ishitani et al. (1993)
Aphanothece halophytica	2,000	~0.4 μmol/10^7 cells	7 days	Incharoensakdi and Waditee (2000)
Aphanothece halophytica	1,500	~40,000 μmol/gFW	10 days	Waditee et al. (2007)
Aphanothece halophytica	2,000	20.1 μmol/gFW	15 days	Waditee-Sirisattha et al. (2015)

Heterologous production

Production strain	Native strain	Salinity (mM)	Production capacity	Cultivation time	Reference
Arabidopsis thaliana	*Aphanothece halophytica*	100	~2 μmol/gFW	15 days	Waditee et al. (2005)
Nicotiana tabacum	*Aphanothece halophytica*	0	0.4 μmol/gFW	28 days	He et al. (2011)
Synechococcus PCC 7942	*Aphanothece halophytica*	500	~1.5 μmol/gFW	NA	Waditee et al. (2005)
Anabaena sp. PCC 7120	*Aphanothece halophytica*	140	0.04 μmol/gFW	7 days	Waditee-Sirisattha et al. (2012)
Anabaena doliolum	*Aphanothece halophytica*	500	12.92 μmol/gDW	10 days	Singh et al. (2013)
Synechocystis sp. PCC 6803	*Aphanothece halophytica*	510	64.29 μmol/gDW	4 days	This work
Escherichia coli XL1-Blue	*Ectothiorhodospira halochloris*	300	78 μmol/gDW	NA	Nyyssola et al. (2000)
Escherichia coli BL21	*Aphanothece halophytica*	300	~23 μmol/gDW	3 h	Waditee et al. (2003)
Escherichia coli BL21	*Aphanothece halophytica*	300	~2,000 μmol/mg protein	3 h	Waditee et al. (2007)
Escherichia coli BL21	*Aphanothece halophytica*	300	~80 μmol/L	2 h	He et al. (2011)
Escherichia coli DH5α	*Aphanothece halophytica*	500	6 μmol/gDW	24 h	Waditee-Sirisattha et al. (2012)
Escherichia coli DH5α	*Aphanothece halophytica*	0	80.62 μmol/gDW	ON	Singh et al. (2013)
Pseudomonas denitrificans	*Aphanothece halophytica*	0	NA*	1 day	Shkryl et al. (2020)

*ON, overnight; NA, not available; DW, dry weight; FW, fresh weight; *—Identified by HPLC-MS.*

toward the production of CS could also explain the increased amount of GB produced in the presence of NaCl.

The implementation of the GB device into *Synechocystis* wild-type led to a small decrease in growth in all conditions tested (**Figure 6**). As predicted by the metabolic flux model, the device may drain the cell's resources imposing a metabolic burden, causing growth impairment. This can be explained by the redirection of part of the photosynthetically fixed carbon to the synthesis of CS, which is no longer available for biomass formation, similarly to what was reported for the production of mannitol (Wu et al., 2020). In contrast to what was observed for the WT, the introduction of the GB device into the Δ*ggpS* mutant resulted in an increased salt tolerance with the concomitant growth improvement, enabling its survival under 5% NaCl. This phenotype was maintained under long-term cultivation periods up to 25 days (data not shown), suggesting that GB can compensate for the absence of GG. Conversely, the implementation of the GB device in the Δ*sps*Δ*ggpS* mutant did not improve its performance under salinity conditions. However, it remains unclear if this outcome is due to: 1) insufficient production of glycine betaine to allow cell survival or 2) the absence of both native compatible solutes (sucrose and GG).

In terms of production, the highest GB amount was obtained for the Δ*ggpS* cultivated in BG11 supplemented with 3% NaCl for 4 days (1.89 μmol GB/mg protein, corresponding to 64.29 μmol/gDW, and a volumetric productivity of 13.67 μg/L/h) (**Figure 8B**). Unexpectedly, the production of GB was not higher at 5% NaCl, which may be due to the limited capacity of the cells to survive in such conditions. Extending the cultivation period up to 16 days does not seem to affect the synthesis of GB in any condition tested (**Supplementary Figure S7**), suggesting that the process is stable. In addition, the negligible GB amounts detected in the extracellular medium show that this CS can be exported. Since product secretion facilitates recovery and reduces costs, this aspect should be addressed in the establishment of a GB-cell factory.

The production of GB using native organisms and heterologous hosts (with the synthesis of the solute mainly based on the metabolic pathway described for *A. halophytica*), has been previously reported (**Table 2**). However, a direct comparison is difficult since different normalization methods were used, and the cultivation conditions/time periods need also to be taken into consideration. Generally, the use of native GB producers such as the hypersaline cyanobacterium *A. halophytica* can render high amounts of the solute. This entails major disadvantages related to the high salt concentrations required, such as the reduced durability of the bioreactors, long processes, and detrimental impact on the environment. In contrast, with heterologous hosts the salinity concentrations used are at least 1/3 of those employed for *A. halophytica* (**Table 2**—heterologous production). Considering the photoautotrophic organisms, the amounts obtained using plants are low and require rather long cultivation periods. The most promising results were obtained using the filamentous cyanobacterium *Anabaena doliolum* that produced 12.92 μmol GB/gDW after 10 days of cultivation (Singh et al., 2013). Using our *Synechocystis* Δ*ggpS* chassis, we report a production level ~5-fold higher than that of *A. doliolum* in just 4 days of cultivation (64.29 μmol GB/gDW). Regarding the heterotrophic chassis, the GB amounts obtained using different *Escherichia coli* strains were only up to 1.25-fold higher than with *Synechocystis* Δ*ggpS*. Cultivation times are significantly reduced for heterotrophic bacteria, but the use of photoautotrophic

chassis enables CO_2 fixation promoting bio-mitigation and surpassing the need to supply a carbon source. Additionally, the highest GB production by our *Synechocystis* Δ*ggpS* chassis was achieved under 510 mM NaCl, opening up the possibility of large-scale cultivation with seawater (salinity range 3.1–3.8%). This does not seem as viable with *E. coli* since increasing the salt concentration to 500 mM has a substantial detrimental impact on the GB production (Waditee-Sirisattha et al., 2012).

CONCLUSION

The heterologous production of the compatible solute glycine betaine (GB) was successfully achieved in different *Synechocystis*-based chassis. The characterization of these compatible solutes (CS) deficient chassis (Δ*sps*, Δ*ggpS*, and Δ*sps*Δ*ggpS*) revealed that under saline conditions, the carbon fluxes are redirected from the synthesis of glycogen toward the production of CS and extracellular polysaccharides. In fact, the maximum amount of GB was obtained in Δ*ggpS* harboring the GB device, under 3% NaCl (64.29 μmol/gDW). This production level is promising and not far from applications using *E. coli*. Considering that the knowledge generated by the characterization of the CS deficient mutants will allow the identification of potential targets to optimize our chassis, that our GB production is based on sunlight and CO_2 fixation, and that there is the possibility of using seawater, *Synechocystis* emerges as a feasible photoautotrophic chassis for large-scale heterologous production of GB or other CS.

DATA AVAILABILITY STATEMENT

The original contributions presented in the study are included in the article/**Supplementary Material**, further inquiries can be directed to the corresponding author.

AUTHOR CONTRIBUTIONS

CCP, EAF, FP, and PT were involved in the conceptual design of the work. The experimental design and strain engineering were carried out by EAF, CCP, JSR, and FP. Characterization and data analysis were performed by EAF and CCP. CS quantification by proton NMR was carried out by PL. EAF, DF, and JU were involved in the curation, simulations, and analyses involving the *i*Syn metabolic model. Data interpretation and article preparation was performed by EAF, CCP, DF (*i*Syn metabolic model), and PT. All authors have revised and approved the submitted version of the article.

FUNDING

This work was financed by Portuguese funds through the Fundação para a Ciência e a Tecnologia (FCT)/Ministério da Ciência, Tecnologia e Ensino Superior within the scope of UIDB/04293/2020, and UIDP/04293/2020. We also greatly acknowledge FCT for the scholarship SFRH/BD/117508/2016 (EAF) and the Assistant Researcher contracts CEECIND/00259/2017 (CCP) and 2020.01953.CEECIND (FP). The NMR data were acquired at CERMAX, ITQB-NOVA, Oeiras, Portugal with equipment funded by FCT, project AAC 01/SAICT/2016.

ACKNOWLEDGMENTS

The authors acknowledge the technical and scientific support of the i3S Scientific Platform "Cell Culture and Genotyping" in the RT-qPCR experiments. We are grateful to: Prof. Paula Gomes, Dr. Luísa Aguiar, and Mélanie Fonte (LAQV-REQUIMTE, Faculdade de Ciências, Universidade do Porto) for providing the equipment and technical assistance regarding compatible solutes extraction; Dr. Paulo Oliveira (i3S) for all the support provided, the scientific discussions, and suggestions; and Dr. Maria Siurana (UPV) for the scientific discussions regarding the *i*Syn metabolic model. The content of this article is available as a preprint at: https://doi.org/10.21203/rs.3.rs-1031622/v1 (Ferreira et al., 2021).

SUPPLEMENTARY MATERIAL

The Supplementary Material for this article can be found online at: https://www.frontiersin.org/articles/10.3389/fbioe.2021.821075/full#supplementary-material

REFERENCES

Ananya, A. K., and Ahmad, I. Z. (2014). Cyanobacteria" the Blue green Algae" and its Novel Applications: A Brief Review. *IJIAS* 7, 251–261.

Baran, R., Lau, R., Bowen, B. P., Diamond, S., Jose, N., Garcia-Pichel, F., et al. (2017). Extensive Turnover of Compatible Solutes in Cyanobacteria Revealed by Deuterium Oxide (D_2O) Stable Isotope Probing. *ACS Chem. Biol.* 12, 674–681. doi:10.1021/acschembio.6b00890

Bustin, S. A., Benes, V., Garson, J. A., Hellemans, J., Huggett, J., Kubista, M., et al. (2009). The MIQE Guidelines: Minimum Information for Publication of Quantitative Real-Time PCR Experiments. *Clin. Chem.* 55, 611–622. doi:10.1373/clinchem.2008.112797

Caldas, T., Demont-Caulet, N., Ghazi, A., and Richarme, G. (1999). Thermoprotection by glycine Betaine and Choline. *Microbiol* 145, 2543–2548. doi:10.1099/00221287-145-9-2543

Canton, B., Labno, A., and Endy, D. (2008). Refinement and Standardization of Synthetic Biological Parts and Devices. *Nat. Biotechnol.* 26, 787–793. doi:10.1038/nbt1413

Cholewa, J. M., Guimarães-Ferreira, L., and Zanchi, N. E. (2014). Effects of Betaine on Performance and Body Composition: a Review of Recent Findings and Potential Mechanisms. *Amino Acids* 46, 1785–1793. doi:10.1007/s00726-014-1748-5

Cleland, D., Krader, P., McCree, C., Tang, J., and Emerson, D. (2004). Glycine Betaine as a Cryoprotectant for Prokaryotes. *J. Microbiol. Methods* 58, 31–38. doi:10.1016/j.mimet.2004.02.015

Costello, A., and Badran, A. H. (2021). Synthetic Biological Circuits within an Orthogonal Central Dogma. *Trends Biotechnol.* 39, 59–71. doi:10.1016/j.tibtech.2020.05.013

Day, C. R., and Kempson, S. A. (2016). Betaine Chemistry, Roles, and Potential Use in Liver Disease. *Biochim. Biophys. Acta (BBA) - Gen. Subjects* 1860, 1098–1106. doi:10.1016/j.bbagen.2016.02.001

Desplats, P., Folco, E., and Salerno, G. L. (2005). Sucrose May Play an Additional Role to that of an Osmolyte in *Synechocystis* sp. PCC 6803 Salt-Shocked Cells. *Plant Physiol. Biochem.* 43, 133–138. doi:10.1016/j.plaphy.2005.01.008

Dikilitas, M., Simsek, E., and Roychoudhury, A. (2020). "Role of Proline and glycine Betaine in Overcoming Abiotic Stresses," in *Protective Chemical Agents in the Amelioration of Plant Abiotic Stress: Biochemical and Molecular Perspectives*. Editors A. Roychoudhury and D. K. Tripathi (John Wiley & Sons), 1–23. doi:10.1002/9781119552154.ch1

Du, W., Liang, F., Duan, Y., Tan, X., and Lu, X. (2013). Exploring the Photosynthetic Production Capacity of Sucrose by Cyanobacteria. *Metab. Eng.* 19, 17–25. doi:10.1016/j.ymben.2013.05.001

Dubois, M., Gilles, K. A., Hamilton, J. K., Rebers, P. A., and Smith, F. (1956). Colorimetric Method for Determination of Sugars and Related Substances. *Anal. Chem.* 28, 350–356. doi:10.1021/ac60111a017

DuPont (2015). Betafin® Natural Betaine Sustainable and Substantiated. Available at: http://animalnutrition.dupont.com/fileadmin/user_upload/live/animal_nutrition/documents/open/Betafin__Natural_Betaine_Lifecycle_Analysis.pdf (Accessed October 14, 2021).

Eklund, M., Bauer, E., Wamatu, J., and Mosenthin, R. (2005). Potential Nutritional and Physiological Functions of Betaine in Livestock. *Nutr. Res. Rev.* 18, 31–48. doi:10.1079/nrr200493

Ernst, A., Kirschenlohr, H., Diez, J., and Böger, P. (1984). Glycogen Content and Nitrogenase Activity in *Anabaena Variabilis*. *Arch. Microbiol.* 140, 120–125. doi:10.1007/bf00454913

Ferreira, E. A., Pacheco, C. C., Pinto, F., Pereira, J., Lamosa, P., Oliveira, P., et al. (2018). Expanding the Toolbox for *Synechocystis* sp. PCC 6803: Validation of Replicative Vectors and Characterization of a Novel Set of Promoters. *Synth. Biol. (Oxf)* 3, ysy014. doi:10.1093/synbio/ysy014

Ferreira, E. A., Pacheco, C. C., Rodrigues, J. S., Pinto, F., Lamosa, P., Fuente, D., et al. (2021). Heterologous Production of glycine Betaine Using *Synechocystis* sp. PCC 6803-based Chassis Lacking Native Compatible Solutes, Preprint. *Res. Square* (Accessed November 22, 2021). doi:10.21203/rs.3.rs-1031622/v1

Gopalakrishnan, S., Pakrasi, H. B., and Maranas, C. D. (2018). Elucidation of Photoautotrophic Carbon Flux Topology in *Synechocystis* PCC 6803 Using Genome-Scale Carbon Mapping Models. *Metab. Eng.* 47, 190–199. doi:10.1016/j.ymben.2018.03.008

Grossman, E. B., and Hebert, S. C. (1989). Renal Inner Medullary Choline Dehydrogenase Activity: Characterization and Modulation. *Am. J. Physiology-Renal Physiol.* 256, F107–F112. doi:10.1152/ajprenal.1989.256.1.f107

Guinn, E. J., Pegram, L. M., Capp, M. W., Pollock, M. N., and Record, M. T. (2011). Quantifying Why Urea Is a Protein Denaturant, whereas glycine Betaine Is a Protein Stabilizer. *Proc. Natl. Acad. Sci.* 108, 16932–16937. doi:10.1073/pnas.1109372108

Hagemann, M. (2013). "Genomics of Salt Acclimation," in *Adv Bot Res*. Editor C. C.-C. Franck Chauvat (Academic Press), 65, 27–55. doi:10.1016/b978-0-12-394313-2.00002-0

Hays, S. G., and Ducat, D. C. (2015). Engineering Cyanobacteria as Photosynthetic Feedstock Factories. *Photosynth Res.* 123, 285–295. doi:10.1007/s11120-014-9980-0

He, Y., He, C., Li, L., Liu, Z., Yang, A., and Zhang, J. (2011). Heterologous Expression of *ApGSMT2* and *ApDMT2* Genes from *Aphanothece Halophytica* Enhanced Drought Tolerance in Transgenic Tobacco. *Mol. Biol. Rep.* 38, 657–666. doi:10.1007/s11033-010-0152-9

Heidorn, T., Camsund, D., Huang, H.-H., Lindberg, P., Oliveira, P., Stensjö, K., et al. (2011). "Synthetic Biology in Cyanobacteria," in *Methods Enzymol*. Editor C. Voigt (Academic Press), 497, 539–579. doi:10.1016/b978-0-12-385075-1.00024-x

Heikkila, H. O., Melaja, J. A., Millner, D. E., and Virtanen, J. J. (1982). Betaine Recovery Process. US4359430A.

Heirendt, L., Arreckx, S., Pfau, T., Mendoza, S. N., Richelle, A., Heinken, A., et al. (2019). Creation and Analysis of Biochemical Constraint-Based Models Using the COBRA Toolbox v.3.0. *Nat. Protoc.* 14, 639–702. doi:10.1038/s41596-018-0098-2

Holmström, K. O., Somersalo, S., Mandal, A., Palva, T. E., and Welin, B. (2000). Improved Tolerance to Salinity and Low Temperature in Transgenic Tobacco Producing glycine Betaine. *J. Exp. Bot.* 51, 177–185. doi:10.1093/jexbot/51.343.177

Huang, H.-H., Camsund, D., Lindblad, P., and Heidorn, T. (2010). Design and Characterization of Molecular Tools for a Synthetic Biology Approach towards Developing Cyanobacterial Biotechnology. *Nucleic Acids Res.* 38, 2577–2593. doi:10.1093/nar/gkq164

Iijima, H., Nakaya, Y., Kuwahara, A., Hirai, M. Y., and Osanai, T. (2015). Seawater Cultivation of Freshwater Cyanobacterium *Synechocystis* sp. PCC 6803 Drastically Alters Amino Acid Composition and Glycogen Metabolism. *Front. Microbiol.* 6, 326. doi:10.3389/fmicb.2015.00326

Iijima, H., Watanabe, A., Sukigara, H., Shirai, T., Kondo, A., and Osanai, T. (2020). Simultaneous Increases in the Levels of Compatible Solutes by Cost-effective Cultivation of *Synechocystis* sp. PCC 6803. *Biotechnol. Bioeng.* 117, 1649–1660. doi:10.1002/bit.27324

Incharoensakdi, A., and Waditee, R. (2000). Degradation of Glycinebetaine by Betaine-Homocysteine Methyltransferase in *Aphanothece halophytica*: Effect of Salt Downshock and Starvation. *Curr. Microbiol.* 41, 227–231. doi:10.1007/s002840010125

Ishitani, M., Takabe, T., Kojima, K., and Takabe, T. (1993). Regulation of Glycinebetaine Accumulation in the Halotolerant Cyanobacterium *Aphanothece Halophytica*. *Funct. Plant Biol.* 20, 693–703. doi:10.1071/pp9930693

Jittawuttipoka, T., Planchon, M., Spalla, O., Benzerara, K., Guyot, F., Cassier-Chauvat, C., et al. (2013). Multidisciplinary Evidences that *Synechocystis* PCC6803 Exopolysaccharides Operate in Cell Sedimentation and protection against Salt and Metal Stresses. *PLoS One* 8, e55564. doi:10.1371/journal.pone.0055564

Joshi, C. J., Peebles, C. A. M., and Prasad, A. (2017). Modeling and Analysis of Flux Distribution and Bioproduct Formation in *Synechocystis* sp. PCC 6803 Using a New Genome-Scale Metabolic Reconstruction. *Algal Res.* 27, 295–310. doi:10.1016/j.algal.2017.09.013

Kaleta, C., Schäuble, S., Rinas, U., and Schuster, S. (2013). Metabolic Costs of Amino Acid and Protein Production in *Escherichia coli*. *Biotechnol. J.* 8, 1105–1114. doi:10.1002/biot.201200267

Kanesaki, Y., Shiwa, Y., Tajima, N., Suzuki, M., Watanabe, S., Sato, N., et al. (2012). Identification of Substrain-specific Mutations by Massively Parallel Whole-Genome Resequencing of *Synechocystis* sp. PCC 6803. *DNA Res.* 19, 67–79. doi:10.1093/dnares/dsr042

Kar, J. R., Hallsworth, J. E., and Singhal, R. S. (2015). Fermentative Production of glycine Betaine and Trehalose from Acid Whey Using *Actinopolyspora Halophila* (MTCC 263). *Environ. Tech. Innovation* 3, 68–76. doi:10.1016/j.eti.2015.02.001

Kirsch, F., Klähn, S., and Hagemann, M. (2019). Salt-regulated Accumulation of the Compatible Solutes Sucrose and Glucosylglycerol in Cyanobacteria and its Biotechnological Potential. *Front. Microbiol.* 10, 2139. doi:10.3389/fmicb.2019.02139

Kirsch, F., Pade, N., Klähn, S., Hess, W. R., and Hagemann, M. (2017). The Glucosylglycerol-Degrading Enzyme GghA Is Involved in Acclimation to Fluctuating Salinities by the Cyanobacterium *Synechocystis* sp. Strain PCC 6803. *Microbiol* 163, 1319–1328. doi:10.1099/mic.0.000518

Klähn, S., and Hagemann, M. (2011). Compatible Solute Biosynthesis in Cyanobacteria. *Environ. Microbiol.* 13, 551–562. doi:10.1111/j.1462-2920.2010.02366.x

Knoll, A. H. (2008). "Cyanobacteria and Earth History," in *The Cyanobacteria: Molecular Biology, Genomics, and evolution*. Editors F. G. Flores and A. Herrero (Caister Academic Press), 1–19.

Landfald, B., and Strøm, A. R. (1986). Choline-glycine Betaine Pathway Confers a High Level of Osmotic Tolerance in *Escherichia coli*. *J. Bacteriol.* 165, 849–855. doi:10.1128/jb.165.3.849-855.1986

Leitão, E., Pereira, S., Bondoso, J., Ferreira, D., Pinto, F., Moradasferreira, P., et al. (2006). Genes Involved in the Maturation of Hydrogenase(s) in the

Nonheterocystous Cyanobacterium *Lyngbya Majuscula* CCAP 1446/4. *Int. J. Hydrogen Energ.* 31, 1469–1477. doi:10.1016/j.ijhydene.2006.06.012

Lever, M., and Slow, S. (2010). The Clinical Significance of Betaine, an Osmolyte with a Key Role in Methyl Group Metabolism. *Clin. Biochem.* 43, 732–744. doi:10.1016/j.clinbiochem.2010.03.009

Lindblad, P. (2018). "Hydrogen Production Using Novel Photosynthetic Cell Factories. Cyanobacterial Hydrogen Production: Design of Efficient Organisms," in *Microalgal Hydrogen Production: Achievements and Perspectives*. Editors G. Torzillo and M. Seibert (UK: G. Royal Society of Chemistry), 323–334.

Meeks, J. C., and Castenholz, R. W. (1971). Growth and Photosynthesis in an Extreme Thermophile, *Synechococcus Lividus* (Cyanophyta). *Archiv. Mikrobiol.* 78, 25–41. doi:10.1007/bf00409086

Miao, X., Wu, Q., Wu, G., and Zhao, N. (2003). Sucrose Accumulation in Salt-Stressed Cells Ofagpgene Deletion-Mutant in cyanobacterium *Synechocystis* sp. PCC 6803. *FEMS Microbiol. Lett.* 218, 71–77. doi:10.1111/j.1574-6968.2003.tb11500.x

Montagud, A., Navarro, E., Fernández de Córdoba, P., Urchueguía, J. F., and Patil, K. R. (2010). Reconstruction and Analysis of Genome-Scale Metabolic Model of a Photosynthetic Bacterium. *BMC Syst. Biol.* 4, 156. doi:10.1186/1752-0509-4-156

Montagud, A., Zelezniak, A., Navarro, E., de Córdoba, P. F., Urchueguía, J. F., and Patil, K. R. (2011). Flux Coupling and Transcriptional Regulation within the Metabolic Network of the Photosynthetic Bacterium *Synechocystis* sp. PCC6803. *Biotechnol. J.* 6, 330–342. doi:10.1002/biot.201000109

Mota, R., Guimarães, R., Büttel, Z., Rossi, F., Colica, G., Silva, C. J., et al. (2013). Production and Characterization of Extracellular Carbohydrate Polymer from *Cyanothece* sp. CCY 0110. *Carbohydr. Polym.* 92, 1408–1415. doi:10.1016/j.carbpol.2012.10.070

Nsimba, Z. F., Paquot, M., Mvumbi, L. G., and Deleu, M. (2010). Glycine Betaine Surfactant Derivatives: Synthesis Methods and Potentialities of Use. *Biotechnol. Agron. Soc. Envir* 14, 737–748.

Nyyssölä, A., Kerovuo, J., Kaukinen, P., von Weymarn, N., and Reinikainen, T. (2000). Extreme Halophiles Synthesize Betaine from glycine by Methylation. *J. Biol. Chem.* 275, 22196–22201. doi:10.1074/jbc.m910111199

Oren, A., Heldal, M., Norland, S., and Galinski, E. (2002). Intracellular Ion and Organic Solute Concentrations of the Extremely Halophilic Bacterium *Salinibacter Ruber*. *Extremophiles* 6, 491–498. doi:10.1007/s00792-002-0286-3

Orth, J. D., Thiele, I., and Palsson, B. Ø. (2010). What Is Flux Balance Analysis? *Nat. Biotechnol.* 28, 245–248. doi:10.1038/nbt.1614

Pacheco, C. C., Ferreira, E. A., Oliveira, P., and Tamagnini, P. (2021). "Synthetic Biology of Cyanobacteria," in *The Autotrophic Biorefinery: Raw Materials from Biotechnology*. Editors R. Kourist and S. Schmidt, 131–172. doi:10.1515/9783110550603-006

Pereira, S. B., Santos, M., Leite, J. P., Flores, C., Eisfeld, C., Büttel, Z., et al. (2019). The Role of the Tyrosine Kinase Wzc (Sll0923) and the Phosphatase Wzb (Slr0328) in the Production of Extracellular Polymeric Substances (EPS) by *Synechocystis* PCC 6803. *Microbiologyopen* 8, e00753. doi:10.1002/mbo3.753

Pinto, F., Pacheco, C. C., Ferreira, D., Moradas-Ferreira, P., and Tamagnini, P. (2012). Selection of Suitable Reference Genes for RT-qPCR Analyses in Cyanobacteria. *PLoS One* 7, e34983. doi:10.1371/journal.pone.0034983

Pinto, F., Pacheco, C. C., Oliveira, P., Montagud, A., Landels, A., Couto, N., et al. (2015). Improving a *Synechocystis*-Based Photoautotrophic Chassis through Systematic Genome Mapping and Validation of Neutral Sites. *DNA Res.* 22, 425–437. doi:10.1093/dnares/dsv024

Rady, M. O. A., Semida, W. M., Abd El-Mageed, T. A., Hemida, K. A., and Rady, M. M. (2018). Up-regulation of Antioxidative Defense Systems by glycine Betaine Foliar Application in Onion Plants Confer Tolerance to Salinity Stress. *Scientia Horticulturae* 240, 614–622. doi:10.1016/j.scienta.2018.06.069

Rathinasabapathi, B., Burnet, M., Russell, B. L., Gage, D. A., Liao, P.-C., Nye, G. J., et al. (1997). Choline Monooxygenase, an Unusual Iron-Sulfur Enzyme Catalyzing the First Step of glycine Betaine Synthesis in Plants: Prosthetic Group Characterization and cDNA Cloning. *Proc. Natl. Acad. Sci.* 94, 3454–3458. doi:10.1073/pnas.94.7.3454

Rodrigues, J. S., and Lindberg, P. (2021). "Engineering Cyanobacteria as Host Organisms for Production of Terpenes and Terpenoids," in *Cyanobacteria Biotechnology*. Editors S. L. Jens Nielsen, G. Stephanopoulos, and P. Hudson (WILEY-VCH GmbH), 267–300. doi:10.1002/9783527824908.ch9

Sadvakasova, A. K., Kossalbayev, B. D., Zayadan, B. K., Bolatkhan, K., Alwasel, S., Najafpour, M. M., et al. (2020). Bioprocesses of Hydrogen Production by Cyanobacteria Cells and Possible Ways to Increase Their Productivity. *Renew. Sust. Energ. Rev.* 133, 110054. doi:10.1016/j.rser.2020.110054

Sambrook, J., and Russel, D. (2001). *Molecular Cloning: A Laboratory Manual*. 3rd ed. NY, USA: Cold Spring Harbor Laboratory Press.

Santos, H., Lamosa, P., and Borges, N. (2006). "Characterization and Quantification of Compatible Solutes in (Hyper)thermophilic Microorganisms," in *Methods in Microbiology*. Editors F. A. Rainey and A. Oren (Academic Press), 35, 173–199. Extremophiles. doi:10.1016/s0580-9517(08)70011-4

Schäfer, A., Tauch, A., Jäger, W., Kalinowski, J., Thierbach, G., and Pühler, A. (1994). Small Mobilizable Multi-Purpose Cloning Vectors Derived from the *Escherichia coli* Plasmids pK18 and pK19: Selection of Defined Deletions in the Chromosome of *Corynebacterium Glutamicum*. *Gene* 145, 69–73. doi:10.1016/0378-1119(94)90324-7

Shkryl, Y., Degtyarenko, A., Grigorchuk, V., Balabanova, L., and Tekutyeva, L. (2020). Betaine Biosynthesis in a Heterologous Expression System Based on the B12 Producer Pseudomonas Denitrificans. Paper presented at the E3S Web of Conferences .

Silva-Rocha, R., Martínez-García, E., Calles, B., Chavarría, M., Arce-Rodríguez, A., de las Heras, A., et al. (2013). The Standard European Vector Architecture (SEVA): a Coherent Platform for the Analysis and Deployment of Complex Prokaryotic Phenotypes. *Nucleic Acids Res.* 41, D666–D675. doi:10.1093/nar/gks1119

Singh, M., Sharma, N. K., Prasad, S. B., Yadav, S. S., Narayan, G., and Rai, A. K. (2013). The Freshwater Cyanobacterium *Anabaena Doliolum* Transformed with *ApGSMT-DMT* Exhibited Enhanced Salt Tolerance and protection to Nitrogenase Activity, but Became Halophilic. *Microbiol* 159, 641–648. doi:10.1099/mic.0.065078-0

Stadmiller, S. S., Gorensek-Benitez, A. H., Guseman, A. J., and Pielak, G. J. (2017). Osmotic Shock Induced Protein Destabilization in Living Cells and its Reversal by glycine Betaine. *J. Mol. Biol.* 429, 1155–1161. doi:10.1016/j.jmb.2017.03.001

Stanier, R. Y., Kunisawa, R., Mandel, M., and Cohen-Bazire, G. (1971). Purification and Properties of Unicellular Blue-green Algae (Order *Chroococcales*). *Bacteriol. Rev.* 35, 171–205. doi:10.1128/br.35.2.171-205.1971

Sun, H., Luo, M., Zhou, X., Zhou, Q., Sun, Y., Ge, W., et al. (2020). Exogenous glycine Betaine Treatment Alleviates Low Temperature-Induced Pericarp browning of 'Nanguo' Pears by Regulating Antioxidant Enzymes and Proline Metabolism. *Food Chem.* 306, 125626. doi:10.1016/j.foodchem.2019.125626

Tamagnini, P., Troshina, O., Oxelfelt, F., Salema, R., and Lindblad, P. (1997). Hydrogenases in *Nostoc* sp. Strain PCC 73102, a Strain Lacking a Bidirectional Enzyme. *Appl. Environ. Microbiol.* 63, 1801–1807. doi:10.1128/aem.63.5.1801-1807.1997

Trautmann, D., Voss, B., Wilde, A., Al-Babili, S., and Hess, W. R. (2012). Microevolution in Cyanobacteria: Re-sequencing a Motile Substrain of *Synechocystis* sp. PCC 6803. *DNA Res.* 19, 435–448. doi:10.1093/dnares/dss024

Waditee, R., Bhuiyan, M. N. H., Rai, V., Aoki, K., Tanaka, Y., Hibino, T., et al. (2005). Genes for Direct Methylation of glycine Provide High Levels of glycinebetaine and Abiotic-Stress Tolerance in *Synechococcus* and *Arabidopsis*. *Proc. Natl. Acad. Sci.* 102, 1318–1323. doi:10.1073/pnas.0409017102

Waditee, R., Bhuiyan, N. H., Hirata, E., Hibino, T., Tanaka, Y., Shikata, M., et al. (2007). Metabolic Engineering for Betaine Accumulation in Microbes and Plants. *J. Biol. Chem.* 282, 34185–34193. doi:10.1074/jbc.m704939200

Waditee, R., Tanaka, Y., Aoki, K., Hibino, T., Jikuya, H., Takano, J., et al. (2003). Isolation and Functional Characterization of N-Methyltransferases that Catalyze Betaine Synthesis from Glycine in a Halotolerant Photosynthetic Organism *Aphanothece halophytica*. *J. Biol. Chem.* 278, 4932–4942. doi:10.1074/jbc.m210970200

Waditee-Sirisattha, R., Kageyama, H., Fukaya, M., Rai, V., and Takabe, T. (2015). Nitrate and Amino Acid Availability Affects glycine Betaine and Mycosporine-2-glycine in Response to Changes of Salinity in a Halotolerant cyanobacterium *Aphanothece halophytica*. *FEMS Microbiol. Lett.* 362, fnv198. doi:10.1093/femsle/fnv198

Waditee-Sirisattha, R., Singh, M., Kageyama, H., Sittipol, D., Rai, A. K., and Takabe, T. (2012). *Anabaena* sp. PCC7120 Transformed with glycine Methylation Genes from *Aphanothece Halophytica* Synthesized glycine

Betaine Showing Increased Tolerance to Salt. *Arch. Microbiol.* 194, 909–914. doi:10.1007/s00203-012-0824-z

Wang, L., Chen, L., Yang, S., and Tan, X. (2020). Photosynthetic Conversion of Carbon Dioxide to Oleochemicals by Cyanobacteria: Recent Advances and Future Perspectives. *Front. Microbiol.* 11, 634. doi:10.3389/fmicb.2020.00634

Williams, J. G. K. (1988). [85] Construction of Specific Mutations in Photosystem II Photosynthetic Reaction center by Genetic Engineering Methods in *Synechocystis* 6803. *Methods Enzymol.* 167, 766–778. doi:10.1016/0076-6879(88)67088-1

Wu, W., Du, W., Gallego, R. P., Hellingwerf, K. J., van der Woude, A. D., and Branco dos Santos, F. (2020). Using Osmotic Stress to Stabilize Mannitol Production in *Synechocystis* sp. PCC6803. *Biotechnol. Biofuels* 13, 117. doi:10.1186/s13068-020-01755-3

You, L., Song, Q., Wu, Y., Li, S., Jiang, C., Chang, L., et al. (2019). Accumulation of glycine Betaine in Transplastomic Potato Plants Expressing Choline Oxidase Confers Improved Drought Tolerance. *Planta* 249, 1963–1975. doi:10.1007/s00425-019-03132-3

Conflict of Interest: The authors declare that the research was conducted in the absence of any commercial or financial relationships that could be construed as a potential conflict of interest.

Supplementary Material

Supplementary Material

Ferreira *et al.* 2021

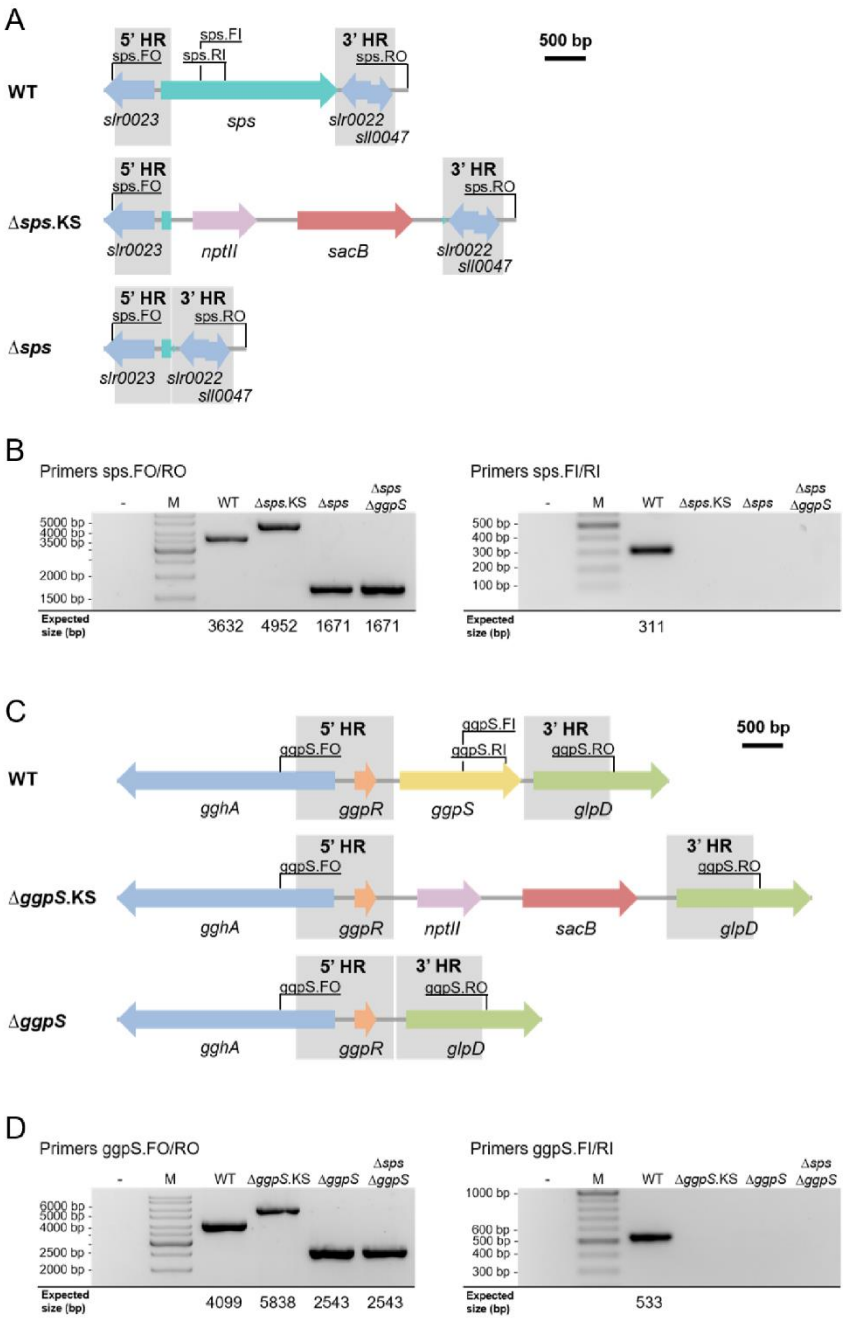

Fig. S1 - Schematic representation of the position of the primers (A and C) and PCR analysis confirming the segregation of the *Synechocystis* Δ*sps*, Δ*ggpS* and Δ*sps*Δ*ggpS* mutants (B and D). PCR reactions were performed using inner and outer primers for *sps* (sps.FI/RI and sps.FO/RO, respectively) and *ggpS* (ggpS.FI/RI and ggpS.FO/RO, respectively). Primers are listed in Table S2. The expected band sizes are indicated. -, negative control (absence of template); M, molecular marker: GeneRuler DNA Ladder Mix (Thermo Scientific™); WT, wild-type; bp, base pairs.

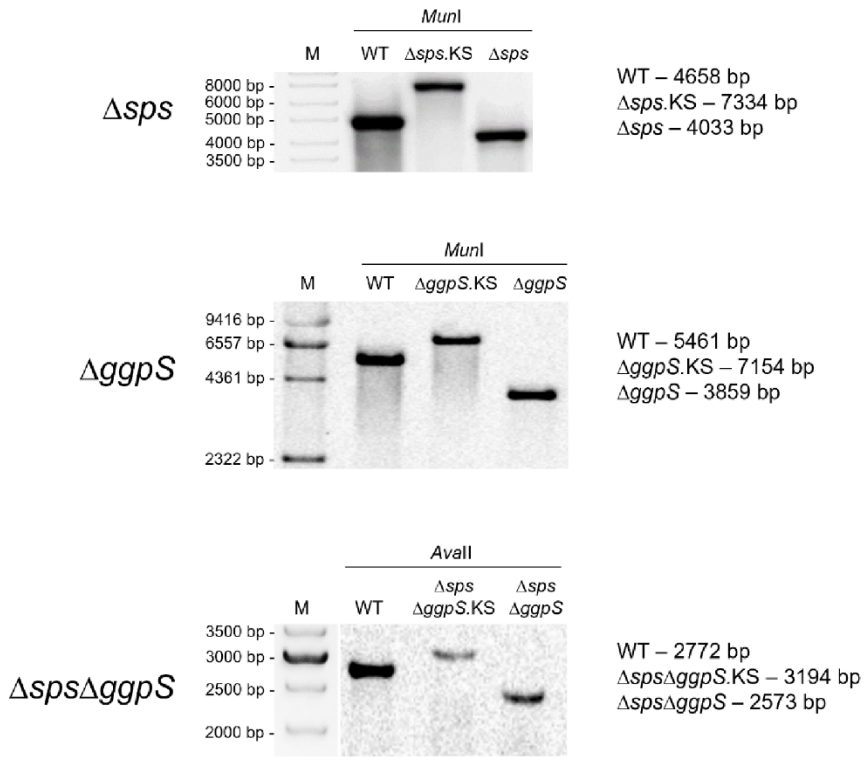

Fig. S2 - Southern blot analysis confirming the segregation of the *Synechocystis* Δ*sps*, Δ*ggpS* and Δ*sps*Δ*ggpS* mutants. The DNA was digested with the endonucleases *Mun*I (WT, Δ*sps*.KS, Δ*sps*, Δ*ggpS*.KS and Δ*ggpS*) and *Ava*II (WT, Δ*sps*Δ*ggpS*.KS and Δ*sps*Δ*ggpS*). Digoxigenin-labelled probes covering the 3'-flanking region of *sps* and the 5'-flanking region of *ggpS* were used (see the *Materials* section for details). The sizes of the DNA fragments hybridizing with the probe are indicated. M, molecular marker: GeneRuler DNA Ladder Mix (Thermo Scientific™) for Δ*sps* and Δ*sps*Δ*ggpS* and lambda DNA/HindIII marker (Thermo Scientific™) for Δ*ggpS*; WT, wild-type; bp, base pairs.

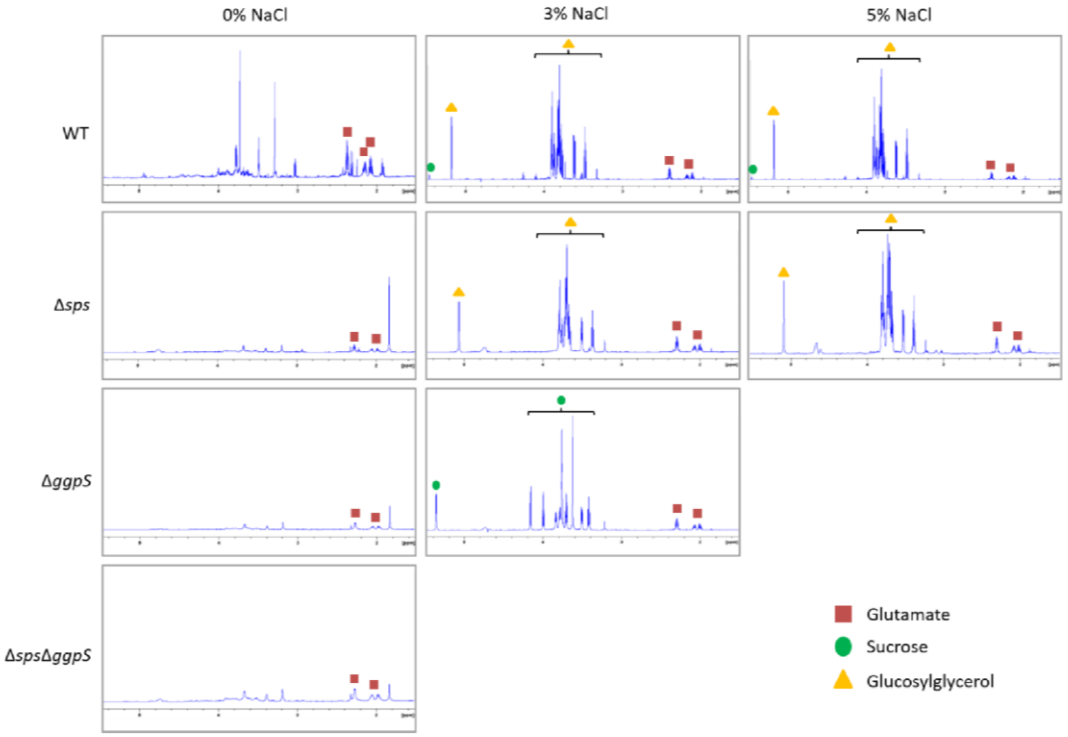

Fig. S3 - Proton nuclear magnetic resonance (NMR) spectra of *Synechocystis* cell-free extracts for the detection of the compatible solutes glutamate, sucrose and glucosylglycerol. Cell-free extracts were obtained from *Synechocystis* wild-type (WT) and the Δ*sps*, Δ*ggpS* and Δ*sps*Δ*ggpS* mutants, grown in BG11 or BG11 supplemented with 3% or 5% (wt/vol) NaCl (left, middle or right panel, respectively). Spectra were acquired at 25 °C on an AVANCE III 800 spectrometer (Bruker) using a four channel inverse detection probe head with solvent pre-saturation and a recycle delay of 60s to allow full relaxation of the resonances.

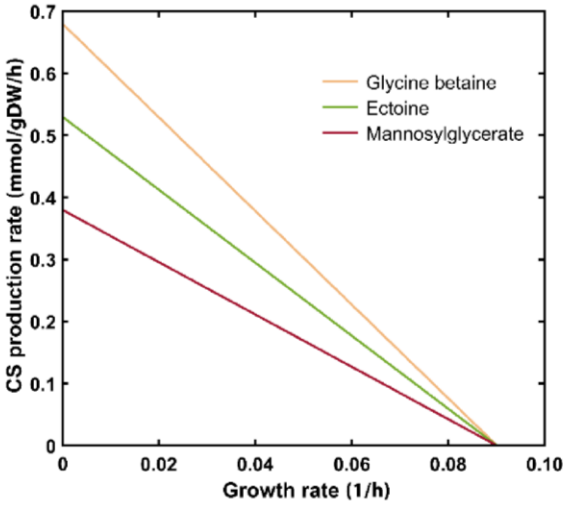

Fig. S4 - Theoretical productivity of the heterologous compatible solutes glycine betaine, ectoine and mannosylglycerate, as predicted by the updated version of the genome-scale metabolic model *i*Syn811 (Montagud *et al.*, 2011). The lines represent the compatible solute production rate as a function of *Synechocystis* wild-type growth under autotrophic conditions.

5

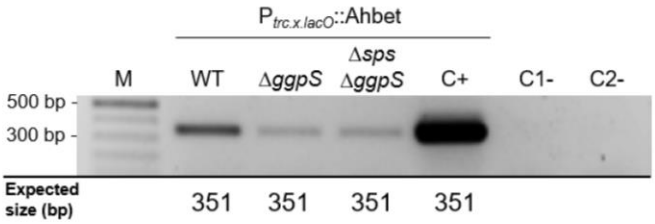

Fig. S5 - PCR analysis confirming the presence of the plasmid containing the glycine betaine synthetic device (pSEVA351 $P_{trc.x.lacO}$::Ahbet) in *Synechocystis* wild-type (WT) and Δ*ggpS* and Δ*sps*Δ*ggpS* mutants. PCR reactions were performed using SD_GSMT_F/R (primers listed in Table S2). The expected band sizes are indicated. C+, positive control (plasmid DNA pSEVA351 $P_{trc.x.lacO}$::Ahbet); C1-, negative control (*Synechocystis* WT genomic DNA); C2-, negative control (no template); M, molecular marker: GeneRuler DNA Ladder Mix (Thermo Scientific™); bp, base pairs.

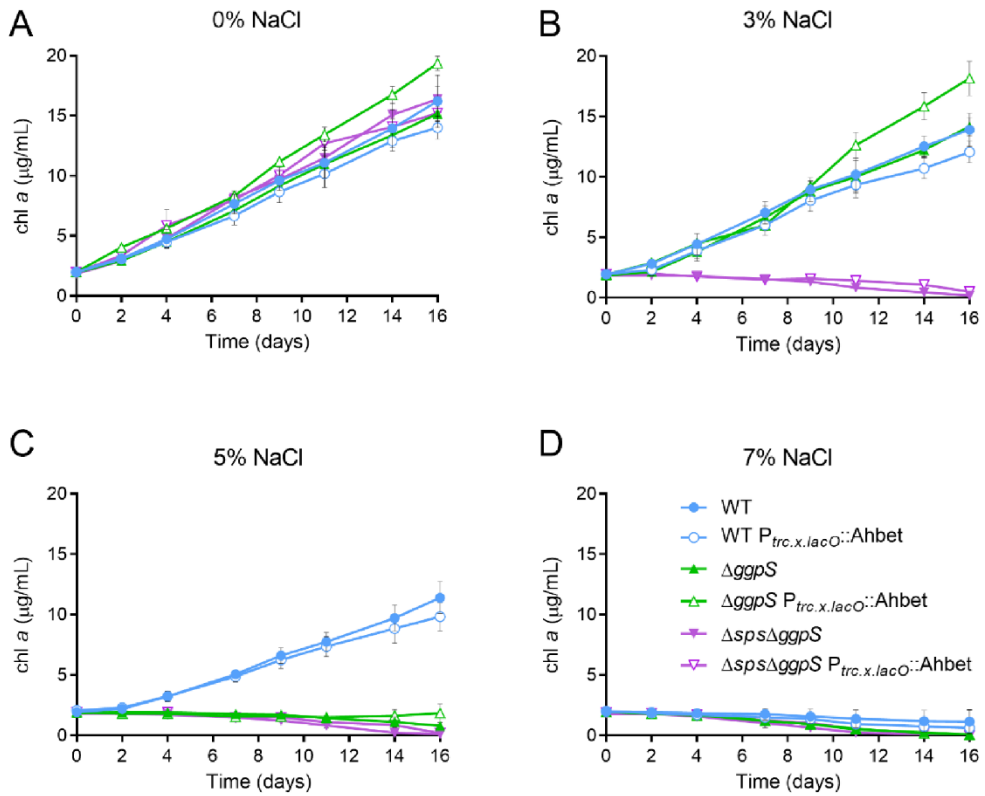

Fig. S6 - Growth curves of *Synechocystis* wild-type (WT), Δ*ggpS*, Δ*sps*Δ*ggpS* and the corresponding strains harboring the glycine betaine synthetic device ($P_{trc.x.lacO}$::Ahbet). Cultures were grown in BG11 (**A**) or BG11 supplemented with 3% (**B**), 5% (**C**) or 7% (**D**) (wt/vol) NaCl, at 30 ºC with orbital shaking (150 rpm) under a 12 h light (25 µE/m²/s) / 12 h dark regimen. Growth was monitored by measuring chlorophyll *a* (chl *a*) expressed as µg per mL of culture. Error bars correspond to standard deviations from, at least, three biological replicates with technical duplicates.

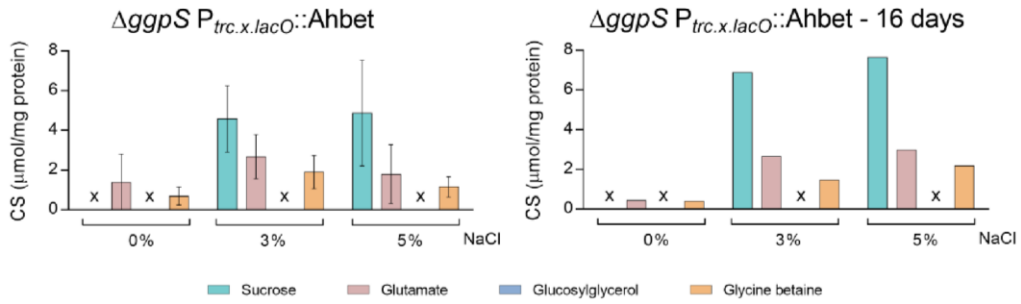

Fig. S7 - Effect of NaCl on the synthesis of native compatible solutes sucrose, glutamate and glucosylglycerol and the heterologous glycine betaine in *Synechocystis* Δ*ggpS* $P_{trc.x.lacO}$::Ahbet after 4 days (A) and 16 days (B) of cultivation. Cultures were grown in BG11 or BG11 supplemented with 3% or 5% (wt/vol) NaCl, at 30 ºC with orbital shaking (150 rpm) under a 12 h light (25 µE/m²/s) / 12 h dark regimen. Compatible solutes were quantified by H-NMR, and the results were normalized per mg of protein. x - not detected. Error bars correspond to standard deviations from three biological replicates for 4 days of cultivation and one biological replicate for 16 days of cultivation.

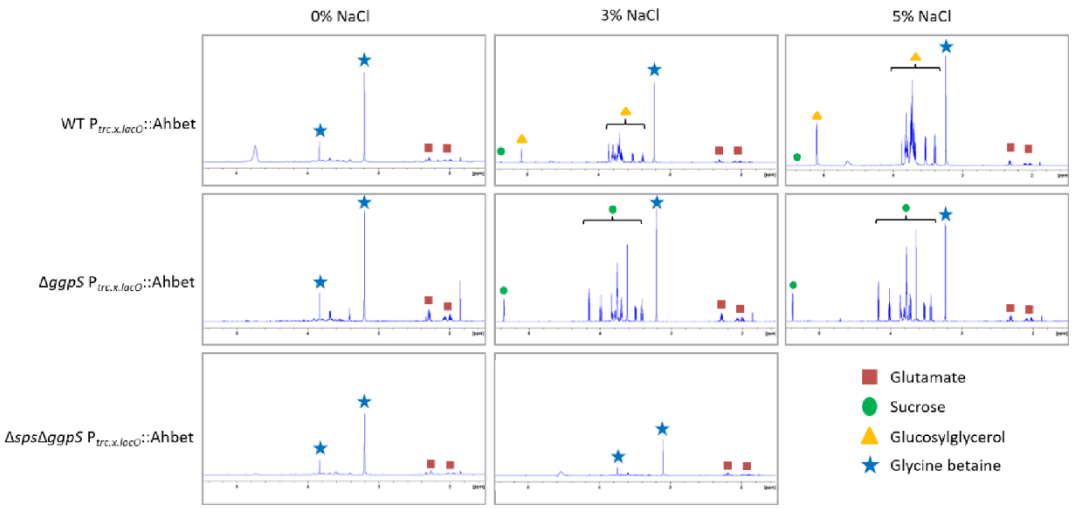

Fig. S8 - Proton NMR spectra of *Synechocystis* cell-free extracts for the detection of the compatible solutes glutamate, sucrose, glucosylglycerol and glycine betaine. Cell-free extracts were obtained from *Synechocystis* WT $P_{trc.x.lacO}$::Ahbet, Δ*ggpS* $P_{trc.x.lacO}$::Ahbet and Δ*sps*Δ*ggpS* $P_{trc.x.lacO}$::Ahbet, grown in BG11 or BG11 supplemented with 3% or 5% (wt/vol) NaCl (left, middle or right panel, respectively). Spectra were acquired at 25 °C on an AVANCE III 800 spectrometer (Bruker) using a four channel inverse detection probe head with solvent pre-saturation and a recycle delay of 60s to allow full relaxation of the resonances.

Table S1 - Growth decrease (OD_{730}) of *Synechocystis* wild-type (WT), Δ*sps*, Δ*ggpS*, Δ*sps*Δ*ggpS* and mutants harboring $P_{trc.x.lacO}$::Ahbet in 3%, 5% or 7% (wt/vol) NaCl compared with 0% NaCl at day 16.

Strain	Growth decrease[a] compared with 0% NaCl		
	3% NaCl (510 mM)	5% NaCl (860 mM)	7% NaCl (1200 mM)
Mutants			
WT	22.5%	43.4%	85.6%
Δ*sps*	28.7%	55.3%	88.7%
Δ*ggpS*	17.0%	87.8%	91.6%
Δ*sps*Δ*ggpS*	91.0%	92.3%	93.1%
Mutants harboring the glycine betaine device			
WT $P_{trc.x.lacO}$::Ahbet	31.0%	43.4%	89.0%
Δ*ggpS* $P_{trc.x.lacO}$::Ahbet	17.8%	81.2%	92.0%
Δ*sps*Δ*ggpS* $P_{trc.x.lacO}$::Ahbet	90.3%	92.0%	93.3%

[a]Statistical significance of $P \leq 0.0001$.

Table S2 - RT-qPCR data of *gsmt*, *dmt* and *metX* relative expression in *Synechocystis* chassis (WT, Δ*ggpS* and Δ*sps*Δ*ggpS*) harboring the glycine betaine synthetic device. RNA was obtained from cells grown in BG11 or BG11 supplemented with 3% and 5% (wt/vol) NaCl, at 30 ºC with orbital shaking (150 rpm) under a 12 h light (25 μE/m^2/s) / 12 h dark regimen. The ΔCq represents the expression of the target genes relative to WT $P_{trc.x.lacO}$::Ahbet 0% NaCl. The data was obtained from three biological replicates and three technical replicates. Statistical analysis was performed by means of One-way ANOVA (*P*-value).

	Target genes								
	gsmt			*dmt*			*metX*		
	Relative expression (ΔCq)	SEM (lg)	*P*-value	Relative expression (ΔCq)	SEM (lg)	*P*-value	Relative expression (ΔCq)	SEM (lg)	*P*-value
WT $P_{trc.x.lacO}$::Ahbet 0% NaCl	1.00	0.70	N.A.	1.00	0.95	N.A.	1.00	0.97	N.A.
WT $P_{trc.x.lacO}$::Ahbet 3% NaCl	0.28	0.32	0.075	0.21	0.63	0.117	0.19	0.78	0.124
WT $P_{trc.x.lacO}$::Ahbet 5% NaCl	1.15	0.96	0.873	0.36	1.61	0.470	0.26	1.80	0.398
Δ*ggpS* $P_{trc.x.lacO}$::Ahbet 0% NaCl	0.34	0.41	0.128	0.13	0.78	0.076	0.11	0.91	0.074
Δ*ggpS* $P_{trc.x.lacO}$::Ahbet 3% NaCl	0.37	0.17	0.119	0.15	0.32	0.051	0.10	0.17	0.027
Δ*ggpS* $P_{trc.x.lacO}$::Ahbet 5% NaCl	0.62	0.14	0.385	0.09	1.79	0.166	0.19	0.09	0.071
Δ*sps*Δ*ggpS* $P_{trc.x.lacO}$::Ahbet 0% NaCl	1.46	0.44	0.543	1.02	0.71	0.985	0.79	0.86	0.807
Δ*sps*Δ*ggpS* $P_{trc.x.lacO}$::Ahbet 3% NaCl	0.97	0.50	0.966	0.84	0.77	0.849	0.74	0.92	0.757

SEM: Standard Error of the Mean; N.A.: not applicable.

Table S3 - Quantification of glycine betaine in the extracellular medium used for the cultivation of *Synechocystis* chassis (WT, Δ*ggpS* and Δ*sps*Δ*ggpS*) harboring the glycine betaine device. Glycine betaine was quantified by H-NMR and the results are presented as the average ± standard deviation from three biological replicates, except for the Δ*ggpS* $P_{trc.x.lacO}$::Ahbet grown for 16 days (one biological replicate).

Mutant	Glycine betaine (µM)		
	0% NaCl	3% NaCl (510 mM)	5% NaCl (860 mM)
WT $P_{trc.x.lacO}$::Ahbet	2.50 ± 0.12	2.69 ± 0.56	1.55 ± 0.08
Δ*ggpS* $P_{trc.x.lacO}$::Ahbet	0.49 ± 0.12	0.24 ± 0.05	0.36 ± 0.22
Δ*sps*Δ*ggpS* $P_{trc.x.lacO}$::Ahbet	2.20 ± 1.25	0.09 ± 0.02	-
Δ*ggpS* $P_{trc.x.lacO}$::Ahbet – 16 days	0.72	2.12	0.18

Table S4 - List of primers used in this study.

Primer name	Sequence*	T_a (ºC)**	Purpose	Reference/ Source
pUC_F	AGGGTTTTCCCAGTCACGAC	57	Amplification of Ahbet synthetic construction	This study
pUC_R	ACACAGGAAACAGCTATGAC			
PS1	AGGGCGGCGGATTTGTCC	60	Confirmation of construct in pSEVA /strains harboring the GB device	Silva-Rocha *et al.* (2013)
PS2	GCGGCAACCGAGCGTTC			
ggpS.5-O	GCTGGCTCGAGAACACCGTAGGGCAGGGAATAGGTC	60	Generation of the Δ*ggpS* mutant / Southern probe	Ferreira *et al.* (2018)
ggpS.5-I	GATTACAACCGGTTGTAATCACGGCTAATGCACCCGACTTCCCGGAACCCAAGTTAATTC			
ggpS.3-O	CTGGCTTTAACCCTGTCGAGGGAACCATCATAG	60	Generation of the Δ*ggpS* mutant	Ferreira *et al.* (2018)
ggpS.3-I	GATTACAACCGGTTGTAATCGTGGTCGGCGGATGGTAACCAAATAACCATTGTC			
sps.5-O	CGCCGCTCGAGGCAATGAATTGGGCGGTGGAATAG	60	Generation of the Δ*sps* mutant	This study
sps.5-I	GATTACACCCGGGTGTAATCAGTTCCAGCACATATTTGGTTTGCCCGCCGGTGTC			
sps.3-O	AAGGTTTCTCGCCACAATAGGTCAGGCTGGCATAG	60	Generation of the Δ*sps* mutant / Southern probe	This study
sps.3-I	GATTACACCCGGGTGTAATCCTGGCCCATTACCGCTTCTTTGAGTTGTTAGACCC			
NeoSacB2F	GCTGGAATTCAGGAAGCGGAACACGTAGAAAG	60	Amplification of the *nptII/sacB* cassette	Schafer *et al.* (1994)
NeoSacB3R	CTACCAATTGCGTAACAGATGAGGGCAAGCGGATGG			
Km.KmScFwd	CTGACCCCGGGTGAATGTCAGCTACTGG	58	Amplification of the *nptII/sacB* cassette	Pinto *et al.* (2015)
KmRev	CAAACCCGGGCGATTTACTTTTCGACCTC			
sps.FO	TAGATCTTGGGCTTGGTTGAGG	63	Confirmation of segregation of Δ*sps* mutant	This study
sps.RO	TGGTGAACATCGGCTTGTC			
sps.FI	CGTCTCCTGCTCAGTGGGATTAAAG	56		
sps.RI	GGTCGGGACAAAGCGAGGATAATAG			
ggpS.FO	GACAAATGGCCGCTTCGCTGTCTTC	63	Confirmation of segregation of Δ*ggpS* mutant	This study
ggpS.RO	CTGCTGGCATCACCCGGTTAGTTTC			
ggpS.FI	CGTGGGCACCAATCCGGCAAATATC	56		Ferreira *et al.* (2018)
ggpS.RI	GGTTAGTCAACACCGCATCGGGTAG			
rnpBF1	CGTTAGGATAGTGCCACAG	56	RNA control PCRs	Pinto *et al.* (2012a)
rnpBR1	CGCTCTTACCGCACCTTTG			

BD16SF1	CACACTGGGACTGAGACAC	56	cDNA control PCRs	Pinto *et al.* (2012b)
BD16SR1	CTGCTGGCACGGAGTTAG			
SD_GSMT_F	TGCTAAGCGGGTACTAGATGC	56	RT-qPCR	This study
SD_GSMT_R	CCTTCGTCCAAGATCAAATCG			
SD_DMT_F	ATTTATGATGCCTCCGTGCG	56		
SD_DMT_R	GCTTCTTCCATCACTTTCCGC			
SD_metX_F	TGAGACACCGGAGCTAATGC	56		
SD_metX_R	AAGCGGGTCTTGTCAGTAGGC			

*Restriction enzyme recognition sites are underlined

**T_a – annealing temperature

Table S5 - Amplicon sizes and parameters derived from RT-qPCR data analysis.

Gene	Amplicon size (bp)	Amplicon Tm (°C)	NTC* (Cq)	Amplification efficiency (E)	R^2	Slope	y-interception
gsmt	351	82.0	N.D.	89.2	0.998	-3.611	23.405
dmt	335	83.0	72.0**	92.0	0.998	-3.529	21.098
metX	312	82.0	N.D.	94.5	0.998	-3.462	19.014

*: no template control, **: primer dimer, N.D.: not detected

References

Ferreira, E. A., Pacheco, C. C., Pinto, F., Pereira, J., Lamosa, P., Oliveira, P. *et al.* (2018). Expanding the toolbox for *Synechocystis* sp. PCC 6803: validation of replicative vectors and characterization of a novel set of promoters. *Synth Biol, 3*.

Montagud, A., Zelezniak, A., Navarro, E., de Cordoba, P. F., Urchueguia, J. F., & Patil, K. R. (2011). Flux coupling and transcriptional regulation within the metabolic network of the photosynthetic bacterium *Synechocystis* sp. PCC 6803. *Biotechnol J, 6*, 330-342.

Pinto, F., Pacheco, C. C., Ferreira, D., Moradas-Ferreira, P., & Tamagnini, P. (2012a). Selection of suitable reference genes for RT-qPCR analyses in cyanobacteria. *PLoS One, 7*, e34983.

Pinto, F., Pacheco, C. C., Oliveira, P., Montagud, A., Landels, A., Couto, N. *et al.* (2015). Improving a *Synechocystis*-based photoautotrophic chassis through systematic genome mapping and validation of neutral sites. *DNA Res, 22*, 425-437.

Pinto, F., van Elburg, K. A., Pacheco, C. C., Lopo, M., Noirel, J., Montagud, A. *et al.* (2012b). Construction of a chassis for hydrogen production: physiological and molecular characterization of a *Synechocystis* sp. PCC 6803 mutant lacking a functional bidirectional hydrogenase. *Microbiol, 158*(2), 448-464.

Schafer, A., Tauch, A., Jager, W., Kalinowski, J., Thierbach, G., & Puhler, A. (1994). Small mobilizable multi-purpose cloning vectors derived from the *Escherichia coli* plasmids pK18 and pK19: selection of defined deletions in the chromosome of *Corynebacterium glutamicum*. *Gene, 145*, 69-73.

Silva-Rocha, R., Martínez-García, E., Calles, B., Chavarría, M., Arce-Rodríguez, A., de las Heras, A. *et al.* (2013). The Standard European Vector Architecture (SEVA): a coherent platform for the analysis and deployment of complex prokaryotic phenotypes. *Nucleic Acids Res, 41*, D666-D675.

Supplementary Datasheet S2

pSEVA351 $P_{trc.x.lacO}$::Ahbet

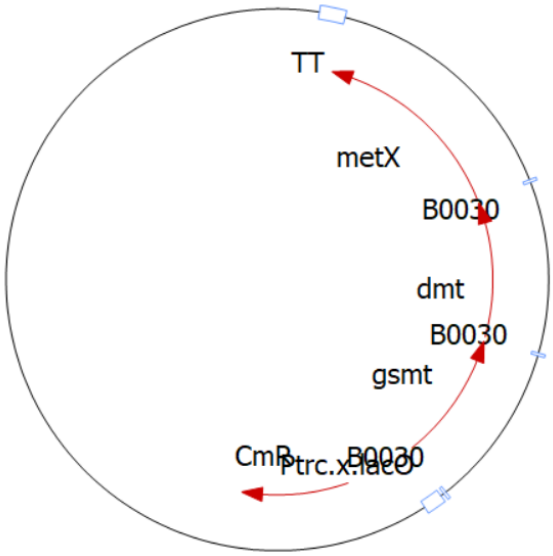

>Ptrc.x.lacO::Ahbet

AATTGTGAGCGCTCACAATTTTCTGAAATGAGCTGTTGACAATTAATCATCCGGCTCGTA
TAATGTGTGGAATTGTGAGCGGATAACAATTTCACACATACTAGAGTACTAGAGATTAAA
GAGGAGAAATACTAGATGGCGATTAAAGAGAAACAGGTGCAAGACTACGGTGAGAATCCC
ATTGAAGTTCGTGACAGCGATCACTATCAAAACGAATACATCGAAGGGTTTGTTGAGAAA
TGGGACGAACTTATTAATTGGCATGCCAGGTCAAGCTCCGAGGGCGAGTTCTTTATTAAG
ACCCTTAAAGAACATGGTGCTAAGCGGGTACTAGATGCGGCCACAGGTACCGGCTTTCAT
TCTATTCGACTAATTGAAGCCGGTTTCGATGTGGCCTCCGTTGATGGGAGCGTGGAAATG
CTGGTTAAAGCCTTTGAGAACGCTACGCGCAAAGACCAGATCCTCCGCACCGTGCACTCC
GACTGGCGTCAAGTTACACGTCATATTCAGGAAAGGTTTGATGCCGTGATTTGTCTAGGG
AATAGTTTTACTCATCTATTTTCCGAGGAAGATCGCCGAAAGACATTAGCTGAGTTCTAT
AGTGTATTGAAGCATGATGGGATTTTGATTCTTGACCAACGCAATTACGATTTGATCTTG
GACGAAGGTTTTAAGAGCAAACATACCTACTACTACTGTGGGGATAATGTAAAGGCCGAA
CCCGAATATGTTGACGATGGTTTGGCGCGCTTTAGATATGAGTTTCCAGATCAAAGCGTA
TATCATCTGAACATGTTTCCCTTGAGGAAGGATTATGTTCGTCGCCTACTGCATGAAGTG
GGTTTCCAGGATATTACGACCTATGGAGATTTTCAAGAAACCTATCACCAAGACGATCCC
GATTTTTATATTCATGTGGCTAAAAAAGATTAATAATACTAGAGATTAAAGAGGAGAAAT
ACTAGATGACAAAAGCCGATGCTGTAGCCAAACAAGCTCAAGACTACTATGATAGTGGAT
CTGCCGATGGATTTTATTACAGGATTTGGGGGGGGGAGGACCTTCACATTGGGATTTATA
ATACCCCCGATGAGCCCATTTATGATGCCTCCGTGCGCACCGTATCAAGGATTTGTGATA
AAATTAAAAACTGGCCCGCCGGAACCAAAGTCCTGGACCTGGGGGCAGGGTATGGTGGCT
CCGCGCGTTATATGGCGAAACATCATGGGTTTGATGTCGATTGCCTAAATATTTCCTTAG
TCCAAAATGAACGGAATCGCCAGATGAATCAAGAACAAGGCCTGGCGGACAAGATCCGGG

TGTTTGATGGGAGCTTTGAGGAACTGCCATTCGAAAATAAATCCTATGATGTGCTTTGGA
GCCAAGATTCCATATTGCATAGTGGCAACCGGCGGAAAGTGATGGAAGAAGCAGATAGGG
TGTTAAAGTCCGGAGGTGATTTTGTTTTTACCGATCCGATGCAAACTGATAACTGCCCCG
AAGGCGTATTGGAGCCTGTTTTAGCTCGAATCCATCTGGATTCTCTCGGCTCTGTCGGAT
TTTACCGGCAAGTGGCCGAGGAACTAGGTTGGGAGTTTGTGGAGTTTGATGAACAAACCC
ACCAACTCGTCAATCATTACAGCCGCGTGCTTCAAGAGCTAGAAGCCCATTATGATCAGT
TGCAACCTGAATGTAGCCAAGAGTACCTAGACCGTATGAAAGTGGGGCTCAATCATTGGA
TCAATGCTGGCAAAAGTGGGTATATGGCCTGGGGTATCTTAAAGTTTCATAAGCCCTAAT
AACCTAGGATTAAAGAGGAGAAATACTAGATGACCGAAGGGCACCCGGATAAAGTATGTG
ATCAAATTAGCGATACAATTTTGGACGCGTTACTGACCCTTGATCCCAATTCCCGCGTTG
CCGCCGAAACAGTCGTTAACACCGGATTAACGTTGGTTACCGGCGAAATTACTTCCCAAG
CCCACATCAACTTTGTAGAGTTGATTCGCCAAAAAATCGCGGAAATTGGTTATACTAATG
CCGATAATGGCTATTCCGCCAACTCCTGTGCGGTTATGTTAGCTATCGACGAGCAAAGTC
CCGATATCTCCCAGGGGGTGACAGCCGCTCAGGAACAGCGTCACGCGTTAAGTGACGACG
AACTGGATAAAATTGGGGCGGGGGATCAAGGTCTGATGTTTGGTTACGCCTGTAATGAGA
CACCGGAGCTAATGCCCCTACCTATTAGTTTGGCCCATAGAATTGCGCTGCGGCTTTCCG
AAGTGCGCAAATCCGGCCAACTAGCGTACCTCAGGCCAGATGGTAAGACCCAAGTCAGTA
TTTTGTACGAAGATGGTTCCCCTGTAGCTATTGATACTATTTTAATCTCCACTCAACATG
ACGAGCACATTGGGGATATTACCGATAACGATGCCGTTCAAGCCAAAATCAAAGCTGATT
TGTGGGACGTGGTAGTCGGGCACTGTTTTTCTGATATTGCCTTGAAGCCTACTGACAAGA
CCCGCTTTATTGTAAACCCAACGGGCAAGTTCGTGGTTGGCGGTCCCCAGGGTGATGCGG
GTCTGACTGGCCGCAAGATTATCGTTGATACCTATGGCGGGTACTCCCGGCATGGCGGGG
GAGCTTTTTCTGGCAAAGATCCTACTAAAGTTGACCGGAGTGCCGCTTACGCCGCCCGTT
ACGTTGCAAAAAACATCGTCGCCGCGGGTTTAGCCGATAAATGTGAAGTCCAAGTATCTT
ATGCCATTGGGGTTGCGCGGCCAGTTTCGGTTTTGATCGATACGTTCGGAACCGGCAAAG
TGGACGAGGAAAAACTCTTGGAAGTGGTCTTGGCCAACTTTGAATTGCGTCCAGCGGGGA
TCATTCAATCTTTGAACCTCCGCAACCTCCCCGCCGAACGCGGGGGTCGTTTCTATCAAG
ATGTGGCCGCGTACGGCCACTTTGGTCGTAATGATCTCGACCTCCCCTGGGAGTACACCG
ACAAAGTTGACGTTTTGAAGGCCGCCTTTGCGTCAAGTCCTCAAGCTGTGGCTGTTTAAT
AACCTAGGCCAGGCATCAAATAAAACGAAAGGCTCAGTCGAAAGACTGGGCCTTTCGTTT
TATCTGTTGTTTGTCGGTGAACGCTCTCTACTAGAGTCACACTGGCTCACCTTCGGGTGG
GCCTTTCTGCGTTTATA

Chapter V. Design and assembly of devices for the production of other compatible solutes in *Synechocystis* sp. PCC 6803

5.1 Introduction

Microorganisms can accumulate large amounts of specific small organic molecules, named compatible solutes, to balance the intra and extracellular osmotic pressure (Kempf & Bremer, 1998). The solutes accumulated by extremophilic bacteria, also referred to as extremolytes, are crucial to enable their survival in hostile habitats (Brown, 1976; Lentzen & Schwarz, 2006). Under extreme salinity conditions, extremophilic bacteria can accumulate ectoine, hydroxyectoine, proline, mannitol, glycine betaine, and trehalose whereas, under extreme temperatures, the preferential compatible solutes are glucosylglycerol, glucosylglycerate, mannosylglycerate and mannosylglyceramide (Becker & Wittmann, 2020).

Among the variety of compatible solutes, ectoine (1,4,5,6-tetrahydro-2-methyl-4-pyrimidinecarboxylic acid) and its hydroxylated derivative hydroxyectoine (1,4,5,6-tetrahydro-2-methyl-5-hydroxy-4-pyrimidinecarboxylic acid) are ubiquitous compounds (Galinski & Trüper, 1994; Inbar & Lapidot, 1988). L-aspartate-β-semialdehyde is the precursor for the synthesis of these compatible solutes, and it is produced from L-aspartate, which is phosphorylated by aspartate kinase (AsK) and then converted to the L-aspartate-β-semialdehyde by the dehydrogenase AsD. L-aspartate-β-semialdehyde is then converted by L-diaminobutyric acid transaminase (EctB) into L-2,4-diaminobutyrate that is subsequently acetylated to *N*-acetyl-2,4-diaminobutyrate by the enzyme L-diaminobutyric acid acetyltransferase (EctA). Finally, ectoine is synthesized through the cyclic condensation of *N*-acetyl-2,4-diaminobutyrate that is catalysed by the enzyme ectoine synthase (EctC). In an additional step, the enzyme ectoine hydroxylase (EctD) catalyses the hydroxylation of ectoine to hydroxyectoine (Figure 1A) (Pastor *et al.*, 2010; Vargas *et al.*, 2008). In addition to acting as osmotic protective agents, ectoine and hydroxyectoine are also excellent biofunctional stabilizers (Barth *et al.*, 2000; Bünger *et al.*, 2001; Graf *et al.*, 2008; Lippert & Galinski, 1992) and skin protectors against ageing, dehydration, inflammation or UV radiation (Buenger & Driller, 2004; Bünger *et al.*, 2001; Graf *et al.*, 2008; Heinrich *et al.*, 2007; Motitschke *et al.*, 2000). These compatible solutes have potential therapeutic uses against atopic dermatitis, lung inflammation, small bowel ischemia and amyloid formation in diabetes and Alzheimer's diseases (Arora *et al.*, 2004; Kanapathipillai *et al.*, 2005; Marini *et al.*, 2014; Sydlik *et al.*, 2009; Wei *et al.*, 2009). The widespread application of these solutes in biotechnology, cosmetics, and medicine has increased their demand and thus they have become added-value compounds. Currently, ectoine is produced in large scale through the "bacterial milking" process using the halophilic bacterium *Halomonas elongata* (Kunte *et al.*, 2014). In this process, high salt concentrations are required for product formation and subsequently, a hypo-osmotic shock is applied to promote the cellular release of ectoine to the medium (Sauer & Galinski, 1998). More

recently, “super-leaky” mutants of *H. elongata* were generated to excrete ectoine during high-salt production, avoiding the need for a hypo-osmotic shock to recover the product (Kunte *et al.*, 2014). However, the high salinity makes the wastewater treatment process difficult, has high costs related to design/durability of the bioreactors, increases the process length and leads to relatively low production yields (Becker *et al.*, 2013; Lang *et al.*, 2011; Onraedt *et al.*, 2005; Schubert *et al.*, 2007). To overcome these disadvantages, efforts have been made to develop and optimize systems that uncouple ectoine production from high osmolarity, using metabolic engineered microorganisms, such as *Halomonas hydrothermalis*, *Escherichia coli* or *Corynebacterium glutamicum* (Gießelmann *et al.*, 2019; Ning *et al.*, 2016; Zhao *et al.*, 2019). The next generation strategies may be focused on the potential of ectoine-producing strains that use inexpensive carbon sources, such as cyanobacteria that can convert CO_2 into bioproducts, which is also beneficial for the environment by sequestrating the excess of atmospheric carbon (Zhang *et al.*, 2017).

Mannosylglycerate is one of the most widespread compatible solutes among marine hyperthermophiles (Santos *et al.*, 2007). This compound is synthesized via a two-step pathway: the enzyme mannosyl-3-phosphoglycerate synthase (MpgS) catalyses the reaction of GDP-mannose and 3-phosphoglycerate into mannosyl-3-phosphoglycerate, which is subsequently dephosphorylated by mannosyl-3-phosphoglycerate phosphatase (MpgP) generating mannosylglycerate (Borges *et al.*, 2014; Martins *et al.*, 1999). Interestingly, the mesophilic bacterium *Dehalococcoides mccartyi* (formerly *Dehalococcoides ethenogenes*) harbours a single gene (*mgsD*), encoding an enzyme with two domains that has high sequence homology to the known MpgS and MpgP (Empadinhas *et al.*, 2004). This compatible solute showed to be one of the best protein stabilizers tested *in vitro* (Borges *et al.*, 2002; Faria *et al.*, 2008). Importantly, mannosylglycerate acts as an enhancer for cosmetic ingredients penetration and can be used as potential treatment for diseases such as Alzheimer’s or Parkinson’s, making mannosylglycerate very attractive for cosmetic and medical industries (Faria *et al.*, 2013; Ryu *et al.*, 2008; Schwarz, 2005). Initially, mannosylglycerate has been obtained by extracting it from the hyperthermophilic species of Archaea, *Pyrococcus furiosus* (Martins & Santos, 1995). More recently, the heterologous expression of MgsD was successfully achieved in *Saccharomyces cerevisiae* and the production of mannosylglycerate was optimized by metabolic engineering (Empadinhas *et al.*, 2004; Faria *et al.*, 2018). However, both for native and heterologous production, the efficiency is low and the overall performance is rather weak (Becker & Wittmann, 2020).

Aiming at producing (hydroxy)ectoine using the photoautotrophic cyanobacterium *Synechocystis* sp. PCC 6803 (hereafter *Synechocystis*), we designed and synthesized two

constructs. For the production of mannosylglycerate, a device was constructed and implemented into the *Synechocystis* wild-type and Δ*ggpS* chassis.

5.2 Material and Methods

5.2.1 Reagents and enzymes

The media components and other reagents were obtained from Fisher Scientific (USA), Merck (Germany) or Sigma Aldrich (USA), and noble agar from Difco (USA). All DNA-modifying enzymes and polymerases were purchased from Thermo Fisher Scientific (USA) and Promega (USA), and standard molecular biology kits were obtained from NZY Tech (Portugal). The Sanger sequencing and oligo synthesis services were provided by STAB VIDA, Lda. (Portugal).

5.2.2 Organisms and culture conditions

Wild-type and mutants of the unicellular, non-motile cyanobacterium *Synechocystis* sp. PCC 6803 substrain GT-Kazusa (Kanesaki *et al.*, 2012; Trautmann *et al.*, 2012) (obtained from the Pasteur Culture Collection, France) were maintained in Erlenmeyer flasks batch cultures with BG11 medium (Stanier *et al.*, 1971) at 30 ºC with orbital shaking (150 rpm) under a 12 h light /12 h dark regimen. Light intensity was 25 µE/m^2/s in all experiments and Cosine-corrected irradiance was measured using a Dual Solar/Electric Quantum Meter (Spectrum Technologies, Inc.; USA). For solid BG11, the medium was supplemented with 1.5% (wt/vol) noble agar, 0.3% (wt/vol) sodium thiosulfate and 10 mM TES-KOH buffer, pH 8.2 (Stanier *et al.*, 1971). For the selection and maintenance of mutants, BG11 medium was supplemented with kanamycin (Km, 10-25 µg/mL). For cloning purposes, *E. coli* strains MG1655, DH5α and TOP10 were used. Cells were grown at 37 ºC in LB medium (Sambrook & Russel, 2001), supplemented with ampicillin (Amp, 100 µg/mL) or Km (50 µg/mL).

5.2.3 DNA and RNA extraction

Cyanobacterial genomic DNA (gDNA) extraction was carried out according to the procedure described previously (Tamagnini *et al.*, 1997). For RNA extraction, 50 mL of *Synechocystis* culture at $OD_{730} \approx 1$, grown in BG11 or BG11 supplemented with 3% or 5% (wt/vol) NaCl (in the conditions described above), were centrifuged for 10 min at 4,470 *g*; cell pellets were treated with RNAprotect Bacteria Reagent (Qiagen, Germany) according to instructions, and stored at -80 °C. RNA was extracted using the TRIzol® Reagent (Ambion) according to the method described previously (Leitão *et al.*, 2006) with adaptations. Cells were disrupted using a FastPrep®-24 (MP Biomedicals) in 2 cycles of 1 min at 4.0 m/s and the

RNA samples were treated with 1 U of RQ1 RNase-Free DNase (Promega) according to manufacturer's instructions.

5.2.4 Design, DNA synthesis and assembly of the devices

Two synthetic constructs meant for the production of (hydroxy)ectoine were designed. One was based on the information available for *Chromohalobacter salexigens* - Cs(h)ect - and includes the Open Reading Frames (ORFs) from *ectA* (L-diaminobutyric acid acetyltransferase), *ectB* (L-diaminobutyric acid transaminase), *ectC* (ectoine synthase) and *ectD* (ectoine hydroxylase) genes. The other construct was based on the metabolic pathway described for *Methylomicrobium alcaliphilum* - Ma(h)ect - containing the ORFs from *ectABCD* and *asK* (aspartate kinase) genes. All the ORF sequences were codon optimized for *Synechocystis* using the Gene Designer 2.0 software (DNA 2.0, Inc.; USA), the restriction sites incompatible with BioBrick™ standard RFC[10] were eliminated and double stops codons included. Each ORF is preceded by the BioBrick™ (BB) ribosome binding site (RBS) B0030 and, the double terminator B0015 was included after the *ectD* or *asK* ORFs. In addition, the synthetic constructs are flanked by the prefix and suffix sequences of the BB RFC[10] standard. All the BB sequences were retrieved from the Registry of Standard Biological Parts (parts.igem.org). Subsequently, the sequences of the two synthetic constructs Cs(h)ect and Ma(h)ect were synthesized and cloned into *Sma*I digested pSB3K3 or pBluescript II SK(-) (Epoch Life Science, Inc.; USA), respectively (Table 1). These plasmids were cut with *Xba*I and *Pst*I and the plasmids (pJ201) with the promoters $P_{trc.x.tetO2}$ or $P_{trc.x.lacO}$ were cut with *Spe*I and *Pst*I.

The device for the synthesis of mannosylglycerate harbours the *mgsD* ORF sequence from *D. mccartyi* that encodes the bifunctional protein able to catalyse the synthesis of this compatible solute. For the construction of the mannosylglycerate device, the *mgsD* ORF was PCR-amplified from the plasmid pRS425 with the primers BB.mgsD.F/R (Table 2), using Phusion high-fidelity DNA polymerase, according to the manufacturer's instructions. The PCR product was purified using NZYGelpure kit, digested with *EcoR*I and *Spe*I and cloned in pSB1A2 plasmid (Table 1), digested with the same restriction enzymes. The P_{rnpB} B0030 fragment (Ferreira *et al.*, 2018) was excised from pSB1A2 using *EcoR*I and *Spe*I and cloned upstream of *mgsD* ORF in pSB1A2 (cut with *EcoR*I and *Xba*I). The generated device P_{rnpB}::*mgsD* (Table 1) was cut from pSB1A2 with *EcoR*I and *Spe*I and transferred to pSEVA251 shuttle vector, obtained from the "Standard European Vector Architecture" repository (Silva-Rocha *et al.*, 2013), digested with *Xba*I and *EcoR*I and dephosphorylated (Table 1). The assembly of the device was confirmed by PCR, restriction analysis and Sanger sequencing.

Table 1. List of plasmids used in this study.

Designation	Plasmid	Description	Source
Cs(h)ect	pSB3K3	(Hydroxy)ectoine construct based on *C. salexigens*	This study
Ma(h)ect	pBSK	(Hydroxy)ectoine construct based on *M. alcaliphilum*	This study
mgsD	pRS425	Mannosylglycerate ORF based on *D. mccartyi*	Provided by Prof. H. Santos (ITQB)
mgsD	pSB1A2	Mannosylglycerate ORF based on *D. mccartyi*	This study
P_{rnpB} B0030 *mgsD*	pSB1A2 / pSEVA251	Mannosylglycerate device	This study

Table 2. List of primers used in this study.

Primer name	Sequence*	T_a (ºC)**	Purpose	Reference /Source
BB.mgsD.F	GTTTCTTCGAATTCGCGGCCGCTTCTAGATGCGCATTGAAAGCCTGCGTCCC	72	Amplification of *mgsD* ORF	This study
BB.mgsD.R	GTTTCTTCCTGCAGCGGCCGCTACTAGTATTATTATTATTCCATGGGCAGTATTATATC			
mgsD.F	GCCTGGCAGTTATCTATCAC	54	Confirmation of the presence of pSEVA251 P_{rnpB}::*mgsD* in *Synechocystis*	This study
PS2	GCGGCAACCGAGCGTTC			Silva-Rocha *et al.* (2013)
BD16SF1	CACACTGGGACTGAGACAC	56	RNA and cDNA control PCRs	Pinto *et al.* (2012)
BD16SR1	CTGCTGGCACGGAGTTAG			
RT_mgsD.F	GAGATGGTAGACCAACAGGC	56	RT-PCR	This study
RT_mgsD.R	GCGGATAAGCCCGTCTTTAC			

*Restriction enzyme recognition sites are underlined

** T_a – annealing temperature

5.2.5 Introduction of the mannosylglycerate device into *Synechocystis*

The pSEVA251 plasmid containing the device P_{rnpB}::*mgsD* was introduced into *Synechocystis* by electroporation following the protocol previously described (Ferreira *et al.*, 2018). The presence of the device was confirmed in *Synechocystis* transformants by PCR using specific primers (Table 2), as described by Ferreira *et al.* (2018).

5.2.6 Transcription analysis by RT-PCR

After RNA extraction, RNA concentration and purity (the ratios A_{260}/A_{280} and A_{260}/A_{230}) were measured using a NanoDrop ND-1000 spectrophotometer (NanoDrop Technologies, Inc.; USA). The quality and integrity of the RNA samples was also inspected in 1% (wt/vol) agarose gel performed by standard protocols using TAE buffer. The absence of genomic DNA contamination was checked by PCR, in reaction mixtures containing: 0.5 U of GoTaq® G2 Flexi DNA Polymerase, 1x Green GoTaq Flexi buffer, 200 µM of each dNTP, 1.5 mM

$MgCl_2$, 0.25 µM of each BD16S primers (Table 2), and 200 ng of total RNA. The PCR profile was: 5 min at 95 °C followed by 25 cycles of 20 s at 95 °C, 20 s at 56 °C and 20 s at 72 °C, and a final extension at 72 °C for 5 min. The PCR reactions were run on 1% (wt/vol) agarose gel as described above. For cDNA synthesis, 1 µg of total RNA was transcribed with the iScript™ Select cDNA Synthesis Kit (Bio-Rad) in a final volume of 20 µL, following the manufacturer's instructions. A control PCR was performed using 1 µL of cDNA as template, the BD16S primers (Table 2), and the same reaction conditions and PCR program described above. RT-PCR was performed using 1 µL of template cDNA and the primer pair RT_mgsD.F/R (Table 2). The absence/presence and size of the amplicon were checked by agarose gel electrophoresis.

5.2.7 Compatible solutes quantification

Cultures of *Synechocystis* wild-type (WT) and the Δ*ggpS* mutant harbouring the P_{rnpB}::*mgsD* device were grown in BG11 supplemented with 3% (wt/vol) NaCl, in the conditions described above, at an initial OD_{730}≈0.5. The quantification of the compatible solutes - sucrose, glutamate, glucosylglycerol and mannosylglycerate - was performed using 500 mL of culture (distributed in 50 mL cultures in 100 mL Erlenmeyer flasks). Four days after inoculation, cells were harvested by centrifugation at 4,470 *g* for 10 min at RT. Cells were washed by adding 100 mL of cold distilled water with 3% (wt/vol) NaCl solution (identical to the growth medium). Centrifugation was repeated and the cell pellet was resuspended in 50 mL of the respective solution. From this suspension, a 0.5 mL aliquot was centrifuged and stored at -20 ºC to be used later for protein quantification. The remaining cell suspension was centrifuged at 4 ºC and the cell pellet was stored at -20 ºC. Ethanol-chloroform extraction of the compatible solutes was performed as described in Ferreira *et al.* (2018) with adaptations. Briefly, cell pellets were suspended in 25 mL of 80% (vol/vol) ethanol and subsequently transferred to a 100 mL round flask containing a magnetic stirrer. The flask was connected to a coil condenser (circulating cold water) and heated at 100 ºC with stirring, for 10 min. The suspension was transferred to a 50 mL tube and centrifuged at 4,000 *g* for 10 min at RT. The supernatant was stored, and the pellet resuspended in 20 mL of 80% (vol/vol) ethanol for a new extraction process. The remainder protocol was performed as described in Santos *et al.* (2006), and the detection, identification and quantification of compatible solutes was performed by Proton NMR (at ITQB magnetic resonance center, CERMAX). For the normalization of the compatible solutes concentration, protein content was determined using crude cell extracts obtained by sonication, as described by Pinto *et al.* (2015); and protein quantification was performed using the Bio-Rad Protein Assay. The compatible solutes concentration was expressed as µmol per mg of protein.

5.3 Results and Discussion

5.3.1 (Hydroxy)ectoine

Envisaging the heterologous production of (hydroxy)ectoine in *Synechocystis*, two constructs were designed based on the biosynthetic pathways described for the halophilic bacteria *Chromohalobacter salexigens* (Cs) and *Methylomicrobium alcaliphilum* (Ma) (Figure 1A, Garcia-Estepa *et al.* (2006); Reshetnikov *et al.* (2006)). The two constructs, Cs(h)ect and Ma(h)ect, contain the Open Reading Frames (ORFs) *ectABC* for the synthesis of ectoine, and additionally the *ectD* for the synthesis of hydroxyectoine. The enzymes aspartate kinase (AsK) and L-aspartate-β-semialdehyde dehydrogenase (AsD), also involved in the production of (hydroxy)ectoine, are natively synthesized by *Synechocystis*. In the case of the Ma(h)ect construct, the *asK* ORF was included since, in *M. alcaliphilum*, it is part of the same operon *ectABCasK* (Reshetnikov *et al.*, 2006). The sequences of all the ORFs were codon optimized for *Synechocystis*. For an approximate indication of the likely success of expression of the codon-optimized sequences in *Synechocystis*, the codon adaptation index (CAI) was calculated, since it is a measurement of the relative adaptiveness of the codon usage of a gene toward the codon usage of highly expressed genes (Puigbò *et al.*, 2008). The results obtained indicate that the optimized sequences are more likely to be expressed in *Synechocystis* than the original ones (Table 3).

Table 3. Codon adaptation index (CAI) of the original and codon optimized sequences of *ectA*, *ectB*, *ectC*, *ectD* and *asK* from *C. salexigens* (Cs) or *M. alcaliphilum* (Ma) for *Synechocystis* sp. PCC 6803.

Sequence	CAI - original	CAI - optimized
Cs_*ectA*	0.65	0.75
Cs_*ectB*	0.67	0.76
Cs_*ectC*	0.67	0.75
Cs_*ectD*	0.65	0.74
Ma_*ectA*	0.69	0.73
Ma_*ectB*	0.72	0.73
Ma_*ectC*	0.71	0.77
Ma_*ectD*	0.66	0.76
Ma_*asK*	0.72	0.74

In addition, the restriction sites incompatible with the BioBrick standard RFC[10] were eliminated. The RBS B0030 and double stop codons (TAATAA) were included before and after each ORF, respectively. A double terminator (B0015) was included in the end of the synthetic constructs (Figure 1B, Cs(h)ect and Ma(h)ect), that were flanked by the prefix and

suffix sequences of the BioBrick RFC[10] standard (Canton *et al.*, 2008), enabling the use of the standard assembly method to include the regulatory element (promoter).

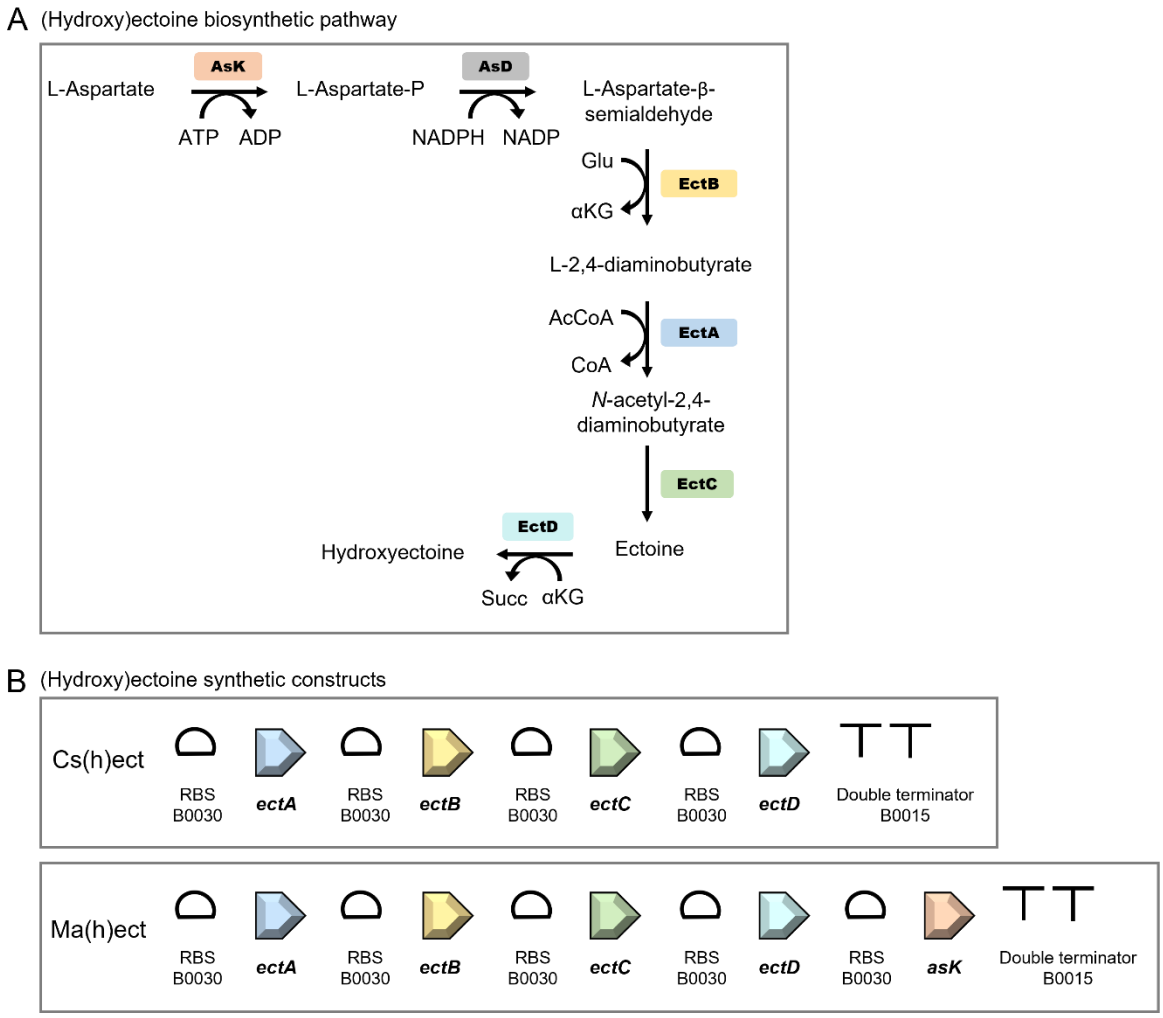

Figure 1. (Hydroxy)ectoine biosynthetic pathway based on *Chromohalobacter salexigens* (Cs) or *Methylomicrobium alcaliphilum* (Ma). Ask - Aspartate kinase, AsD - L-aspartate-β-semialdehyde dehydrogenase, EctB - L-diaminobutyric acid transaminase, EctA - L-diaminobutyric acid acetyltransferase, EctC - Ectoine synthase, EctD - Ectoine hydroxylase, Glu – Glutamate, αKG - α-ketoglutarate, AcCoA - Acetyl-coenzyme A, CoA - Coenzyme A, Succ - Succinate (A). The (hydroxy)ectoine synthetic constructs Cs(h)ect and Ma(h)ect include the RBS B0030, the ORFs *ectA, ectB, ectC, ectD, asK* codon optimized for *Synechocystis* sp. PCC 6803, and the double terminator B0015 (B).

After the synthesis of the constructs, we attempted to clone them under control of $P_{trc.x.lacO}$ or $P_{trc.x.tetO2}$ (for more details see Chapter III), in TOP10 or MG1655 *E. coli* strains. However, no transformant colonies were obtained. This could be due to a metabolic burden at the transcriptional level caused by the strength of the promoters used or other unknown factors. Possible ways to surpass the metabolic burden would be to use a weak promoter such as

P_{rnpB} (Huang *et al.*, 2010) or to use an *E. coli* strain harbouring the regulators LacI or TetR to repress the transcription. However, further experiments are needed to reach definitive conclusions.

5.3.2 Mannosylglycerate

For the heterologous production of mannosylglycerate in *Synechocystis*, a device was designed based on the metabolic pathway described for the mesophilic bacterium *D. mccartyi* (Figure 2A) (Empadinhas *et al.*, 2004). This device comprises *mgsD* that encodes the mannosyl-3-phosphoglycerate synthase and mannosyl-3-phosphoglycerate phosphatase (Empadinhas *et al.*, 2004). The codon adaptation index (CAI) was above 0.69, indicating a high probability of successful expression in *Synechocystis* and thus, the sequence was not codon optimized for *Synechocystis*. The reference cyanobacterial constitutive promoter P_{rnpB} (Huang *et al.*, 2010) and the RBS B0030 were cloned upstream of the *mgsD* ORF, originating the P_{rnpB}::*mgsD* device (Figure 2B).

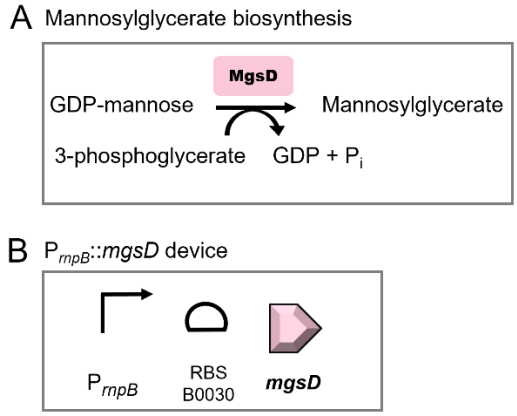

Figure 2. Mannosylglycerate biosynthesis based on *Dehalococcoides mccartyi* involves MgsD (mannosyl-3-phosphoglycerate synthase and mannosyl-3-phosphoglycerate phosphatase) (A). The P_{rnpB}::*mgsD* device for the production of mannosylglycerate in *Synechocystis* sp. PCC 6803 includes the promoter P_{rnpB}, the RBS B0030 and the *mgsD* ORF (B).

The P_{rnpB}::*mgsD* device was implemented into the *Synechocystis* wild-type (WT) and the Δ*ggpS* chassis (for more details on this mutant see Chapter IV), using the replicative plasmid pSEVA251. The presence of the device was confirmed by PCR (Figure 3).

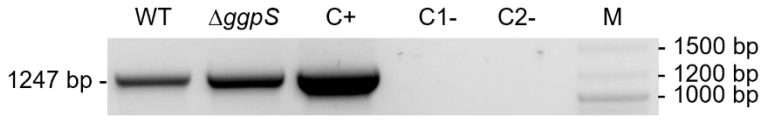

Figure 3. PCR analysis confirming the presence of pSEVA251 P_{rnpB}::*mgsD* in *Synechocystis* sp. PCC 6803 wild-type (WT) and the Δ*ggpS* mutant. PCR reactions were performed using mgsD.F and PS2 primers (primers listed in Table 2). The expected amplicon size is indicated to the left. C+, positive control (pSEVA251 P_{rnpB}::*mgsD*); C1-, negative control (*Synechocystis* WT genomic DNA); C2-, negative control (no DNA template); M, molecular marker: GeneRuler DNA Ladder Mix (Thermo Fisher Scientific™); bp, base pairs.

For the transcriptional analysis, cultures of *Synechocystis* WT and the Δ*ggpS* mutant harbouring the P_{rnpB}::*mgsD* device were grown in BG11 or BG11 supplemented with 3% or 5% NaCl and harvested for RNA extraction. The transcription of *mgsD* was analyzed by RT-PCR. Preliminary results showed that *mgsD* is transcribed in the two transformants (WT and Δ*ggpS*) and in all conditions tested (0%, 3% and 5% NaCl, Figure 4).

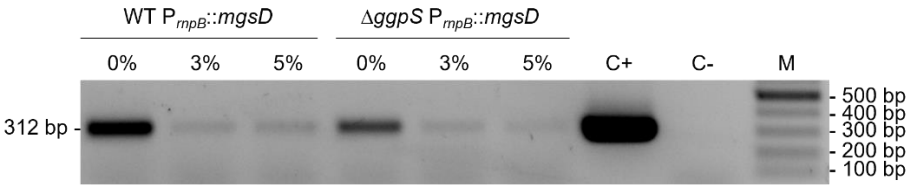

Figure 4. RT-PCR detection of *mgsD* transcript in *Synechocystis* sp. PCC 6803 WT and Δ*ggpS* mutant harbouring the device P_{rnpB}::*mgsD*. The total RNA was isolated from cultures grown in BG11 or BG11 supplemented with 3% or 5% (wt/vol) NaCl. RT-PCRs were performed using RT_mgsD.F/R primers (primers listed in Table 2). The expected amplicon size is indicated to the left. C+, positive control (pSEVA251 P_{rnpB}::*mgsD*); C-, negative control (no DNA template); M, molecular marker: GeneRuler DNA Ladder Mix (Thermo Fisher Scientific™); WT, wild-type; bp, base pairs.

In addition to the transcriptional analysis, the compatible solutes pools of *Synechocystis* WT P_{rnpB}::*mgsD* and Δ*ggpS* P_{rnpB}::*mgsD* were analysed by H-NMR. Preliminary results showed that no mannosylglycerate could be detected in cultures grown under 3% NaCl. The amount of the native compatible solutes sucrose, glutamate or glucosylglycerol was very similar to the ones obtained for the respective backgrounds in 3% NaCl [see Chapter IV, Figure 2A (WT) and Figure 2C (Δ*ggpS*)].

The fact that mannosylglycerate was not detected could be related to low transcript levels of *mgsD*, as the P_{rnpB} promoter used in the device is weak (Huang *et al.*, 2010). This could be solved by replacing it by a stronger promoter, e.g. $P_{trc.x.tetO2}$ or $P_{trc.x.lacO}$ (Ferreira *et al.*, 2018). However, the absence of mannosylglycerate could also be due to the unavailability or low availability of the required precursors, GDP-mannose or 3-phosphoglycerate. This issue could be addressed by supplementing the culture medium with these precursors. Alternatively, the synthesis of the precursors could be enhanced by overexpressing part of the respective pathways. Previously, Empadinhas *et al.* (2004) did not obtain synthesis of mannosylglycerate in *E. coli* containing the *mgsD* from *D. mccartyi*, perhaps because the required substrates were not available (Empadinhas *et al.*, 2004). Recently, *Saccharomyces cerevisiae*, containing *mgsD*, was metabolically engineered to enhance the synthesis of GDP-mannose by overexpressing the genes encoding mannose-6-phosphate isomerase and GDP-mannose pyrophosphorylase, which increased the yield and productivity of mannosylglycerate (Faria *et al.*, 2018).

5.4 Acknowledgements

We wish to acknowledge Catarina Pacheco (i3S/IBMC) for the conceptual design of the work and all the support provided; Filipe Pinto (i3S/IBMC) for designing the (hydroxy)ectoine constructs; Prof. Helena Santos (ITQB, Universidade Nova de Lisboa) for kindly providing the *mgsD* ORF and Pedro Lamosa (ITQB, Universidade Nova de Lisboa) for the quantification of compatible solutes by proton NMR. We are also grateful to Prof. Paula Gomes, Luísa Aguiar and Mélanie Fonte (LAQV-REQUIMTE, Faculdade de Ciências, Universidade do Porto) for providing the equipment and technical assistance regarding compatible solutes extraction.

5.5 References

Arora, A., Ha, C., & Park, C. B. (2004). Inhibition of insulin amyloid formation by small stress molecules. *FEBS Lett, 564*(1-2), 121-125.

Barth, S., Huhn, M., Matthey, B., Klimka, A., Galinski, E. A., & Engert, A. (2000). Compatible-solute-supported periplasmic expression of functional recombinant proteins under stress conditions. *Appl Environ Microbiol, 66*(4), 1572-1579.

Becker, J., Schafer, R., Kohlstedt, M., Harder, B. J., Borchert, N. S., Stoveken, N., Bremer, E., & Wittmann, C. (2013). Systems metabolic engineering of *Corynebacterium glutamicum* for production of the chemical chaperone ectoine. *Microb Cell Fact, 12*(110).

Becker, J., & Wittmann, C. (2020). Microbial production of extremolytes - high-value active ingredients for nutrition, health care, and well-being. *Curr Opin Biotechnol, 65*, 118-128.

Borges, N., Jorge, C. D., Gonçalves, L. G., Gonçalves, S., Matias, P. M., & Santos, H. (2014). Mannosylglycerate: structural analysis of biosynthesis and evolutionary history. *Extremophiles, 18*(5), 835-852.

Borges, N., Ramos, A., Raven, N. D., Sharp, R. J., & Santos, H. (2002). Comparative study of the thermostabilizing properties of mannosylglycerate and other compatible solutes on model enzymes. *Extremophiles, 6*(3), 209-216.

Brown, A. (1976). Microbial water stress. *Bacteriol Rev, 40*(4), 803-846.

Buenger, J., & Driller, H. (2004). Ectoin: An effective natural substance to prevent UVA-induced premature photoaging. *Skin Pharmacol Physiol, 17*(5), 232-237.

Bünger, J., Degwert, J., & Driller, H. (2001). The protective function of compatible solute ectoin on the skin, skin cells and its biomolecules with respect to UV radiation, immunosuppression and membrane damage. *IFSCC Mag, 4*(2), 127-131.

Canton, B., Labno, A., & Endy, D. (2008). Refinement and standardization of synthetic biological parts and devices. *Nat Biotechnol, 26*, 787-793.

Empadinhas, N., Albuquerque, L., Costa, J., Zinder, S. H., Santos, M. A., Santos, H., & da Costa, M. S. (2004). A gene from the mesophilic bacterium *Dehalococcoides ethenogenes* encodes a novel mannosylglycerate synthase. *J Bacteriol, 186*(13), 4075-4084.

Faria, C., Borges, N., Rocha, I., & Santos, H. (2018). Production of mannosylglycerate in *Saccharomyces cerevisiae* by metabolic engineering and bioprocess optimization. *Microb Cell Fact, 17*(1), 1-11.

Faria, C., Jorge, C. D., Borges, N., Tenreiro, S., Outeiro, T. F., & Santos, H. (2013). Inhibition of formation of α-synuclein inclusions by mannosylglycerate in a yeast model of Parkinson's disease. *Biochim Biophys Acta, 1830*(8), 4065-4072.

Faria, T. Q., Mingote, A., Siopa, F., Ventura, R., Maycock, C., & Santos, H. (2008). Design of new enzyme stabilizers inspired by glycosides of hyperthermophilic microorganisms. *Carbohydr Res, 343*(18), 3025-3033.

Ferreira, E. A., Pacheco, C. C., Pinto, F., Pereira, J., Lamosa, P., Oliveira, P., Kirov, B., Jaramillo, A., & Tamagnini, P. (2018). Expanding the toolbox for *Synechocystis* sp. PCC 6803: validation of replicative vectors and characterization of a novel set of promoters. *Synth Biol, 3*.

Galinski, E. A., & Trüper, H. G. (1994). Microbial behaviour in salt-stressed ecosystems. *FEMS Microbiol Rev, 15*(2-3), 95-108.

Garcia-Estepa, R., Argandona, M., Reina-Bueno, M., Capote, N., Iglesias-Guerra, F., Nieto, J. J., & Vargas, C. (2006). The *ectD* gene, which is involved in the synthesis of the compatible solute hydroxyectoine, is essential for thermoprotection of the halophilic bacterium *Chromohalobacter salexigens*. *J Bacteriol, 188*(11), 3774-3784.

Gießelmann, G., Dietrich, D., Jungmann, L., Kohlstedt, M., Jeon, E. J., Yim, S. S., Sommer, F., Zimmer, D., Mühlhaus, T., & Schroda, M. (2019). Metabolic engineering of *Corynebacterium glutamicum* for high-level ectoine production: design, combinatorial assembly, and implementation of a transcriptionally balanced heterologous ectoine pathway. *Biotechnol J, 14*(9), 1800417.

Graf, R., Anzali, S., Buenger, J., Pfluecker, F., & Driller, H. (2008). The multifunctional role of ectoine as a natural cell protectant. *Clin Dermatol, 26*(4), 326-333.

Heinrich, U., Garbe, B., & Tronnier, H. (2007). In vivo assessment of ectoin: a randomized, vehicle-controlled clinical trial. *Skin Pharmacol Physiol, 20*(4), 211-218.

Huang, H. H., Camsund, D., Lindblad, P., & Heidorn, T. (2010). Design and characterization of molecular tools for a Synthetic Biology approach towards developing cyanobacterial biotechnology. *Nucleic Acids Res, 38*, 2577-2593.

Inbar, L., & Lapidot, A. (1988). The structure and biosynthesis of new tetrahydropyrimidine derivatives in actinomycin D producer Streptomyces parvulus. Use of 13C-and 15N-labeled L-glutamate and 13C and 15N NMR spectroscopy. *J Biol Chem, 263*(31), 16014-16022.

Kanapathipillai, M., Lentzen, G., Sierks, M., & Park, C. B. (2005). Ectoine and hydroxyectoine inhibit aggregation and neurotoxicity of Alzheimer's beta-amyloid. *FEBS Lett, 579*(21), 4775-4780.

Kanesaki, Y., Shiwa, Y., Tajima, N., Suzuki, M., Watanabe, S., Sato, N., Ikeuchi, M., & Yoshikawa, H. (2012). Identification of substrain-specific mutations by massively parallel whole-genome resequencing of *Synechocystis* sp. PCC 6803. *DNA Res, 19*, 67-79.

Kempf, B., & Bremer, E. (1998). Uptake and synthesis of compatible solutes as microbial stress responses to high-osmolality environments. *Arch Microbiol, 170*(5), 319-330.

Kunte, H. J., Lentzen, G., & Galinski, E. (2014). Industrial production of the cell protectant ectoine: protection mechanisms, processes, and products. *Curr Biotechnol, 3*(1), 10-25.

Lang, Y.-j., Bai, L., Ren, Y.-n., Zhang, L.-h., & Nagata, S. (2011). Production of ectoine through a combined process that uses both growing and resting cells of *Halomonas salina* DSM 5928 T. *Extremophiles, 15*(2), 303-310.

Leitão, E., Pereira, S., Bondoso, J., Ferreira, D., Pinto, F., Moradas-Ferreira, P., & Tamagnini, P. (2006). Genes involved in the maturation of hydrogenase(s) in the nonheterocystous cyanobacterium *Lyngbya majuscula* CCAP 1446/4. *Int J Hydrog Energy, 31*, 1469-1477.

Lentzen, G., & Schwarz, T. (2006). Extremolytes: Natural compounds from extremophiles for versatile applications. *Appl Microbiol Biotechnol, 72*(4), 623-634.

Lippert, K., & Galinski, E. A. (1992). Enzyme stabilization be ectoine-type compatible solutes: protection against heating, freezing and drying. *Appl Microbiol Biotechnol, 37*, 61-65.

Marini, A., Reinelt, K., Krutmann, J., & Bilstein, A. (2014). Ectoine-containing cream in the treatment of mild to moderate atopic dermatitis: a randomised, comparator-controlled, intra-individual double-blind, multi-center trial. *Skin Pharmacol Physiol, 27*(2), 57-65.

Martins, L. O., Empadinhas, N., Marugg, J. D., Miguel, C., Ferreira, C., da Costa, M. S., & Santos, H. (1999). Biosynthesis of mannosylglycerate in the thermophilic bacterium *Rhodothermus marinus*: biochemical and genetic characterization of a mannosylglycerate synthase. *J Biol Chem, 274*(50), 35407-35414.

Martins, L. O., & Santos, H. (1995). Accumulation of mannosylglycerate and di-*myo*-inositol-phosphate by *Pyrococcus furiosus* in response to salinity and temperature. *Appl Environ Microbiol, 61*(9), 3299-3303.

Motitschke, L., Driller, H., & Galinski, E. (2000). Ectoin and ectoin derivatives as moisturizers in cosmetics. Patent US060071.

Ning, Y., Wu, X., Zhang, C., Xu, Q., Chen, N., & Xie, X. (2016). Pathway construction and metabolic engineering for fermentative production of ectoine in *Escherichia coli*. *Metab Eng, 36*, 10-18.

Onraedt, A. E., Walcarius, B. A., Soetaert, W. K., & Vandamme, E. J. (2005). Optimization of ectoine synthesis through fed-batch fermentation of *Brevibacterium epidermis*. *Biotechnol Prog, 21*(4), 1206-1212.

Pastor, J. M., Salvador, M., Argandoña, M., Bernal, V., Reina-Bueno, M., Csonka, L. N., Iborra, J. L., Vargas, C., Nieto, J. J., & Cánovas, M. (2010). Ectoines in cell stress protection: Uses and biotechnological production. *Biotechnol Adv, 28*(6), 782-801.

Pinto, F., Pacheco, C. C., Oliveira, P., Montagud, A., Landels, A., Couto, N., Wright, P. C., Urchueguía, J. F., & Tamagnini, P. (2015). Improving a *Synechocystis*-based photoautotrophic chassis through systematic genome mapping and validation of neutral sites. *DNA Res, 22*, 425-437.

Pinto, F., van Elburg, K. A., Pacheco, C. C., Lopo, M., Noirel, J., Montagud, A., Urchueguía, J. F., Wright, P. C., & Tamagnini, P. (2012). Construction of a chassis for hydrogen production: physiological and molecular characterization of a *Synechocystis* sp. PCC 6803 mutant lacking a functional bidirectional hydrogenase. *Microbiol, 158*(2), 448-464.

Puigbò, P., Bravo, I. G., & Garcia-Vallvé, S. (2008). E-CAI: a novel server to estimate an expected value of Codon Adaptation Index (eCAI). *BMC Bioinformatics, 9*(1), 1-7.

Reshetnikov, A. S., Khmelenina, V. N., & Trotsenko, Y. A. (2006). Characterization of the ectoine biosynthesis genes of haloalkalotolerant obligate methanotroph "*Methylomicrobium alcaliphilum* 20Z". *Arch Microbiol, 184*(5), 286-297.

Ryu, J., Kanapathipillai, M., Lentzen, G., & Park, C. B. (2008). Inhibition of β-amyloid peptide aggregation and neurotoxicity by α-d-mannosylglycerate, a natural extremolyte. *Peptides, 29*(4), 578-584.

Sambrook, J., & Russel, D. (2001). *Molecular Cloning: a laboratory manual* (3rd ed.): Cold Spring Harbor Laboratory Press, NY, USA.

Santos, H., Lamosa, P., & Borges, N. (2006). Characterization and quantification of compatible solutes in (hyper)thermophilic microorganisms. In F. A. Rainey & A. Oren (Eds.), *Extremophiles* Vol. 35, 173-199: Methods in Microbiology, Academic Press.

Santos, H., Lamosa, P., Faria, T. Q., Borges, N., & Neves, C. (2007). The physiological role, biosynthesis, and mode of action of compatible solutes from (hyper)thermophiles. In C. Gerday & N. Glansdorff (Eds.), *Physiology and biochemistry of extremophiles* 86-103: ASM Press.

Sauer, T., & Galinski, E. A. (1998). Bacterial milking: a novel bioprocess for production of compatible solutes. *Biotechnol Bioeng, 57*(3), 306-313.

Schubert, T., Maskow, T., Benndorf, D., Harms, H., & Breuer, U. (2007). Continuous synthesis and excretion of the compatible solute ectoine by a transgenic, nonhalophilic bacterium. *Appl Environ Microbiol, 73*(10), 3343-3347.

Schwarz, T. (2005). Use of beta-mannosylglycerate and derivatives in cosmetic and dermatological formulations. US20050100534.

Silva-Rocha, R., Martínez-García, E., Calles, B., Chavarría, M., Arce-Rodríguez, A., de las Heras, A., Páez-Espino, A. D., Durante-Rodríguez, G., Kim, J., Nikel, P. I., Platero, R., & de Lorenzo, V. (2013). The Standard European Vector Architecture (SEVA): a coherent platform for the analysis and deployment of complex prokaryotic phenotypes. *Nucleic Acids Res, 41*, D666-D675.

Stanier, R., Kunisawa, R., Mandel, M., & Cohen-Bazire, G. (1971). Purification and properties of unicellular blue-green algae (order *Chroococcales*). *Bacteriol Rev, 35*, 171-205.

Sydlik, U., Gallitz, I., Albrecht, C., Abel, J., Krutmann, J., & Unfried, K. (2009). The compatible solute ectoine protects against nanoparticle-induced neutrophilic lung inflammation. *Am J Respir Crit Care Med, 180*(1), 29-35.

Tamagnini, P., Troshina, O., Oxelfelt, F., Salema, R., & Lindblad, P. (1997). Hydrogenases in *Nostoc* sp. strain PCC 73102, a strain lacking a bidirectional enzyme. *Appl Environ Microbiol, 63*, 1801-1807.

Trautmann, D., Voß, B., Wilde, A., Al-Babili, S., & Hess, W. R. (2012). Microevolution in cyanobacteria: re-sequencing a motile substrain of *Synechocystis* sp. PCC 6803. *DNA Res, 19*, 435-448.

Vargas, C., Argandona, M., Reina-Bueno, M., Rodriguez-Moya, J., Fernandez-Aunion, C., & Nieto, J. J. (2008). Unravelling the adaptation responses to osmotic and temperature stress in *Chromohalobacter salexigens*, a bacterium with broad salinity tolerance. *Saline Syst, 4*(1), 1-9.

Wei, L., Wedeking, A., Büttner, R., Kalff, J. C., Tolba, R. H., & van Echten-Deckert, G. (2009). A natural tetrahydropyrimidine protects small bowel from cold ischemia and subsequent warm in vitro reperfusion injury. *Pathobiol, 76*(4), 212-220.

Zhang, A., Carroll, A. L., & Atsumi, S. (2017). Carbon recycling by cyanobacteria: improving CO_2 fixation through chemical production. *FEMS Microbiol Lett, 364*(16), fnx165.

Zhao, Q., Li, S., Lv, P., Sun, S., Ma, C., Xu, P., Su, H., & Yang, C. (2019). High ectoine production by an engineered *Halomonas hydrothermalis* Y2 in a reduced salinity medium. *Microb Cell Fact, 18*(184), 1-12.

Chapter VI. Final remarks and future perspectives

6.1 Expanding the synthetic biology toolbox for *Synechocystis*

The development of a well-characterized cyanobacterial synthetic biology toolbox is of utmost importance to render cyanobacteria as efficient, sustainable and economically viable cell factories. However, the majority of the available tools have been developed for heterotrophic chassis like *E. coli* or *Saccharomyces cerevisiae* (Liu *et al.*, 2020; Tsai *et al.*, 2015; Xu *et al.*, 2012) and most of the regulatory elements characterized in these organisms function rather poorly or not at all in cyanobacteria, since the performance of biological parts is influenced by the genomic context (Cardinale & Arkin, 2012; Huang *et al.*, 2010). Therefore, we placed a considerable effort on the design and construction of a customized toolbox for *Synechocystis* sp. PCC 6803 (hereafter *Synechocystis*) (Chapter III, Ferreira *et al.* (2018)). The toolbox comprises fourteen promoters: five heterologous promoters well described and routinely used in *E. coli* either from bacterial origin (P_{luxR}, P_{araC}, P_{BADwt}) or bacteriophage-derived ($P_{\lambda cI}$, P_{T7pol}); eight redesigned promoters based on P_{T7pol} ($P_{T7.1.x.lacO}$, $P_{T7.2.x.lacO}$, $P_{T7.3.x.lacO}$), on P_{trc1O} ($P_{trc.x.tetO1}$, $P_{trc.x.tetO2}$, $P_{trc.x.araO}$, $P_{trc.x.lacO}$) and on P_{psbA2} (P_{psbA2*}); and one hybrid (P_{tacI}). This set of promoters was characterized using GFP as reporter and showed a wide range of activities varying from 0.13- to 41-fold compared to the cyanobacterial reference P_{rnpB}. Three of them ($P_{\lambda cI}$, $P_{trc.x.lacO}$ and $P_{trc.x.tetO1}$) were efficiently repressed (up to 99%). The LacI- and TetR-regulated redesigned promoters could be de-repressed (up to 2.3-fold) upon isopropyl β-D-1-thiogalactopyranoside (IPTG) or anhydrotetracycline hydrochloride (aTc) addition, respectively. Moreover, three replicative vectors available at the Standard European Vector Architecture (SEVA) repository (Silva-Rocha *et al.*, 2013) were validated for *Synechocystis* (Chapter III, Ferreira *et al.* (2018)). These vectors were successfully used to transform *Synechocystis* by three different methods (natural transformation, electroporation and conjugation). The presence of the vectors did not lead to an evident phenotype or hindered *Synechocystis* growth, with the majority of the cells (> 90%) able to maintain the replicative vector at least for 16 days, even in the absence of selective pressure.

Overall, the promoters characterized in this study are available to fine-tune the regulation of gene expression systems, and the validation of the use of the SEVA replicative vectors allows the fast generation of *Synechocystis* transformants for screening purposes and testing synthetic devices. Furthermore, the work presented in Chapter III constitutes a solid basis for the development and implementation of more efficient and tightly regulated elements required by applications using cyanobacteria as cell factories.

6.2 Functionality of the synthetic biology toolbox

As a proof-of-concept, the redesigned promoter $P_{trc.x.lacO}$ was assembled with the *ggpS* gene and the synthetic device was introduced into *Synechocystis* using one of the SEVA plasmids (Chapter III, Ferreira *et al.* (2018)). The presence of this device restored the production of glucosylglycerol in a *Synechocystis ggpS* deficient mutant, demonstrating the functionality of the tools/device. Therefore, the tools developed were used to construct a synthetic module, and to introduce it into the chassis. This work opened the possibility to use these tools for the control of gene expression and for the fast implementation of new functionalities in *Synechocystis*, contributing for the establishment of this cyanobacterium as a robust chassis, as it can be seen on section 6.4.

6.3 *Synechocystis* mutants deficient in the synthesis of native compatible solutes

For the sustainable production of heterologous compatible solutes, we started by generating *Synechocystis* mutants deficient in the synthesis of the main native compatible solutes, sucrose or/and glucosylglycerol, to decrease the redundancy (Chapter IV). Under standard laboratory growth conditions, *Synechocystis* wild-type (WT) and Δ*sps*, Δ*ggpS* and Δ*sps*Δ*ggpS* mutants accumulate glycogen (Figure 1, - NaCl), since it is the main strategy for the intracellular storage of carbon and energy (Gruendel *et al.*, 2012). Under saline conditions, the glycogen content decreases and the carbon is redirected for the synthesis of compatible solutes and extracellular polymeric substances (EPS), that are accumulated in a salinity-dependent manner, in all the strains (Figure 1, + NaCl), contributing to the homeostasis and protection of the cells. The comparison of the growth curves of *Synechocystis* WT and Δ*sps*, Δ*ggpS* and Δ*sps*Δ*ggpS* mutants under saline conditions showed the importance of the synthesis of compatible solutes for the *Synechocystis* survival. The most tolerant strain was the WT, followed by Δ*sps*, Δ*ggpS* and Δ*sps*Δ*ggpS*, being all of them unable to grow in BG11 supplemented with 7% NaCl (without NaCl adaptation).

In *Synechocystis* WT, glucosylglycerol was accumulated in higher amounts followed by glutamate and sucrose (Figure 1A). The two main native compatible solutes sucrose and glucosylglycerol could only be detected in presence of NaCl, as it was previously documented (Kirsch *et al.*, 2019). In contrast, glutamate was detected in the absence and presence of NaCl and increased in presence of NaCl, which agrees with the reported accumulation of this amino acid in *Synechocystis* grown in artificial seawater medium and BG11 with KCl (Iijima *et al.*, 2015; Iijima *et al.*, 2020).

For the Δ*sps* mutant grown under 5% NaCl, glucosylglycerol do not reach the levels observed for the WT, and released polysaccharides (RPS) increased significantly (Figure 1B), implying that RPS are crucial for the survival of this mutant under 5% NaCl. Most importantly, our results suggest that sucrose goes beyond osmoprotection, acting as a trigger for signaling cascades, as was previously hypothesized by Desplats *et al.* (2005).

In the Δ*ggpS* mutant, the significant increase in sucrose (Figure 1C) seems to indicate that this compatible solute is able to compensate for the absence of glucosylglycerol, sustaining *Synechocystis* growth under 3% NaCl. This compensation mechanism was also observed in the Δ*agp* mutant that is a mutant unable to produce glucosylglycerol since it is unable to synthesize ADP-glucose (Miao *et al.*, 2003). Notably, in Δ*ggpS* and Δ*agp* mutants, sucrose amounts were similar to glucosylglycerol amounts accumulated in the WT under the same conditions, suggesting that these two compatible solutes may have comparable osmoprotectant capacity when accumulated in similar amounts.

The Δ*sps*Δ*ggpS* mutant does not produce either sucrose and glucosylglycerol and is unable to survive under salt stress conditions (Figure 1D), indicating a minor contribution of glutamate to the salt acclimation process in *Synechocystis*, similar to the reported for the halophilic bacterium *Salinibacter ruber* (Oren *et al.*, 2002).

In summary, the characterization of the different compatible solutes deficient mutants enabled a better understanding of the carbon distribution and identification of some key players in terms of carbon sinks that will allow the chassis optimization for the increased production of heterologous compatible solutes or other carbon-based compounds in *Synechocystis*.

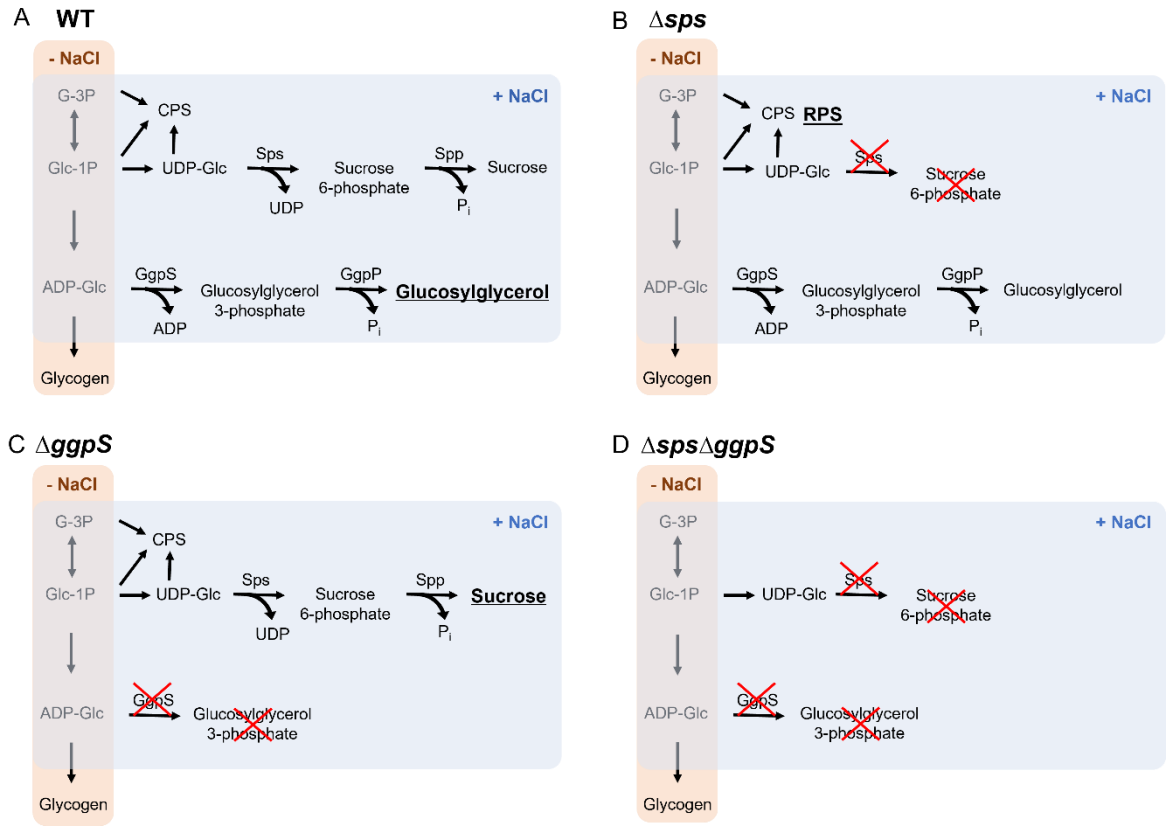

Figure 1. Schematic representation of precursors and reactions leading to the synthesis of sucrose, glucosylglycerol, glycogen, CPS (capsular polysaccharides) and RPS (released polysaccharides) in *Synechocystis* sp. PCC 6803 wild-type (WT) (A), Δ*sps* (B), Δ*ggpS* (C) and Δ*sps*Δ*ggpS* (D) mutants, grown in BG11 ("- NaCl", orange) or BG11 supplemented with NaCl ("+ NaCl", blue). Red crosses indicate that the enzymes and the respective products are absent. Under salinity conditions the carbon fluxes are redirected mainly to the underlined compounds. G-3P - glycerol-3-phosphate; Glc-1P - glucose-1-phosphate; UDP - uridine diphosphate; UDP-Glc - UDP-glucose; ADP - adenosine diphosphate; ADP-Glc - ADP-glucose; P_i - inorganic phosphate; Sps - sucrose phosphate synthase; Spp - sucrose phosphate phosphatase; GgpS - glucosylglycerol phosphate synthase; GgpP - glucosylglycerol phosphate phosphatase.

6.4 Heterologous production of compatible solutes in *Synechocystis*

The updated genome-scale metabolic model *i*Syn811 was used to predict the production rates for heterologous compatible solutes in *Synechocystis*. The analysis showed that the maximum production rate was for glycine betaine, followed by (hydroxy)ectoine and mannosylglycerate (Chapter IV, Additional file 1: Figure S4). Therefore, a synthetic device aiming at producing glycine betaine was implemented into *Synechocystis* wild-type and the customized compatible solutes deficient chassis (Δ*ggpS* and Δ*sps*Δ*ggpS*). The transcript levels were very stable regardless of the chassis or salinity, demonstrating that the

regulatory elements used in the device ensured its insulation from the genetic network of the chassis and that salinity did not influence the transcription. The heterologous production of glycine betaine was successfully achieved in the different *Synechocystis*-based chassis and, unlike transcription, the production increased with salinity (Chapter IV). This could be due to the redirection of carbon fluxes to the production of compatible solutes under salinity conditions. Furthermore, the higher levels of the precursor glycine reported for *Synechocystis* cells grown in artificial seawater medium, compared with BG11 (Iijima *et al.*, 2015), most probably favor the synthesis of glycine betaine. This may explain the fact that the maximum amount of glycine betaine was obtained in the Δ*ggpS* harboring the glycine betaine device, under 3% NaCl (64.29 µmol/gDW, Chapter IV). The production of glycine betaine in this mutant led to a significant growth improvement and supported its survival under 5% NaCl. Previously, glycine betaine was produced heterologously in the plants *Arabidopsis thaliana* and *Nicotiana tabacum*, in the cyanobacteria *Synechococcus* sp. PCC 7942*, Anabaena* sp. PCC 7120 and *Anabaena doliolum* and in *Escherichia coli* XL1-Blue and DH5α (Chapter IV, Table 1). Considering photoautotrophic organisms, plants produced low amounts and require rather long cultivation periods. The filamentous cyanobacterium *A. doliolum* produced 12.92 µmol/gDW under 3% NaCl after 10 days of cultivation, which is ~5-fold less than the production that we obtained using *Synechocystis* Δ*ggpS* chassis grown in the same salinity condition for 4 days. Regarding heterotrophic chassis, the amounts obtained using different *E. coli* strains were only up to 1.25-fold higher compared with ours. The cultivation times are significantly reduced, however, the production of glycine betaine significantly decreased when salt concentration is increased to 500 mM NaCl (~3% NaCl). Altogether, glycine betaine production using our *Synechocystis* Δ*ggpS* chassis not only has the advantage of overcoming the need for a carbon source, but also opens up the possibility of large-scale cultivation with seawater.

Regarding (hydroxy)ectoine and mannosylglycerate, these compatible solutes were previously produced heterologously mainly by *E. coli*, *Corynebacterium glutamicum* and *Saccharomyces cerevisiae* (Table 1). However, next generation strategies for heterologous production may be focused on the potential of strains that use inexpensive carbon sources, such as cyanobacteria (Zhang *et al.*, 2017). In this context, with the aim of producing (hydroxy)ectoine in *Synechocystis*, two synthetic constructs were designed (Chapter V), but further work is needed to reach the final goal. Envisaging the production of mannosylglycerate, a device was constructed and implemented into the *Synechocystis* wild-type and Δ*ggpS* chassis. Our results showed that *mgsD* gene was transcribed but no mannosylglycerate could be detected in preliminary studies using small culture volumes

(Chapter V). Therefore, this work also opens the possibility of producing these added-value compounds using *Synechocystis* / *Synechocystis* chassis.

Overall, this work contributed to expand the molecular toolbox for the cyanobacterium *Synechocystis* by characterizing a set of regulatory elements and validating three replicative vectors. These tools were then used to assemble functional devices, *e.g.* for the heterologous production of glycine betaine, in *Synechocystis* sp. PCC 6803 wild-type and *Synechocystis* mutants deficient in the synthesis of native compatible solutes. Among these customized chassis, the Δ*ggpS* chassis, grown under 3% NaCl, proved to be the best for the production of glycine betaine (64.29 µmol/gDW). The characterization of the different mutants also allowed to unveil compensation mechanisms for the survival of *Synechocystis* under saline conditions and insights on the key players in terms of carbon sinks. Altogether, this work opens up the possibility of optimizing the production of glycine betaine and to produce other heterologous compatible solutes / compounds using photoautotrophic chassis based on *Synechocystis*.

Table 1. Heterologous production of the compatible solutes: ectoine, hydroxyectoine and mannosylglycerate.

Production strain	Native strain	Salinity (M)	Amount	Production	Production rate	Yield (g/g)	Carbon source / Precursor	Reference
Ectoine								
Escherichia coli XL1-Blue	*Marinococcus halophilus* DSM 20408^T	0.86	1000 µmol/gDW	NA	NA	NA	Aspartate	Louis and Galinski (1997)
Escherichia coli DH5α	*Chromohalobacter salexigens* DSM 3043	0.08	NA	6 g/L	0.04 g/L/h	NA	Glucose	Schubert *et al.* (2007)
Escherichia coli DH5α	*Marinococcus halophilus* / *Corynebacterium glutamicum* MH20-22B	0.51	400 µmol/gDW	NA	NA	NA	Aspartate or fumarate	Bestvater *et al.* (2008)
Escherichia coli DH5α	*Acidiphilium cryptum* DSM 2389^T	0.04	NA	1.66 g/L 2.9 g/gDW	0.3 g/gDW/h	0.36	Glycerol	Bethlehem and Moritz (2020)
Escherichia coli K-12 BW25113	*Halomonas elongata*	0.4	NA	63.4 g/L 4 g/gDW	1.04 g/L/h	NA	Aspartate and glycerol	He *et al.* (2015)
Escherichia coli W3110	*Halomonas elongata* / *Corynebacterium glutamicum*	0	NA	25.1 g/L	0.84 g/L/h	0.11	Glucose	Ning *et al.* (2016)
Corynebacterium glutamicum ECT-2	*Pseudomonas stutzeri*	0	36.1 µmol/gDW	4.5 g/L	0.28 g/L/h	NA	Glucose	Becker *et al.* (2013)
Corynebacterium glutamicum Ecto5	*Chromohalobacter salexigens*	0	NA	22 g/L	0.32 g/L/h	0.16	Glucose	Pérez-García *et al.* (2017)
Corynebacterium glutamicum ectABC^{opt}	*Pseudomonas stutzeri*	0.03	NA	65.3 g/L	1.16 g/L/h	0.19	Glucose and molasses	Gießelmann *et al.* (2019)
Hydroxyectoine								
Escherichia coli DH5α	*Pseudomonas stutzeri* DSM 5190^T	0.34	500 µmol/gDW	NA	175 µmol/gDW/h	NA	NA	Seip *et al.* (2011)
Escherichia coli DH5α	*Acidiphilium cryptum* DSM 2389^T	0.09	13800 µmol/gDW	1.6 g/L 2.2 g/gDW	0.2 g/gDW/h	0.34	Glycerol	Bethlehem and Moritz (2020)
Escherichia coli FF4169	*Pseudomonas stutzeri* A1501	0.4	NA	2.13 g/L	0.1 g/L/h	NA	Glucose and ectoine	Czech *et al.* (2016)
Escherichia coli SK51	*Pseudomonas stutzeri* DSM 5190^T	0.4	NA	1.3 g/L 1.2 g/gDW	NA	0.16	Glucose	Czech *et al.* (2018)
Hansenula polymorpha	*Halomonas elongata*	0	365 µmol/gDW	2.8 g/L	NA	NA	MeOH and sorbitol	Eilert *et al.* (2013)
Mannosylglycerate								
Saccharomyces cerevisiae	*Dehalococcoides mccartyi*	0	49 µmol/gDW	0.008 g/gDW	NA	NA	GDP-mannose and 3-phosphoglycerate	Empadinhas *et al.* (2004)
Saccharomyces cerevisiae	*Dehalococcoides mccartyi*	0	NA	0.02 g/gDW	0.002 g/gDW/h	NA	GDP-mannose	Faria *et al.* (2018)

NA – Not available; DW – Dry weight.

6.5 Future perspectives

Although this work contributed to expand the molecular toolbox for the model cyanobacterium *Synechocystis* sp. PCC 6803, there is still room for improvement, *e.g.*, the development of more efficient inducible promoter systems:

(i) by increasing the outer membrane permeability to inducers, using *Synechocystis* mutants impaired in S-layer formation or extracellular polymeric substances (EPS) synthesis, overexpressing the *Synechocystis* TolC transporter protein, or expressing classical *E. coli* porins (OmpF or OmpC).

(ii) by testing optimized promoters that allow the control of gene expression using small-molecule inducers described for the *E. coli* "Marionette" strains (Meyer *et al.*, 2019), since one of these promoters (vanillate-inducible promoter) was recently proved to be functional in *Synechocystis* (Behle *et al.*, 2020).

(iii) by testing hybrid repressors regulated by sugars, *e.g.*, galactose or fructose (Dimas *et al.*, 2019), since cyanobacteria import small sugars by a non-specific mechanism (Kowata *et al.*, 2017).

The compatible solute glycine betaine was successfully produced heterologously in *Synechocystis,* but the production could be improved by *e.g.*,:

(i) implementing genetic switches to enable the shift from the "growth phase" to a "production phase" where cell resources should be devoted to biosynthesis.

(ii) using a *Synechocystis* Δ*gcvT* mutant that accumulates the precursor glycine (Eisenhut *et al.*, 2007).

This work provides an important stepping-stone to produce other compatible solutes in *Synechocystis*, (hydroxy)ectoine and mannosylglycerate, but further efforts are needed, starting by *e.g.*, assembling the constructs using different promoters (constitutive or inducible ones), and other regulatory elements.

6.6 References

Becker, J., Schafer, R., Kohlstedt, M., Harder, B. J., Borchert, N. S., Stoveken, N., Bremer, E., & Wittmann, C. (2013). Systems metabolic engineering of *Corynebacterium glutamicum* for production of the chemical chaperone ectoine. *Microb Cell Fact, 12*(110).

Behle, A., Saake, P., Germann, A. T., Dienst, D., & Axmann, I. M. (2020). Comparative dose–response analysis of inducible promoters in cyanobacteria. *ACS Synth Biol, 9*(4), 843-855.

Bestvater, T., Louis, P., & Galinski, E. A. (2008). Heterologous ectoine production in *Escherichia coli*: by-passing the metabolic bottleneck. *Saline Syst, 4*(1), 1-14.

Bethlehem, L., & Moritz, K. D. (2020). Boosting *Escherichia coli*'s heterologous production rate of ectoines by exploiting the non-halophilic gene cluster from *Acidiphilium cryptum*. *Extremophiles, 24*(5), 733-747.

Cardinale, S., & Arkin, A. P. (2012). Contextualizing context for synthetic biology–identifying causes of failure of synthetic biological systems. *Biotechnol J, 7*(7), 856-866.

Czech, L., Poehl, S., Hub, P., Stoeveken, N., & Bremer, E. (2018). Tinkering with osmotically controlled transcription allows enhanced production and excretion of ectoine and hydroxyectoine from a microbial cell factory. *Appl Environ Microbiol, 84*(2), e01772-01717.

Czech, L., Stöveken, N., & Bremer, E. (2016). EctD-mediated biotransformation of the chemical chaperone ectoine into hydroxyectoine and its mechanosensitive channel-independent excretion. *Microb Cell Fact, 15*(1), 1-16.

Desplats, P., Folco, E., & Salerno, G. L. (2005). Sucrose may play an additional role to that of an osmolyte in *Synechocystis* sp. PCC 6803 salt-shocked cells. *Plant Physiol Biochem, 43*, 133-138.

Dimas, R. P., Jiang, X.-L., Alberto de la Paz, J., Morcos, F., & Chan, C. T. Y. (2019). Engineering repressors with coevolutionary cues facilitates toggle switches with a master reset. *Nucleic Acids Res, 47*(10), 5449-5463.

Eilert, E., Kranz, A., Hollenberg, C. P., Piontek, M., & Suckow, M. (2013). Synthesis and release of the bacterial compatible solute 5-hydroxyectoine in *Hansenula polymorpha*. *J Biotechnol, 167*(2), 85-93.

Eisenhut, M., Bauwe, H., & Hagemann, M. (2007). Glycine accumulation is toxic for the cyanobacterium *Synechocystis* sp. strain PCC 6803, but can be compensated by supplementation with magnesium ions. *FEMS Microbiol Lett, 277*(2), 232-237.

Empadinhas, N., Albuquerque, L., Costa, J., Zinder, S. H., Santos, M. A., Santos, H., & da Costa, M. S. (2004). A gene from the mesophilic bacterium *Dehalococcoides ethenogenes* encodes a novel mannosylglycerate synthase. *J Bacteriol, 186*(13), 4075-4084.

Faria, C., Borges, N., Rocha, I., & Santos, H. (2018). Production of mannosylglycerate in *Saccharomyces cerevisiae* by metabolic engineering and bioprocess optimization. *Microb Cell Fact, 17*(1), 1-11.

Ferreira, E. A., Pacheco, C. C., Pinto, F., Pereira, J., Lamosa, P., Oliveira, P., Kirov, B., Jaramillo, A., & Tamagnini, P. (2018). Expanding the toolbox for *Synechocystis* sp. PCC

6803: validation of replicative vectors and characterization of a novel set of promoters. *Synth Biol, 3*.

Gießelmann, G., Dietrich, D., Jungmann, L., Kohlstedt, M., Jeon, E. J., Yim, S. S., Sommer, F., Zimmer, D., Mühlhaus, T., & Schroda, M. (2019). Metabolic engineering of *Corynebacterium glutamicum* for high-level ectoine production: design, combinatorial assembly, and implementation of a transcriptionally balanced heterologous ectoine pathway. *Biotechnol J, 14*(9), 1800417.

Gruendel, M., Scheunemann, R., Lockau, W., & Zilliges, Y. (2012). Impaired glycogen synthesis causes metabolic overflow reactions and affects stress responses in the cyanobacterium *Synechocystis* sp. PCC 6803. *Microbiol, 158*(12), 3032-3043.

He, Y.-Z., Gong, J., Yu, H.-Y., Tao, Y., Zhang, S., & Dong, Z.-Y. (2015). High production of ectoine from aspartate and glycerol by use of whole-cell biocatalysis in recombinant *Escherichia coli*. *Microb Cell Fact, 14*(1), 1-10.

Huang, H. H., Camsund, D., Lindblad, P., & Heidorn, T. (2010). Design and characterization of molecular tools for a Synthetic Biology approach towards developing cyanobacterial biotechnology. *Nucleic Acids Res, 38*, 2577-2593.

Iijima, H., Nakaya, Y., Kuwahara, A., Hirai, M. Y., & Osanai, T. (2015). Seawater cultivation of freshwater cyanobacterium *Synechocystis* sp. PCC 6803 drastically alters amino acid composition and glycogen metabolism. *Front Microbiol, 6*, 326.

Iijima, H., Watanabe, A., Sukigara, H., Shirai, T., Kondo, A., & Osanai, T. (2020). Simultaneous increases in the levels of compatible solutes by cost-effective cultivation of *Synechocystis* sp. PCC 6803. *Biotechnol Bioeng, 117*, 1649-1660.

Kirsch, F., Klähn, S., & Hagemann, M. (2019). Salt-regulated accumulation of the compatible solutes sucrose and glucosylglycerol in cyanobacteria and its biotechnological potential. *Front Microbiol, 10*, 2139.

Kowata, H., Tochigi, S., Takahashi, H., & Kojima, S. (2017). Outer membrane permeability of cyanobacterium *Synechocystis* sp. strain PCC 6803: studies of passive diffusion of small organic nutrients reveal the absence of classical porins and intrinsically low permeability. *J Bacteriol, 199*(19), e00371-00317.

Liu, Y., Su, A., Li, J., Ledesma-Amaro, R., Xu, P., Du, G., & Liu, L. (2020). Towards next-generation model microorganism chassis for biomanufacturing. *Appl Microbiol Biotechnol, 104*, 9095–9108.

Louis, P., & Galinski, E. A. (1997). Characterization of genes for the biosynthesis of the compatible solute ectoine from *Marinococcus halophilus* and osmoregulated expression in *Escherichia coli*. *Microbiol, 143*(4), 1141-1149.

Meyer, A. J., Segall-Shapiro, T. H., Glassey, E., Zhang, J., & Voigt, C. A. (2019). *Escherichia coli* “Marionette” strains with 12 highly optimized small-molecule sensors. *Nat Chem Biol, 15*(2), 196-204.

Miao, X., Wu, Q., Wu, G., & Zhao, N. (2003). Sucrose accumulation in salt-stressed cells of *agp* gene deletion-mutant in cyanobacterium *Synechocystis* sp. PCC 6803. *FEMS Microbiol Lett, 218*, 71-77.

Ning, Y., Wu, X., Zhang, C., Xu, Q., Chen, N., & Xie, X. (2016). Pathway construction and metabolic engineering for fermentative production of ectoine in *Escherichia coli*. *Metab Eng, 36*, 10-18.

Oren, A., Heldal, M., Norland, S., & Galinski, E. A. (2002). Intracellular ion and organic solute concentrations of the extremely halophilic bacterium *Salinibacter ruber*. *Extremophiles, 6*(6), 491-498.

Pérez-García, F., Ziert, C., Risse, J. M., & Wendisch, V. F. (2017). Improved fermentative production of the compatible solute ectoine by *Corynebacterium glutamicum* from glucose and alternative carbon sources. *J Biotechnol, 258*, 59-68.

Schubert, T., Maskow, T., Benndorf, D., Harms, H., & Breuer, U. (2007). Continuous synthesis and excretion of the compatible solute ectoine by a transgenic, nonhalophilic bacterium. *Appl Environ Microbiol, 73*(10), 3343-3347.

Seip, B., Galinski, E. A., & Kurz, M. (2011). Natural and engineered hydroxyectoine production based on the *Pseudomonas stutzeri ectABCD-ask* gene cluster. *Appl Environ Microbiol, 77*(4), 1368-1374.

Silva-Rocha, R., Martínez-García, E., Calles, B., Chavarría, M., Arce-Rodríguez, A., de las Heras, A., Páez-Espino, A. D., Durante-Rodríguez, G., Kim, J., Nikel, P. I., Platero, R., & de Lorenzo, V. (2013). The Standard European Vector Architecture (SEVA): a coherent platform for the analysis and deployment of complex prokaryotic phenotypes. *Nucleic Acids Res, 41*, D666-D675.

Tsai, C.-S., Kwak, S., Turner, T. L., & Jin, Y.-S. (2015). Yeast synthetic biology toolbox and applications for biofuel production. *FEMS Yeast Res, 15*(1), 1-15.

Xu, P., Vansiri, A., Bhan, N., & Koffas, M. A. (2012). ePathBrick: a synthetic biology platform for engineering metabolic pathways in *E. coli*. *ACS Synth Biol, 1*(7), 256-266.

Zhang, A., Carroll, A. L., & Atsumi, S. (2017). Carbon recycling by cyanobacteria: improving CO_2 fixation through chemical production. *FEMS Microbiol Lett, 364*(16), fnx165.